



UNIVERSITÀ DEGLI STUDI DI MILANO

DOCTORAL PROGRAMME IN NUTRITIONAL SCIENCE

Transcriptional Characterization of Obesity and Type 2
Diabetes: a focus on non-coding RNAs

Doctoral Dissertation of:
Federica REY

Tutor:
Prof. Alessandra BARASSI

Co-Tutor
Dr. Stephana CARELLI

The Chair of the Doctoral Program:
Prof. Coordinator Luciano PINOTTI

2020 – XXXIII

*A Cecilia,
che ha reso tutto più bello*

Abstract

Obesity is defined by the World Health Organization as a condition of abnormal or excessive accumulation of body fat that presents a risk to health. This disease can lead to an increase in associated morbidities for many chronic diseases such as type 2 diabetes, hypertension, coronary artery disease, dyslipidemia, stroke, osteoarthritis, and even certain forms of cancer, with a subsequent increase in mortality rate. The relative contribution of either genetic or the environment in obesity onset and co-morbidities development is not yet completely defined, and RNA biology might play a central role in elucidating new targetable pathways. The aim of this research was the characterization of the transcriptional differences present in the sottocutaneous adipose tissue of obese and obese with type 2 diabetes subjects. Moreover, the work focused on the role of the non-coding part of the genome in disease development, as these molecules are becoming more and more relevant for their function in physiological processes and disease mechanisms. To this aim, RNA-sequencing was performed on sottocutaneous adipose tissue obtained from 5 healthy normal weight females, 5 obese females, and 5 obese females with type 2 diabetes. Three experimental conditions were subsequently analyzed: the differences occurring between obese and healthy subjects, the differences occurring between obese with type 2 diabetes and healthy subjects, and moreover the differences occurring between obese with type 2 diabetes and obese subjects. For each condition, a global bioinformatics characterization of the differentially expressed RNAs and the pathways in which they are involved was performed. These analyses extensively characterized the differentially expressed RNAs, highlighting their localization, interaction, and transcriptional regulation. Gene ontology analysis highlighted the gene-specific molecular functions and biological processes involved, and the most significant pathways in which the differentially expressed RNAs are involved were identified. Moreover, disease-related databases were interrogated and a screening of the gene relations with immunological, oncogenic and metabolic diseases were characterized.

Moreover, a special attention was given to non-coding RNAs, whose prevalence increases when switching from a “pure” obesogenic condition to a comorbidity with diabetes. Specifically, whilst non-coding genes are 6.43% of the differentially expressed RNAs in obese subjects, this percentage increases to up to 32.43% in diabetic subjects, and when considering the molecular underlining responsible for the additional diabetic phenotype (diabetic vs. obese), more than 50% of the differentially expressed RNAs are non-coding RNAs. This highlights how the non-coding epigenome could be of crucial relevance in the development of specific comorbidities, highlighting the possibility of new markers and targets for future therapeutic intervention and prevention. Lastly, functional experiments were performed on long-non coding RNAs deregulated in sottocutaneous adipose tissue from obese subjects, and results highlight how these are highly expressed in differentiated adipocytes, and predominantly regulated by adipogenesis transcription factors such as PPAR γ , C/EBP α , C/EBP β and C/EBP δ . The results clearly highlight the role of the non-coding component in the development of the diabetic comorbidity, and the investigation of this molecules could be of crucial relevance in understanding a new disease-mechanism never before analyzed, and even highlight why certain patients present a higher risk for diabetes development, paving the way for early intervention and precision medicine strategies.

Riassunto

L'obesità è definita dall'Organizzazione Mondiale della Sanità come una condizione di accumulo di grasso corporeo anormale o eccessivo che può presentare un rischio per la salute. Questa malattia può portare all'insorgenza di comorbidità associate quali il diabete di tipo 2, l'ipertensione, malattie cardiovascolari, dislipidemia, infarto, artrite e anche alcuni tipi di cancro, con un conseguente aumento della mortalità. Il contributo relativo di fattori genetici o dell'ambiente nell'insorgenza dell'obesità non è ancora chiaramente definito, e gli RNA regolatori potrebbero avere una funzione fondamentale nell'identificazione di nuovi meccanismi di malattia. Lo scopo di questo lavoro è la caratterizzazione delle differenze trascrizionali presenti nel tessuto adiposo sottocutaneo di pazienti obesi e obesi con diabete di tipo 2. Il lavoro si è inoltre focalizzato sull'analisi del ruolo del genoma non codificante nello sviluppo della malattia, per la loro rilevanza in numerosi processi fisiologici e patologici.

A questo scopo è stato effettuato il sequenziamento dell'RNA presente nel tessuto adiposo sottocutaneo di 5 donne normopeso, 5 donne obese e 5 donne obese con diabete di tipo 2. Tre condizioni sperimentali sono state analizzate: le differenze presenti tra le donne obese e le normopeso, quelle tra le donne obese con il diabete di tipo 2 e le normopeso e quelle tra le donne obese con diabete di tipo 2 e le donne obese senza questa comorbidità. Per ogni condizione è stata effettuata un'analisi bioinformatica globale. Questa analisi ha previsto una caratterizzazione estensiva dei trascritti differenzialmente espressi, indicandone la loro localizzazione, interazione e regolazione trascrizionale. L'analisi di ontologia genica ha permesso di identificare le funzioni molecolari specifiche e i processi biologici in cui essi sono coinvolti, insieme ai loro processi di appartenenza. Sono stati consultati inoltre specifici database contenenti informazioni su numerose malattie, in modo da identificare l'implicazione dei trascritti in malattie immunologiche, oncologiche e metaboliche. Un'attenzione particolare è stata posta sul ruolo degli RNA non codificanti, la cui presenza aumenta significativamente passando da una condizione di obesità "pura" a quella di un'obesità associata alla compresenza di diabete di tipo 2. I trascritti differenzialmente espressi non codificanti sono il 6,43% dei deregolati nella condizione di obesità versus normopeso, il 32,43% nei soggetti diabetici versus normopeso e addirittura più del 50% nell'analisi di soggetti obesi diabetici versus obesi. Questo dimostra come il genoma non codificante potrebbe essere di importanza fondamentale nell'insorgenza di specifiche comorbidità e potrebbe rappresentare un bersaglio per futuri interventi terapeutici e di prevenzione. In questo lavoro sono stati svolti esperimenti funzionali in modo da caratterizzare il ruolo di alcuni RNA non codificanti "a catena lunga" (long non-coding RNAs) nell'obesità, e i risultati hanno dimostrato come questi sono espressi negli adipociti e strettamente regolati da fattori trascrizionali implicati nell'adipogenesi quali PPAR γ , C/EBP α , C/EBP β e C/EBP δ .

I risultati dimostrano chiaramente il ruolo della componente non codificante del genoma nello sviluppo della comorbidità diabetica e un'analisi futura di queste molecole potrebbe essere di cruciale rilevanza nella comprensione di nuovi meccanismi di malattia mai prima caratterizzati. I risultati potrebbero inoltre spiegare perché alcune classi di pazienti obesi hanno un rischio maggiore di sviluppo di comorbidità specifiche, aprendo le porte a possibili strategie terapeutiche preventive e di medicina di precisione.

Abbreviations:

AA: aminoacids; ADIPOQ: Adiponectin; ADNCR: adipocyte differentiation-associated long non-coding RNA; β linc: β -cell long intergenic noncoding RNA; BMI: Body Mass Index; cDNA: complementary DNA; C/EBP: CCAAT-enhancer-binding proteins; DE RNAs: differentially expressed RNAs; FABP4: fatty-acid-binding protein; FBS: Fetal Bovine Serum; FC: Fold Change; FDR: False Discovery Rate; GLUT4: glucose transporter type 4; GO: Gene Ontology; hADSCs: human Adipose Derived Stem Cells; HOTAIR: HOX transcript antisense RNA; IG C pseudogene:inactivated immunoglobulin gene; IMFNCR: intramuscular fat-associated long non-coding RNA; KEGG: Kyoto Encyclopedia of Genes and Genomes; LEP: Leptin; lincRNAs: lincRNAs: long intergenic non-coding RNAs; lncRNAs: long non-coding RNAs; MCE: Mitotic Clonal Expansion phase; MEG3: Maternally Expressed Gene 3; miRNAs: microRNAs; miscRNAs: novel RNAs whose biotype could not be defined by any other parameter; NATs: natural antisense transcripts; NCoR: nuclear receptor co-repressor 1; ncRNAs: non-coding RNAs; NEAT1: Nuclear Enriched Abundant Transcript 1; NJ: Neighbor-Joining; NW: Normal Weight; OBF: Obese Female Subjects; OBT2D: Obese Female Subjects with Type 2 Diabetes; PBMCs: Peripheral Blood Mononuclear Cells; PCA: Principal Component Analysis; PCR: Polymerase Chain Reaction; PLIN: perilipin; PPAR γ : Peroxisome Proliferator-Activated Receptor; PVT1: Plasmacytoma Variant Translocation 1; ribosomal RNA: rRNA; RNA-seq: RNA-sequencing; SAT: Sottocutaneous Adipose Tissue; SD: Standard Deviations; SEM: Standard Error Mean; Sim-1: SIM BHLH Transcription Factor 1; SIRT1: Sirtuin 1; SMRT: silencing mediator for retinoid or thyroid-hormone receptors; snoRNAs: small nucleolar RNAs; snRNAs: small nuclear RNAs; SRA: Steroid Receptor RNA Activator; STAT3: Signal Transducer and Activator of Transcription 3; T2D: type 2 diabetes; TEC: To be Experimentally Confirmed; TFs: Transcription Factors; VAT: Visceral Adipose Tissue; WAGR: Wilms tumor, Aniridia, Genitourinary anomalies and mental Retardation; WGCNA: Weighted Gene Co-expression Network Analysis; WHO: World Health Organization;

Table of Contents

| | |
|---|-----------|
| 1. INTRODUCTION | 1 |
| 1.1. INTRODUCTION TO OBESITY | 1 |
| 1.1.1. <i>Childhood obesity</i> | 3 |
| 1.1.2. <i>Etiology</i> | 4 |
| 1.1.3. <i>Genetics</i> | 5 |
| 1.2. LNCRNAs IN OBESITY AND METABOLIC DISEASES | 6 |
| 1.2.1. <i>LncRNAs: definition and principal functions</i> | 6 |
| 1.2.2. <i>LncRNAs in adipogenesis</i> | 7 |
| 1.2.2.1. Role of lncRNAs in the regulation of early adipogenesis master regulators..... | 8 |
| 1.2.2.2. Role of lncRNAs in the regulation of late adipogenesis master regulators..... | 9 |
| 1.2.3. <i>LncRNAs in obesity</i> | 12 |
| 1.2.4. <i>LncRNAs in T2D</i> | 13 |
| 2. AIM OF THE STUDY..... | 15 |
| 3. MATERIALS AND METHODS | 16 |
| 3.1. ADULT HUMAN ADIPOSE TISSUE COLLECTION, ISOLATION AND DIFFERENTIATION | 16 |
| 3.2. SAT RNA EXTRACTION..... | 16 |
| 3.3. RNA-SEQ AND BIOINFORMATIC DATA ANALYSIS | 17 |
| 3.3.1. <i>Library preparation</i> | 17 |
| 3.3.2. <i>Library sequencing</i> | 17 |
| 3.3.3. <i>Differential expression analysis</i> | 17 |
| 3.3.4. <i>Pathways analysis</i> | 18 |
| 3.3.5. <i>Visualization of RNA-Seq results with R software</i> | 18 |
| 3.3.5.1. Heatmap..... | 18 |
| 3.3.5.2. Principal Component Analysis (PCA) plot | 18 |
| 3.3.5.3. Volcano plot | 18 |
| 3.3.5.4. Dotplot..... | 18 |
| 3.3.5.5. GOChord plot | 19 |
| 3.3.6. <i>Visualization of RNA-Seq results with Cytoscape</i> | 19 |
| 3.3.6.1. NDEx..... | 19 |
| 3.3.6.2. ClueGO..... | 19 |
| 3.3.6.3. BiNGO..... | 19 |
| 3.3.6.4. DisGeNET | 20 |
| 3.3.6.5. iRegulon..... | 20 |
| 3.3.7. <i>String Protein Interaction Network</i> | 20 |
| 3.3.8. <i>Visualization of ncRNAs features and interactors</i> | 20 |
| 3.3.8.1. Coding and ncRNAs co-expression analysis..... | 20 |
| 3.3.8.2. Phylogenetic analysis | 21 |
| 3.3.8.3. RNA secondary structure prediction | 21 |
| 3.3.8.4. Identification of TFs binding sites (CiiDER) | 21 |
| 3.4. hADSCs | 21 |
| 3.4.1. <i>hADSCs' isolation</i> | 21 |
| 3.4.2. <i>Culture of cryopreserved hADSCs</i> | 21 |
| 3.4.3. <i>Adipogenic induction</i> | 22 |
| 3.4.4. <i>Pharmacological treatments</i> | 22 |
| 3.4.5. <i>Gene expression silencing</i> | 22 |
| 3.4.6. <i>hADSCs RNA extraction</i> | 22 |
| 3.4.7. <i>Reverse Transcription-PCR (RT-PCR)</i> | 23 |
| 3.4.8. <i>Real Time PCR</i> | 23 |
| 3.4.9. <i>Statistical analysis for in vitro experiments</i> | 24 |

| | |
|--|------------|
| 4. RESULTS | 25 |
| 4.1. ISOLATION AND CHARACTERIZATION OF SAT FROM NW, OBESE AND T2D PATIENTS..... | 25 |
| 4.1.1. <i>Clinical characteristics of screened subjects</i> | 26 |
| 4.2. TRANSCRIPTIONAL CHARACTERIZATION FROM SAT OF HEALTHY, OBESE AND T2D PATIENTS..... | 26 |
| 4.2.1. <i>Transcriptional characterization of SAT of OBF vs. NW</i> | 28 |
| 4.2.1.1. Expression profiles of SAT of OBF vs. NW..... | 28 |
| 4.2.1.2. Analysis of deregulated genes: a focus on novel risk-genes..... | 30 |
| 4.2.1.3. Characteristics of DE RNAs: interaction, tissue expression and cellular localization..... | 31 |
| 4.2.1.4. Identification of co-regulating TFs..... | 34 |
| 4.2.1.5. GO analyses: Cellular Component, Molecular Function and Biological Processes..... | 35 |
| 4.2.1.6. Pathways characterization: top deregulated processes and implications for metabolic components..... | 38 |
| 4.2.1.7. Role of the immunological component in SAT of OBF vs NW..... | 42 |
| 4.2.1.8. Potential cancer implications: susceptibility in obese patients..... | 44 |
| 4.2.1.9. DE RNAs correlations with nutritional and metabolic diseases..... | 46 |
| 4.2.1.10. Identification of DE RNAs associated diseases..... | 47 |
| 4.2.2. <i>Transcriptional characterization of SAT of OBT2D vs. NW</i> | 48 |
| 4.2.2.1. Expression profiles of SAT of obese OBT2D vs. NW..... | 48 |
| 4.2.2.2. Analysis of deregulated genes: a focus on novel risk-genes..... | 49 |
| 4.2.2.3. Characteristics of DE RNAs: network interaction, tissue expression and cellular compartmentalization..... | 50 |
| 4.2.2.4. Identification of co-regulating TFs..... | 52 |
| 4.2.2.5. GO analyses: Cellular Component, Molecular Function and Biological Processes..... | 53 |
| 4.2.2.6. Pathways characterization: top deregulated processes and implications for metabolic components..... | 56 |
| 4.2.2.7. Analysis of the transcriptional immunological response in OBT2D..... | 58 |
| 4.2.2.8. Potential cancer implications: susceptibility in OBT2D..... | 59 |
| 4.2.2.9. DE RNAs correlations with nutritional and metabolic diseases..... | 60 |
| 4.2.2.10. Identification of DE RNAs associated diseases..... | 61 |
| 4.2.3. <i>Transcriptional characterization of SAT of OBT2D vs. OBF</i> | 62 |
| 4.2.3.1. Expression profiles of SAT of OBT2D vs. OBF..... | 62 |
| 4.2.3.2. Analysis of deregulated genes: a focus on novel risk-genes..... | 63 |
| 4.2.3.3. Characteristics of DE RNAs: network interaction, tissue expression and cellular compartmentalization..... | 64 |
| 4.2.3.4. Identification of co-regulating TFs..... | 66 |
| 4.2.3.5. GO analyses: Cellular Component, Molecular Function and Biological Processes..... | 66 |
| 4.2.3.6. Pathways characterization: top deregulated processes and implications for metabolic components..... | 69 |
| 4.2.3.7. Role of the immunological component in SAT from OBT2D vs. OBF..... | 70 |
| 4.2.3.8. Potential cancer implications: susceptibility in OBT2D vs. OBF..... | 72 |
| 4.2.3.9. DE RNAs correlations with nutritional and metabolic diseases..... | 73 |
| 4.2.3.10. Identification of DE RNAs associated diseases..... | 73 |
| 4.3. ROLE OF NCRNAS IN DISEASE PATHOGENESIS: A FOCUS ON LNCRNAs IN OBESITY..... | 74 |
| 4.3.1. <i>Role of ncRNAs in obesity and diabetes</i> | 74 |
| 4.3.1.1. Increase of the non-coding biological component in the diabetic comorbidity..... | 74 |
| 4.3.1.2. Network interaction of coding and non-coding DE RNAs in obesity and diabetes..... | 75 |
| 4.3.2. <i>Computational and functional analyses of lncRNAs in OBF</i> | 76 |
| 4.3.2.1. Computational characterization of lncRNAs in OBF..... | 76 |
| 4.3.2.2. In vitro characterization of lncRNAs regulation..... | 80 |
| 5. DISCUSSION | 86 |
| 6. ACKNOWLEDGMENTS | 93 |
| 7. BIBLIOGRAPHY | 94 |
| 8. ANNEX A - PUBLICATIONS | 111 |
| 9. ANNEX B – ABSTRACTS | 112 |

1. Introduction

1.1. Introduction to obesity

Obesity is defined as abnormal or excessive fat accumulation, presenting a risk to health (WHO 2020a). The most recent report of the World Health Organization (WHO) shows how the worldwide prevalence of obesity nearly tripled between 1975 and 2016, with over 650 million adults being clinically defined as obese (WHO 2020a). This trend is due to increase even more, as in 2018 more than 40 million children under the age of 5 years were overweight and obese, with studies showing that 70% of obese adolescents will maintain their obese condition as adults, with a significant impact on their physical and psychological health (WHO 2020a, Maclaren et al. 2007, Ogden et al. 2010). Based on these data and multiple epidemiological evidence linking obesity with a range of physical and psychosocial health conditions, it is possible to describe obesity as a public health crisis that severely impairs the health and quality of life of people and furthermore considerably adds to national health-care budgets (Seidell and Halberstadt 2015). Indeed, obesity contributes to increased morbidity and mortality as it is associated to many chronic diseases such as type 2 diabetes (T2D), hypertension, dyslipidemia, coronary artery disease, stroke, osteoarthritis and even certain forms of cancer (Haslam, Sattar, and Lean 2006, Lawrence and Kopelman 2004, WHO 2020a). The emerging link between obesity and multiple cancer types is gaining more and more relevance in recent years (Avgerinos et al. 2019, Kompella and Vasquez 2019, Ungefroren et al. 2015). Specifically, the burden of cancer attributable to obesity, expressed as population attributable fraction, is 11.9% in men and 13.1% in women (Avgerinos et al. 2019). It is fundamental to characterize the molecular underlining of this process, as they could highlight new mechanisms leading to increased susceptibility to cancer. Indeed, one recent research work, authored by me and collaborators, demonstrates how human Adipose Derived Stem Cells (hADSCs) obtained from breast cancer microenvironment present impaired Peroxisome Proliferator-Activated Receptor (PPAR γ) activation and a subsequent inhibition of differentiation (Rey et al. 2019).

The parameter used to measure obesity and classify its different levels of severity is the Body Mass Index (BMI), defined as a person's weight (in kilograms) divided by the square of his or her height (in meters). A person with a BMI of 30 or more is generally considered obese, whilst a person with a BMI equal to or more than 25 is considered overweight (WHO 2020a). The BMI is sufficient for most clinical screening and surveillance purposes as high BMI predicts future morbidity and death. Some research, however, suggests that other measures of body fat, such as skinfold thicknesses, bioelectrical impedance analysis, underwater weighing, and dual energy x-ray absorption, are more accurate than BMI (Duren et al. 2008).

It is possible to try and counteract obesity through a regulation of body weight. Indeed, this is controlled by several complex regulatory systems that respond to internal metabolic and hormonal signals, hedonic properties of food, internal forces of valuation and self-control, and social factors (Bessesen 2011). Each of these steps can be controlled and thus lead to an alteration in body weight. Typically, obesity is the result of excessive food energy intake, lack of physical activity and genetic susceptibility, although in a few cases it can be a secondary consequence of endocrine disorders, medications, sleep deprivation or psychiatric diseases

(Figure 1) (Hossain, Kawar, and El Nahas 2007, Tsai and Bessesen 2019, van der Klaauw and Farooqi 2015).

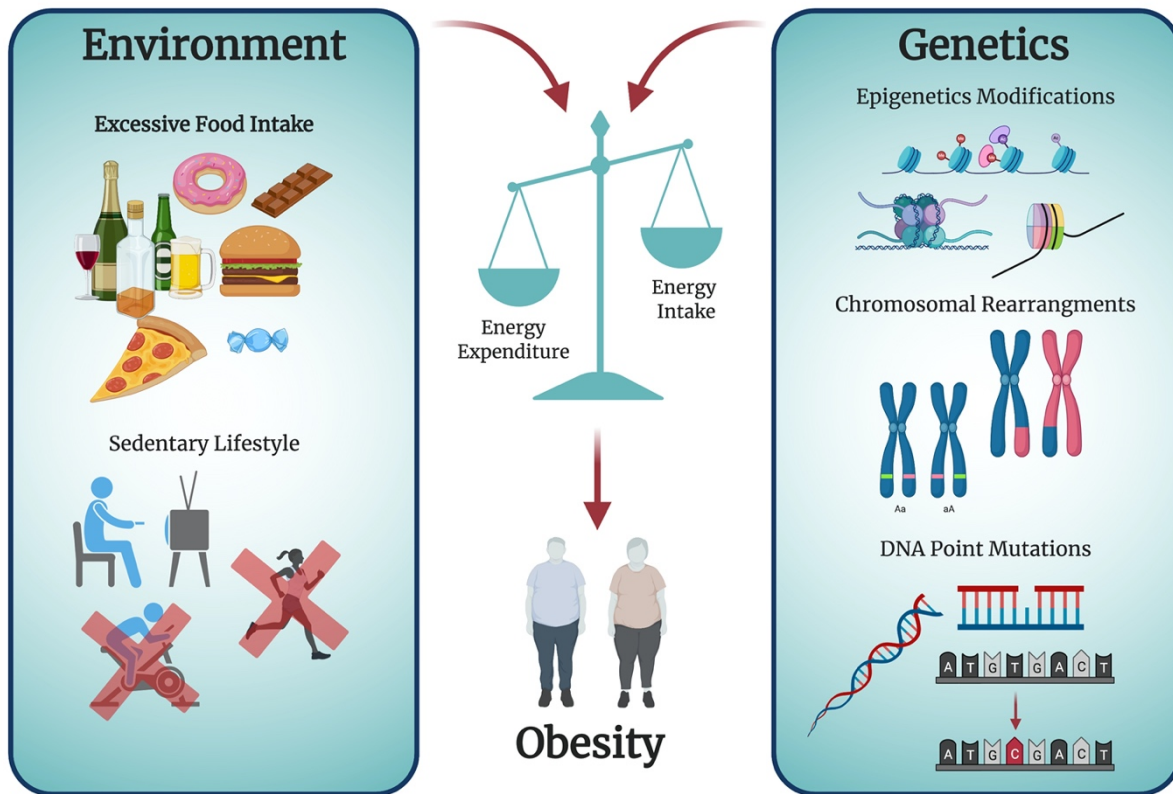


Figure 1: Contribution of the environment and genetics to obesity development. Created with BioRender.com.

All these factors that can influence body weight regulation ultimately act by a chronic modification of the energy balance equation:

$$\text{Energy stored} = \text{energy intake} - \text{energy lost in feces and urine} - \text{energy expenditure}$$

Even a slight imbalance between energy intake and energy expenditure may lead to severe obesity: an excess of energy intake by 5% every day can result in a gain of 5 kg fat mass over one year, and to morbid obesity over several years (Jéquier 2002).

Consequently to this, canonical approaches to counteract obesity involve decreasing energy intake by choosing a suitable diet and increasing the energy expenditure with exercise, but these two approaches alone are not always sufficient (Wyatt 2013) (Figure 2). It is important to stress that also a moderate weight loss (-5-10% of initial weight) should be encouraged because of proven health benefits and clinical complications improvement induced by a negative energy balance. Combinatory approaches involve high-intensity counselling, and, as the psychological and neurological component can be relevant in this disease, neuromodulation and neurofeedback treatments are also starting to be employed (Tronieri et al. 2019, Dalton, Campbell, and Schmidt 2017). To this day, the most commonly used anti-obesity medications are phentermine, orlistat, topiramate, lorcaserin, naltrexone, liraglutide and various medicinal plants (Saunders et al. 2018, Park et al. 2016). Medications approved for chronic weight management could help patients improve the diet plan adherence sustaining long term weight loss but, even in this case, they do not lead to a long-term resolution of the disease. The

discovery of monogenic forms of the disease and of several disease-causing pathways (e.g. the leptin (LEP)-melanocortin axis, the opioid system, Glucagon-like peptide-1 system, and Fibroblast growth factor 21/ Fibroblast growth factor Receptor 1c/b-Klotho axis) is leading to the development of new drug candidates which can avoid previous issues and directly target the obesity-causing molecule of choice (Jackson et al. 2015). Other innovative therapies involve microbiome replacement/supplementation and non-surgical devices (Jackson et al. 2015). For adult patients with severe obesity and complications, bariatric surgery should be encouraged and in adolescents should be performed (Beamish and Reinehr 2017, Childerhose et al. 2017, Thenappan and Nadler 2019, Beamish, Johansson, and Olbers 2015). This surgical approach is now endorsed by many international societies of experts to be an effective treatment for weight loss, which also offers significant improvement in associated co-morbidities, especially T2D (Ryan and Kahan 2018, Durrer Schutz et al. 2019, Stefater et al. 2012).

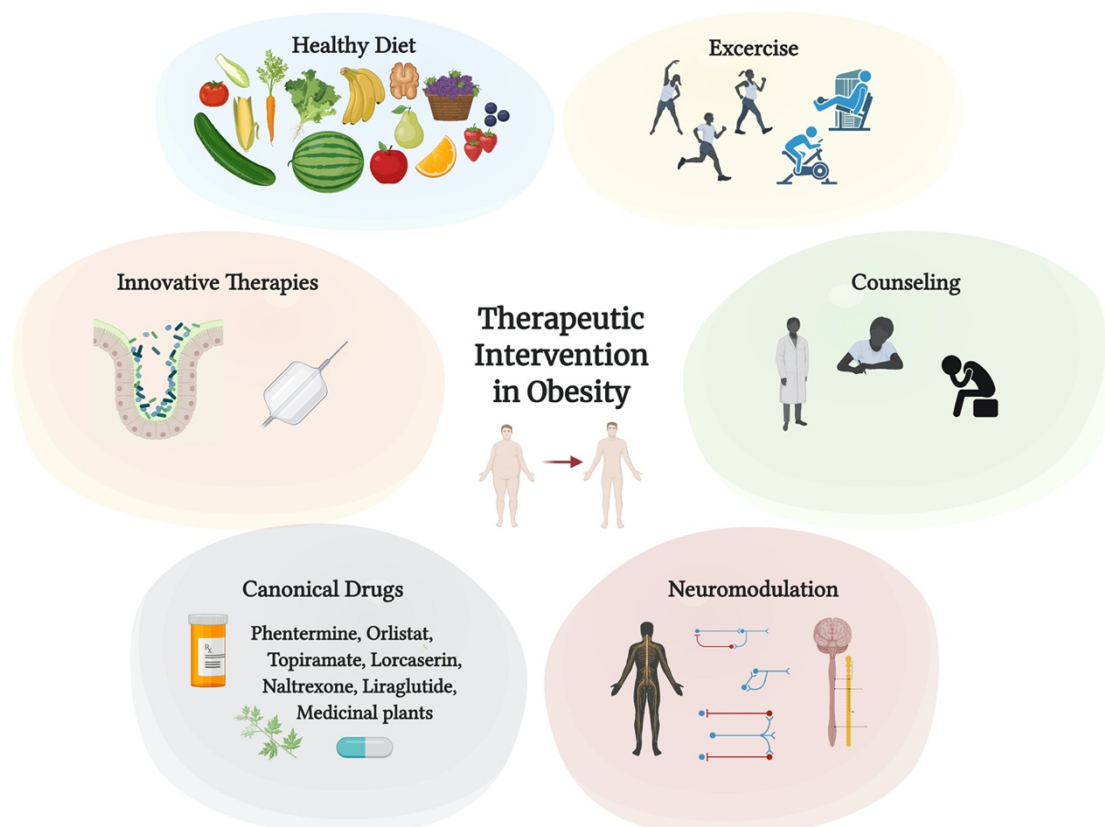


Figure 2: Strategies for therapeutic intervention in obesity. Created with BioRender.com.

At a tissue level, obesity is characterized by the accumulation of adipose tissue that expands due to an increase in adipose size (hypertrophy) and number (hyperplasia) and imbalances in adipogenesis (the process through which stem cells mature into adipocytes) can also lead to increased obesity and may represent a new promising therapeutic strategy in the treatment of the disease (Ghaben and Scherer 2019, Tseng, Cypess, and Kahn 2010).

1.1.1. Childhood obesity

Childhood obesity is a global problem, and since the 1980s the worldwide prevalence of childhood overweight and obesity has increased by 47%, both in developing and developed countries (Bleich et al. 2018, Ng et al. 2014). In children under 5 years of age obesity is defined

as weight-for-height 3 standard deviations (SD) above the WHO Child Growth Standards reference median. For children aged 5–19 years, obesity is defined as BMI-for-age 2 SD above the WHO Growth Standards reference median (WHO 2020b). Indeed, the WHO reports that in 2018 an estimated 40 million children under the age of 5 were classified as overweight or obese, and over 340 million children and adolescents aged 5-19 were overweight or obese in 2016 (WHO 2020a). As previously mentioned, many reports identify childhood obesity as a risk factor of obesity problems in adults, and there is thus a need for early intervention in order to modify this trend (Haidar and Cosman 2011). Interestingly, pediatric obesity could be influenced as early as in the “first 1000 days of life”, as within this defined time frame, three main steps of human dietary development can be identified: (1) the prenatal period; (2) breast vs. formula feeding; and (3) complementary diet (Mameli, Mazzantini, and Zuccotti 2016). In this time frame, nutrition, the microbiome and the epigenome can strongly influence the child’s development and future health. Indeed, maternal nutrition through over/undernutrition, vitamin D status, dietary methyl donors, and food pollutants, along with neonatal and infant nutrition (human or formula milk, prebiotics and probiotics) can deeply influence the child’s growth. When considering the epigenome, the human genome and environmental factors could be of relevance in the child’s future development, whilst microbiome alterations refer to maternal microbiota, antenatal and post-natal antibiotic exposure, and urban or rural environment (Indrio et al. 2017)

Childhood obesity is associated with comorbidities that were previously considered to be "adult" diseases, such as T2D, hypertension, non-alcoholic fatty liver disease, obstructive sleep apnea, and dyslipidemia (Kumar and Kelly 2017). Also in the case of childhood obesity, there is a need for new therapeutic strategies (Kumar and Kelly 2017). Different therapies will depend on the age of the child, the severity of obesity, and the presence of obesity-related comorbidities. Lifestyle interventions resulted in limited effects in severe obese children, and there is reduced information on the efficacy and safety of medications for weight loss in children (Kumar and Kelly 2017). The most invasive approach would be bariatric surgery, possible in adolescents, but again there is limited data on the long-time effect of this therapy (Kumar and Kelly 2017). New innovative approaches need to be considered, and the development of patient-specific therapies aimed at disrupting specifically altered cellular pathways could be of great interest. Indeed, although the adipogenesis process is now mostly elucidated, the differences in this process between obese and healthy subjects are far from characterized.

1.1.2. Etiology

Obesity is typically caused by excess energy consumption relative to energy expenditure, but the etiology of obesity is highly complex and includes genetic, physiologic, environmental, psychological, social, economic, and even political factors that interact in various degrees to promote the development of obesity (Wright and Aronne 2012). Amongst the environmental and social factors, causative for obesity are rising incomes, increasing urban populations, diets high in fats and simple sugars, and a shift toward less physically demanding jobs. Indeed, a lack in physical activity is promoted by automated transport, labor-saving technology in the home and workplace, television, and computer games, which can be very influential in the development of the disease at a young age (Kenney and Gortmaker 2017). Even so,

environmental factors are not the only causes of obesity, and a focus on genetic, epigenetic and metabolic factors controlling this disease is needed.

1.1.3. Genetics

There is now mounting evidence of genetic causes of obesity. Genome Wide Association Studies have allowed the identification of novel mutations and polymorphisms which can be associated to BMI, waist circumference, and waist-to-hip ratio (Singh, Kumar, and Mahalingam 2017). To date, more than 97 loci related to complex obesity that account for approximately 2.7% of BMI, waist circumference, and waist-to-hip ratio variations have been identified (Singh, Kumar, and Mahalingam 2017).

It is possible to classify obesity in syndromic (associated with pre-existing conditions) and non-syndromic (mono-genic or polygenic forms of obesity) (Figure 3). Specifically, syndromic obesity is obesity occurring in the clinical context of a broad range of associated clinical phenotypes, characterized by one or more features including developmental delay, dysmorphic traits, and/or congenital malformations and

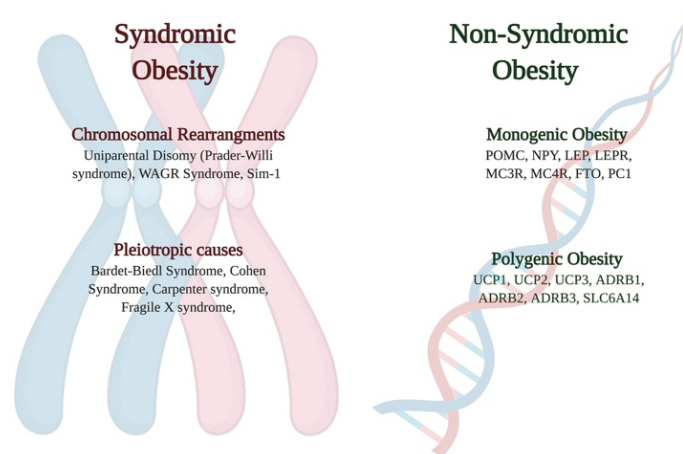


Figure 3: Genetic Basis of Obesity. Created with BioRender.com.

unusual behaviors such as increased energy intake. In the syndromic category it is possible to identify those syndromes due to chromosomal rearrangements, such as uniparental disomy (e.g. Prader-Willi Syndrome), Wilms tumor, aniridia, genitourinary anomalies and mental retardation Syndrome (WAGR), SIM BHLH Transcription Factor 1 (Sim-1) and those due to pleiotropic causes (Bardet-Biedl Syndrome, Cohen Syndrome, Fragile X syndrome, also associated with developmental delays) (Farooqi and O’Rahilly 2016). The non-syndromic forms of obesity include monogenic and polygenic forms of the diseases (Farooqi and O’Rahilly 2004). Monogenic forms of obesity are caused by single-point mutations in specific genes. These forms are rare, severe and typically occur in childhood (Farooqi and O’Rahilly 2004). They typically occur in genes implicated in energy homeostasis and adipogenesis, along with the neural signaling implicated in appetite and satiety regulation (Singh, Kumar, and Mahalingam 2017). Genes more frequently implicated are: POMC, NPY, LEP, LEPR, MC3R, MC4R, FTO, PC1. The most common non-syndromic obesity is associated with MC4R gene mutations with a prevalence, in the general population, of 1-5 : 10 000. Mutation carriers display severe early-onset obesity, hyperphagia and numerous endocrine complications. Polygenic obesity implicates multiple genes affected in the same individual, rendering its study significantly more complex. Even so, it is possible to implicate families of genes thought to be causative for the diseases, and these are: the β -adrenergic receptor family, uncoupling proteins and SLC6A14 (Singh, Kumar, and Mahalingam 2017).

Even considering all these evidence, it is not possible to conclude that obesity can be caused either by the genes or the environment. Indeed, behavior and genes are different levels of the same causal framework. Moreover, epigenetic aspects need to be considered as they are crucial regulators in the translation of environment stimuli on gene expression regulation. “Classic” epigenetic mechanisms include dysregulation of known imprinted genes (also called “genomic imprinting”) and epigenetic mosaicism, a widespread phenomenon documented in many organisms, that may account for differences in body weight and fat accumulation (Stöger 2008, Loh et al. 2019, Allum and Grundberg 2020). In recent years, the role of RNA is changed and its relevance in the regulation of biologic processes is now reconsidered since up to 90% of the genome is transcribed and not translated into a protein. Among the epigenetic modulators there are also long non-coding RNAs (lncRNAs). These transcripts are poorly conserved, frequently unstable, and/or sometimes present in few copies, and new biological roles have emerged for some lncRNAs. The non-coding transcriptome is becoming more and more relevant also in the field of adipogenesis, fat mass expansion and obesity and in this context lncRNAs are emerging as new potential candidate targets for therapeutic development as well as comorbidities regulators (Salem et al. 2019, Landrier, Derghal, and Mounien 2019, Arcinas et al. 2019).

1.2. LncRNAs in obesity and metabolic diseases

As both obesity and other metabolic diseases cannot be clearly defined by genetics or the environment, new players are coming into question when considering possible pathogenic mechanisms. In this framework, the role of the epigenome, with a specific focus on lncRNAs, could prove of fundamental importance.

1.2.1. LncRNAs: definition and principal functions

It is now established knowledge that only 1-2% of the human genome codes for proteins (Mattick 2009, Ponting, Oliver, and Reik 2009, Consortium 2012). For this reason, RNAs can be classified for their coding potential in coding RNAs (transcripts that will subsequently be translated into proteins) and non-coding RNAs (ncRNAs), that do not code for a polypeptide and whose function is still to be fully understood especially in modulating gene expression (Mattick 2009, Ponting, Oliver, and Reik 2009, Consortium 2012). The non-coding part of the genome (ranging from 70 up to 90% of the total RNAs) was initially classified as “junk DNA”, but it is now clear that this definition could not be farther from the true, as the non-coding transcriptome has gained a significant relevance in both health and disease (Maass, Luft, and Bähring 2014, Ponting, Oliver, and Reik 2009, Wang and Chang 2011, Nagano and Fraser 2011, Wu et al. 2013, Batista and Chang 2013, Lekka and Hall 2018). Amongst the ncRNAs, it is possible to distinguish two subclasses: small ncRNAs, molecules smaller than 200bp, and lncRNAs, defined as ncRNA molecules longer than 200bp. Small ncRNAs include: small nuclear RNAs (snRNAs), small nucleolar RNAs (snoRNAs), microRNAs (miRNAs), and piwi-interacting RNAs. LncRNAs include rRNA (ribosomal RNA), long intergenic ncRNAs (lincRNAs) and Natural Antisense Transcripts (NATs) (St Laurent, Wahlestedt, and Kapranov 2015). LncRNAs can also arise from other DNA sequences such as introns, or regulatory elements such as enhancers (St Laurent, Wahlestedt, and Kapranov 2015). Finally, some of them are transcribed from intergenic regions that do not overlap any other known coding gene having their own promoters (St Laurent, Wahlestedt, and Kapranov 2015). Most of them are

RNA polymerase II transcribed so they are similar in structure to protein coding transcripts, possibly presenting cap structures and poly A tails (Zhang, Wang, et al. 2019). After their synthesis, biogenesis and processing, lncRNAs can localize both in the cytoplasm and in the nucleus, depending on their subsequent function (Zhang, Wang, et al. 2019).

LncRNAs can mediate transcriptional regulation in different ways. Indeed these molecules can modulate gene expression at multiple levels, ranging from chromatin re-arrangements, through transcriptional regulation or even translational modulation (Yao, Wang, and Chen 2019). Multiple evidence suggests that they can operate through distinct modes, including working as signals, scaffolds for protein-protein interactions, molecular decoys, and guides to target elements in the genome or transcriptome (Wang and Chang 2011). A primary gene expression regulation takes place in the nucleus, where they can influence chromatin remodeling and interfere with gene transcription (Vance and Ponting 2014). To this end lncRNAs act close to their sites of synthesis regulating the expression of nearby genes on the same chromosome, or target protein coding genes located on different or homologues chromosomes (Vance and Ponting 2014). At this level, lncRNAs act associating with chromatin in multiple ways. Indeed, single-stranded lncRNAs directly interact with complementary double-stranded DNA target sequences through hydrogen bonding to form a RNA-DNA-DNA triplex structure, thus being indirectly recruited to the genome through RNA-Protein-DNA interaction or matching with RNA sequences at their transcribed loci (Vance and Ponting 2014). Consequently, chromatin conformation changes are required to bring two distantly located loci into close spatial proximity and allow lncRNAs' gene regulation.

In the cytosol, lncRNAs influence gene expression through transcriptional regulation. They can interact with miRNAs binding sites acting as molecular decoys or sponges that sequester miRNAs away from other transcripts creating a network that exerts post-transcriptional regulation of gene expression (Zampetaki, Albrecht, and Steinhofel 2018). LncRNAs are also able to inhibit or promote gene expression at a translational level. They are also involved in various post-translational protein modifications such as phosphorylation, ubiquitination and acetylation, thereby regulating protein degradation or formation (Zhang, Wang, et al. 2019). It has been discovered that some cytoplasmic lncRNAs contain smaller open reading frames than the typical cutoff of at least 100 amino acids in eukaryotes, and these encode for micropeptides that have been shown to perform vital biological function such as cell division, transcription regulation and cell signaling (Hartford and Lal 2020). This high degree of complexity in gene expression regulation, and the number of still unknown mechanisms through which lncRNAs could act, indicates a clear need to further investigate these molecules, both in health and disease, as they could provide crucial new insights in cell biology representing promising targets for the development of innovative therapeutic strategies for multiple diseases.

1.2.2. LncRNAs in adipogenesis

The non-coding epigenome is known to play a regulatory role in many developmental contexts, including adipogenesis. In addition to miRNAs, numerous lncRNAs have been demonstrated to be involved in adipogenesis with subsequent implications for obesity and obesity-related complications in adults (Wei et al. 2016) and children (Liu, Ji, et al. 2018). As more and more studies in this field arise every year, there is a need to distinguish between the multiple functions

that the lncRNAs could have. Indeed, results are variable, and a full characterization of the role that lncRNAs play in obesity is far from being present. Numerous lncRNAs have been correlated with adipogenesis, showing a change in their expression levels at different stages of adipocytes differentiation, but a clear mechanism of action is lacking. In other cases, they have been found to regulate key players in adipogenesis (e.g. PPAR γ), associate with adipogenesis-implicated miRNAs and even be significantly deregulated in patients with obesity or murine models of obesity (Chen, Cui, et al. 2015, Sun et al. 2013).

1.2.2.1. Role of lncRNAs in the regulation of early adipogenesis master regulators

Adipogenesis is the process of adipocytes formation into fat-containing cells from stem cells or adipocyte precursors. It involves 2 phases: determination (considered an early stage) and terminal differentiation (late adipogenesis). It is a complex process finely tuned at multiple levels by specific transcription factors (TFs) and protein regulators. Although the transcriptional cascade leading to intracellular lipid uptake (adipogenic differentiation) is well characterized, much remains to be discovered on the implications of lncRNAs on the multiple levels at which this cascade can be regulated.

Early stages of adipogenesis are represented by a Mitotic Clonal Expansion phase (MCE) and by the expression of early regulators such as CCAAT-enhancer-binding proteins (C/EBP) C/EBP β and C/EBP δ (Rosen and MacDougald 2006, Rosen, Eguchi, and Xu 2009, Tang, Otto, and Lane 2003). Amongst the lncRNAs able to influence this stage of adipogenesis, the lncRNA Steroid Receptor RNA Activator (SRA) was one of the first to be described (Xu et al. 2010). Its expression resulted 2-folds higher in differentiated murine 3T3-L1 adipocytes than pre-adipocytes, but the lncRNA seems to also act in early phases of adipogenesis (Sheng et al. 2018). Indeed, it can promote S-phase entry during the MCE phase of adipogenesis controlling cell cycle genes expression (e.g. decreasing the expression of the cyclin-dependent kinase inhibitors cyclin-dependent kinase inhibitor 1 and Cyclin-dependent kinase inhibitor 1B, and increasing phosphorylation of Cyclin-dependent kinase 1) (Xu et al. 2010). Moreover, in the mouse ST2 mesenchymal cell line, SRA is implicated in the regulation of p38 mitogen-activated protein kinase/c-Jun N-terminal kinases phosphorylation inhibition, a crucial step in the early stages of adipogenesis, as well as in stimulating insulin receptor gene expression and downstream signaling (Liu, Xu, et al. 2014, Bost et al. 2005). The Obesity Related lncRNA, whose expression levels increases during adipogenesis, regulates the cell cycle through induction of expression of crucial marker genes such as Proliferating Cell Nuclear Antigen, cyclin B, cyclin D1 and cyclin E, allowing cells entry into the S phase during the MCE (Cai et al. 2019). Modulation of the cell cycle and thus early stages of adipogenesis can also occur through epigenetic modulation, and indeed the lncRNA slincRAD can interact with the DNA Methyl Transferase 1 in the S phase of the cell cycle, guiding it to the promoter of cell cycle-related genes, facilitating the cells entry into the clonal expansion stage of differentiation (Yi et al. 2019).

Through microarray study, a novel lncRNA, lncRNA-Adi, has been identified and found to be highly expressed in the MCE phase. It exerts its effects through the interaction with miR-449a, enhancing the expression of the miRNA target Cyclin-dependent kinase 6. This leads to an

increase in Cyclin-dependent kinase 6 translation and subsequent activation of the retinoblastoma protein - TF E2F1 pathway, involved in early adipogenesis (Chen et al. 2020).

The genetic location of lncRNAs could be of crucial relevance in identifying their target genes. Three recently discovered lncRNAs, Gm15051, Tmem189, and Cebpd genomically locate respectively next to Hoxa1, C/EBP β and C/EBP δ and their expression levels correlate, suggesting that each of them can positively influence the neighboring gene expression having the role of transcriptional regulators (You et al. 2015).

1.2.2.2. Role of lncRNAs in the regulation of late adipogenesis master regulators

As pre-adipocytes mature into adipocytes, C/EBP β and δ target the promoters of C/EBP α and PPAR γ , master regulators of adipocytes terminal differentiation as they activate genes that are involved in insulin sensitivity, lipogenesis and lipolysis. Examples include genes encoding glucose transporter type 4 (GLUT4), fatty-acid-binding protein (FABP4), lipoprotein lipase, sn-1-acylglycerol-3-phosphate acyltransferase 2, perilipin (PLIN) and the well-known secreted adipokines, adiponectin (ADIPOQ) and LEP (Rosen and MacDougald 2006, Rosen, Eguchi, and Xu 2009, Ghaben and Scherer 2019).

This step is critical for late adipocytes differentiation, and indeed numerous lncRNAs have been found to modulate specifically PPAR γ (Figure 4). SRA also plays a role in this context, as it exerts its function via direct association with the PPAR γ protein, promoting its transcriptional activity (Sheng et al. 2018, Xu et al. 2010). Another mode of action through which lncRNAs can modulate PPAR γ is through miRNAs sponging. This is the case of lncRNA IMFNCR (intramuscular fat-associated lncRNA), which has been found to promote intramuscular adipocyte differentiation sponging miR-128-3p and miR-27b-3p, which directly target PPAR γ (Zhang, Li, et al. 2019). There can also be an indirect lncRNAs-miRNAs modulation of PPAR γ , through other epigenetic modulators. The adipocyte differentiation-associated lncRNA (ADNCR) can sponge miR-204, whose target gene, Sirtuin 1 (SIRT1), is known to form a complex with modulators such as nuclear receptor co-repressor 1 (NCoR) and silencing mediator for retinoid or thyroid-hormone receptors (SMRT) to repress PPAR γ activity (Li et al. 2016). An epigenetic modulation can happen at PPAR γ 's promoter, in sites known as CpG islands that when methylated decrease the expression of the respective downstream genes. Indeed, the lncRNA Plnc1, transcribed 25 000 bp upstream of PPAR γ 2, can attenuate the methylation status of its promoter increasing subsequent transcription (Zhu et al. 2019). PPAR γ can also be targeted at the end of specific signal-transduction pathways, as demonstrated for Signal Transducer and Activator of Transcription 3 (STAT3) gene expression regulation (Wang et al. 2009). Specifically, adipogenesis is induced by the activation of STAT3, acting as a molecular switch. This effect was counteracted by PPAR γ 's activation with the agonist troglitazone, suggesting that STAT3 can modulated adipogenic differentiation through a PPAR γ upstream regulation (Wang et al. 2009). The nuclear lncRNA Plasmacytoma Variant Translocation 1 (PVT1) has been found to associate with STAT3, and indeed PVT1 has been found to correlate with increased expression of PPAR γ , but also C/EBP α , FABP4, and genes related to fatty acid synthesis (Zhang et al. 2020). Well renowned lncRNAs, such as Nuclear Enriched Abundant Transcript 1 (NEAT1), widely implicated in numerous cancers, can also have a function in adipogenesis, and indeed NEAT1 has been found to modulate the splicing

of PPAR γ , increasing the expression of the isoform 2 through Serine And Arginine Rich Splicing Factor 5 association (Cooper et al. 2014).

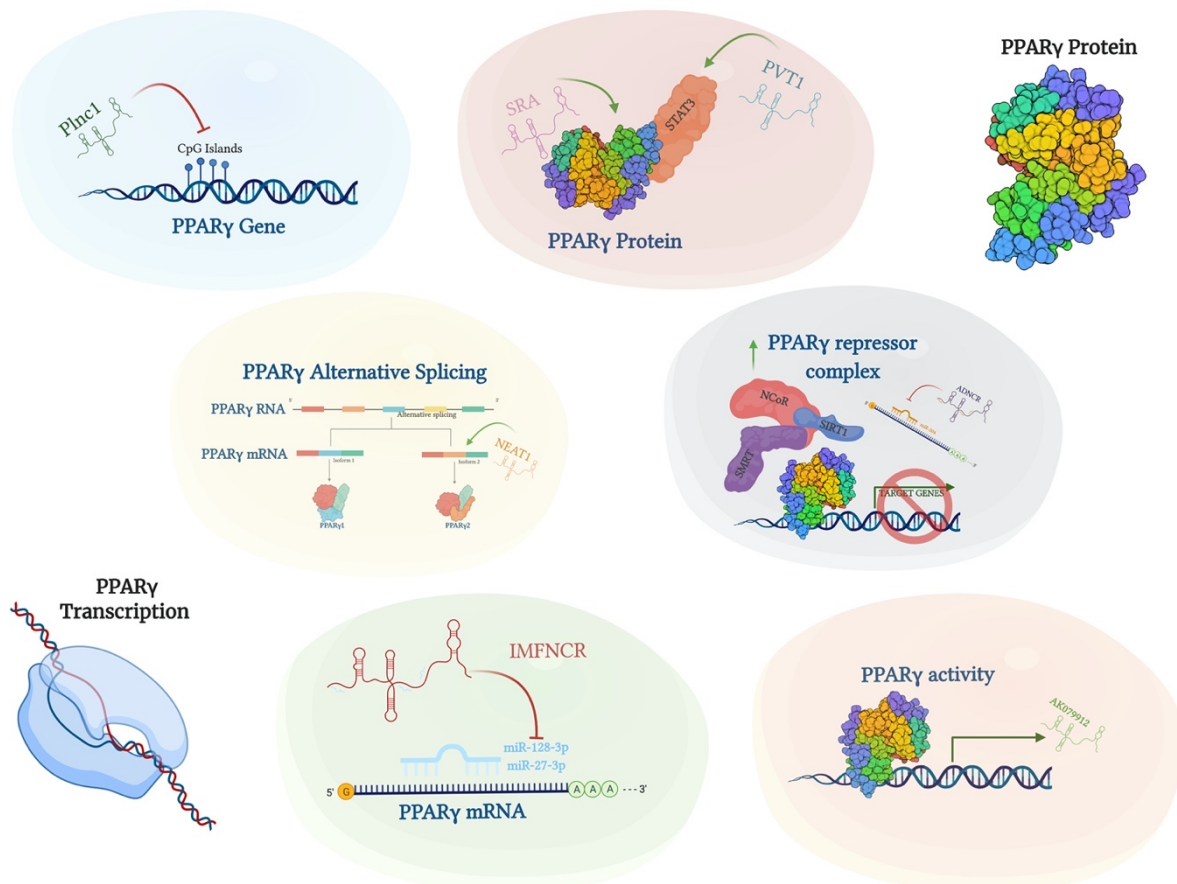


Figure 4: LncRNAs can influence PPAR γ transcription and activity at multiple levels. Specifically, lncRNAs can modulate directly PPAR γ by inhibiting DNA methylation. They can also selectively induce a different PPAR γ mRNA splicing or sponge specific miRNAs which would sequester and lead to degradation of PPAR γ mRNA. They directly bind to the PPAR γ protein being able to inhibit its activity through upregulation of the PPAR γ repressor complex. Lastly, PPAR γ itself can induce the expression of specific lncRNAs. Created with biorender.com.

PPAR γ itself can regulate lncRNAs expression, such as AK079912, a lncRNA correlated to browning of white adipocytes, which presents three conserved PPAR γ binding sites in its promoter region (Xiong et al. 2018). Other adipogenic genes can also induce lncRNAs expression, such as lnc-BATE's induction by C/EBP α , C/EBP β and again, PPAR γ . In this case, lnc-BATE is a specific regulator of brown adipogenesis through interaction with hnRNP-U (Alvarez-Dominguez et al. 2015).

Modulation of late adipogenesis can occur through modulation of other key genes, as demonstrated for the knockdown of the lncRNA HOXA11 Antisense RNA resulting in the inhibition of adipocytes differentiation through a decrease of C/EBP α , diacylglycerolacyltransferase 2, cell death-inducing DFF45-like effector and PLIN, ultimately leading to the decreased lipid accumulation (Nuermaiti et al. 2018). On the other hand, the Tissue differentiation-Inducing Non-protein Coding RNA can form a feedback loop with miR-31 and C/EBP α , leading to the upregulation of miR-31's downstream target C/EBP α , thus promoting adipogenesis (Liu, Wang, et al. 2018). Also in this case, lncRNAs can bind to epigenetic regulators to promote adipogenesis through an upregulation of mature adipocytes-

related genes, as does miR-31 host gene, which is able to promote the binding of H3K4me3 to FABP4's promoter, increasing its expression (Huang et al. 2017). Similarly, the adipogenic differentiation induced ncRNA can recruit Mixed-Lineage Leukemia protein 3/4 histone methyl-transferase complexes increasing H3K4me3 and decreasing H3K27me3 histone modification in the C/EBP α locus during adipogenesis, leading to an increase in its expression (Xiao et al. 2015).

A specific subclass of lncRNAs, defined as NATs, can modulate the expression of their respective sense gene altering processes in which they are involved. For example, PU.1AS can form a RNA-duplex with PU1, a molecule that inhibits adipogenesis, hindering its expression and subsequent protein expression. This indicates that PU.1AS promotes adipogenesis, and indeed its knockdown results in decreased expression of adipogenic modulators such as PPAR γ , fatty acid synthase and ADIPOQ (Pang et al. 2013, Wei et al. 2015). Similarly, ADIPOQ antisense RNA (AdipoQ AS) can modulate ADIPOQ expression. Indeed, during adipogenesis, AdipoQ AS can shuttle from the nucleus to the cytoplasm and form a duplex with adiponectin's mRNA, ultimately suppressing adiponectin's translation and inhibiting adipogenesis (Cai et al. 2018). Although not its NAT, lnc-leptin is directly correlated with LEP, as it is transcribed from an enhancer region upstream of LEP and their expression directly correlates. Lnc-leptin transcript seems to act as a bridge to enhance the interaction between the Lep promoter and enhancer, although specific mechanistic details are yet to be clarified (Lo et al. 2018).

The lncRNAs correlation with adipogenesis can also be negative, as some lncRNAs have been found to be decreased in adipogenesis. For example, overexpression of lnc-U90926 can inhibit lipid accumulation when overexpressed, whereas its inhibition leads to the increased expression of PPAR γ 2, FABP4, C/EBP α and ADIPOQ in murine 3T3-L1 pre-adipocytes (Chen, Liu, et al. 2017). This is the case for other lncRNAs, such as miR-221 host gene and lncRNA H19, whose inhibition increases adipocyte differentiation through an increase in the expression of adipogenic markers such as PPAR γ , FABP4 and C/EBP α respectively in bovine adipocytes and in human Bone Marrow Mesenchymal Stem Cells (Li et al. 2019, Huang et al. 2016).

As the function of most lncRNAs in adipogenesis is still being investigated, it is not surprising that some evidence might be controversial and that further studies might be needed to clarify specific lncRNAs functions in this process. This is the case of Maternally Expressed Gene 3 (Meg3), a novel lncRNA which has been defined as both able to inhibit or promote adipogenesis (Li et al. 2017, Huang et al. 2019). Indeed, a first study reported that silencing of Meg3 promoted adipogenesis through the overexpression of the adipogenesis-related miR-140-5p, as well as crucial adipogenesis master regulators such as PPAR γ and C/EBP α , suggesting that when Meg3 is absent, adipogenesis is induced (Li et al. 2017). On the contrary, a second work described Meg3's role in upregulating Dickkopf-3 through interaction with miR-217, ultimately leading to an upregulation of adipogenesis via the induction of expression of adipogenesis-related genes such as FABP4 (Huang et al. 2019). This might be due to a time-specific effect of the lncRNA's action, or the different cellular context (the first study was performed in human cells whereas the second in murine 3T3-L1 preadipocytes) and further studies will be needed to clarify Meg3's mechanism of action. The Wnt/ β -catenin signaling is also influenced by a novel nuclear lncRNA, AC092834.1. This lncRNA directly promoted an

increase in the expression of Dickkopf-1, which competitively binds to Low-density lipoprotein receptor-related protein 5 to degrade cytosolic β -catenin, ultimately leading to upregulation of adipogenic transcripts such as PPAR γ , FAPB4 and C/EBP α (Fan et al. 2020).

1.2.3. LncRNAs in obesity

Specific studies correlate lncRNAs with the obese phenotype and obesogenic models. Amongst them, SRA has been demonstrated to be strictly associated with obesity, as it has been shown that SRA $-/-$ mice have a phenotype of resistance to high-fat diet induced obesity with decreased fat mass and an increased lean mass, a decreased expression of a subset of adipocyte marker genes in adipose tissues, reduced fatty liver and improved glucose tolerance (Liu, Sheng, et al. 2014).

High-throughput techniques such as RNA-sequencing (RNA-seq) allowed the screening of the whole transcriptome in adipose tissue of patients with obesity versus lean ones, leading to the identification of novel lncRNAs involved in the disease. In one study, two lncRNAs termed adipocyte-specific metabolic related lncRNAs -1 and -2 were identified and found to regulate adipogenesis, lipid mobilization and ADIPOQ secretion (Gao et al. 2018). Another screening was performed in gluteal subcutaneous adipose tissue (SAT) on healthy subjects, identifying 120 adipose-derived lncRNAs (Zhang et al. 2018). Moreover, Lui Y et al, aiming to evaluate whether lncRNAs are involved also in childhood obesity, investigated the differential expression profile of lncRNAs in children with obesity compared with those that do not present the condition (Liu, Ji, et al. 2018). They identified 1268 differentially expressed lncRNAs involved in various biological processes, including the inflammatory response, lipid metabolic process, osteoclast differentiation and fatty acid metabolism. In particular, they indicated that lncRNA RP11-20G13.3, hub lncRNA in children with obesity, attenuated adipogenesis of preadipocytes (Liu, Ji, et al. 2018).

The same has been done in mice, where brown and white adipocytes, preadipocytes, and cultured adipocytes were screened leading to the identification of 175 different lncRNAs that are specifically regulated during adipogenesis (Sun et al. 2013). Similarly, inguinal white adipose tissue has been screened in obese mice compared to wild type ones, identifying 46 differentially expressed lncRNAs (Cai et al. 2019). Moreover, lncRNAs such as PVT1 and Plnc1 were found to be upregulated in obese mice (Zhang et al. 2020, Zhu et al. 2019).

From an anatomical point of view, lncRNAs expression can differ in different fat depots, as it is for HOX transcript antisense RNA (HOTAIR) which has been demonstrated to be highly expressed in gluteal-femoral fat. Interestingly the mechanical stimulation of this area induces exosomal secretion of HOTAIR, which then circulates in the bloodstream resulting in higher serum expression in subjects with obesity and a sedentary lifestyle (Lu et al. 2017). Again, gene expression screening can help find differences also in different adipose depots, as shown by another study reporting differences in the lncRNAs expression profiles of brown versus white adipose tissue, identifying respectively 735 up-regulated and 877 down-regulated lncRNAs (Chen, Cui, et al. 2015). Indeed, the differential lncRNAs regulation in brown adipose tissue was also proven by lnc-Blnc1 induction of thermogenic gene expression through the interaction with EBF TF 2, a TF that controls brown and beige adipocyte morphology (Mi et al. 2017). Lastly, a recent work screened the lncRNAs expression in rat livers with hypertriglyceridemia

and identified the upregulation of a novel lncRNA: lnc19959.2. The knockdown of lnc19959.2 resulted in triglycerides lowering effects in vitro and in vivo both and mechanistic studies revealed that lnc19959.2 upregulated Apolipoprotein A4 expression via ubiquitinated transcription inhibitor factor Transcriptional activator protein Pur-beta, while its specific interaction with Heterogeneous Nuclear Ribonucleoprotein A2/B1 was able to down-regulate the expression of Carnitine Palmitoyltransferase 1A, Transmembrane 7 Superfamily Member 2, and Glycerol-3-Phosphate Acyltransferase, Mitochondrial (Wang et al. 2020).

1.2.4. LncRNAs in T2D

At all ages, the risk of T2D rises with increasing body fat. The prevalence of T2D is three to seven times higher in those who are affected by obesity than in normal weight (NW) adults. It is also 20 times more likely in those with a BMI greater than 35 kg/m². Specifically, T2D is an adult onset, non- insulin-dependent type of diabetes and is strictly linked to obesity (Raut and Khullar 2018). In recent years, an increased incidence of T2D among youth is also reported, with obesity and family history of T2D generally present (Pulgaron and Delamater 2014). Also, in this case, lncRNAs could be crucial players in disease onset and progression.

Indeed, lncRNAs can be both up- and down-regulated during disease progression in different cell types (Figure 5). Expression profiles of lncRNAs in Peripheral Blood Mononuclear Cells (PBMCs) from patients with T2D highlighted how several lncRNAs were significantly increased compared to controls, and these included HOTAIR, MEG3, LET, MALAT1, MIAT, CDKN2BAS1/ANRIL, XIST, PANDA, GAS5, Linc-p21, ENST00000550337.1, PLUTO, and NBR2 (Sathishkumar et al. 2018). The lncRNAs ANRIL and MALAT1 were found increased in the serum of patients with T2D (Zhang and Wang 2019, Liu et al. 2019), and the same was true for NONRATT021972, which also correlated with increased blood glucose and neuropathic pain (Yu et al. 2017). Interestingly, lncRNA-p3134 is highly expressed in serum exosomes of patients with T2D as studies found that it is secreted by islet β -cells (Ruan et al. 2018). Moreover, the lncRNA H19 was found upregulated in plasma of patients with T2D (Fawzy et al. 2020) and the lncRNA KCNQ1OT1 was upregulated in T2D islets (Morán et al. 2012). Evidence can also be obtained from murine models of the disease, as is the case of E330013P06, which was found upregulated firstly in macrophages of diet-induced insulin-resistant T2D mice and subsequently also found upregulated in monocytes from patients with T2D (Reddy et al. 2014).

Interestingly, many lncRNAs have also been reported to be downregulated in patients with T2D. When considering PBMCs screening studies, results showed that multiple lncRNAs were found downregulated. These include LINC00523, LINC00994 (Mansoori et al. 2018), LY86-AS1, HCG27_201 (Saeidi et al. 2018), THRIL and SALRNA1 (Sathishkumar et al. 2018). Moreover, studies showed that levels of GAS5 lncRNA were decreased both in serum and in plasma of patients with T2D (Carter et al. 2015, Fawzy et al. 2020). Lastly, the lncRNA HILNC45 was found downregulated in T2D islets (Morán et al. 2012).

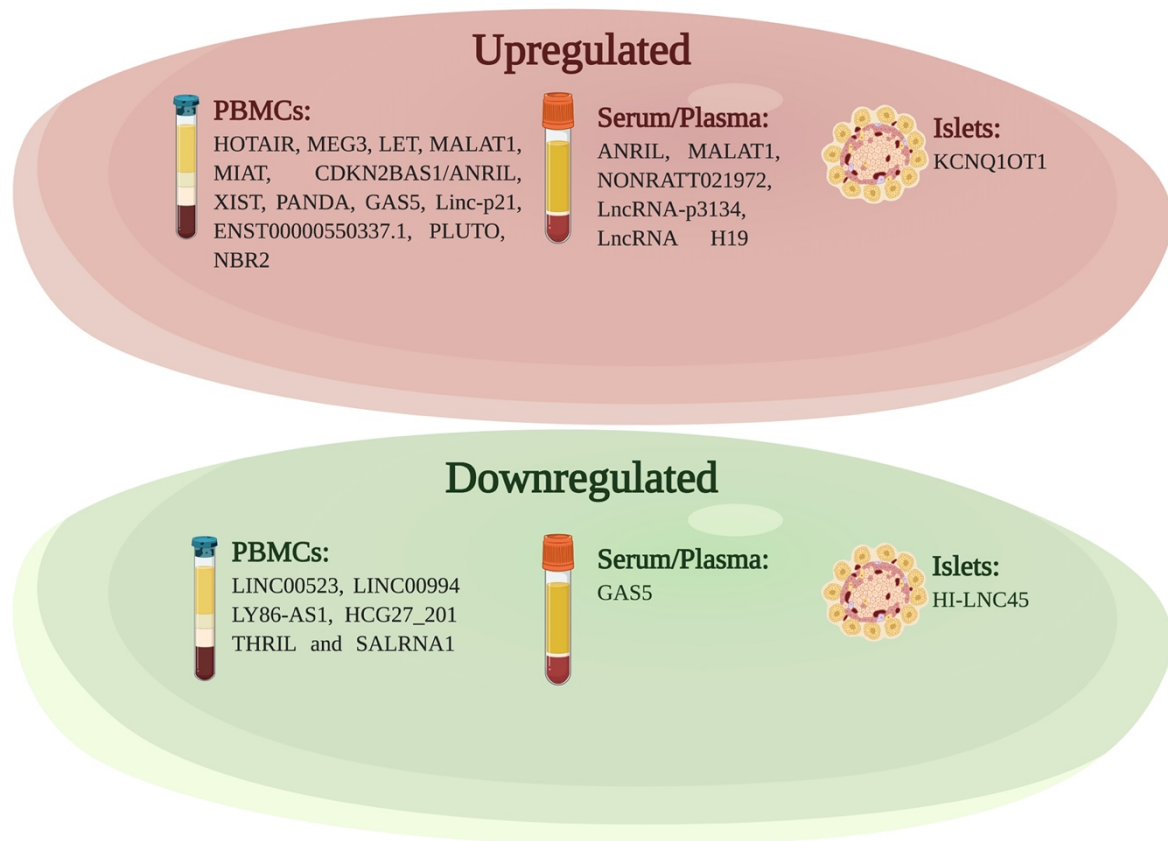


Figure 5: Summary of lncRNAs upregulated or downregulated in specific tissues of T2D patients. Created with biorender.com.

Indeed, lncRNAs can modulate the cellular activity of pancreatic β cells. LncRNA-p3134 seems to act as a new signaling molecule that maintains β -cell mass and enhances insulin synthesis and secretion and indeed it has been seen that lncRNA-p3134 can contribute to reverse the insufficient insulin secretion in T2D (Ruan et al. 2018). Moreover, the lncRNA β -cell long intergenic noncoding RNA (β linc1) can coordinate the regulation of neighboring islet-specific TFs and it is in fact necessary for the specification and function of insulin-producing β cells. In particular, in adult mice it has been shown that deletion of β linc1 leads to a defective islet development and disruption of glucose homeostasis (Arnes et al. 2016). In pediatric age, Liu Y et al. reported that several lncRNAs involved in regulation of glucose metabolic process and insulin resistance, such as RP11-559N14.5, RP11-363E7.4, RP11-707P17.1, were significantly up or down regulated in children with obesity compared to controls, even in the absence of diabetes (Liu, Ji, et al. 2018). Considering that hyperglycemia and T2D develop when the pancreas cannot match the increased insulin demands resulting from insulin resistance, lncRNAs could play a crucial role in the onset of the disease.

2. Aim of the Study

Obesity is defined as abnormal or excessive fat accumulation, presenting a risk to health. The most recent report of the WHO shows how the worldwide prevalence of obesity nearly tripled between 1975 and 2016, with over 650 million adults being clinically defined as obese. This trend is due to increase even more, as in 2018 more than 40 million children under the age of 5 years were overweight and obese, with studies showing that 70% of obese adolescents will maintain their obese condition as adults, with a significant impact on their physical and physiological health. Based on these data and multiple epidemiological evidence linking obesity with a range of physical and psychosocial health conditions, it is possible to describe obesity as a public health crisis that severely impairs the health and quality of life of people and furthermore considerably adds to national health-care budgets. Indeed, obesity contributes to increased morbidity and mortality as it is associated to many chronic diseases such as T2D, hypertension, dyslipidemia, coronary artery disease, stroke, osteoarthritis and certain forms of cancer.

The first aim of this research work is the identification of transcriptional differences present in SAT from normal weight, obese and diabetic subjects. Indeed, the identification of deregulated transcripts could lead to the investigation of new disease-changing mechanisms and possible targetable pathways. Moreover, the analysis of the transcriptional differences highlighted in diabetic obese versus obese subjects could highlight which targets are responsible for the development of the diabetic co-morbidity. Through numerous bioinformatics tools and database analyses, the deregulated targets will be investigated for their possible function, ontology, and disease implication.

The second aim of this work is the identification and characterization of ncRNAs deregulated in SAT from NW, obese and diabetic subjects. The identified lncRNAs will be characterized with bioinformatic tools, and their specific role in adipogenesis will be assessed in vitro.

3. Materials and Methods

3.1. Adult human adipose tissue collection, isolation and differentiation

The present study is in accordance with the Declaration of Helsinki and it was approved by the Ethical Committee of IRCCS Istituto Auxologico Italiano (Ethical Committee approval code #19C723_2017). The study was conducted in collaboration with Dr. Raffaella Canello from IRCCS Istituto Auxologico Italiano and Prof Simona Bertoli from IRCCS Istituto Auxologico Italiano and University of Milan. A signed informed consent was obtained from each enrolled patient for tissue sampling. Biopsies of SAT were collected from a total of 15 subjects: 5 healthy NW females (age 37 ± 6.7 years, BMI 24.3 ± 0.9 kg/m²), 5 obese females (age 41 ± 12.5 years, BMI 38.2 ± 4.6 kg/m²), and 5 obese females with T2D (age 54.6 ± 14.9 years, BMI 38.1 ± 11.8 kg/m²).

Surgical biopsies of whole abdominal SAT were collected pre-operatively from obese female patients during bariatric surgery procedures and from NW women before aesthetic plastic surgery or abdominal surgery for non-inflammatory diseases. Each collected biopsy was weighed and stored in 1 ml of DMEM (Invitrogen Corporation, Jefferson City, MO) supplemented with 2.5% Bovine Serum Albumin (Sigma, St. Louis, MO) per gram of collected tissue. The biopsy was immediately transferred to the laboratory and processed. A fragment of the whole adipose tissue biopsy was immediately frozen in liquid nitrogen for RNA extraction (see below), another fragment was formalin-fixed and the remaining material was digested with 1 mg/ml collagenase type 2 (Sigma, St. Louis, MO) for at least 1 h at 37°C under shaking. The digested tissue was then filtered through a sterile gauze and a nylon filter (BD Bioscience 1 Becton Drive Franklin Lakes, NJ). The SVF cells were isolated by centrifugation and then treated with a buffer containing 154 mM NH₄Cl, 10 mM KHCO₃, and 0.1 mM EDTA for lysis of red blood cells. Stroma-Vascular Fraction cells were plated and cultured in a medium containing a 1:1 mixture of Ham's F12/DMEM (Invitrogen Corporation, Jefferson City, MO) supplemented with 10% Fetal Bovine Serum (FBS, Sigma, St. Louis, MO) until confluence. At confluence, cells were differentiated into mature adipocytes using AdipoStemPro (Invitrogen) for 10 days. Intracellular triglyceride accumulation levels were assessed by AdipoRed staining, according to the manufacturer protocol (Lonza, Milan, Italy).

3.2. SAT RNA extraction

Approximately 500 mg of frozen SAT was homogenized in RLT buffer (Qiagen). RNA from SAT was extracted using the RNeasy Mini Kit (Qiagen) according to the manufacturer protocol and samples were then treated with the RNase-Free DNase Set (Qiagen). Concentration and quality of the extracted RNA were determined by the NanoDropH ND-1000 spectrophotometer (NanoDrop Technologies, USA) and RNA integrity verified by gel-electrophoresis. PLIN, FABP4, LEP and ADIPOQ gene expression levels were assessed starting from 10 ng of complementary DNA (cDNA) using TaqMan probes (assay on demand, Applied Biosystems).

3.3. RNA-Seq and bioinformatic data analysis

3.3.1. Library preparation

RNA-seq libraries were prepared with the CORALL Total RNA-Seq Library Prep Kit (Lexogen) using 150 ng total RNAs from 5 healthy females, 5 obese females and 5 obese females with T2D. The RiboCop rRNA Depletion Kit (Lexogen) was used to remove rRNA, as this makes up more than 80% of total cellular RNA, and as it was not the research focus its presence could greatly reduce the useful transcript coverage in the following sequencing step. Briefly, a double-stranded cDNA library was prepared via random priming and reverse transcription. After purification of the generated fragmented cDNA, sequencing adapters were ligated to both ends of the fragments and the library were amplified via Polymerase Chain Reaction (PCR). The quality of sequencing libraries were assessed with the D1000 ScreenTape Assay using the 4200 TapeStation System (Agilent) and quantified with Qubit™ dsDNA HS Assay Kit (Invitrogen).

3.3.2. Library sequencing

Libraries were sequenced in paired-end with the Illumina NextSeq 550 sequencer. The sequencing step relies on the NGS technologies which relies on an in vitro cloning step (clonal amplification) to amplify each fragmented cDNA molecule in a cell-free system. The Illumina Genome Analyzer performs a so-called bridge PCR amplification, in which the adapter linked, single-stranded cDNA fragments are first immobilized on a glass slide by oligonucleotide hybridization in a bridging way, followed by clonal PCR amplification. Clonal amplification resulted in a population of identical templates, each of which was subjected to the following sequencing reaction. This process generated raw reads representing the sequence of each fragment. The more a transcript is abundant, the more reads it will generate.

3.3.3. Differential expression analysis

The raw reads were used as starting material of the computational biology analysis. Raw data were examined for high quality scores for base calls, guanine-cytosine content matching the expected distribution, the over representation of particularly short sequence motifs, and an unexpectedly high read duplication rate (Conesa et al. 2016). Transcripts were then aligned to the human reference genome. Reads that align equally well to multiple locations must be identified and either removed, aligned to one of the possible locations, or aligned to the most probable location. FastQ files were generated via Illumina bcl2fastq2 (Version 2.17.1.14 - <https://support.illumina.com/downloads/bcl2fastq-conversion-software-v2-20.html>) starting from raw sequencing reads produced by Illumina NextSeq sequencer. Quality of individual sequences were evaluated using FastQC software after adapter trimming with cutadapt software. Lastly, short reads generated by RNA-seq were aligned to the reference genome. To do that, gene and transcript intensities were computed using STAR/RSEM software using Gencode Release 27 (GRCh38) as a reference, using the “strandness forward” option. The STAR software package enables highly accurate and ultra-fast alignment of RNA-seq reads to a reference genome. STAR can align spliced sequences of any length with moderate error rates providing scalability for emerging sequencing technologies. STAR generates output files that can be used for many downstream analyses such as transcript/gene expression quantification,

differential gene expression, novel isoform reconstruction, signal visualization, and so forth (Dobin and Gingeras 2016). Transcript abundance was obtained using the BlueBee® Genomics Platform (Lexogen).

In this work, differential expression analysis was performed using the R package DESeq2, selected because of its superior performance in identifying isoforms differential expression. Genes were analyzed according to Fold Change (FC), i.e the ratio of a gene expression between conditions, and to False Discovery Rate (FDR), that measures the proportion of false discoveries among a set of hypothesis tests called significant (Chen, Robinson, and Storey 2019). The FDR is often employed to determine significance thresholds and quantify the overall error rate when testing a large number of hypotheses simultaneously (Chen, Robinson, and Storey 2019). In particular, genes showing $|\log_2FC| \geq 1$ and an $FDR \leq 0.1$ were considered as differentially expressed. This choice was motivated by the decision to maximize the sensitivity of this analysis, in order to perform a massive screening and identify candidate genes to be validated with a wider sample population with real-time analysis.

3.3.4. Pathways analysis

Gene enrichment analysis was performed on coding genes. Kyoto Encyclopedia of Genes and Genomes (KEGG) pathway analysis (<http://www.genome.ad.jp/kegg>) and WikiPathways analysis (<https://www.wikipathways.org/index.php/WikiPathways>) of differentially expressed coding genes via enrichR web tool was performed. Moreover, Gene Ontology (GO) analysis for biological processes, cellular components and molecular function was executed.

3.3.5. Visualization of RNA-Seq results with R software

3.3.5.1. Heatmap

Heatmap was obtained using the *heatmap.2* function from the R *ggplots* package. The data was displayed in a grid where each row represents a gene and each column represents a sample. The color and intensity of the boxes was used to represent changes (not the absolute values) of gene expression.

3.3.5.2. Principal Component Analysis (PCA) plot

The PCA plot was obtained using the *prcomp* function from the R *ggplots* package. It allowed the identification of groups of samples that were similar and identify which variables make one group different from another.

3.3.5.3. Volcano plot

Volcano plot is a type of scatterplot that shows statistical significance (P value) versus magnitude of change (FC). In this work the volcano plot was obtained through the R *EnhancedVolcano* package, omitting genes with counts <20.

3.3.5.4. Dotplot

The enriched pathways were displayed with the dot plot graph. In this work the dot plot was obtained using *ggplot* R package. Specifically, the y axis represents the name of the pathways whereas the x axis indicates the Gene Ratio or Rich factor, meaning the ratio of differentially expressed gene numbers annotated in that particular pathway term to all genes annotated in that

particular pathway term. The greater the Rich factor is, the greater the degree of pathway enrichment is. The dot size represents the number of differentially expressed genes present in the particular pathway and the color indicates the adjusted p value (meaning the p value modified taking into account the FDR).

3.3.5.5. GOChord plot

GO terms were displayed by using the *GOPlot* R package. The relationship between GO terms and genes was displayed through the GOChord plot. Thanks to this particular method of visualization it is possible to better understand the relationship between genes and terms. On the right the GO term for the category were considered, whereas on the left the corresponding genes ordered according to log₂FC were reported. Segments connected each term to the respective involved gene.

3.3.6. Visualization of RNA-Seq results with Cytoscape

The Cytoscape software was used for other representations of functional enrichment, allowing visualization of gene clustering and specific biological annotations (Shannon et al. 2003).

3.3.6.1. NDEx

The NDEx plugin allows gene annotation pertaining to specific biological conditions (Pratt et al. 2015). Specifically, in this work it allowed to group the differentially expressed genes according to their tissue expression (each gene was linked to all the tissues where it was annotated as expressed), their subcellular localization (each gene was linked to all the organelles where it was annotated as expressed) and their prognosis in specific cancer types (each gene was linked to all the cancer types, with a different color of the link indicating either a favorable or unfavorable prognosis).

3.3.6.2. ClueGO

The ClueGO plug-in allows the visualization of non-redundant biological terms for large clusters of genes in a functionally grouped network (Bindea et al. 2009). In this work, the list of deregulated genes was uploaded and the results for GO Cellular Component, GO Molecular Function, GO Biological Process, GO Immune System Processes, KEGG, WikiPathways, Reactome and ClinVar were visualized. From the ontology sources used, the terms with $p < 0.05$ were selected. The related terms which share similar associated genes can be fused to reduce redundancy. The ClueGO network is created with kappa statistics and reflects the relationships between the terms based on the similarity of their associated genes. The network was summarized in a pie chart highlighting all the relevant terms.

3.3.6.3. BiNGO

The BiNGO plugin was used to determine which GO categories are statistically overrepresented in the set of differentially expressed genes. BiNGO maps the predominant functional themes of a given gene set on the GO hierarchy, and outputs this mapping as a Cytoscape graph (Maere, Heymans, and Kuiper 2005).

3.3.6.4. DisGeNET

The DisGeNET plugin allows to visualize, query and analyze a network representation of the gene, and variant-disease associations in DisGeNET using the current version (7.0) of the DisGeNET data. DisGeNET is a discovery platform that integrates human gene and variant-disease associations from various expert curated databases and the scientific literature, and includes Mendelian, rare, complex and environmental diseases, as well as abnormal phenotypes and traits (Piñero et al. 2020). In this work, DisGeNET was used to correlate the deregulated gene sets with immune system diseases, cancers, obesity, diabetes, and nutritional and metabolic associated diseases.

3.3.6.5. iRegulon

The iRegulon plug in allows the identification of TFs binding sites in a provided gene set (Janky et al. 2014). The iRegulon plugin allows the identification of regulons using motif and track discovery in an existing network or in a set of co-regulated genes. Motif discovery can be performed in proximal and distal sequences, across ten vertebrate genomes, using nearly 10 thousand candidate motifs (position weight matrices). In this work, the iRegulon plugin was used to identify TFs binding sites in the deregulated genes, grouping together those under a common regulator.

3.3.7. String Protein Interaction Network

The protein interaction network was obtained using the STRING database (Szklarczyk et al. 2019). This network view summarizes the network of predicted associations for a particular group of proteins, specifically the subset of deregulated genes. The network nodes are proteins. The edges represent the predicted functional associations. The combined score is computed by combining the probabilities from the different evidence channels and corrected for the probability of randomly observing an interaction.

3.3.8. Visualization of ncRNAs features and interactors

3.3.8.1. Coding and ncRNAs co-expression analysis

Coding and ncRNAs co-expression analysis was performed using Weighted gene co-expression network analysis (WGCNA) R package (<https://CRAN.R-project.org/package=WGCNA>). WGCNA is a popular systems biology method used not only to construct gene networks but also to detect gene modules and identify the central players (e.g. hub genes) within modules (Li et al. 2018). Three conditions were investigated: obese female patients compared to healthy controls, obese diabetic patients compared to healthy controls and diabetic patients compared to obese patients. For each condition, coding and non-coding genes with a deregulation ≥ 1 in terms of $|\text{Log}_2\text{FC}|$ were subjected to this analysis. The soft thresholding power was chosen considering the criterion of approximate scale-free topology. Network nodes represent gene expression profiles, while undirected edges values are the pairwise correlations between gene expressions. Cytoscape software (<http://www.cytoscape.org/>) was used for network import and visualization.

3.3.8.2. Phylogenetic analysis

Phylogenetic analysis was performed using Geneious software (Geneious version 2020.1 created by Biomatters. Available from <https://www.geneious.com>). The transcript sequence was used as query to search the sequences with high similarity in databases using Megablast (Chen, Ye, et al. 2015). Sequences with high pairwise identity were chosen and used as input for multiple alignment. Multiple alignment was performed using Clustal Omega (Sievers and Higgins 2014). The final sequence alignment was used to perform phylogenetic analysis employing the distance-based neighbor-joining (NJ) method implemented in the PHYML program (Guindon et al. 2010). The genetic distance for NJ method was calculated through the Tamura-Nei model.

3.3.8.3. RNA secondary structure prediction

RNA secondary structure was predicted using the RNA Fold Web Server (<http://rna.tbi.univie.ac.at/cgi-bin/RNAWebSuite/RNAfold.cgi>) based on Vienna RNA Fold (Lorenz et al. 2011) with default settings. The base pair probability of binding was used as color scale.

3.3.8.4. Identification of TFs binding sites (CiiiDER)

For identification of TFs binding sites in lncRNAs, the CiiiDER software was used (Gearing et al. 2019). CiiiDER can retrieve promoter sequences from a gene list or use FASTA format sequences and scan for TFs binding sites using supplied position frequency matrices. In this research work, the promoters of lncRNAs of interest were scanned with the CiiiDER software using the JASPAR2020 matrices.

3.4. hADSCs

3.4.1. hADSCs' isolation

Primary cell cultures from human adipose tissue samples were obtained from voluntary patients undergoing elective liposuction procedures under local anesthesia. The cells were isolated after directly plating the pellet without centrifugation in complete DMEM prepared with DMEM (Euro Clone) containing 1g/l D-glucose 10% heat-inactivated FBS supplemented with antibiotics at 37°C in a humidified, 5% CO₂ incubator (HERAcell 150- Thermo electron, USA).

All cell cultures were maintained at 37°C in humidified atmosphere containing 5% CO₂. After 2 weeks, the non-adherent fraction was removed and the adherent cells were cultured continuously, while the medium was changed every 3 days. Before seeding, cell samples were tested for viability by means of Trypan blue exclusion test. To prevent spontaneous differentiation, cells were maintained at a sub- confluent culture level; therefore, when cells reached 85% confluence, they were detached with 0.05% trypsin/EDTA solution, collected by centrifugation (1300 x g for 10') and expanded in culture for subsequent passages.

3.4.2. Culture of cryopreserved hADSCs

hADSCs were cryopreserved with 10% of Dimethyl Sulfoxide, 10% DMEM and 80% FBS using a controlled-rate freezing container (CoolCell®). To recovery from cryopreservation, the vials containing the cells were placed into a 37°C water bath for few seconds. Thawed cells were then seeded on a plate in complete DMEM.

3.4.3. Adipogenic induction

hADSCs were differentiated in adipogenic medium composed of DMEM High Glucose (Euroclone) supplemented with 10% Fetal Bovine Serum (GIBCO™), antibiotics (1% Penicillin/Streptomycin, 0.3% Amphotericin B) (Euroclone), 1% L-Glutamine (Euroclone), 1 µmol/L dexamethasone (Sigma-Aldrich), 0.5 mM 3-isobutyl-1-methyl-xanthine (Sigma-Aldrich), 10 µM insulin (Sigma-Aldrich) and 200 µM indomethacin (Sigma-Aldrich). Alternatively, hADSCs were also differentiated with standard adipogenic medium but with DMEM Low Glucose instead of High Glucose, or standard adipogenic medium supplemented with a 10% lipid mixture (Sigma-Aldrich) in order to mimic a high-fat diet. The medium was changed every 3 days. Adipogenic induction required 7 days (Kawaji et al. 2010, Carelli et al. 2015, Rey et al. 2019).

3.4.4. Pharmacological treatments

PPAR γ was activated using the activator troglitazone (Galateanu et al. 2012, Hausman et al. 2009). 1 µg/mL troglitazone (Sigma-Aldrich) was added to the standard culture medium for 7 days, and medium was changed every 2 days. PPAR γ was inhibited with the selective PPAR γ antagonist T0070907 (Sigma-Aldrich)(Lee et al. 2002). 1 µM of T0070907 was added to the standard culture medium for 7 days, and the medium was changed every 2 days (Rey et al. 2019).

3.4.5. Gene expression silencing

RNA interference was used to suppress specific gene expression, thus mimicking loss-of-function mutation and enabling in vitro and in vivo gene function analysis. For each transfection, a un-specific siRNA was used as negative control designed to have no known computationally derived target in the cells being transfected, and are thus commonly called a scrambled control. Briefly, two days before transfection, 6 000 cells/cm² were plated in standard growth medium. On the day of transfection, the Lipofectamine® RNAiMAX Reagent and the siRNA agent were diluted in the appropriate volume of Opti-MEM® Medium in two separate eppendorfs. The diluted siRNA was added to the diluted Lipofectamine® RNAiMAX Reagent (1:1 ratio) carefully avoiding contact with the plastic walls of the eppendorfs. Samples were incubated for <15 minutes at room temperature. Cells were washed in PBS and the medium was substituted with the appropriate composition lacking antibiotics. The siRNA-lipid complex was gently dropped in the wells containing the cells, which were then incubated for 72h days at 37°C in a CO₂ incubator.

3.4.6 hADSCs RNA extraction

Total RNA was isolated using TRIzol Reagent™ (Invitrogen) in accordance with manufacturer's instructions. TRIzol Reagent™ maintains the integrity of the RNA while disrupting cells and dissolving cell components during sample homogenization. Briefly, 0.5 ml of TRIzol Reagent™ were added directly to the sample to be extracted and samples were incubated for 5 minutes to permit complete dissociation of the nucleoproteins complex. 0.1 ml of chloroform were then added and samples were then incubated for further 5 minutes and subsequently centrifuged for 15 minutes at 12,000×g at 4°C.

The mixture then separated into a lower pink phenol-chloroform organic phase (containing protein), an interphase (containing DNA), and a colorless upper aqueous phase (containing RNA). The aqueous phase containing the RNA was transferred to a new tube, and 0.25 mL of isopropanol were added. Samples were then incubated for 10 minutes and subsequently centrifuged for 10 minutes at $12,000 \times g$ at 4°C . Total RNA precipitate formed a pellet at the bottom of the tube. The supernatant was then discarded and 0.5 mL of 75% ethanol was added. Samples were then centrifuged for 5 minutes at $7500 \times g$ at 4°C . The supernatant was then discarded, samples were air dried for 5 minutes and the pellet was then resuspended in 21 μl of RNase-free water. RNA was then stored at -80°C .

3.4.7. Reverse Transcription-PCR (RT-PCR)

This technique is used to convert the RNA to cDNA. The kit iScriptTM Reverse Transcription Supermix for RT-qPCR (BioRad) was used following manufacturer's instructions. The enzyme is the Reverse Transcriptase (4 μl) and 500 μg RNA was retrotranscribed in a final volume of 20 μl . The RNA must be diluted in nuclease-free water to reach the desired final concentration. The complete reaction mix is incubated in a thermal cycler with a priming step (5 minutes at 25°C), a reverse transcription step (20 minutes at 46°C) and a RT inactivation step (1 minute at 95°C). cDNA samples can be stored at -20°C until further use.

3.4.8. Real Time PCR

Real time PCR, also known as quantitative PCR is a laboratory technique that quantifies the amplification of a targeted molecule in the template. Real Time PCR was performed with StepOnePlusTM Real Time PCR System (Thermo Fisher) using Sso SYBR Green Supermix (Bio-Rad). SYBR green is a fluorescent dye, and the relative fluorescence emission is directly proportioned to the amount of specific cDNA detected, as amplified with each specific primer. Each sample was analyzed in triplicate, using a no-template control (NTC) as control, in which water is added instead of cDNA.

The reaction mix was composed of 5 μl of SsoAdvancedTM Universal SYBR Green Supermix, 0.3 μl of Primer Forward (10 μM), 0.3 μl of Primer Reverse (10 μM), 3.4 μl of DNase and RNase free water, and 1 μl of cDNA. Amplification conditions for 40 cycles were polymerase activation and DNA denaturation (95°C for 30 seconds), annealing (60°C for 30 seconds), extension (60°C for 30 seconds). Samples were analyzed with the $2^{-\Delta\Delta\text{Ct}}$ method, where $\Delta\Delta\text{Ct} = \Delta\text{Ct sample} - \Delta\text{Ct reference}$ (Livak and Schmittgen 2001).

Primers were designed using human gene sequences available from NCBI (www.ncbi.nlm.nih.gov/nucleotide), and selected using NCBI's Primer-BLAST tool at the exon junctions' level to optimize amplification from RNA templates and avoiding nonspecific amplification products. Primers were designed to have a sequence of about 20 bp and perform a PCR product size of maximum 250 bp. 18S and GAPDH were used as housekeeping genes, as these are stably expressed across different cellular phenotypes. The specific genes amplification was thus normalized on the respective expression of the housekeeping gene, in order to ensure that the detected variability was indeed due to a differential expression.

Primer used are shown in Table 1:

Table 1: List of Primers used

| Primer Name | Primer Sequence |
|---------------------|--------------------------------|
| GAPDH-FW | CTTTTGCCTCGCCAG |
| GAPDH-REV | TTGATGGCAACAATATCCAC |
| 18S-FW | AGTACGCACGGGCCGGTACAGTGAAGTGGC |
| 18S-REV | CGGGTTGGTTTTGATCTGATAAATGCACGC |
| SMIM25-FW | CCTTCCTTCTGCCTCCACTG |
| SMIM25-REV | TTGCTGTGGACTGATGTGGG |
| COL4A2-AS2-FW | CTCTCAGGTCATGCCCATCC |
| COL4A2-AS2-REV | CTGAGTCCTGTGCACGTCTT |
| COL4A2-FW | CAGGCCTGTATGGCGAGATT |
| COL4A2-REV | CCCCGATGTCACCGAAATCA |
| CTEPHA1-FW | CAGCTGCAACTTTGACGCAT |
| CTEPHA1-REV | CAAAGGGCCCCCATCAATCT |
| RPS21-AS-FW | TCTGCCATCCCATGTTTCAC |
| RPS21-AS-REV | TCTAGCACTACGACAAACGC |
| RPS21-FW | TCACAGGCAGGTTTAATGGC |
| RPS21-REV | TGACTCACCCATCCTACGAATG |
| PPAR γ -FW | CAAGAGTACCAAAGTGCAATCAAAGTGGAG |
| PPAR γ -REV | GTTCTCCGGAAGAAACCCTTGCATCCTTCA |
| FABP4-FW | CTGGGCCAGGAATTTGACGA |
| FABP4-REV | ACCAGGACACCCCATCTAA |
| C/EBP α -FW | GGAGCAAATCGTGCCTTGTC |
| C/EBP α -REV | CTTCTCTCATGGGGGTCTGC |
| C/EBP β -FW | GGGAGCCCGTCGGTAATTTT |
| C/EBP β -REV | CATGTGCGGTTGGTTTGGAC |
| C/EBP δ -FW | TGGGACATAGGAGCGCAAAG |
| C/EBP δ -REV | ACACGTTTAGCTTCTCTCGCA |

3.4.9. Statistical analysis for in vitro experiments

Statistics was evaluated using GraphPad Prism 8.0a version (GraphPad Software Inc, La Jolla, USA). When two conditions were analyzed, Student's unpaired t test was used. When three or more conditions were analyzed, one-way ANOVA was used followed by Tukey's post-test. For all in vitro experiments, data are reported as mean \pm Standard Error Mean (SEM). The level of statistical significance was set at $p=0.05$.

4. Results

4.1. Isolation and characterization of SAT from NW, Obese and T2D patients

The principal aim of this research work was the identification of transcriptional differences present in SAT from NW, obese and diabetic subjects. The SAT tissue highly differs in obese subjects versus lean ones, appearing to be hypertrophic when compared to SAT from lean subjects (Figure 6a). Moreover, Figure 6b shows how the tissue presents an inflammatory component (flogosis, top panels) and is highly fibrotic (lower panels). In vitro differentiation of SAT and Visceral Adipose Tissue (VAT) was performed and the adipocytes stained with AdipoRed, and results show the most efficient differentiation in SAT from obese subjects, followed by SAT from obese subjects with diabetes and ultimately a less efficient differentiation in lean subjects (Figure 6c). Moreover, the expression of PLIN, FABP4, LEP and ADIPOQ was assessed in SAT and VAT from obese and obese patients with diabetes. These markers are highly expressed in the SAT, with PLIN and ADIPOQ's expression being slightly higher in diabetic subjects (Figure 6d).

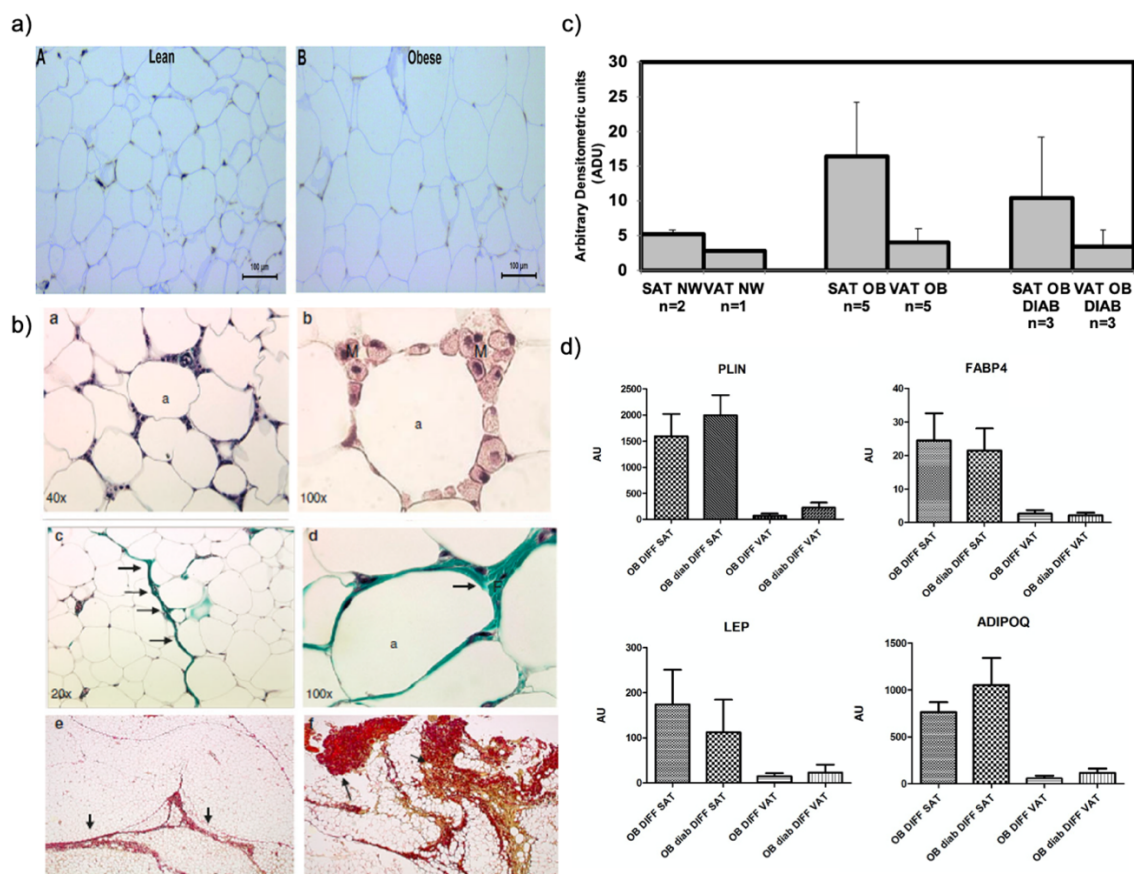


Figure 6: (a) Histological analysis of SAT tissue in lean and obese subjects. Scale bar 100 μm (b) Histological acquisition of SAT from obese subjects shows a highly flogotic and fibrotic tissue (c) In vitro differentiation of SAT and VAT and adipocytes staining with AdipoRed. (d) RNA expression of PLIN, FABP4, LEP and ADIPOQ in SAT and VAT from obese and obese patients with diabetes.

4.1.1. Clinical characteristics of screened subjects

The clinical characteristics of the 15 Females whose SAT was used for RNA-seq are reported in Table 2, analyzed with Tukey-Kramer Multiple comparisons test.

Table 2: Clinical characteristics of screened subjects

| | NW N=5 | Obese Patients N=5 | T2D Obese Patients N=5 | p value (p) |
|------------------------|-----------|-----------------------|---------------------------|----------------|
| Age, years | 37±6.7 | 41±12.5 | 54.6±14.9 | ns |
| Weight , Kg | 64.6±7.7 | 102±12.3* | 102.4±31.6* | *p=0.017 vs NW |
| Height , cm | 162.8±7.8 | 164.4±4.6 | 164.2±52.9 | ns |
| BMI, Kg/m ² | 24.3±0.9 | 38.2±4.6* | 38.1±11.8* | *p=0.016 vs NW |

4.2. Transcriptional characterization from SAT of Healthy, Obese and T2D patients

One of the main focuses of this research was the transcriptional characterization of SAT obtained from 5 healthy NW females (NW), 5 obese females (OBF), and 5 obese females with T2D (OBT2D). The aim was to characterize the differences in the transcriptome of these patients, and to do so, RNA-seq technologies was used and three experimental conditions were analyzed: the differences occurring between OBF and NW, the differences occurring between OBT2D and NW, and moreover the differences occurring between OBT2D and OBF. The quality of the RNA-seq experiment was firstly assessed. After sequencing, it is important to evaluate the clusters formation through the cluster density, which indicates the number of clusters formed per mm² and should fall within 170K/mm²-200K/mm², and the clusters passing filter, an indication of signal purity from each cluster which should be >80%. In this analysis, the cluster density was 174K/mm², whereas the cluster passing filter was 90.4%, indicating that the raw data obtained was in line with the expected values required for subsequent analyses. Table 3 reports the number of raw reads obtained for each sample.

Table 3: Number of raw reads obtained for each sample.

| Category | Raw reads |
|----------|------------|
| NW1 | 13 752 422 |
| NW2 | 15 050 528 |
| NW3 | 13 266 542 |
| NW4 | 58 309 280 |
| NW5 | 16 620 389 |
| OBF1 | 15 848 430 |
| OBF2 | 12 943 781 |
| OBF3 | 19 063 202 |
| OBF4 | 17 319 231 |
| OBF5 | 13 239 222 |
| OBT2D1 | 15 613 467 |
| OBT2D2 | 18 224 278 |
| OBT2D3 | 14 557 877 |
| OBT2D4 | 15 286 804 |
| OBT2D5 | 12 553 629 |

Table 4 reports the number and relative % of mapped reads obtained after alignment of raw sequences with the reference genome. The high number of uniquely mapped reads indicates a successful alignment.

Table 4: Number and relative % of mapped reads obtained after alignment of raw sequences with the reference genome.

| Sample | Uniquely mapped | Mapped to multiple loci | Mapped to too many loci | Unmapped: too short | Unmapped: other |
|--------|------------------|-------------------------|-------------------------|---------------------|-----------------|
| NW1 | 11473544 (83.4%) | 985245 (7.2%) | 8112 (0.1%) | 1282771 (9.3%) | 2750 (0.0%) |
| NW2 | 12408995 (82.4%) | 1058145 (7.0%) | 6636 (0.0%) | 1573743 (10.5%) | 3009 (0.0%) |
| NW3 | 11782503 (88.8%) | 662257 (5.0%) | 6470 (0.0%) | 812656 (6.1%) | 2656 (0.0%) |
| NW4 | 50742827 (87%) | 2974477 (5.1%) | 51391 (0.1%) | 4493955 (7.7%) | 46630 (0.1%) |
| NW5 | 14085422 (84.7%) | 1193487 (7.2%) | 44280 (0.3%) | 1267265 (7.6%) | 29935 (0.2%) |
| OBF1 | 13758992 (86.8%) | 1003312 (6.3%) | 47672 (0.3%) | 998818 (6.3%) | 39636 (0.3%) |
| OBF2 | 11462047 (88.6%) | 578220 (4.5%) | 4453 (0.0%) | 896470 (6.9%) | 2591 (0.0%) |
| OBF3 | 16205258 (85%) | 1343711 (7.0%) | 53216 (0.3%) | 1430500 (7.5%) | 30517 (0.2%) |
| OBF4 | 15059598 (87%) | 1027932 (5.9%) | 8071 (0.0%) | 1220164 (7.0%) | 3466 (0.0%) |
| OBF5 | 10889211 (82.2%) | 738989 (5.6%) | 7538 (0.1%) | 1599515 (12.1%) | 3969 (0.0%) |
| OBT2D1 | 12814208 (82.1%) | 1296440 (8.3%) | 14434 (0.1%) | 1483700 (9.5%) | 4685 (0.0%) |
| OBT2D2 | 15641892 (85.8%) | 1152298 (6.3%) | 13930 (0.1%) | 1408868 (7.7%) | 7290 (0.0%) |
| OBT2D3 | 12241157 (84.1%) | 784349 (5.4%) | 7258 (0.0%) | 1523656 (10.5%) | 1457 (0.0%) |
| OBT2D4 | 13022570 (85.2%) | 1045164 (6.8%) | 6364 (0.0%) | 1209651 (7.9%) | 3055 (0.0%) |
| OBT2D5 | 9420441 (75%) | 2062397 (16.4%) | 9939 (0.1%) | 1058341 (8.4%) | 2511 (0.0%) |

When filtering for transcripts with >20 reads, 30327 total variables were identified, 18674 of which were coding genes and 11653 of which were non-coding transcripts.

4.2.1. Transcriptional characterization of SAT of OBF vs. NW

The first experimental condition analyzed was that concerning the transcriptional changes occurring between OBF and NW. In this case, a full characterization of the expression profile, along with the identification of deregulated pathways and disease-implication, was performed.

4.2.1.1. Expression profiles of SAT of OBF vs. NW

After RNA-Seq analysis, genes were analyzed according to FC, i.e. the ratio of a gene expression between obese and control samples, and to FDR, that measures the proportion of false discoveries among a set of hypothesis tests called significant (Chen, Robinson, and Storey 2019). Genes showing $|\log_2FC| \geq 1$ and an $FDR \leq 0.1$ were considered as differentially expressed (DE RNAs).

Heatmap (Figure 7a) and PCA (Figure 7b) were displayed to evaluate the expression profiles obtained through the analysis. Both visualizations highlighted different expression profiles, suggesting that obesity might strongly impact cellular features and gene expression in SAT.

In particular, the heatmap (Figure 7a) displayed differentially expressed genes through a color code, where in green were represented the up-regulated genes and in red the down-regulated ones. The clustering analysis reported in the top part of the heatmap showed that the SAT from female OBF versus female NW (CTRL) belonged to two different "families", i.e. CTRL colored in light blue and OBF in pink. Indeed, in the bottom part of the graph it was possible to appreciate that OBF (N=5) were grouped together and separately from CTRL (N=5). This clustering was performed automatically based on the differential gene expression: the fact that the two conditions were "similar", indicated that the replicates within the group all presented with similar expression profiles.

The PCA visualization (Figure 7b) also showed that the samples per each condition appeared separated and grouped together, indicating a similarity amongst CTRL and OBF, but relevant differences between the two conditions. These two methods of data visualization revealed that OBF present a different transcription profile in SAT, with a high number of DE RNAs and thus a global alteration in gene expression.

DE RNAs were also displayed through a volcano plot to visualize the distribution of single up- and down-regulated genes (Figure 7c). On the x axis the \log_2FC is reported whereas on the y axis the P value in logarithmic scale is reported. The volcano plot was built considering a total of 30 327 genes. Genes that respected the condition in terms of \log_2FC and FDR were reported in red. Non differentially expressed genes were represented in grey, while genes that respected only one condition were represented in blue, i.e. genes respecting the FDR condition and not the \log_2FC one. The three dotted lines represents the conditions imposed in the analysis to consider the significant differentially expressed genes. In particular, the vertical lines regard the \log_2FC whereas the horizontal line the FDR. Already from the graph it is possible to appreciate how there is a majority of up-regulated genes.

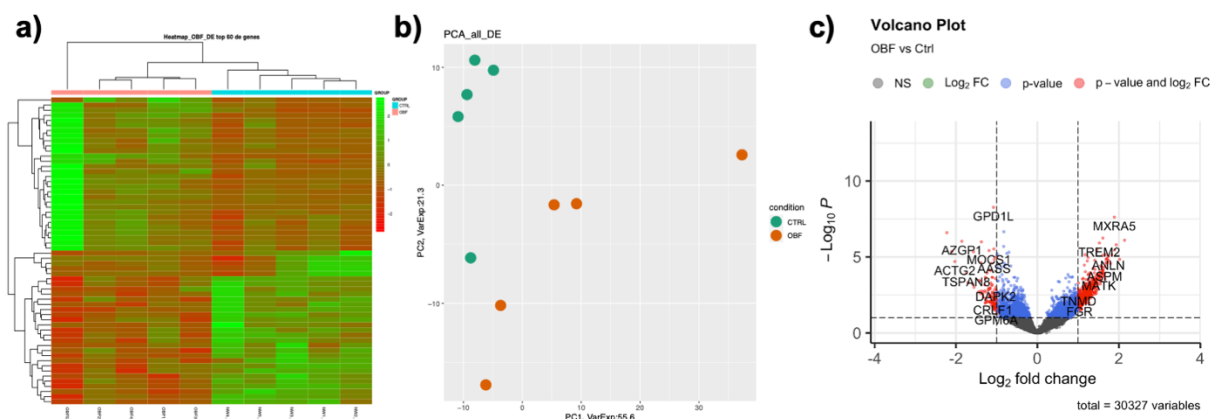


Figure 7: Transcriptomic profiles of SAT from OBF and CTRL (a) Expression profiles of differentially expressed genes in OBF versus CTRL reported as a Heatmap. (B), PCA of differentially expressed genes in OBF versus CTRL (C) Volcano plot showing deregulated genes between OBF and CTRL. On the x axis is reported the log₂FC whereas on the y axis is reported the P value in logarithmic scale.

Specifically, a total of 171 differentially expressed RNAs (DE RNAs) were detected in SAT tissue from OBF versus NW (Table 5). Of these, 160 were coding genes (mRNAs; 127 up-regulated DE RNAs and 33 down-regulated DE RNAs) and 11 were non-coding genes (ncRNAs; 8 up-regulated DE RNAs and 3 down-regulated DE RNAs) (Table 5).

Table 5: Number of differentially expressed genes in the SAT of OBF vs. NW.

| OBF vs. NW | | | |
|-----------------------|------------|-----------|------------|
| | mRNAs | ncRNAs | Total |
| Up-Regulated | 127 | 8 | 135 |
| Down-Regulated | 33 | 3 | 36 |
| Total | 160 | 11 | 171 |

The full characterization of the ncRNAs is reported in Table 6 with a classification of these ncRNAs for their specific biotype. It is possible to observe how the most abundant category are NATs, followed by lincRNAs, both lincRNAs.

Table 6: Biotype characterization of differentially expressed ncRNAs. TEC: To be Experimentally Confirmed; IG_C pseudogene: inactivated immunoglobulin gene.

| ncRNAs | | | |
|---|--------------|----------------|-----------|
| | Up-Regulated | Down-Regulated | Total |
| NATs | 3 | 1 | 4 |
| lincRNAs | 2 | 0 | 2 |
| Processed pseudogene | 0 | 1 | 1 |
| TEC | 0 | 1 | 1 |
| Transcribed unprocessed pseudogene | 1 | 0 | 1 |
| IG_C_pseudogene | 1 | 0 | 1 |
| Unprocessed pseudogene | 1 | 0 | 1 |
| Total | 8 | 3 | 11 |

4.2.1.2. Analysis of deregulated genes: a focus on novel risk-genes

A bibliographic analysis of previous literature was performed, in order to identify how many, amongst the 171 DE RNAs had been previously associated with obesity. This analysis (Figure 8) revealed that almost half of the deregulated genes (47.37%) had never been associated with the obesity condition. Moreover, most of the studies concerning the 90 obesity-associated genes were observational studies, correlating the genes to an obese phenotype. An in-depth functional characterization is needed to elucidate the role of SAT-deregulated genes in obese subjects. The results hereby reported could provide new insights in the molecular basis of obesity, providing 81 novel targets (Table 7).

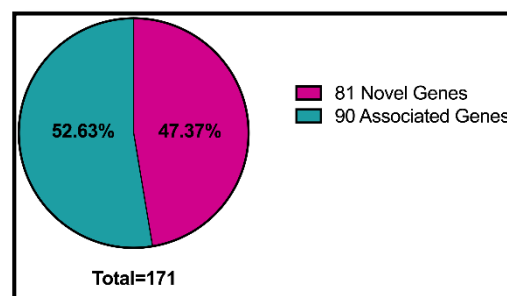


Figure 8: Genes previously associated with obesity.

Table 7: List of 81 DE RNAs which were never previously associated to obesity.

| Gene | Log2FC | Gene | Log2FC | Gene | Log2FC |
|------------------|--------|------------|--------|------------|--------|
| COL4A2-AS2 | 5.93 | BUB1 | 2.60 | MKX | -1.82 |
| TM4SF19 | 4.98 | NCAPH | 2.49 | SNX20 | 1.81 |
| DCSTAMP | 4.63 | FCGBP | 2.48 | RASGRP1 | 1.78 |
| CHRNA1 | 4.39 | AP1S3 | 2.47 | GAPT | 1.78 |
| PDE6G | 4.32 | TYROBP | 2.47 | LINC01094 | 1.74 |
| URAD | 4.18 | AL121832.2 | 2.36 | TNFSF8 | 1.70 |
| TM4SF19-TCTEX1D2 | 4.12 | CRABP2 | 2.34 | PTPN22 | 1.67 |
| SDS | 4.10 | MXRA5Y | 2.33 | MFSD12 | 1.66 |
| ACTG2 | -3.57 | PTPN7 | 2.28 | SPTB | -1.64 |
| ANLN | 3.49 | ITGB2-AS1 | 2.23 | DOK3 | 1.62 |
| COL11A1 | 3.49 | SPINT1 | 2.22 | GPR137B | 1.58 |
| SIGLEC15 | 3.35 | CD48 | 2.12 | GLULP4 | -1.54 |
| FCMR | 3.27 | ROR2 | 2.10 | PLCXD1 | -1.49 |
| RRM2 | 3.27 | LGALS9 | 2.09 | FAT2 | 1.48 |
| ST14 | 3.21 | HAVCR2 | 2.07 | PGF | 1.46 |
| CCL22 | 3.15 | SPTA1 | 2.03 | HLA-DRB5 | 1.37 |
| SLAMF7 | 3.09 | SLC19A2 | -2.01 | GLYCTK | -1.36 |
| MYH11 | -3.00 | NPL | 1.97 | BTBD8 | -1.35 |
| ADGRE4P | 2.97 | LILRB1 | 1.96 | RUNX3 | 1.33 |
| CILP2 | 2.94 | KCNJ5 | 1.95 | MOCS1 | -1.31 |
| ASPM | 2.91 | PARP15 | 1.95 | TENM4 | 1.30 |
| SPOCD1 | 2.88 | RUNX2 | 1.93 | CKB | -1.24 |
| GZMK | 2.86 | TPX2 | 1.92 | AASS | -1.16 |
| SLC6A12 | 2.82 | CD22 | 1.92 | ACER2 | -1.15 |
| UBD | 2.80 | AC134669.1 | 1.90 | AC015813.6 | -1.08 |
| SMIM25 | 2.74 | CIT | 1.84 | AL158206.1 | -1.07 |
| IGHGP | 2.66 | DOK2 | 1.82 | ADCY7 | 1.06 |

4.2.1.3. Characteristics of DE RNAs: interaction, tissue expression and cellular localization

The top 20 deregulated genes based on their log₂FC are reported in Table 8.

Table 8: FC of Top 20 DE RNAs. Protein function description was obtained from the STRING database.

| Gene Name | FC | p value | Gene Function |
|------------------|-------|------------|---|
| COL4A2-AS2 | 5.93 | 0.00014 | Unknown. |
| MMP7 | 5.72 | 0.000018 | Matrilysin; Degrades casein, gelatins of types I, III, IV, and V, and fibronectin. |
| DES | -5.67 | 0.00000026 | Desmin; Muscle-specific type III intermediate filament essential for proper muscular structure and function. |
| ADAMDEC1 | 5.26 | 0.000018 | Important role in the control of the immune response. |
| TREM2 | 5.20 | 0.0000011 | Triggering receptor expressed on myeloid cells 2; Forms a receptor signaling complex with TYROBP. |
| SPP1 | 5.09 | 0.0000071 | Osteopontin; Binds tightly to hydroxyapatite. Forms an integral part of the mineralized matrix. Important to cell-matrix interaction. |
| TM4SF19 | 4.98 | 0.0000034 | Transmembrane 4 L six family member 19; Belongs to the L6 tetraspanin family. |
| MMP8 | 4.70 | 0.000028 | Neutrophil collagenase; Can degrade fibrillar type I, II, and III collagens; Belongs to the peptidase M10A family. |
| DCSTAMP | 4.63 | 0.000025 | Dendritic cell-specific transmembrane protein; Cell surface receptor, roles in cellular fusion, cell differentiation, bone and immune homeostasis. Role in TNFSF11-mediated osteoclastogenesis. |
| APOC4-APOC2 | 4.63 | 0.00083 | Unknown. |
| CHRNA1 | 4.39 | 0.00088 | Acetylcholine receptor subunit alpha; After binding acetylcholine, the AChR responds changing conformation and this leads to opening of a ion-conducting channel across the plasma membrane. |
| PDE6G | 4.32 | 0.000016 | Retinal rod rhodopsin-sensitive cGMP 3',5'-cyclic phosphodiesterase subunit gamma; Implicated in transmission of the visual signal. |
| URAD | 4.18 | 0.00034 | Putative 2-oxo-4-hydroxy-4-carboxy-5-ureidoimidazole decarboxylase; Catalyzes the stereoselective decarboxylation of 2-oxo-4-hydroxy-4-carboxy-5-ureidoimidazole (OHCU) to (S)-allantoin. |
| TM4SF19-TCTEX1D2 | 4.12 | 0.00011 | Unknown. |
| SDS | 4.10 | 0.000015 | L-serine dehydratase/L-threonine deaminase; Serine dehydratase. |
| TNNI2 | 3.96 | 0.00021 | Troponin I, fast skeletal muscle; Inhibitory subunit of troponin, the thin filament regulatory complex which confers calcium-sensitivity to striated muscle actomyosin ATPase activity. |
| PLA2G7 | 3.78 | 0.00028 | Platelet-activating factor acetylhydrolase; Modulates the action of platelet-activating factor (PAF) by hydrolyzing the sn-2 ester bond. |
| CD300LB | 3.77 | 0.000038 | CMRF35-like molecule 7; Acts as an activating immune receptor through its interaction with ITAM-bearing adapter TYROBP, and also independently by recruitment of GRB2. |
| APOC1 | 3.75 | 0.00000075 | Apolipoprotein C-I; Inhibitor of lipoprotein binding to the low density lipoprotein (LDL) receptor, LDL receptor-related protein, and very low density lipoprotein (VLDL) receptor. |
| CD52 | 3.73 | 0.000013 | CAMPATH-1 antigen; May play a role in carrying and orienting carbohydrate, as well as having a more specific role. |

It is worth noticing that the top deregulated gene is a lncRNA, COL4A2-AS2, whose function is currently unknown, whilst the other 19 genes are all protein coding. Among the deregulated genes it is possible to highlight an implication for genes of the immune system, as ADAMDEC1, TREM2, DCSTAMP, CD300LB and CD52 are all involved in the immune response. There seems to be also a re-modelling of the surrounding tissue, as MMP7, SPP1, MMP8, DCSTAMP all play a role in this process. DES and TNNI2, which control the biology of striatal muscle, are also deregulated. Indeed, obesity can cause a decline in contractile function of skeletal muscle, reducing mobility and leading to the development of more obesity-associated health risks (Tallis, James, and Seebacher 2018).

The STRING database was used to construct an interaction network of deregulated genes where the nodes are proteins and the edges represent the predicted functional associations (Figure 9). The combined score is computed by combining the probabilities from the different evidence channels and corrected for the probability of randomly observing an interaction. It is possible to see that the proteins encoded by the genes interact in two main networks, with evidence which are both from curated databases and experimentally determined.

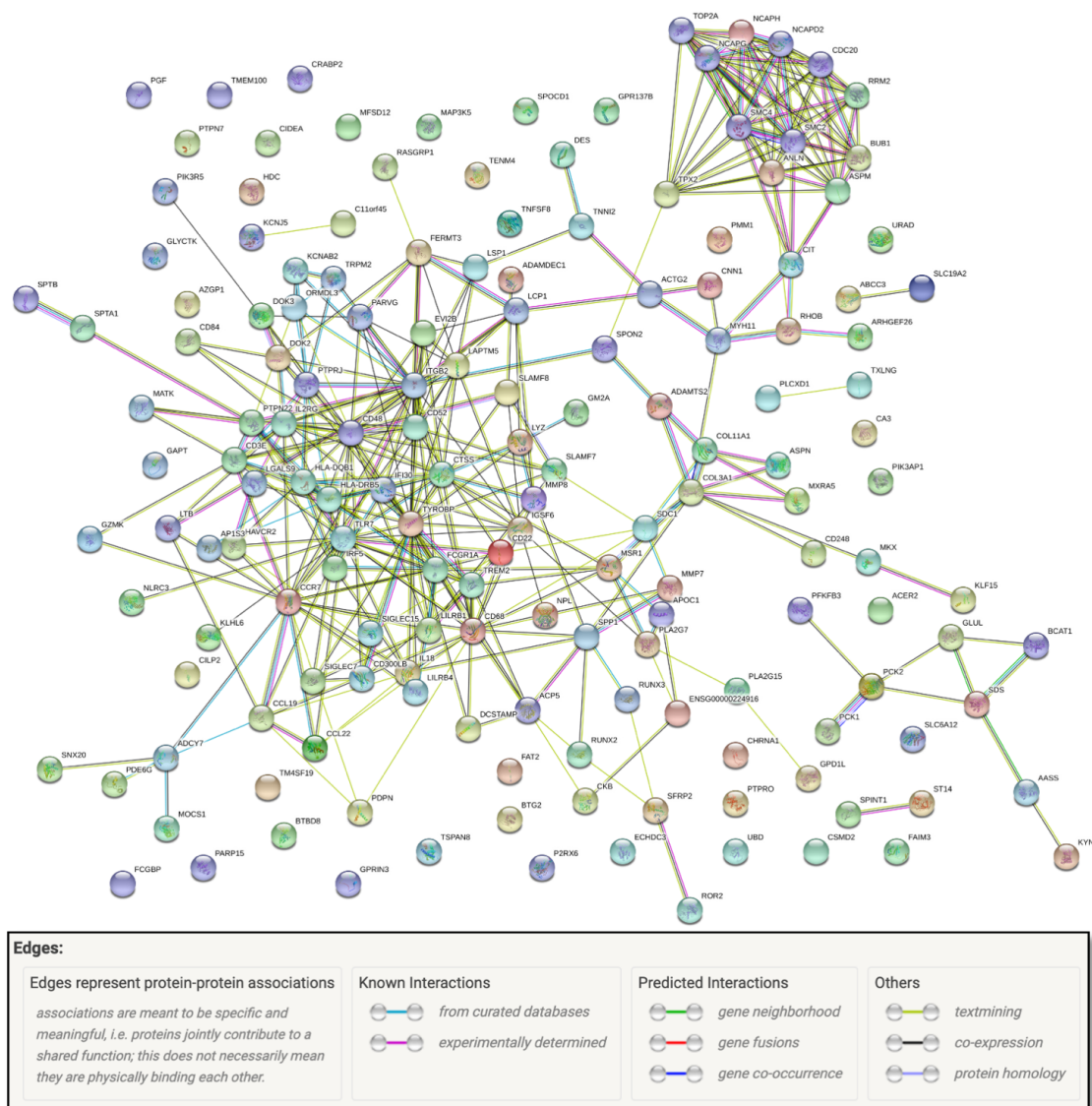


Figure 9: STRING Protein Network Interaction.

With the NDEx plugin of the Cytoscape software it was also possible to investigate the genes expression and cellular localization. The genes deregulated in OBF are also expressed in a high number of other tissues (Figure 10). These include also neural specific tissues, such as the cerebellum, the caudate and the hippocampus, tissues implicated in the genitourinary apparatus, such as the fallopian tube, the endometrium, the urinary bladder, the seminal vesicle etc., and also the muscle tissue (e.g. skeletal muscle, heart muscle). These results could potentially suggest that the genes found deregulated in SAT could have a profound impact also in other un-related tissues, if their deregulation is confirmed in these locations.

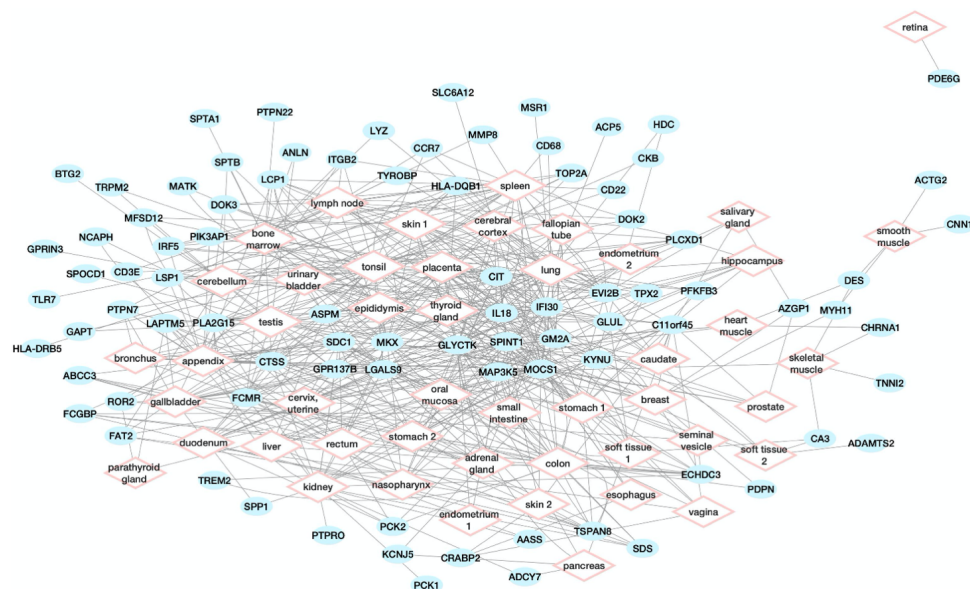


Figure 10: Specific tissue expression of deregulated genes as obtained with the NDEx database.

Moreover, in Figure 11 it is possible to observe the known subcellular localization of the DE RNAs. A high number of variable organelles emerge, it is possible to suggest that the cells of the SAT present with ubiquitary perturbations, in the nucleus as well as the cytoplasm, the mitochondria, and the cytoskeleton indicating a profound alteration in all cellular functions.

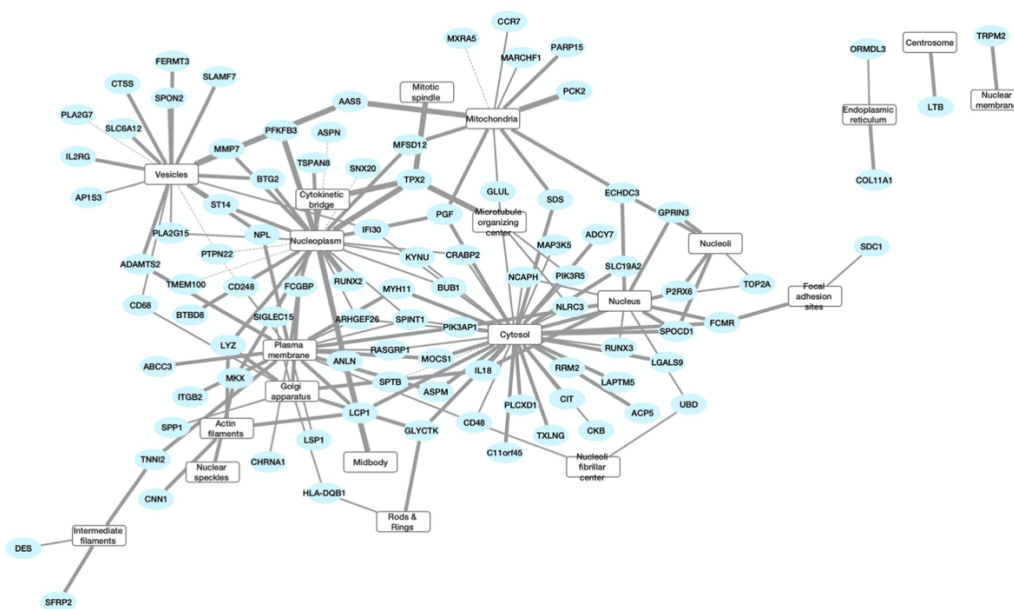


Figure 11: Subcellular localization of deregulated genes as obtained with the NDEx database.

4.2.1.4. Identification of co-regulating TFs

The following aim was the identification of TFs binding sites in the DE RNAs gene set. Indeed, it was then possible to group together these genes under common regulators, as shown in Figure 12. The main transcriptional regulator influencing the DE RNAs network seems to be SPI1, as it presents the highest number of targets. Interestingly, this TF, namely implicated in the activation of gene expression during myeloid and B-lymphoid cell development, has been also shown to be implicated in adipogenesis (Dispirito et al. 2013, Lefterova et al. 2014). Indeed, when it is expressed in mature adipocytes, it leads to the increased expression of macrophage genes and a global repression of genes with nearby adipocyte-specific PPAR γ binding sites (Dispirito et al. 2013, Lefterova et al. 2014). Moreover, it has been implicated in insulin resistance, and its knock out promotes insulin sensitivity in high-fat diet-fed obese mice (Lin et al. 2012, Lackey et al. 2019). Other TFs implicated in adipogenesis and regulators in this network are HSF1 (Ma et al. 2015), EP300 (Lee et al. 2019, Takahashi et al. 2002), EBF1 (Jimenez et al. 2007, Gao et al. 2014), NFkB1 (Berg et al. 2004), SRF (Rosenwald et al. 2017, Jones et al. 2020), CREB1 (Reusch, Colton, and Klemm 2000), TWIST2 (Lee et al. 2003, Franco et al. 2011), TP53 (Krstic et al. 2018, Huang et al. 2014), and, of course, C/EBP δ , key regulator of early adipogenesis (Hishida et al. 2009, Lee et al. 2019). Moreover, PTC1 knock out has been correlated with adult-onset obesity (Perks et al. 2017), whilst early over-nutrition leads to a decrease of PDX1 (Glavas et al. 2019). Members of the NFAT family have been implicated in adipogenesis and insulin resistance, but NFATc1 specifically was never reported to have a role in this process (Yang et al. 2006). EVX2, ZNF622, C9orf156, MTA3 and FLI1 have not been correlated with adipogenesis to date. The identification of adipogenesis-related TFs integrates current knowledge of how these regulate the process, as this analysis specifically correlates them with DE RNAs and could thus enrich the knowledge on adipogenesis and/or obesity transcriptional regulators and targets. Moreover, as a number of DE RNAs are co-regulated by TFs never before associated with adipogenesis or obesity, these results could prove helpful in directing scientists towards their characterization in these contexts.

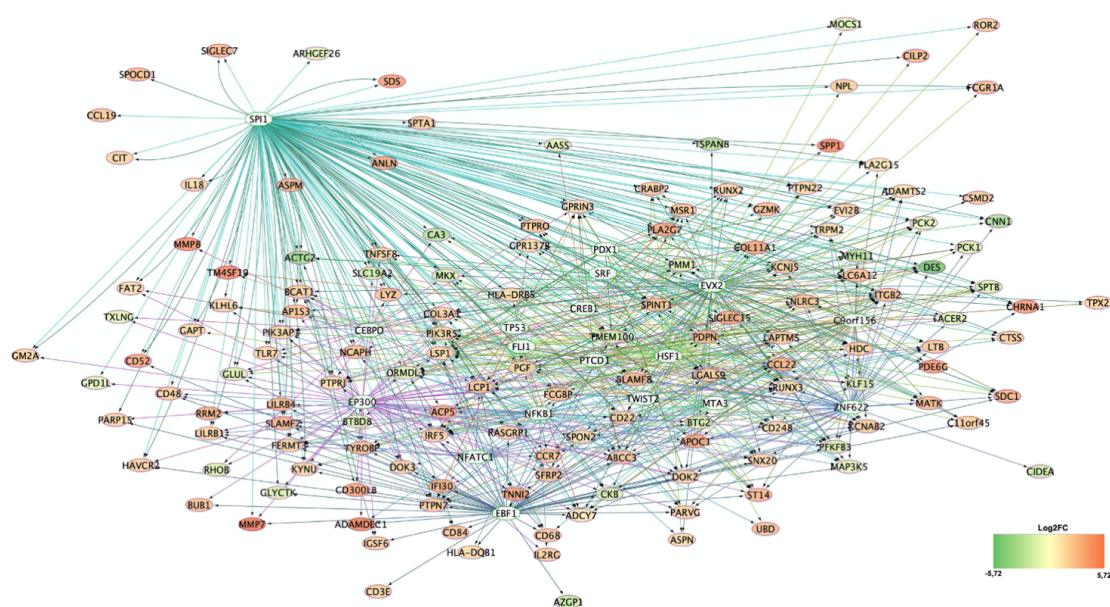


Figure 12: Regulon identification of DE RNAs. TFs are reported as white-filled hexagon shapes whereas DE RNAs are reports as ellipses color-filled. The color of DE RNAs indicates the respective log₂FC deregulation.

4.2.1.5. GO analyses: Cellular Component, Molecular Function and Biological Processes

Gene expression profiles of SAT tissue from OBF versus NW were then analyzed for GO terms enrichment, in order to better understand the possible genes cellular localization (Cellular Component), Molecular Functions and Biological Processes. Coding genes with $|\log_2FC| \geq 1$ were subjected to pathways analysis through enrichR web tool, and the outcomes were ordered according the adjusted p value, i.e. the p value adjusted taking into account the FDR (Chen, Robinson, and Storey 2019), and for each category only the top 10 GO terms were considered. Then, for each category, the outcomes were displayed through a GO Chord graph, which was obtained through R software. Thanks to this visualization strategy it was possible to better understand the relationship between genes and terms. On the right of the graph, the top 10 GO term for the category considered, whereas on the left the corresponding genes ordered according to \log_2FC . Segments connected each term to the respective involved gene. For each category, GO analysis was performed also with the ClueGO and BiNGO plugins, in order to compare the three interpretations and obtain more significant information.

The GO terms analysis in Cellular Component highlighted 112 pathways. The top 10 GO Cellular Component strongly implicated the vesicle formation component, with terms such as “clathrin-coated endocytic vesicle membrane”, “clathrin-coated endocytic vesicle”, but even pathways related specific granules formation and lytic vacuoles (Figure 13).

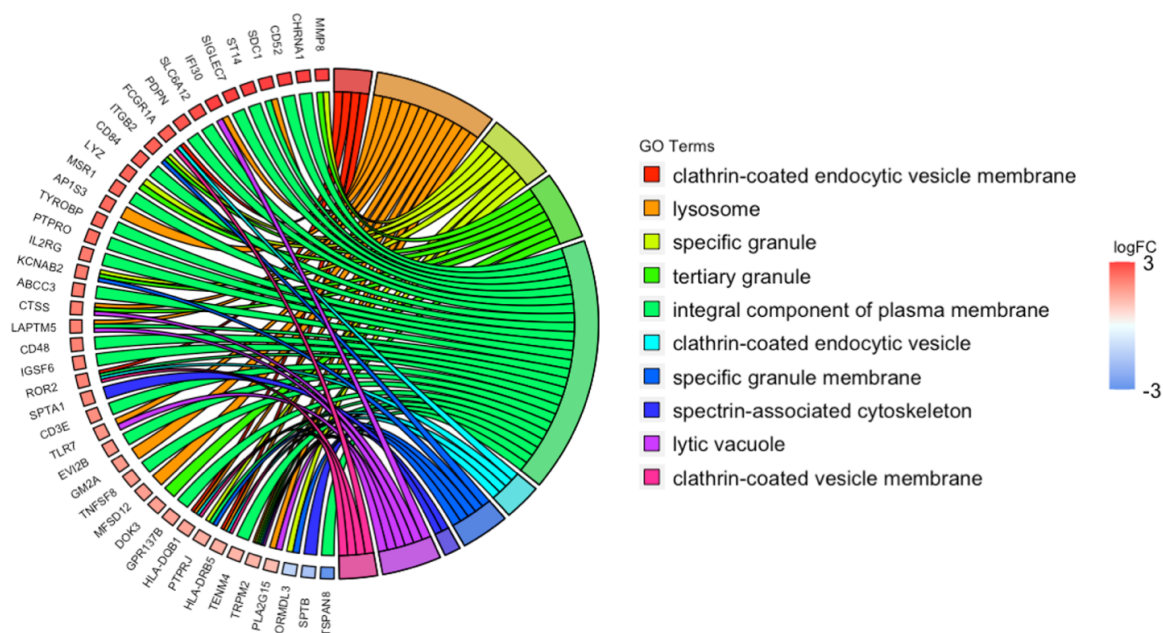


Figure 13: GO Chord Cellular Component analysis for DE genes in SAT from in OBF vs. NW. On the right the top 10 significant GO term for cellular component, whereas on the left the corresponding genes ordered according to \log_2FC . Segments connected each term to the respective involved gene.

Moreover, the ClueGO analysis (Figure 14a) implicates a significant deregulation in plasma lipoproteins ($p < 0.01$), along with again the vesicle and granule component ($p < 0.01$) and, interestingly, an association with the immunological synapse ($p < 0.05$). Supporting these results, the BiNGO analysis highlights how the most overrepresented terms are related to morphological changes in the plasma membrane, the lysosome and the extracellular regions (Figure 14b).

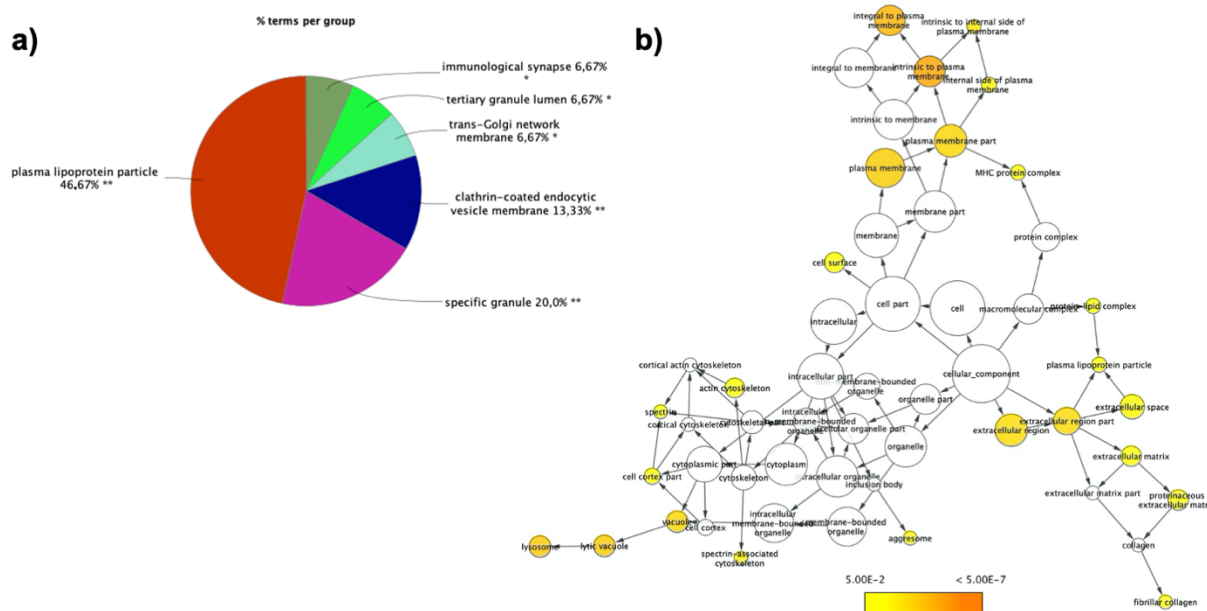


Figure 14: GO Cellular Component analysis. (a) ClueGO analysis for Cellular Component in OBF vs. NW. Each pie segment refers to the % of terms present per group (* $p < 0.05$, ** $p < 0.01$ vs NW) (b) BiNGO analysis for Cellular Component in in OBF vs. NW. The hubs reported show the overrepresented terms and the color intensity refers to the node significance.

The GO terms analysis in Molecular Function highlighted 207 pathways. The top 10 GO terms implicated morphological components, such as actin and integrin binding, along with matrix remodeling with metallopeptidase activity, biochemical alterations such as carboxy-lyase and phosphoric ester hydrolase activity and signal transduction complexes such as the PI3K regulator subunit, phosphatase activity and protein tyrosine phosphatase activity (Figure 15).

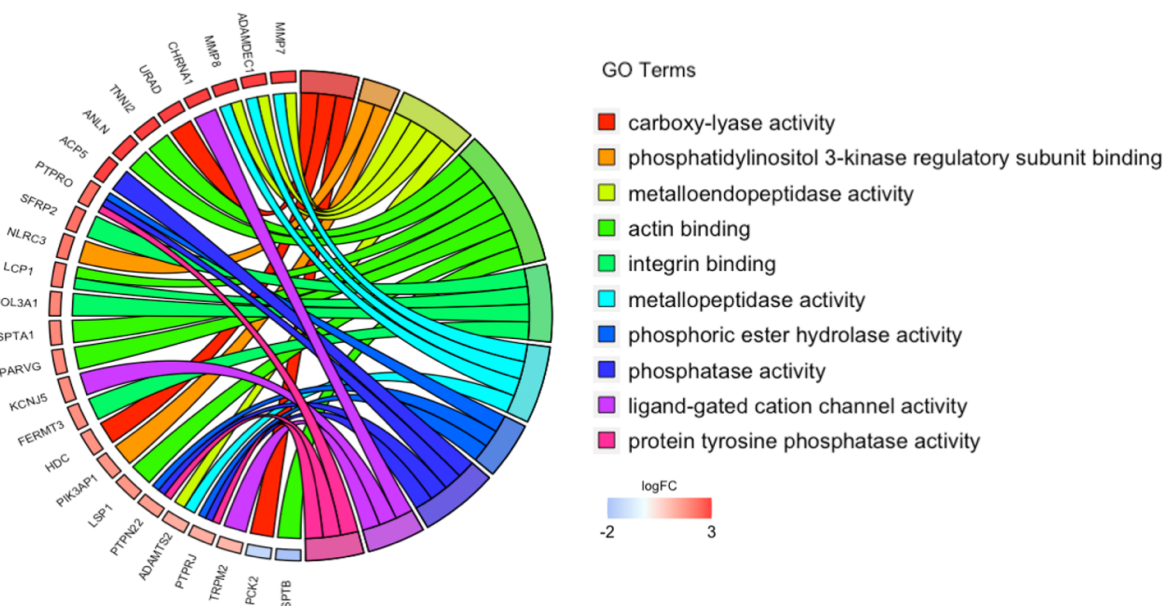


Figure 15: GO Chord Molecular Function analysis for DE genes in in OBF vs. NW. On the right the top 10 significant GO term for molecular functions, whereas on the left the corresponding genes ordered according to log₂FC. Segments connected each term to the respective involved gene.

Along with the previously mentioned components, the ClueGO analysis (Figure 16a) implicates a significant deregulation lipid-related activity, such as lipid kinase activity ($p < 0.05$), lipoprotein particle binding ($p < 0.01$) and lipase activity ($p < 0.05$). Moreover, the BiNGO analysis highlights how the most overrepresented terms are related to catalytic activities (Figure 16b).

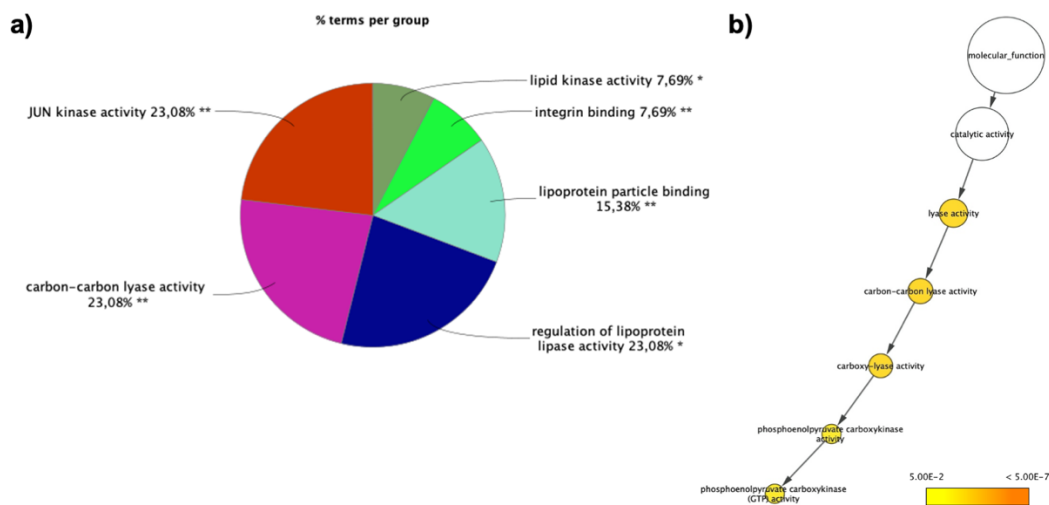


Figure 16: GO Molecular Function. (a) ClueGO analysis for Molecular Function in in OBF vs. NW. Each pie segment refers to the % of terms present per group ($*p < 0.05$, $**p < 0.01$ vs NW) (b) BiNGO analysis for Molecular Function in in OBF vs. NW. The hubs reported show the overrepresented terms and the color intensity refers to the node significance.

The GO terms analysis for Biological Processes highlighted 1243 deregulated pathways, and the GO Chord graph reports the top 10 deregulated processes according to their significance (Figure 17). Remarkably, all these processes pertained immune-related functions, indicating a highly inflammatory phenomenon occurring in SAT of obese patients, indeed, the deregulated terms are all upregulated but one, and this analysis highlights the key molecular genes responsible for immune activation.

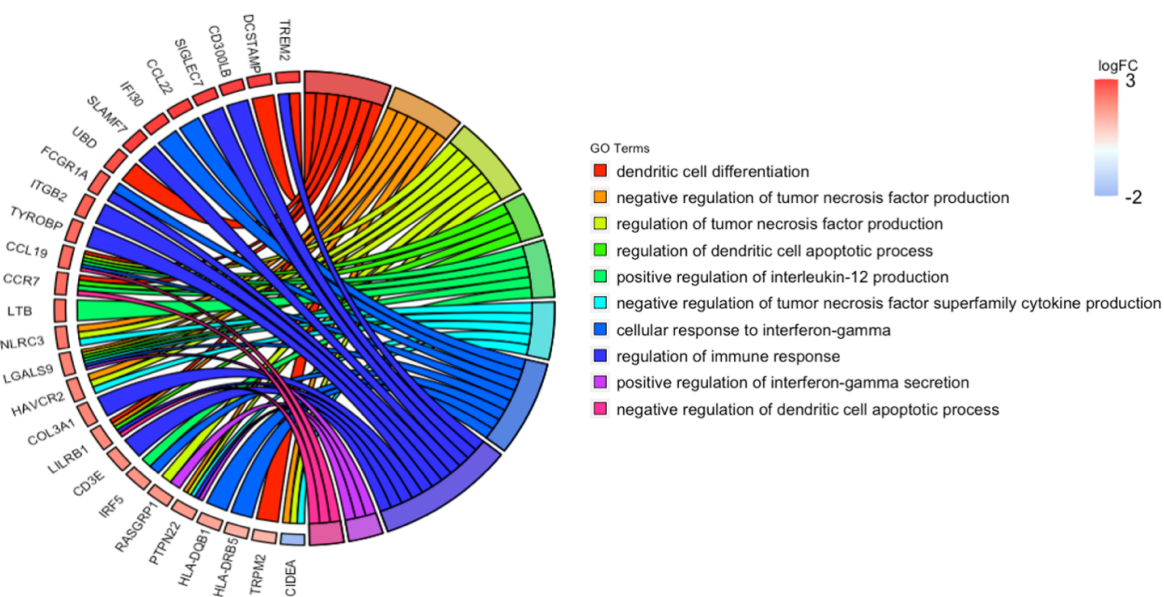


Figure 17: GO Biological Processes analysis for DE genes in SAT from in OBF vs. NW. On the right the top 10 significant GO terms for Biological processes, whereas on the left the corresponding genes ordered according to log2FC. Segments connected each term to the respective involved gene.

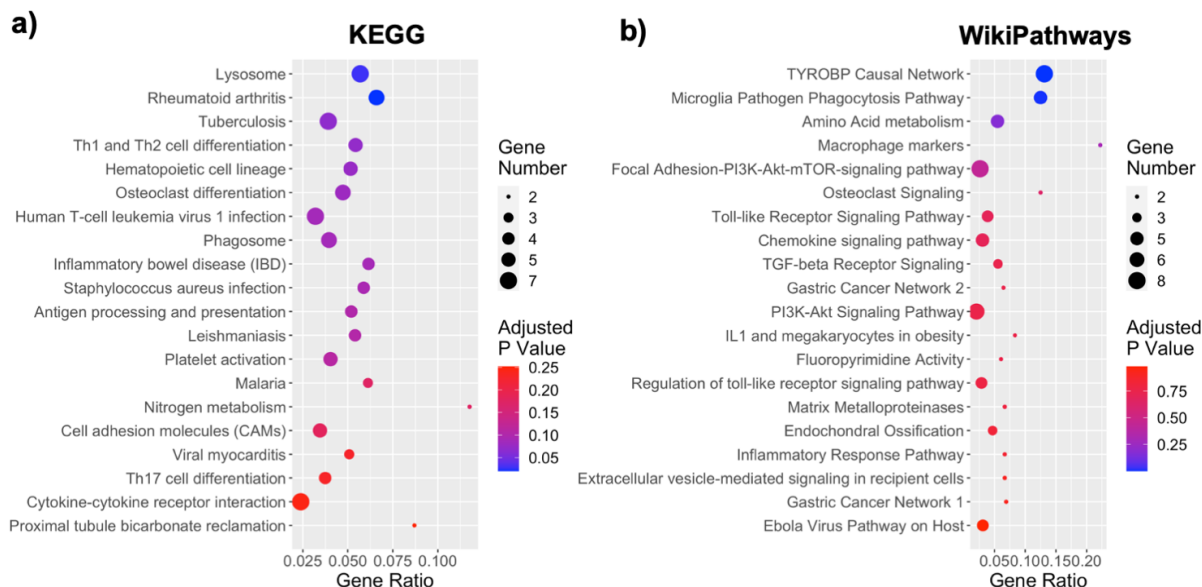


Figure 19: Dotplot of top 20 KEGG 2019 (a) and WikiPathways (b) analyses. The y-axis represents the name of the pathway, the x-axis represents the Rich factor, dot size represents the number of different genes and the color indicates the adjusted p-value.

The most significant pathway deregulation was also investigated using the ClueGO plugin, for KEGG (Figure 20a), WikiPathways (Figure 20b) and Reactome (Figure 20c) databases. The results again implicated immunological responses (viral protein interaction with cytokine and cytokine receptor for KEGG, microglia pathogen phagocytosis pathway for WikiPathways, immunoregulatory interactions between a lymphoid and a non-lymphoid cell for Reactome), together with an implication for auto-immune diseases such as rheumatoid arthritis, known to be associated with obesity (Stavropoulos-Kalinoglou et al. 2011).

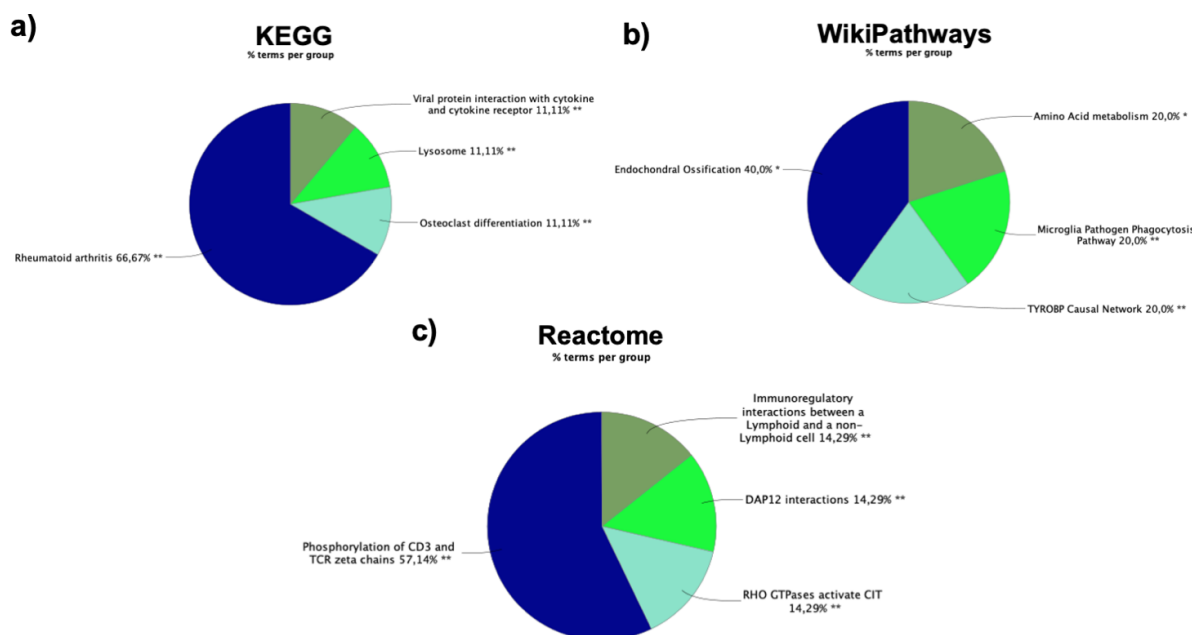


Figure 20: ClueGO analysis for KEGG (a), WikiPathways (b) and Reactome (c) in OBF vs NW. Each pie segment refers to the % of terms present per group (* $p < 0.05$, ** $p < 0.01$ vs Control SAT).

As metabolic complications of obesity can lead to the development of metabolic diseases, a focus was given on those pathways identified as correlated with dysfunctions in specific

metabolisms (Grundy et al. 2004). Indeed, cellular metabolism is typically defined as the sum of biochemical processes that either produce or consume energy (DeBerardinis and Thompson 2012). These metabolic processes can be simplified in pathways involving three main classes of nutrients: carbohydrates, fatty acids and aminoacids (aa), necessary for maintaining energy homeostasis (DeBerardinis and Thompson 2012). The deregulated metabolic pathways are reported in Figure 21.

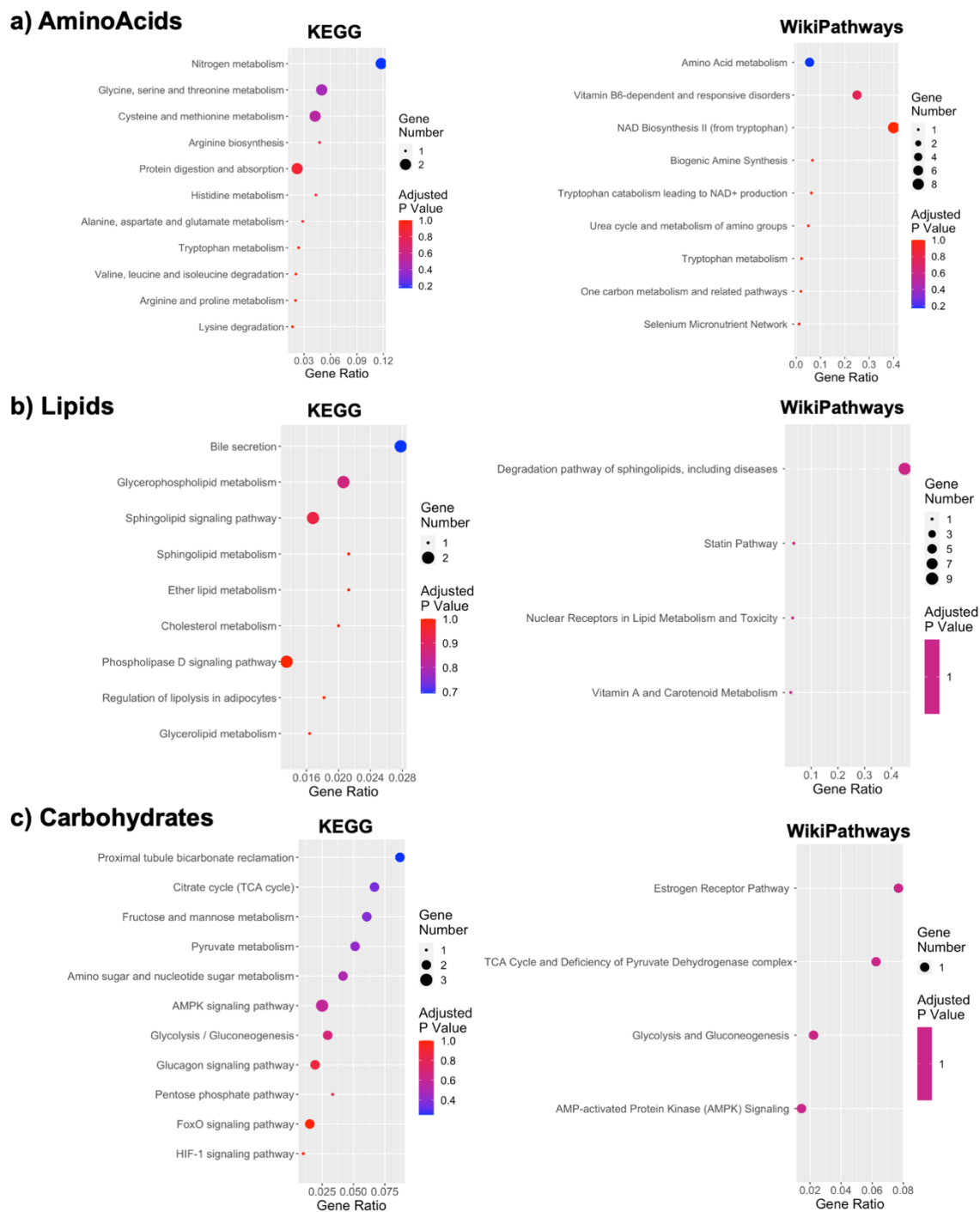


Figure 21: Dotplot of KEGG 2019 and WikiPathways analysis of pathways correlated with (a) aa metabolism, (b) lipids metabolism and (c) carbohydrates metabolism. The y-axis represents the name of the pathway, the x-axis represents the Rich factor, dot size represents the number of different genes and the color indicates the adjusted p-value.

It is interesting to note that the highest number of deregulated pathways is correlated with aa metabolism, followed by carbohydrates. The lipids component seems to be the least affected by the gene perturbation, as it includes the lowest number of deregulated pathways. Indeed, changes in blood concentrations of essential aa and their derivatives, in particular branched chain aa, sulfur aa, tyrosine, and phenylalanine, are apparent with obesity and insulin resistance, often before the onset of clinically diagnosed T2D. A model was even proposed linking the free fatty acids-rich environment of obesity patients with diminution of branched chain aa catabolic enzyme activity, changes in methionine oxidation and cysteine/cystine generation, and tissue redox balance (NADH/NAD⁺) (Adams 2011). Even so, most studies focused on the peripheral or muscular deregulation in aa present in obese patients (Suzuki et al. 2019, Adams 2011, Takashina et al. 2016, Guillet et al. 2016), and it is remarkable to note that this is also observable also in the SAT tissue (Figure 21a). Moreover, when studying the specific DE RNAs implicated in these processes, new target modulators could be identified.

Concerning lipids metabolism, it has been shown that obesity is associated with increased basal lipolysis in adipose tissue, and elevated circulating free fatty acids (Singla, Bardoloi, and Parkash 2010). Indeed, obese people commonly have increased tissue lipid accumulation in the liver, skeletal muscle, and heart (Shulman 2014, Galgani, Cortés, and Carrasco 2014). It appears that elevated fat content in ectopic locations is more deleterious for whole-body and tissue metabolic homeostasis as indeed excessive fat accumulation in non-adipose cells seems to be causative of insulin resistance in obese individuals (Galgani, Cortés, and Carrasco 2014). Notably, in the DE RNAs dataset, a number of them have been found to correlate also with sphingolipids metabolism and cholesterol metabolisms, with even an implication for nuclear receptors involved in these processes (Figure 21b).

Obesity has also been correlated with carbohydrates metabolism, as more and more studies are identifying glucose uptake into fat as modulator of systemic glucose homeostasis (Singla, Bardoloi, and Parkash 2010). Indeed, in all forms of obesity, there is a downregulation of GLUT4, a major factor contributing to the impaired insulin-stimulated glucose transport in adipocytes (Shepherd et al. 1993). Moreover, there is reduced glucose disposal in adipose tissue in obese subjects (Singla, Bardoloi, and Parkash 2010), and it is of increasing relevance the identification of the molecular signature responsible for these changes. Deregulated pathways concerning carbohydrates metabolism include glycolysis and gluconeogenesis, the pentose signaling pathway, pyruvate metabolism, the citrate cycle and fructose and mannose metabolisms (Figure 21c). Interestingly, subjects fed with large doses of fructose versus glucose for several weeks tend to present exacerbated visceral and ectopic fat accumulation (Stanhope et al. 2009).

Other deregulated metabolisms found in SAT of obese patients include vitamin, pyrimidine, and even specific drug metabolisms, suggesting a global alteration in the SAT metabolome of obese patients (Figure 22).

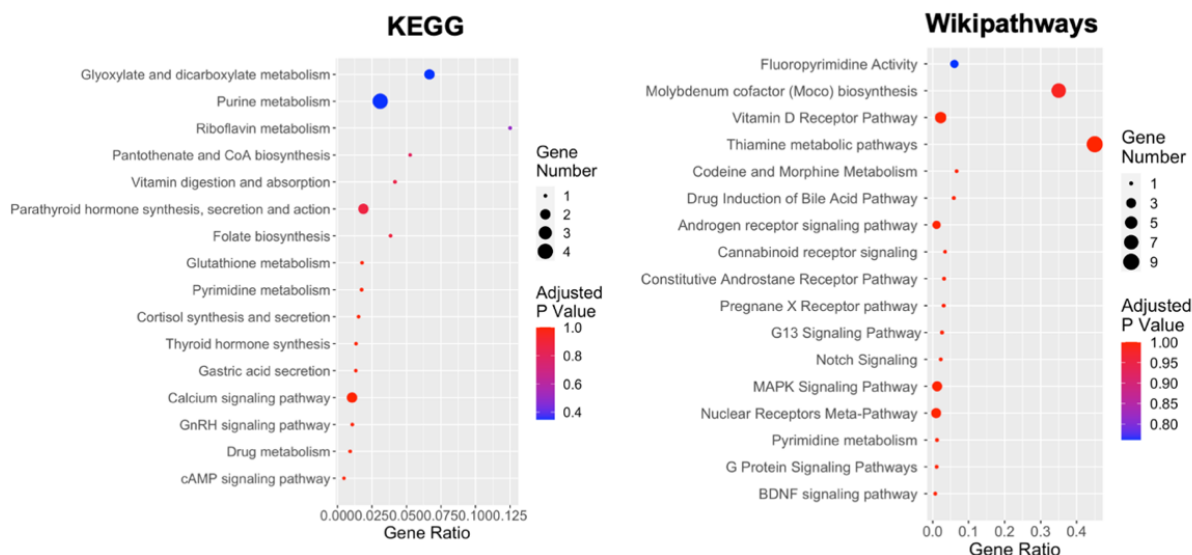


Figure 22: Dotplot of KEGG 2019 and WikiPathways analysis of pathways correlated with other metabolisms. The y-axis represents the name of the pathway, the x-axis represents the Rich factor, dot size represents the number of different genes and the color indicates the adjusted p-value.

Lastly, the specific pathways concerning adipogenesis were highlighted, and are reported in Figure 23. These included a deregulation in adipocytokines, PPAR and insulin signaling pathways, adipocytes differentiation and even thermogenesis (Figure 23).

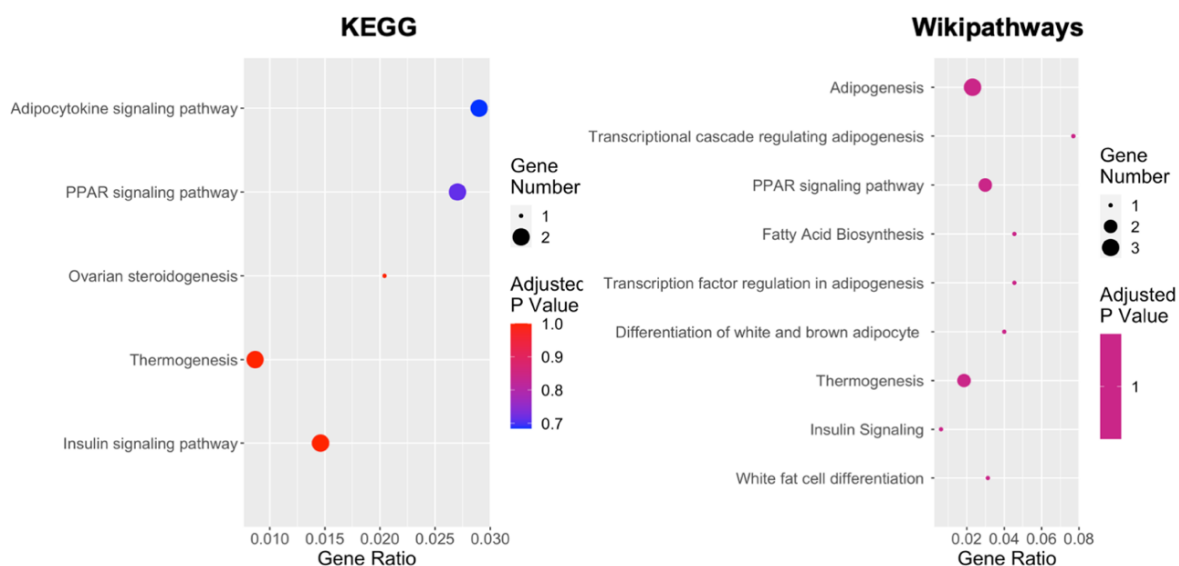


Figure 23: Dotplot of the KEGG 2019 and WikiPathways analysis of pathways correlated with adipogenesis. The y-axis represents the name of the pathway, the x-axis represents the Rich factor, dot size represents the number of different genes and the color indicates the adjusted p-value.

4.2.1.7. Role of the immunological component in SAT of OBF vs NW

As all the previous results directed towards a strong implication for the immunological system in the SAT obtained from obese patients, a more in-depth analysis was performed concerning these processes. First of all, the specific immune-related pathways were highlighted in the KEGG and WikiPathways enrichment and displayed as a dotplot ranked for their significance (Figure 24). Specifically, 67 out of the 171 KEGG deregulated terms (39%) and 44 out of the 158 WikiPathways deregulated terms (28%) were correlated with the immune system,

suggesting that the DE RNAs deregulation reported profoundly impacts this system, with a higher susceptibility for subsequent co-morbidities insurgence.

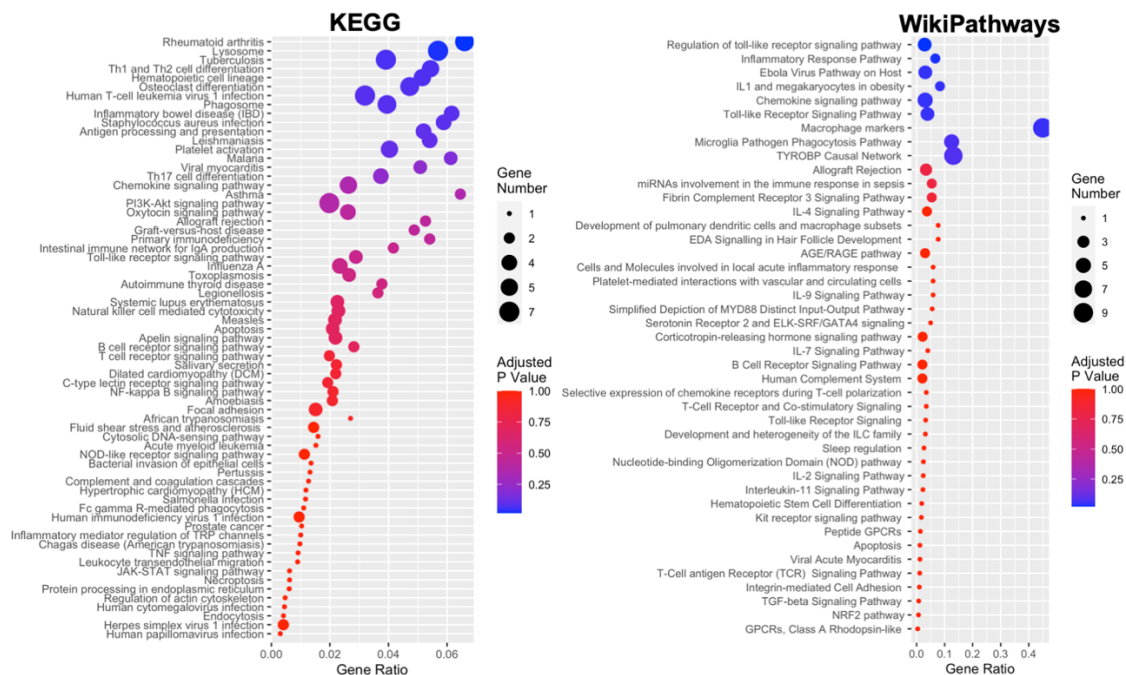


Figure 24: Dotplot of KEGG 2019 and WikiPathways analysis of pathways correlated with the immune system. The y-axis represents the name of the pathway, the x-axis represents the Rich factor, dot size represents the number of different genes and the color indicates the adjusted p-value.

Moreover, via ClueGO analysis it was possible to interrogate the GO Immune System Processes database, obtaining the significant terms pertaining to these processes from the DE RNAs (Figure 25). 5 equally represented categories were identified, implicating dendritic cells, antigen processing and presentation, and T cell activation. Indeed, it is these three mechanisms which seem to be most deregulated and their modulation could lead to an improved outcome in the case of co-insurgence of obesity secondary diseases or infections.

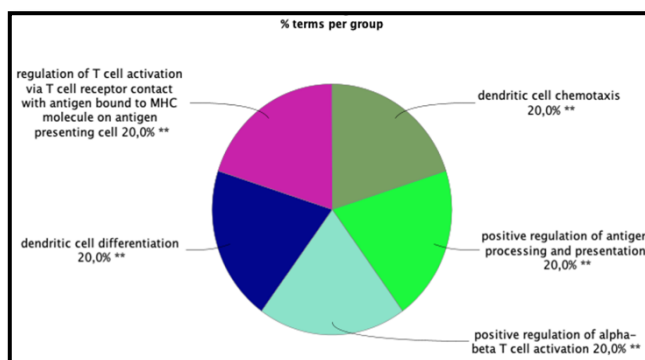


Figure 25: ClueGO analysis for GO Immune System Processes in OBF vs NW. Each pie segment refers to the % of terms present per group (** $p < 0.01$ vs NW).

The following step was to interrogate the DisGeNET database, which consists of an integrated analysis of all the known and predicted interactions between a set of genes and a disease class. Specifically, Figure 26 reports the known interaction of the DE RNAs with diseases of the Immune System, obtained from curated databases. It is thus possible to appreciate which specific genes deregulated in SAT lead to increased susceptibility for specific immune diseases, with possible implications for precision therapies when certain co-morbidities occur. The numerous diseases implicated include multiple types of diabetes, known complication of obesity, but also autoimmune diseases such as Lupus Erythematosus Systemic, Rheumatoid

Arthritis, Immunologic Deficiency Syndromes, Multiple Sclerosis, defects in the leucocyte adhesion process, dermal diseases etc.

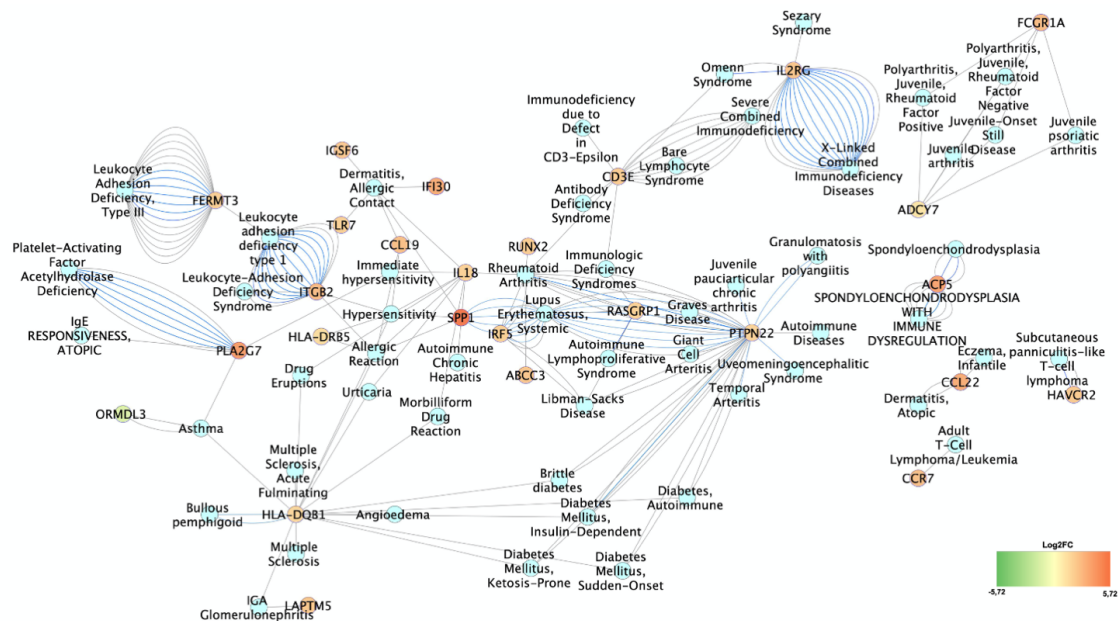


Figure 26: DisGeNET analysis shows the terms implicated in Immune Diseases OBF vs. NW. The lines connecting the genes to the disease term represent the literature evidence for the terms' implication in the disease. The color scale represents the genes FC.

4.2.1.8. Potential cancer implications: susceptibility in obese patients

The emerging link between obesity and multiple cancer types is gaining more and more relevance in recent years (Avgerinos et al. 2019, Kompella and Vasquez 2019, Ungefroren et al. 2015). Indeed, worldwide, the burden of cancer attributable to obesity, expressed as population attributable fraction, is 11.9% in men and 13.1% in women (Avgerinos et al. 2019). For this reason, the identification of the molecular signature occurring in obesity responsible for the insurgence of related carcinogenesis is of crucial importance. Firstly, the oncogenic-related pathways were highlighted in the KEGG and WikiPathways analysis and displayed as a dotplot ranked for their significance (Figure 27). Specifically, 25 out of the 171 KEGG deregulated terms (15%) and 31 out of the 158 WikiPathways deregulated terms (20%) were correlated with the oncogenic phenomenon and diseases, suggesting a strong implication for the DE RNAs dataset in secondary carcinogenesis occurrence.

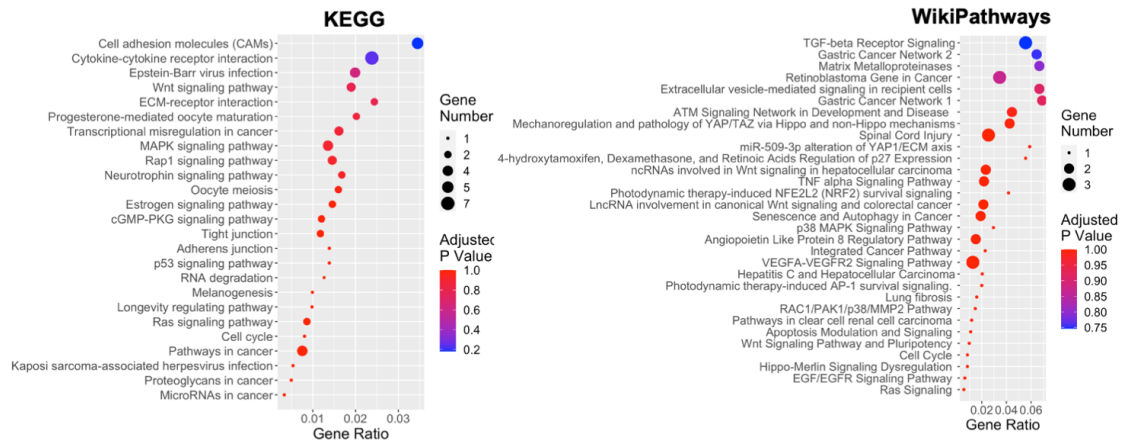


Figure 27: Dotplot of KEGG 2019 and WikiPathways analysis of oncogenesis-related pathways. The y-axis represents the name of the pathway, the x-axis represents the Rich factor, dot size represents the number of different genes and the color indicates the adjusted p-value.

As this kind of analysis does not allow for gene visualization, the DisGeNET database was investigated in order to elucidate all known interactions between cancers and DE RNAs (Figure 28). It is possible to note how most genes involved are upregulated, correlating with numerous different cancer types. These include breast cancer, urinary cancer, lung cancer, colorectal cancer and many more.

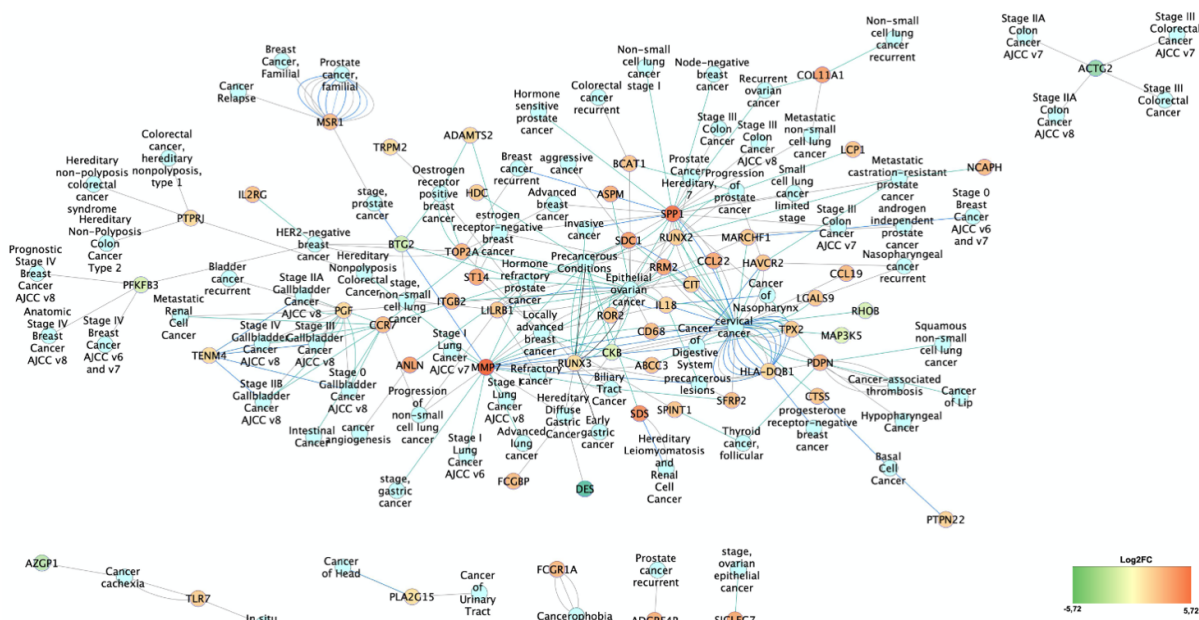


Figure 28: DisGeNET analysis shows the terms implicated in cancer in SAT from OBF vs. NW. The lines connecting the genes to the disease term represent the literature evidence for the terms' implication in the disease. The color scale represents the genes FC.

Even so, this type of analysis does not allow for prognosis correlation. Indeed, although in most cases an excessive body weight is associated with carcinogenesis development and poor outcome, some new studies are now highlighting how this might not always be the case. Studies are highlighting how obesity can be a predictor of better overall survival in metastatic patients (Tsang et al. 2016) and moreover, in lung cancer, renal cell carcinoma and melanoma, obesity was found to be protective in terms of outcome (Petrelli et al. 2020). For this reason, the NDEX

plugin was used to construct a network where the edges are correlated with disease prognosis (Figure 29). It is interestingly to note how, for example, that in liver cancer most of the downregulated genes in the network are correlated with a favorable prognosis, indicating an overall higher susceptibility. Furthermore, a relevant number of unfavorable genes for renal and pancreatic cancer are reported to be upregulated. In depth studies will allow to predict and specifically address the risk for cancer development in obese patients.

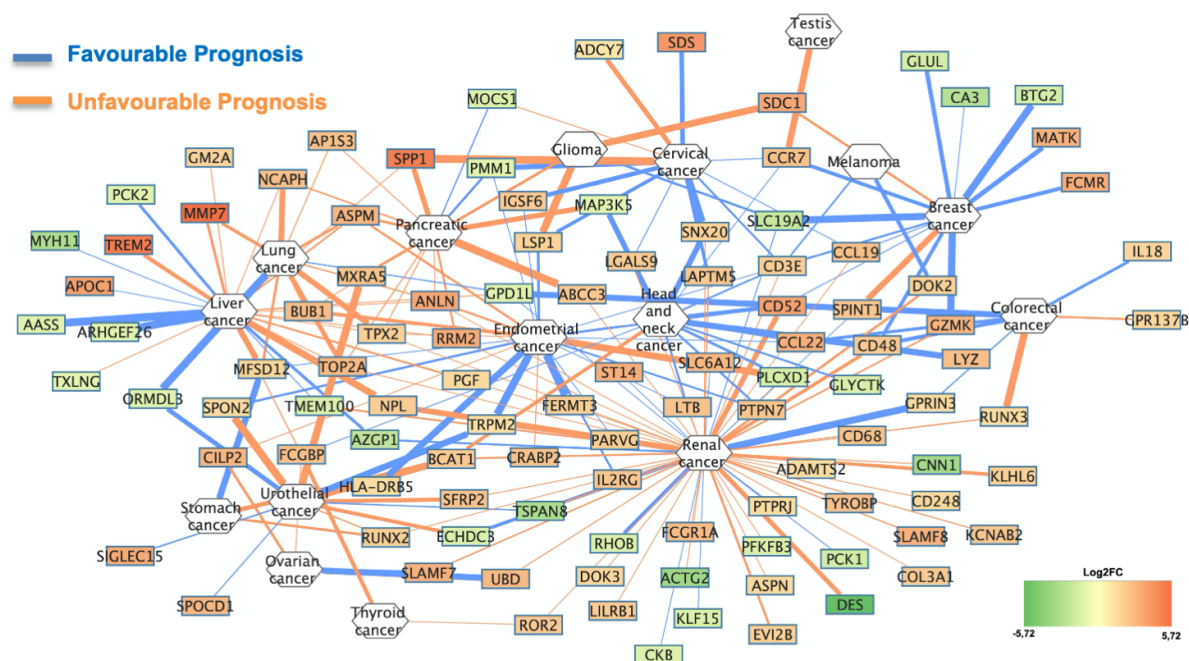


Figure 29: Gene-Cancer correlation network as obtained with the NDEx database. The edges color indicates the prognosis (favorable in blue and unfavorable in orange) and the color scale for the genes represents the genes FC.

4.2.1.9. DE RNAs correlations with nutritional and metabolic diseases

As previously reported, metabolic complications of obesity can lead to the development of metabolic diseases (Grundy et al. 2004), and for this reason the DisGeNET database was investigated in order to identify the interactions between DE RNAs and Nutritional and Metabolic Diseases, as obtained from curated databases (Figure 30). It is possible to notice how these diseases include also central nervous system diseases with a metabolic component, such as central nervous system inborn metabolic diseases, brain metabolic diseases, amyotrophic lateral sclerosis, semantic dementia etc., along with other metabolic diseases such as celiac disease, Tay-Sachs diseases and many more.

As obesity and diabetes are the main focus of this thesis work, these two diseases were specifically investigated expanding the search to all known databases and depicting all known correlations (Figure 31b). 49 genes were found to be associated with obesity (Figure 31a) and 35 with diabetes. It would be especially interesting to see if modulating disease parameters the deregulation in these DE RNAs would revert, and moreover specific attention should be put to those that are diabetes susceptibility genes, in order to prevent the development of the diabetic co-morbidity.

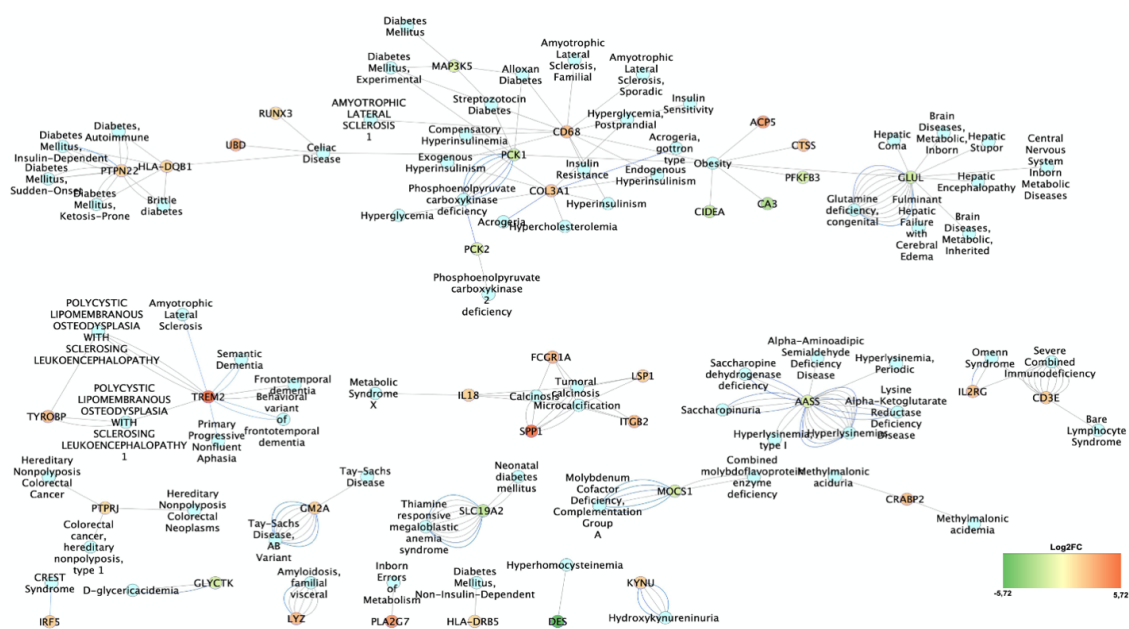


Figure 30: DisGeNET analysis shows the terms implicated in nutritional and metabolic diseases in SAT from OBF vs NW. The lines connecting the genes to the disease term represent the literature evidence for the terms' implication in the disease. The color scale represents the genes FC.

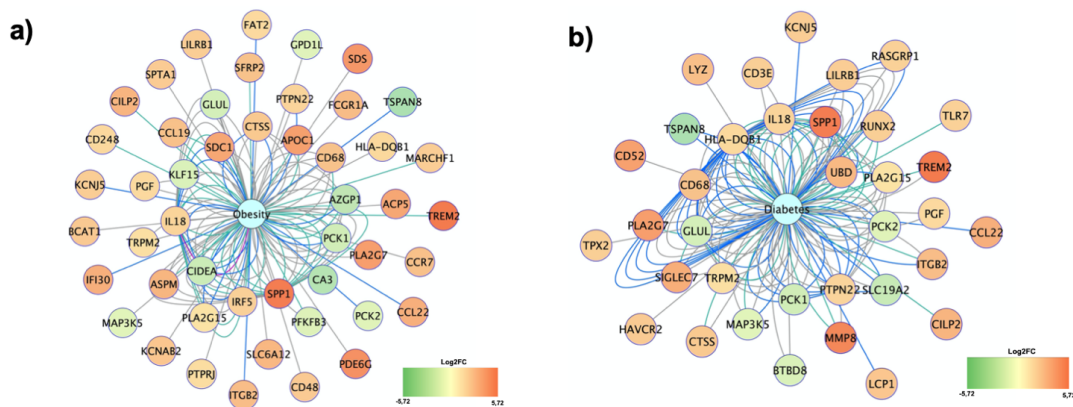


Figure 31: DisGeNET analysis shows the terms implicated in obesity (a) and diabetes (b) in SAT from OBF vs NW. The lines connecting the genes to the disease term represent the literature evidence for the terms' implication in the disease. The color scale represents the genes FC.

4.2.1.10. Identification of DE RNAs associated diseases

The last analysis performed for this dataset consisted in investigating the ClinVar database. This highlights all diseases potentially associated with a list of DE RNAs (Figure 32). An incredibly high number of diseases emerge, suggesting that obesity could be correlated with the insurgence of even more pathogeneses than we thought.

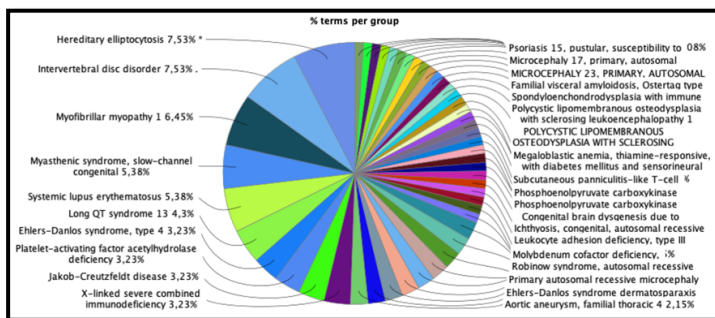


Figure 32: ClueGO analysis for GO Immune System Processes. Each pie segment refers to the % of terms present per group (*p<0.05 vs NW).

4.2.2. Transcriptional characterization of SAT of OBT2D vs. NW

The second experimental condition analyzed was the transcriptional changes occurring between OBT2D and NW. Also in this case, a full characterization of the expression profile, along with the identification of significant deregulated pathways and disease-implications was performed.

4.2.2.1. Expression profiles of SAT of obese OBT2D vs. NW

Heatmap (Figure 33a) and PCA (Figure 33b) were displayed to evaluate the expression profiles obtained through the analysis. Both visualizations highlighted different expression profiles, showing that also T2D strongly impacts cellular features and gene expression in SAT. The clustering analysis reported in the top part of the heatmap showed that the SAT from OBT2D (DIABETES) and from NW (CTRL) belonged to two different "families", i.e. CTRL colored in light blue and DIABETES in pink. The PCA visualization (Figure 33b) also showed that the samples per each condition appeared separated and grouped together, indicating a similarity amongst CTRL and DIABETES, but relevant differences between the two conditions. The single genes found were displayed through a volcano plot (Figure 33c) and the DE RNAs were reported in red.

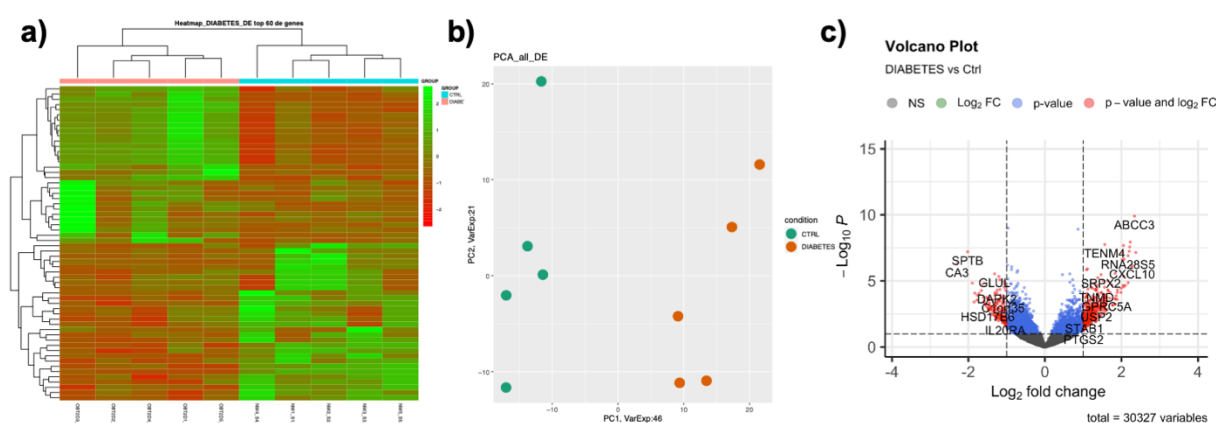


Figure 33: Transcriptional profile between SAT of T2D (DIABETES) and NW (CTRL) reported as heatmap (a) PCA (b), and volcano plot (c) where genes that respected the condition in terms of \log_2FC and FDR are reported in red, non-differentially expressed genes in grey, while genes that respected only one condition in blue.

Specifically, a total of 259 DE RNAs were detected in SAT tissue from obese OBT2D versus NW (Table 9). Of these, 175 were coding genes (mRNAs; 101 up-regulated DE RNAs and 74 down-regulated DE RNAs) and 84 were non-coding genes (ncRNAs; 71 up-regulated DE RNAs and 13 down-regulated DE RNAs).

Table 9: Number of DE RNAs in SAT of OBT2D vs. NW subjects.

| OBT2D vs. NW | | | |
|-----------------------|------------|-----------|------------|
| | mRNAs | ncRNAs | Total |
| Up-Regulated | 101 | 71 | 172 |
| Down-Regulated | 74 | 13 | 87 |
| Total | 175 | 84 | 259 |

The full list characterization of the ncRNAs is reported in Table 10, with a classification of these ncRNAs for their specific biotype. It is possible to observe how the most abundant

category are both snoRNAs and novel RNAs whose biotype could not be defined by any other parameter (miscRNAs).

Table 10: Biotype characterization of differentially expressed ncRNAs.

| | ncRNAs | | |
|------------------------------------|--------------|----------------|-----------|
| | Up-Regulated | Down-Regulated | Total |
| NATs | 0 | 4 | 4 |
| lncRNAs | 9 | 0 | 9 |
| Mt tRNA | 0 | 4 | 4 |
| Processed pseudogene | 5 | 2 | 7 |
| Transcribed unprocessed pseudogene | 1 | 0 | 1 |
| Transcribed processed pseudogene | 0 | 2 | 2 |
| Unprocessed pseudogene | 2 | 0 | 2 |
| miscRNA | 19 | 0 | 19 |
| scaRNA | 3 | 0 | 3 |
| scRNA | 1 | 0 | 1 |
| snRNAs | 9 | 0 | 9 |
| snoRNAs | 19 | 0 | 19 |
| TEC | 2 | 0 | 2 |
| IG C Gene | 1 | 0 | 1 |
| TR C Gene | 0 | 1 | 1 |
| Total | 71 | 13 | 84 |

4.2.2.2. Analysis of deregulated genes: a focus on novel risk-genes

Firstly, a bibliographic analysis of previous literature was performed, in order to identify how many, amongst the 259 DE RNAs had been previously associated with T2D. This analysis (Figure 34) revealed that more than two thirds of the deregulated genes (63.3%) had never been associated with the diabetic condition. Even more in this condition, It is clear the need for functional investigation of DE RNAs, to obtain new insights in the molecular basis of diabetes.

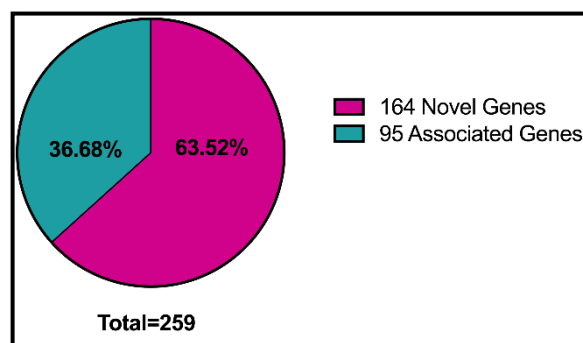


Figure 34: Ratio of novel and known genes for T2D.

The list of the un-characterized novel genes is the following: ABCC1; AC005921.4; AC006963.1; AC006978.1; AC007242.1; AC009812.4; AC010655.2; AC010655.3; AC036222.2; AC073082.1; AC073283.3; AC079601.1; AC113410.1; ACEA_U3; ACEA_U3, RNU3, U3; ACEA_U3, RNU3A1, U3-2B, U3a, U3b1, U3b2; ACEA_U3, U3; ACTG2; ADAMTS10; ADAMTS2; AF093117.1; AKR1B15; AL109920.1; AL133243.4; AL133330.1; AL135938.1; AL138762.1; AL139407.1; AL356273.5; AL513523.1; AL513523.2; ALDH1L1-AS2; ANKDD1A; AP006222.1; ARHGEF26; ATP6V1FNB; BCYRN1; C1orf35;

CASQ2; CD209; CECR2; CES1P2; CHST2; CNKSR2; CNN1; COL12A1; CRISPLD2; CTH; DES; DSCC1; EYA1; FAM161A; FANCE; FAT2; FAT3; FCGBP; FJX1; FTH1P15; GCHFR; GOLGA8H; GOLGA8J; GOLGA8T; GPR137B; HNRNPA1P66; HOMEZ; IFI44; ISG20; ITK; KLHL29; KLRC4-KLRK1; KRT7; LENG1; MARCHF1; MBNL1-AS1; MIR155HG; MIR4435-2HG; MOCS1; MT-TA; MT-TE; MT-TN; MT-TQ; MUC20; NAALAD2; NDRG4; NKD1; NR1D1; NSA2P2; OASL; P2RX6; PAG1; PAIP2B; PDCL3P5; PGM5P3-AS1; PI15; PIK3R5; PKNOX2; PKP2; PMAIP1; POLR2I; PPP1R10; PRSS36; PRUNE2; RASL10B; RASSF5; REC8; RFX2; RN7SL381P; RN7SL471P; RN7SL720P; RN7SL88P; RNA28S5; RNU1-1; RNU1-27P; RNU1-28P; RNU4-1; RNU4-2; RNVU1-15; RNVU1-18; RNVU1-29; RNVU1-7; RNY3P1; RP11-469M7.1; RPL23AP7; SCARNA13; SCARNA5; SCARNA6; SCUBE3; SECTM1; SH3TC1; SLC7A1; SLC7A5; SLCO4A1; SNHG3; SNORA16A; SNORA23; SNORA68; SNORA73A; SNORA73B; SNORA7A; SNORA7B; SNORD10; SNORD17; SNORD3A; SNORD3B-1; SNORD3B-2; SNORD3C; SNORD89; SPTB; SRPX2; ST13P15; STOX1; SYT17; TM7SF2; TMEM25; TSTD1; TUBB2A; TUBB2B; TUBB2BP1; UPP1; URAD; XYLT1; ZNF232; ZNF425; ZNF763.

4.2.2.3. Characteristics of DE RNAs: network interaction, tissue expression and cellular compartmentalization

Amongst all the DE RNAs, the top 20 deregulated genes based on their log₂FC are reported in Table 11. Along with protein coding genes, this list also includes tRNAs, rRNAs, lncRNAs and miscRNAs, suggesting an implication for the ncRNAs categories in diabetes. In this disease condition the immune system implication is even more relevant, with genes such as CSF3, CXCL10, CXCL11, GREM2, and LIF all implicated in this system.

Table 11: Top20 DE RNAs. Protein function description was obtained from the STRING database while a bibliographic search was performed for ncRNAs.

| Gene Name | FC | p value | Gene Function |
|-----------|-------|------------|--|
| CYP1A1 | -5.20 | 0.00049 | Cytochrome P450 1A1. In liver microsomes, this enzyme is involved in an NADPH-dependent electron transport pathway. It oxidizes a variety of structurally unrelated compounds, including steroids and fatty acids. |
| CSF3 | 4.96 | 0.00033 | Granulocyte colony-stimulating factor; Controls the production, differentiation, and function of granulocytes. |
| CXCL10 | 4.68 | 0.00000064 | C-X-C motif chemokine 10; Chemotactic for monocytes and T-lymphocytes. Binds to CXCR3; Belongs to the integrin alpha family. |
| MMP7 | 4.62 | 0.00054 | Matrilysin; Degrades casein, gelatins of types I, III, IV, and V, and fibronectin. Activates procollagenase. |
| URAD | 4.42 | 0.00012 | Catalyzes the stereoselective decarboxylation of 2-oxo- 4-hydroxy-4-carboxy-5-ureidoimidazole (OHCU) to (S)-allantoin. |
| CXCL11 | 4.41 | 0.000050 | C-X-C motif chemokine 11; Chemotactic for interleukin-activated T-cells but not unstimulated T-cells, neutrophils or monocytes. Induces calcium release in activated T-cells. Binds to CXCR3. |
| OASL | 4.14 | 0.00000090 | 2'-5'-oligoadenylate synthase-like protein; Can bind double-stranded RNA. Belongs to the 2-5A synthase family. |
| PI15 | -4.13 | 0.00017 | Peptidase inhibitor 15; Serine protease inhibitor which displays weak inhibitory activity against trypsin. |
| GREM2 | -3.99 | 0.00083 | Gremlin-2; Cytokine that inhibits the activity of BMP2 and BMP4 in a dose-dependent manner, and thereby modulates signaling by BMPs. |

| | | | |
|-------------------|-------|-------------|---|
| SERPINE1 | 3.96 | 0.0012 | Plasminogen activator inhibitor 1; Serine protease inhibitor. Its rapid interaction with PLAT may be a control point in fibrinolysis. |
| CA3 | -3.85 | 0.00000047 | Carbonic anhydrase 3; Reversible hydration of carbon dioxide. |
| DES | -3.84 | 0.00039 | Desmin; Muscle-specific type III intermediate filament essential for proper muscular structure and function. |
| MT-TQ | -3.68 | 0.00050 | Mt_tRNA, Mitochondrially encoded tRNA glutamine. |
| RNA28S5 | 3.63 | 0.00000011 | Processed pseudogene, represents the portion of one rDNA repeat encoding for 28S rRNA. |
| BMP3 | -3.59 | 0.000089 | Bone morphogenetic protein 3; Negatively regulates bone density. Antagonizes the ability of certain osteogenic BMPs to induce osteoprogenitor differentiation and ossification. |
| LIF | 3.54 | 0.000072 | Leukemia inhibitory factor; has the capacity to induce terminal differentiation in leukemic cells. |
| AL138762.1 | 3.48 | 0.000016 | misc_RNA, NAT to FAM178A. |
| SCUBE3 | -3.42 | 0.000015 | Signal peptide, CUB and EGF-like domain-containing protein 3; Binds to TGFBR2 and activates TGFB signaling. |
| MIR15HG | 3.35 | 0.00084 | lncRNA, microRNA host gene. Expressed at high levels in lymphoma and may function as an oncogene. |
| AC113410.1 | 3.27 | 0.000000091 | misc_RNA, unknown. |

The STRING database was used to visualize protein interaction networks in coding DE RNAs (Figure 35). It is possible to see that the proteins encoded by the genes interact in one main network, mainly comprising proteins of the immune system, and one smaller network, comprising of subunits of the RNA Polymerase II suggesting a disruption in transcription.

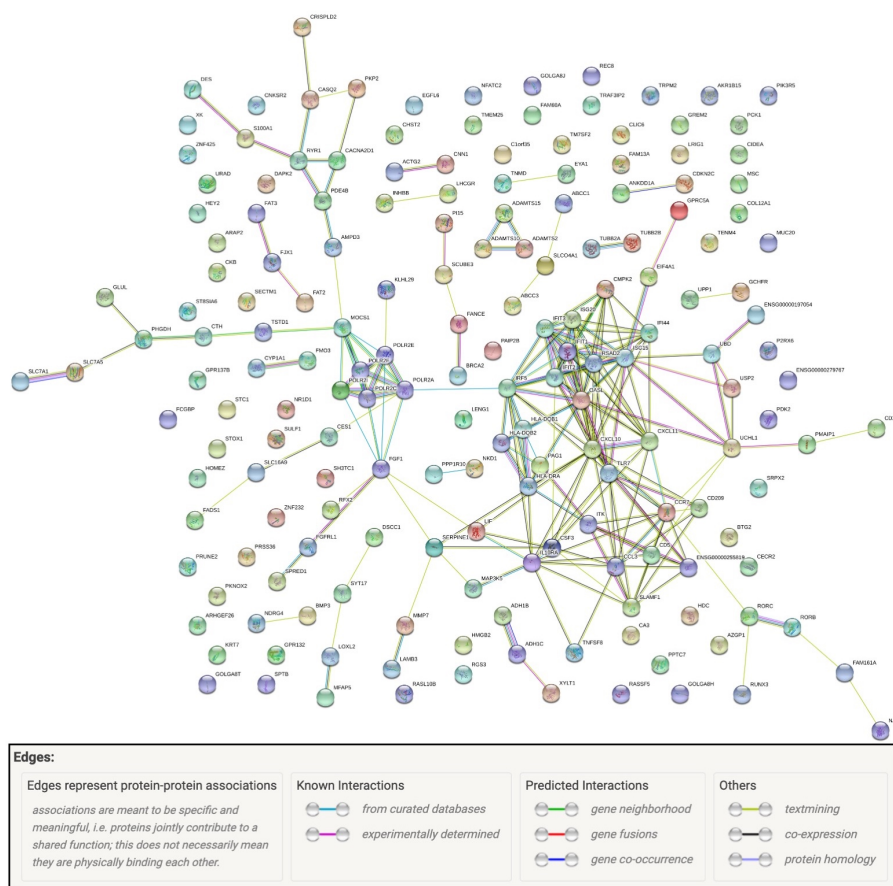


Figure 35: STRING Protein Network Interaction.

The genes expression and cellular localization were then investigated (Figure 36). Concerning tissue expression, genes deregulated in SAT of OBT2D are ubiquitary (Figure 36). These include muscle tissues, the genitourinary apparatus, the digestive system, the lymph node and many more (Figure 36a). The deregulated genes are ubiquitarily localized in the cytosol and nucleus, along with other organelles, and this kind of representation gives possible insights into where to functionally investigate the DE RNAs for further in vivo biological investigation (Figure 36b).

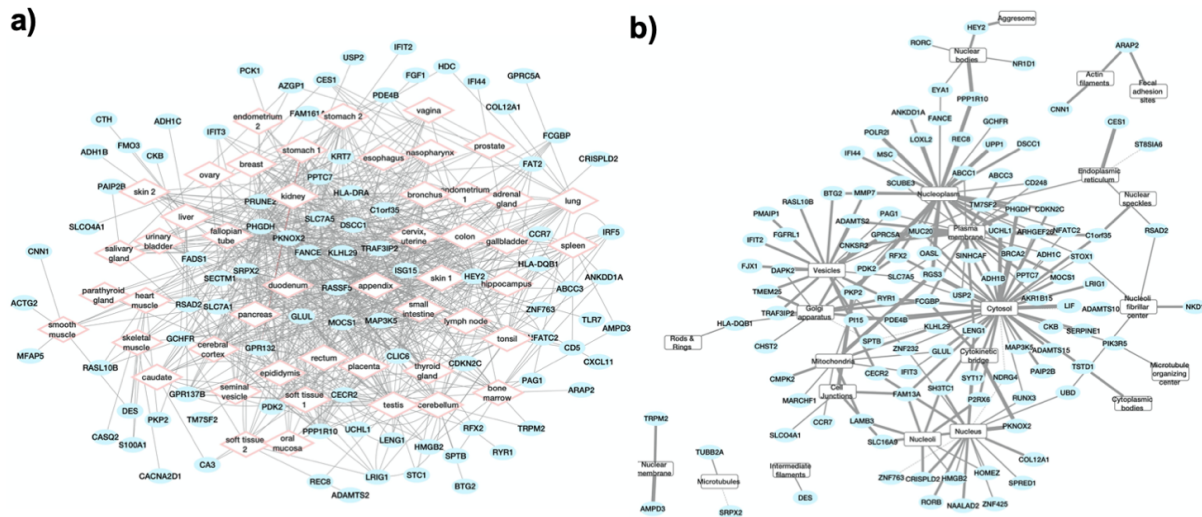


Figure 36: Tissue (a) and subcellular (b) localization of deregulated genes as obtained with the NDEx database.

4.2.2.4. Identification of co-regulating TFs

The TFs binding sites in the DE RNAs gene set were then identified (Figure 37). There does not seem to be a predominant regulator, and 17 TFs were identified. NFIC (Muhammad et al. 2017), MTA3 (He et al. 2016), STAT5 (Jackerott et al. 2006), NFE2 (Jin et al. 2020, Xiao et al. 2019), HSF1 (Chen, Ding, et al. 2017) have been previously correlated with T2D. HSF1 inhibition has been correlated with glucolipototoxicity-induced β -cells apoptosis (Purwana et al. 2017). Interestingly, the TF FOXM1 was found to be induced by obesity and stimulate β -cells proliferation, revitalizing their replicative potential and enhancing insulin secretion (Davis et al. 2010, Golson et al. 2015), whilst mice with the knock out in the TF PGR, present in this regulation network, have an improved glucose homeostasis secondary to β -cells proliferation (Picard et al. 2002). SMAD4 and SMAD1 impact autoimmune diabetes development (Kim, Lee, and Jun 2017, Seong, Manoharan, and Ha 2018, Kim et al. 2007) whilst LTF has also been found very recently to be differentially expressed in a Chinese cohort of type 1 diabetic patients (Yang et al. 2020). Moreover, SRY has been correlated with insulin resistance (Goldsworthy et al. 2008). FLI1 and NFATc1 were previously identified to regulate also the obesity DE RNAs network (Figure 12) and were never previously correlated to either diabetes or obesity. POLR2A, belonging to the polymerase category and with thus a constitutive function (Fagerberg et al. 2014) has never been correlated with obesity nor diabetes. Other TFs which were never correlated to diabetes before include T (TBXT), ELF1 and BCLAF1. This analysis allowed the association of TFs with specific targets in SAT of diabetes patients, thus providing new transcriptional pathways worth investigating.

The implication of the MHC complex and Golgi cisterna was supported by ClueGO analysis (Figure 39a) whilst the BiNGO analysis highlighted how the extracellular region and the sarcoplasmic reticulum are amongst the most overrepresented terms (Figure 39b).

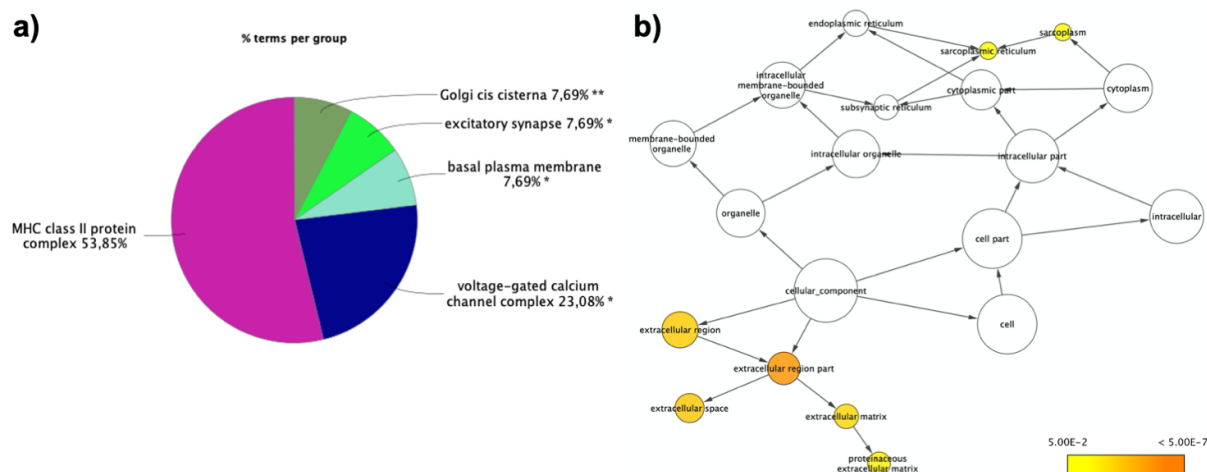


Figure 39: GO Cellular Component analysis. (a) ClueGO analysis for Cellular Component OBT2D vs NW. Each pie segment refers to the % of terms present per group (* $p < 0.05$, ** $p < 0.01$ vs NW) (b) BiNGO analysis for overrepresented Cellular Component terms in OBT2D vs NW. The hubs reported show the overrepresented terms.

The GO terms analysis in Molecular Function highlighted 281 pathways. The top 10 GO Molecular Functions supported the observation made in the cellular component analysis, as half of the terms relate to immunological activities (Figure 40). Interestingly, RNA polymerase II TF activity is also impaired, suggesting profound transcriptional deregulation.

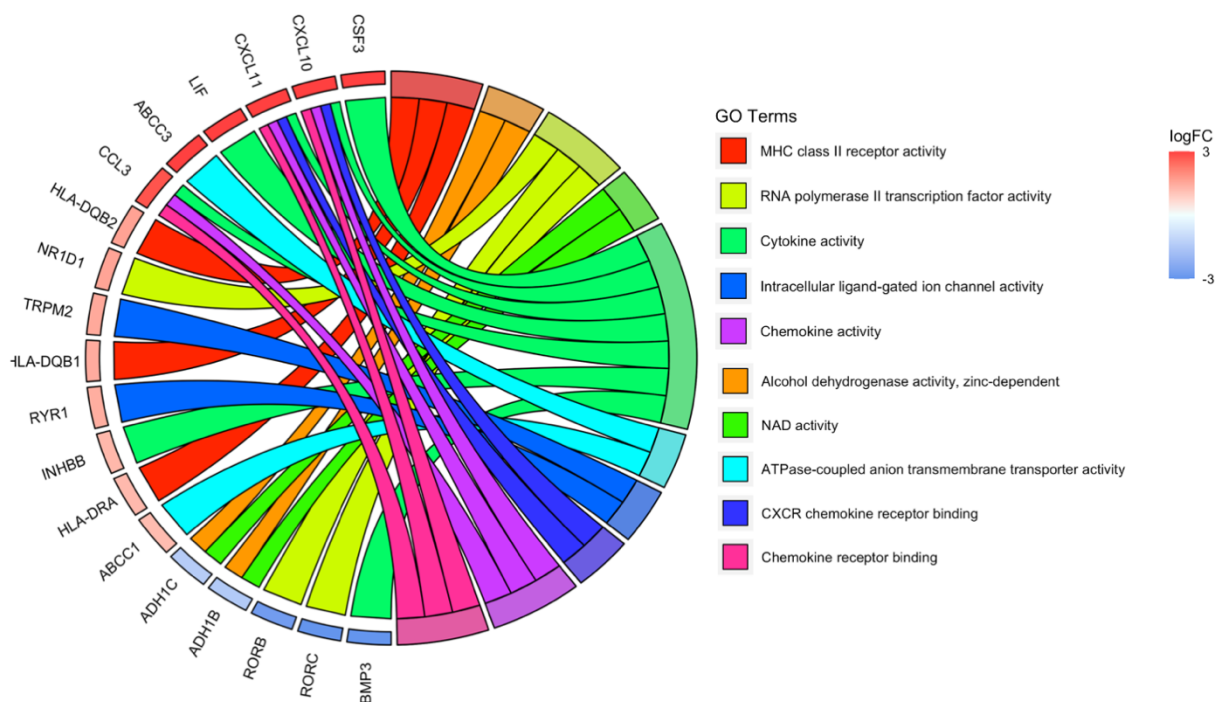


Figure 40: GO Chord Molecular Function analysis for DE genes in OBT2D vs NW. On the right the top 10 significant GO terms, whereas on the left the corresponding genes ordered according to \log_2FC .

Along with the previously mentioned components, the ClueGO analysis (Figure 41a) implicates nuclear receptor activity, heparin binding, and lyase activity, also found as an overrepresented term in BiNGO analysis (Figure 41b).

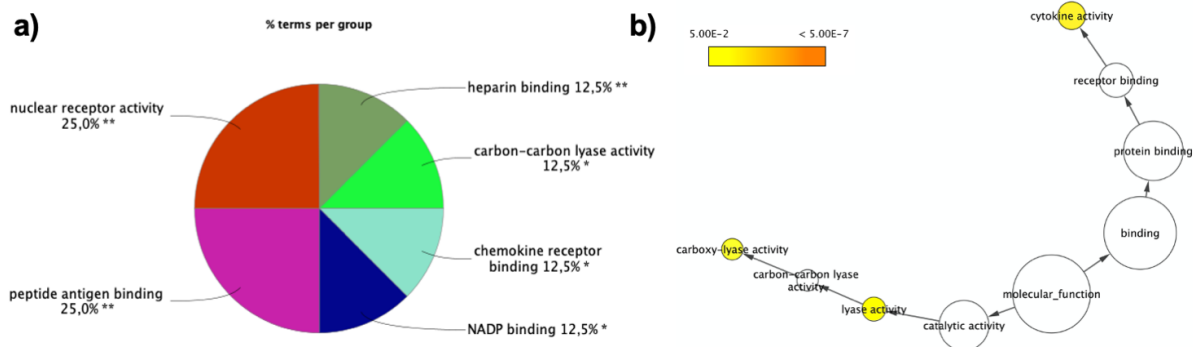


Figure 41: GO Molecular Function (a) ClueGO analysis in OBT2D vs NW. Each pie segment refers to the % of terms present per group (* $p < 0.05$, ** $p < 0.01$ vs NW) (b) BiNGO analysis in OBT2D vs NW. The hubs reported show the overrepresented terms.

The GO terms analysis for Biological Processes highlighted 1390 deregulated pathways, and the GO Chord graph reports the top 10 deregulated processes according to their significance (Figure 42). Again, 7 out of 10 of these processes pertained immune-related functions, indicating a highly inflammatory phenomenon occurring in T2D patients.

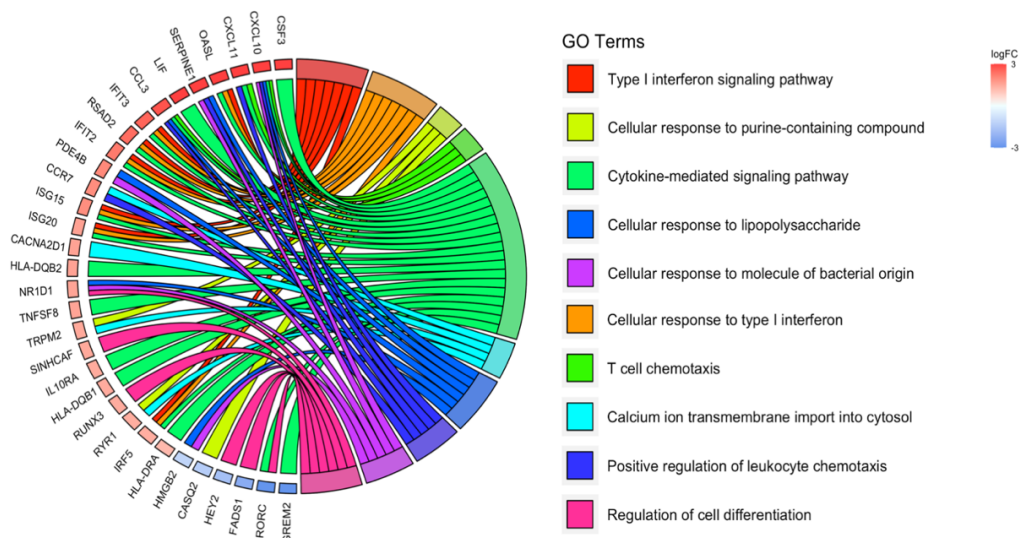


Figure 42: GO Biological Processes analysis for DE genes in SAT from OBT2D vs NW. On the right the top 10 significant GO terms, whereas on the left the corresponding genes ordered according to \log_2FC .

The ClueGO (Figure 43a) and BiNGO (Figure 43b) analyses support the immunological implication, and moreover ClueGO implicates calcium transport, angiogenesis, apoptosis, neuroinflammatory response and DNA catabolic processes.

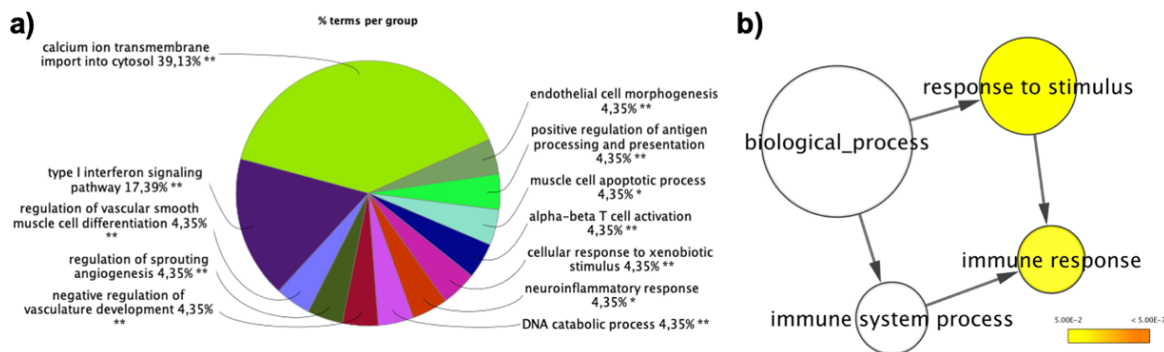


Figure 43: GO Biological Process. (a) ClueGO analysis in OBT2D vs NW. Each pie segment refers to the % of terms present per group (* $p < 0.05$, ** $p < 0.01$ vs NW) (b) BiNGO analysis in OBT2D vs NW. The hubs reported show the overrepresented terms.

4.2.2.6. Pathways characterization: top deregulated processes and implications for metabolic components.

The top 20 deregulated pathways ranked for their significance were visualized for KEGG (Figure 44a) and WikiPathways (Figure 44b). A strong metabolic component is represented, with nitrogen metabolism, glycolysis/gluconeogenesis, metabolism of xenobiotics, fatty acid omega oxidation, aa metabolism and many more found deregulated. Several pathways also implicated in immunological responses and also in this case there is a deregulation in the gene expression signature correlated with specific diseases.

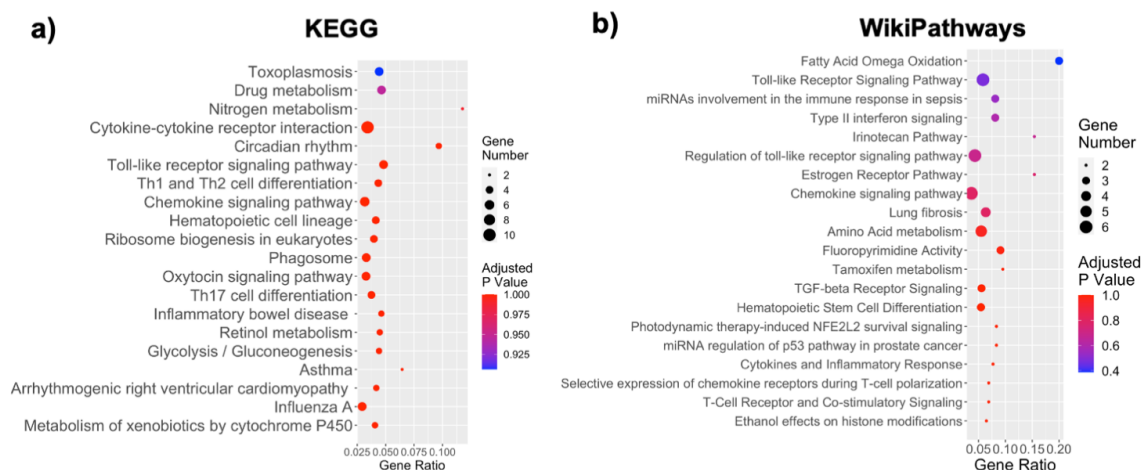


Figure 44: Dotplot of top 20 deregulated pathways after KEGG 2019 (a) and WikiPathways (b) analyses. The y-axis represents the name of the pathway, the x-axis represents the Rich factor, dot size represents the number of different genes and the color indicates the adjusted p-value.

The ClueGO analysis for KEGG interestingly highlighted RNA transport as the most significantly deregulated component ($p < 0.01$, Figure 45a) suggesting a strong impairment of physiologic functions. WikiPathways implicated the immunological response with a focus also on COVID-19 infection (Figure 45b). The Reactome database highlighted mostly immunological components (Figure 45c).

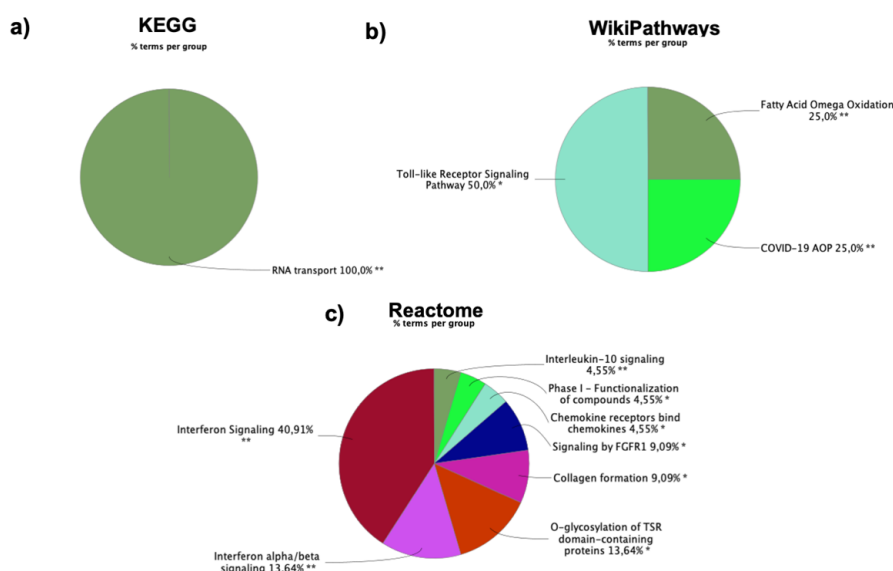


Figure 45: ClueGO analysis for KEGG (a), WikiPathways (b) and Reactome (c) in OBT2D vs NW. Each pie segment refers to the % of terms present per group (* $p < 0.05$, ** $p < 0.01$ vs NW).

Metabolic complications can aggravate obesity and be highly dysfunctional in diabetic patients (Grundy et al. 2004, Goetzman et al. 2018). The deregulated pathways related to these metabolisms are reported in Figure 46. Specifically, 10/170 KEGG and 7/183 terms for WikiPathways related to aa (Figure 46a), 6/170 for KEGG and 5/183 for WikiPathways related to lipids (Figure 46b) and 7/170 for KEGG and 2/183 for WikiPathways related to Carbohydrates (Figure 46c).

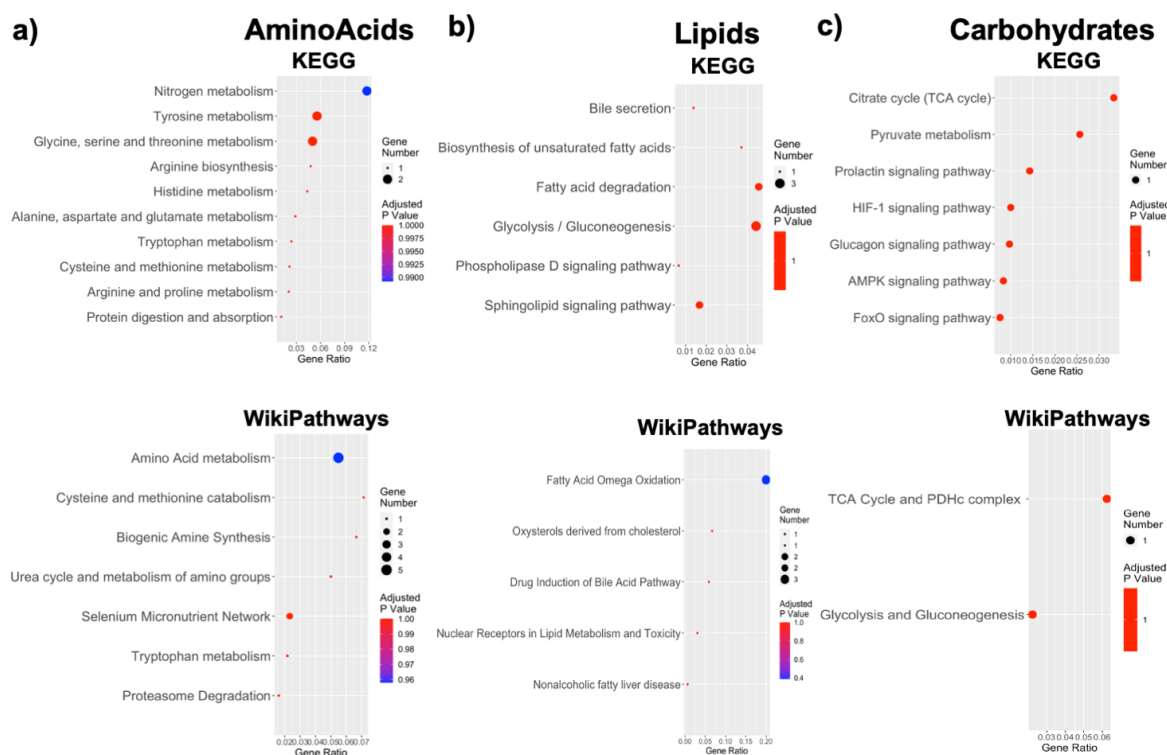


Figure 46: Dotplot of KEGG 2019 and WikiPathways analysis of pathways correlated with (a) aa metabolism, (b) lipids metabolism and (c) carbohydrates metabolism. The y-axis represents the name of the pathway, the x-axis represents the Rich factor, dot size represents the number of different genes and the color indicates the adjusted p-value.

Other deregulated metabolisms found in OBT2D include ABC transporters, vitamins, pyrimidine, specific drug metabolisms with many more suggesting a global alteration in the SAT metabolome of T2D patients (Figure 47).

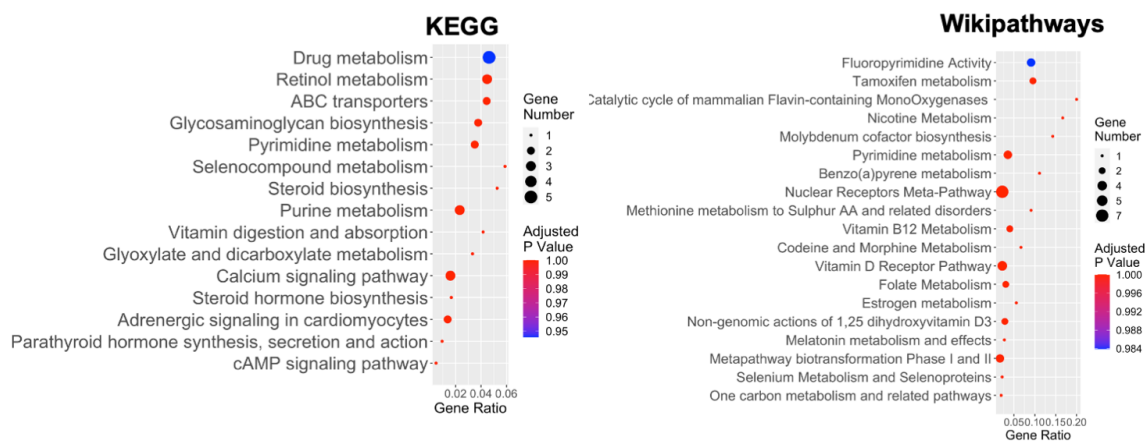


Figure 47: Dotplot of KEGG 2019 and WikiPathways analysis of pathways correlated with other metabolisms. The y-axis represents the name of the pathway, the x-axis represents the Rich factor, dot size represents the number of different genes and the color indicates the adjusted p-value.

Lastly, the specific pathways concerning adipogenesis were highlighted, and are also present when patients develop diabetes. These included a deregulation in adipogenesis, PPAR and insulin signaling pathways, and even thermogenesis (Figure 48).

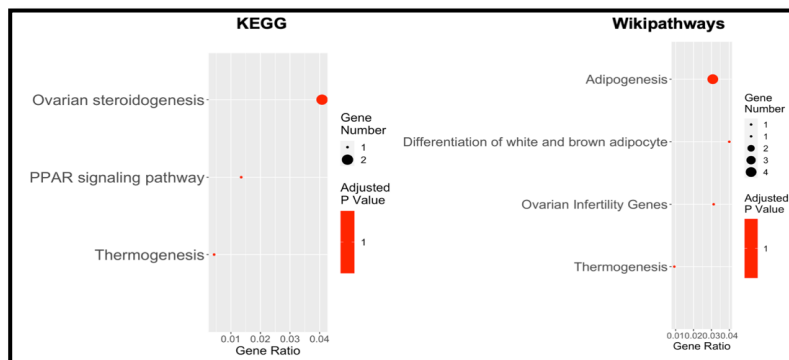


Figure 48: Dotplot of KEGG and WikiPathways analysis of pathways correlated with adipogenesis.

4.2.2.7. Analysis of the transcriptional immunological response in OBT2D

A more in depth analysis was then performed concerning immunological processes. 67 out of the 170 KEGG deregulated terms (39%) and 41 out of the 183 WikiPathways deregulated terms (22%) were correlated with the immunogenic phenomenon, suggesting that the DE RNAs deregulation reported profoundly impacts this system, with a higher susceptibility for subsequent co-morbidities insurgence (Figure 49).

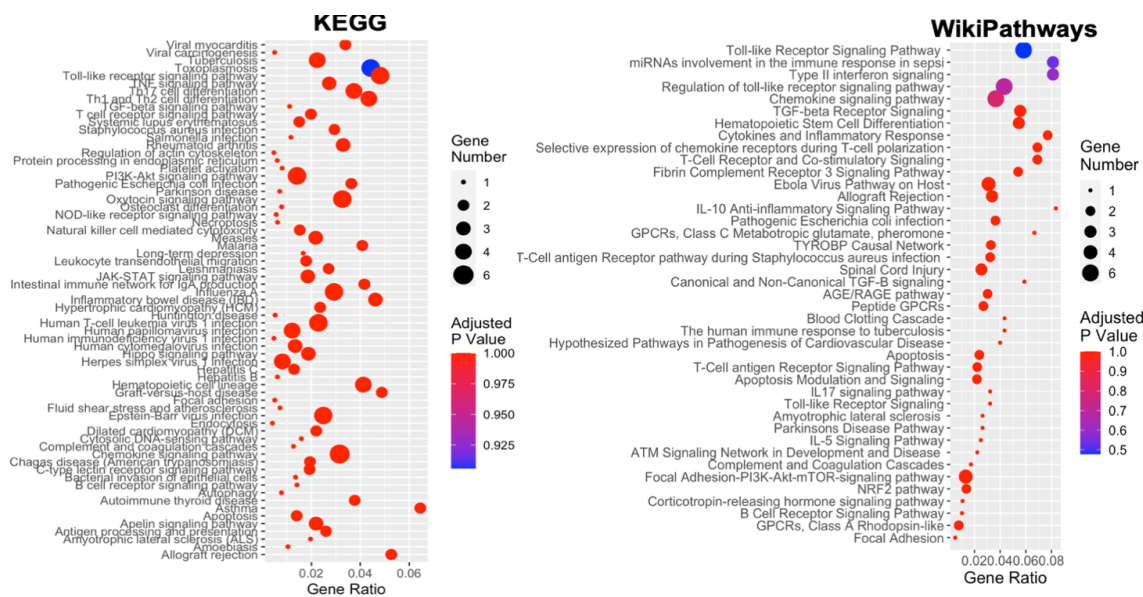


Figure 49: Dotplot of KEGG 2019 and WikiPathways analysis of immune system-related pathways. The y-axis represents the pathway, the x-axis represents the Rich factor, dot size represents the number of genes and the color the adjusted p-value.

Moreover, via ClueGO GO Immune System Processes database, it was possible to see that the two most represented categories concerned type I interferon signaling pathway and the positive regulation of antigen processing and presentation (Figure 50).

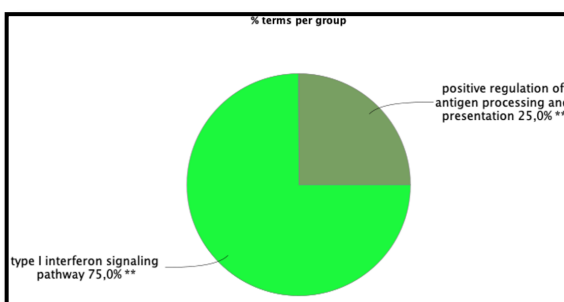


Figure 50: ClueGO analysis in OBT2D vs NW. Each pie segment refers to the % of terms present per group (**p<0.01 vs NW).

The following step was to interrogate the DisGeNET curated database, noting numerous deregulated genes linked with multiple immunological diseases (Figure 51). The upregulated CSF2 and HLA-DQB1 appear to be the genes implicated in the highest number of conditions, respectively mainly lymphoma and diabetes.

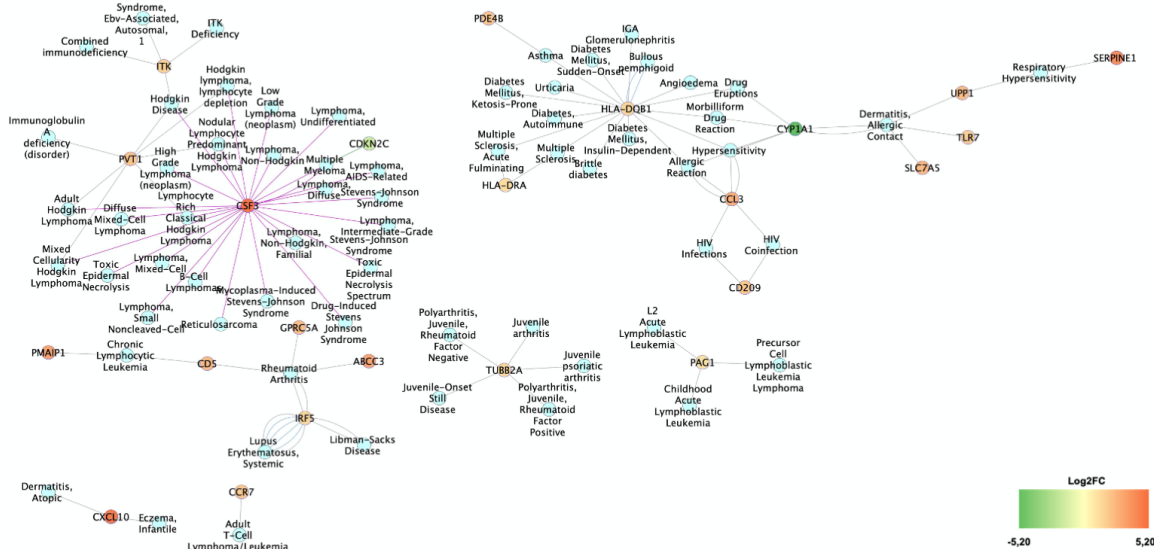


Figure 51: DisGeNET analysis shows the terms implicated in Immune Diseases in OBT2D vs NW. The lines connecting the genes to the disease term represent the literature evidence for the terms' implication in the disease.

4.2.2.8. Potential cancer implications: susceptibility in OBT2D

As it is with obesity and cancer, there is also a known correlation between diabetes and cancer (Giovannucci et al. 2010). The study thus aimed at the identification of the cancer-susceptibility signature in obese diabetic patients. 26 out of the 170 KEGG deregulated terms (15%) and 42 out of the 183 WikiPathways deregulated terms (23%) were correlated with oncogenesis (Figure 52).

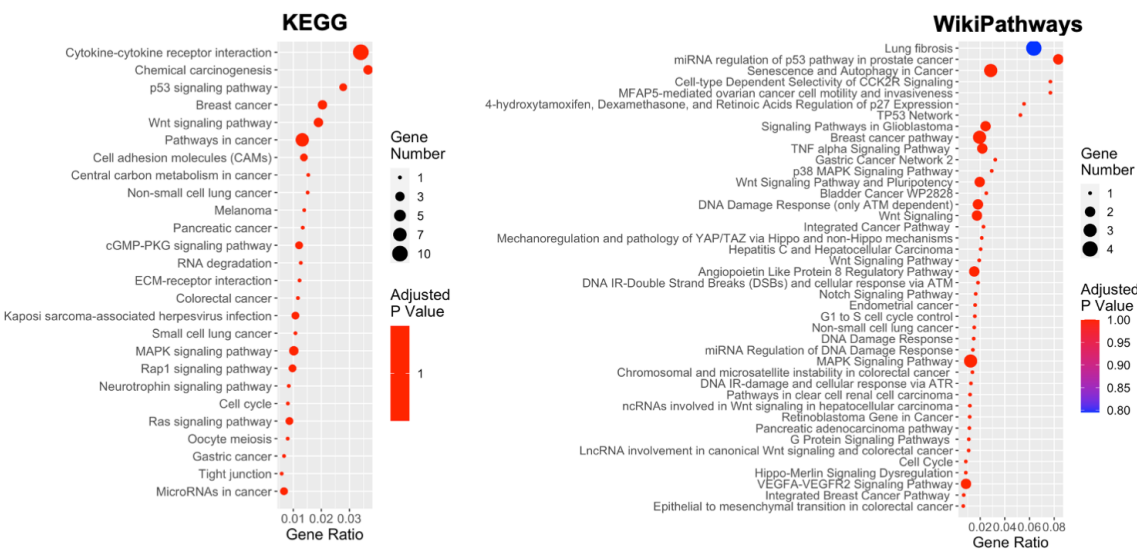


Figure 52: Dotplot of KEGG 2019 and WikiPathways analysis of oncogenesis-related pathways. The y-axis represents the name of the pathway, the x-axis represents the Rich factor, dot size represents the number of genes and the color indicates the adjusted p-value.

The DisGeNET database was investigated highlighting a susceptibility network reduced when compared to the obesity one, but still interesting (Figure 53). Indeed, it highlights how BRCA2, known for its implications in breast cancer, is upregulated, and there is also a deregulation in many genes, such as MMP7 and SERPINE1 implicated in gastric cancer.

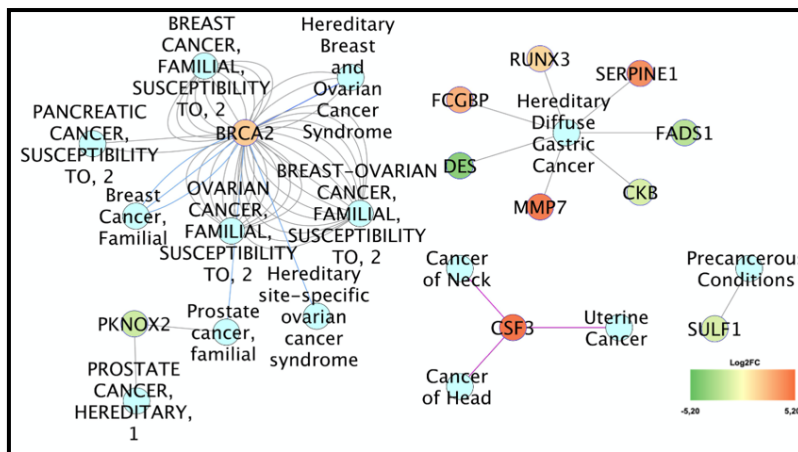


Figure 53: DisGeNET analysis shows the terms implicated in cancer in OBT2D vs NW. The lines connecting the genes to the disease term represent the literature evidence for the terms' implication in the disease. The color scale represents the genes FC.

The investigation of the NDEX database allowed the identification of a higher number of implicated genes (Figure 54). Also in this case, there seems to be a high number of genes with unfavorable prognosis correlated with renal cancer, whilst there seems to be reduced expression of genes correlating with a favorable prognosis for breast cancer.

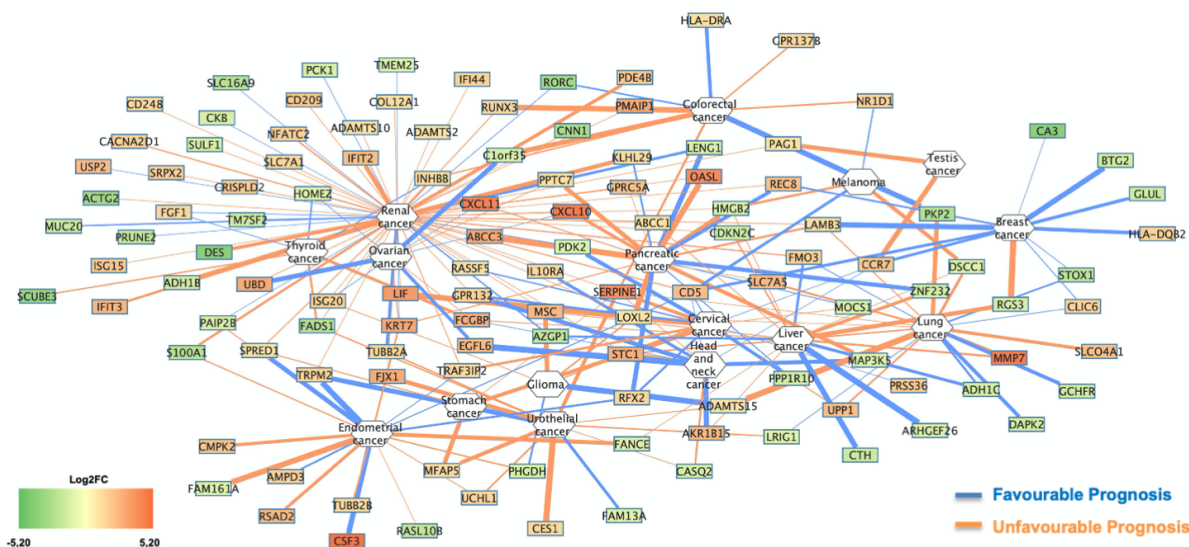


Figure 54: Gene-Cancer correlation network as obtained with the NDEX database. The edges color indicates the prognosis (favorable in blue and unfavorable in orange) and the color scale for the genes represents their FC.

4.2.2.9. DE RNAs correlations with nutritional and metabolic diseases

The DisGeNET database was investigated in order to identify the interactions between DE RNAs and Nutritional and Metabolic Diseases, as obtained from curated databases (Figure 55). It is possible to notice how these diseases include also central nervous system diseases with a metabolic component, along with other metabolic diseases such as Fanconi Anemia, celiac disease, and many more.

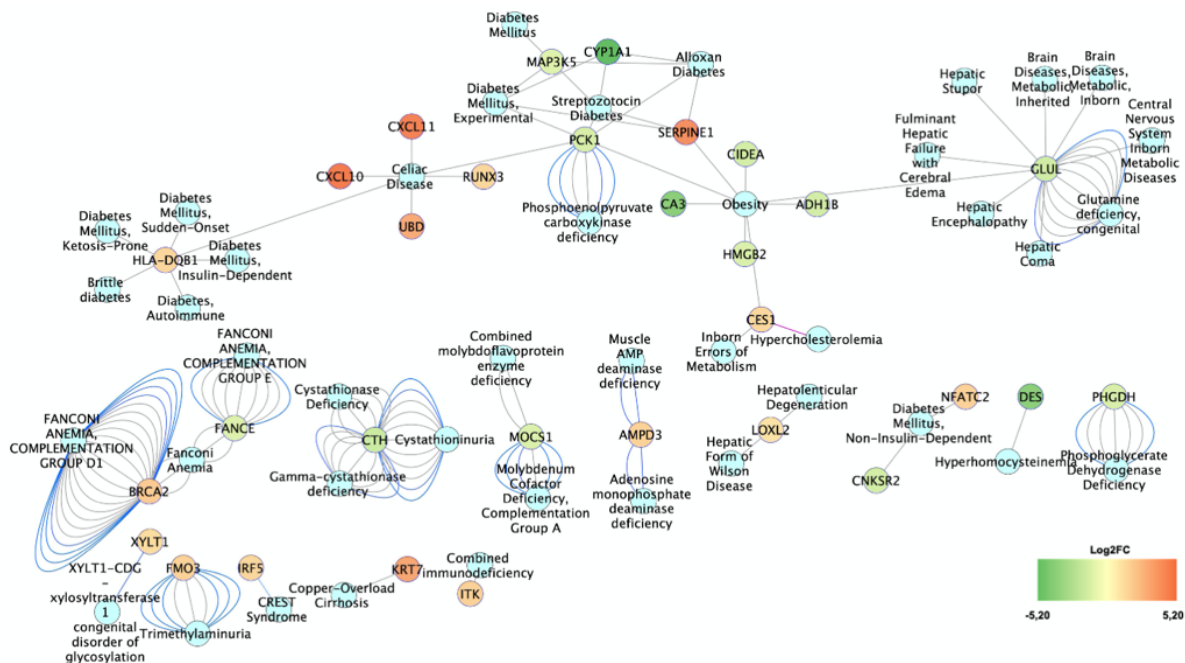


Figure 55: DisGeNET analysis shows the terms implicated in nutritional and metabolic diseases OBT2D vs NW.

When expanding the search to all known databases 48 genes were found to be associated with obesity (Figure 56a) and 40 with diabetes (Figure 56b). The most annotated gene correlated with obesity appears to be SERPINE1, whilst the most correlated with diabetes appears to be HLA-DQB1.

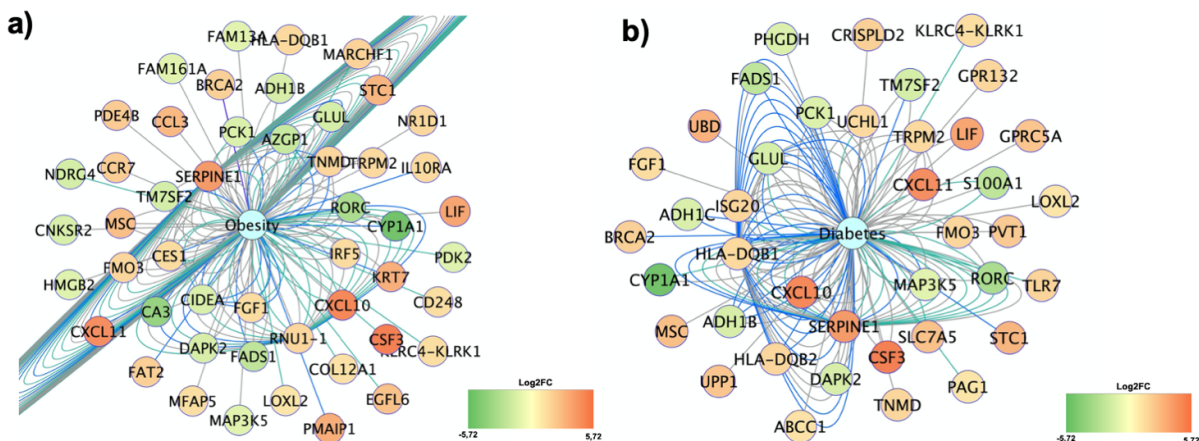


Figure 56: DisGeNET analysis shows the terms implicated in obesity (a) and diabetes (b) in SAT from OBT2D vs NW.

4.2.2.10. Identification of DE RNAs associated diseases

The last analysis performed for this dataset consisted in investigating the ClinVar database. This highlights all diseases potentially associated with a list of DE RNAs (Figure 57). Interestingly, 5 conditions emerge, and these are: susceptibility to HIV, cardiomyopathy, Alcohol dependence, Fanconi anemia and PD.

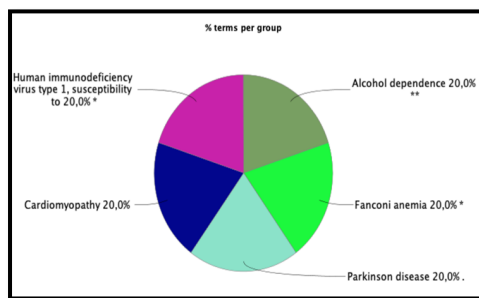


Figure 57: ClueGO analysis for ClinVar in OBT2D vs NW (* $p < 0.05$, ** $p < 0.01$ vs NW).

4.2.3. Transcriptional characterization of SAT of OBT2D vs. OBF

The last experimental condition analyzed was the transcriptional difference occurring between OBT2D and OBF. The aim was to identify the molecular signature responsible for the development of the diabetic comorbidity. Also in this case, a full characterization of the expression profile, along with the identification of deregulated pathways and disease-implication was performed.

4.2.3.1. Expression profiles of SAT of OBT2D vs. OBF

Heatmap (Figure 58a) and PCA (Figure 58b) were displayed to evaluate the expression profiles obtained through the analysis. Both visualizations highlighted different expression profiles, suggesting also T2D strongly impacts cellular features and gene expression in SAT. The clustering analysis reported in the top part of the heatmap showed that the SAT from OBT2D (DIABETES) and from OBF belonged to two different "families" except for one sample.

The PCA visualization (Figure 58b) also showed that the samples per each condition appeared separated and grouped together, indicating a highly differential expression. The single genes found were displayed through a volcano plot (Figure 58c) and the DE RNAs were reported in red. Indeed, it is possible to observe in this case how genes are mostly up-regulated.

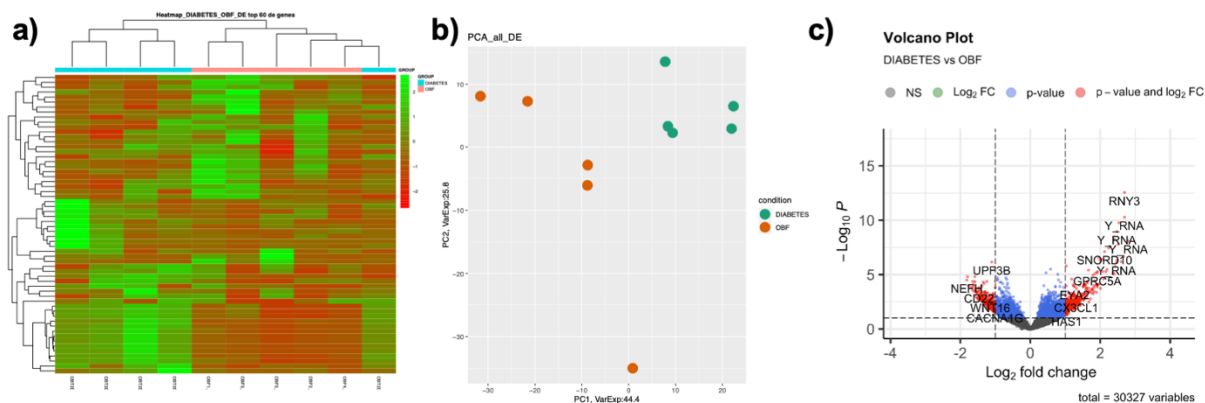


Figure 58: Transcriptional profile between SAT of DIABETES and OBF reported as heatmap (a) PCA (b), and volcano plot (c) where genes that respected the condition in terms of \log_2FC and FDR are reported in red, non-differentially expressed genes in grey, while genes that respected only one condition in blue.

Specifically, a total of 149 DE RNAs were detected in OBT2D versus OBF (Table 12). Of these, 71 were coding genes (mRNAs; 25 up-regulated DE RNAs and 46 down-regulated DE RNAs) and 78 were non coding genes (ncRNAs; 69 up-regulated DE RNAs and 9 down-regulated DE RNAs).

Table 12: Number of DE RNAs in the SAT of OBT2D vs. OBF.

| OBT2D vs. OBF | | | |
|----------------|-----------|-----------|------------|
| | mRNAs | ncRNAs | Total |
| Up-Regulated | 25 | 69 | 94 |
| Down-Regulated | 46 | 9 | 55 |
| Total | 71 | 78 | 149 |

The full list characterization of the ncRNAs is reported in Table 13, with a full classification of these ncRNAs for their specific biotype. It is possible to observe how the most abundant categories are both snRNAs (21 DE RNAs) and miscRNAs (24 DE RNAs). Another class highly represented are snoRNAs, with 14 DE RNAs. A number of other categories are represented, such as NATs lincRNAs, lincRNAs and other lincRNAs classes. Moreover, transcribed unprocessed, transcribed processed and unprocessed pseudogenes are also found deregulated, one for each category, along with one rRNA and one sense intronic RNA.

Table 13: Biotype characterization of differentially expressed ncRNAs.

| ncRNAs | | | |
|------------------------------------|--------------|----------------|-----------|
| | Up-Regulated | Down-Regulated | Total |
| NATs | 0 | 2 | 2 |
| lincRNAs | 2 | 1 | 3 |
| Other lincRNAs | 3 | 1 | 4 |
| Processed pseudogene | 1 | 2 | 3 |
| Transcribed unprocessed pseudogene | 0 | 1 | 1 |
| Transcribed processed pseudogene | 0 | 1 | 1 |
| Unprocessed pseudogene | 0 | 1 | 1 |
| miscRNA | 24 | 0 | 24 |
| rRNA | 1 | 0 | 1 |
| scaRNA | 2 | 0 | 2 |
| Sense intronic | 1 | 0 | 1 |
| snRNAs | 21 | 0 | 21 |
| snoRNAs | 14 | 0 | 14 |
| Total | 69 | 9 | 78 |

4.2.3.2. Analysis of deregulated genes: a focus on novel risk-genes

Firstly, a bibliographic analysis of previous literature was performed, in order to identify how many, amongst the 149 DE RNAs had been previously associated with either obesity or diabetes. This analysis (Figure 59) revealed that 71.14% of the genes had never been associated with either the diabetic or obesogenic condition. Even more in this condition, this highlights the need for functional investigation of DE RNAs, to obtain new insights in the molecular basis of diabetes. The list of the un-characterized novel genes is the following: 5_8S_rRNA; AC006963.1; AC007242.1; AC008158.1; AC009131.1; AC016705.2; AC017007.1; AC024051.1; AC024051.11; AC024051.2; AC024051.3; AC024051.4; AC024051.6; AC024051.7; AC024575.1; AC036222.2; AC051619.7; AC079601.1;

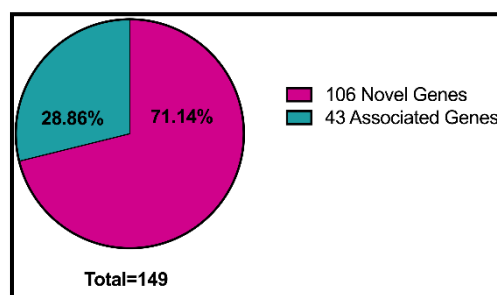


Figure 59: Ratio of novel and known genes for diabetes and obesity.

AC090181.2; AC090527.1; AC107021.2; AC113410.1; AF093117.1; AL109920.1; AL135938.1; AL138762.1; AL160313.1; AL356273.5; AL356299.1; AL391647.2; AL513523.1; AL513523.2; AL845331.2; CFDP1; CIR1; DIRAS1; FHAD1; FRMPD4; GABRB3; GOLGA6L17P; GPR78; GRIN3A; KCNE1B; KIF26B; LEO1; MAGED4; MFAP1; MUC20; MUC20P1; NEFH; NKX3-1; NRK; NSA2P2; OASL; PIEZO2; PLCXD1; PRRG3; PTMS; PYCR1; RFX2; RNA28S5; RNU1-1; RNU1-2; RNU1-27P; RNU1-28P; RNU1-3; RNU1-4; RNU2-1; RNU4-1; RNU4-2; RNVU1-18; RNVU1-28; RNVU1-29; RNVU1-2A; RNVU1-7; RNY3P1; ROR2; RP11-469M7.1; RP11-815I9.4; RP3-461P17.10; RPL23AP7; SCARNA13; SCARNA6; SEL1L2; SLC28A3; SLC7A5; SMARCE1P3; SNORA23; SNORA48; SNORA54; SNORA63; SNORA68; SNORA7A; SNORA7B; SNORD10; SNORD13; SNORD17; SNORD33; SNORD3C; TCEAL3; TMEM79; TXNDC2; UPF3B; WDR74; ZMIZ1-AS1; ZNF425.

4.2.3.3. Characteristics of DE RNAs: network interaction, tissue expression and cellular compartmentalization

Amongst all the DE RNAs, the top 20 deregulated genes based on their log₂FC are reported in Table 14. The majority of this list consisted in miscRNAs, indicating that ncRNAs could be of crucial relevance in disease progression and that there is a lot yet to be characterized which could be responsible of the development of the diabetic comorbidity.

Table 14: FC of top20 DE RNAs.

| Gene Name | FC | p value | Gene Function |
|------------|-------|--------------|---|
| AL391647.2 | 5.99 | 0.0000059 | misc_RNA; unknown function |
| CXCL8 | 5.56 | 0.000099 | Interleukin-8; IL-8 is a chemotactic factor that attracts neutrophils, basophils, and T-cells, but not monocytes. It is released from several cell types in response to an inflammatory stimulus. |
| 5_8S_rRNA | 5.55 | 0.00048 | rRNA; unknown function. |
| AC016705.2 | -5.20 | 0.00082 | lncRNA; unknown function. |
| AC008158.1 | 5.10 | 0.000079 | misc_RNA; unknown function. |
| AC036222.2 | 4.95 | 0.00000024 | misc_RNA; sense intronic to SKAP1, unknown function. |
| TXNDC2 | -4.91 | 0.00038 | Thioredoxin domain-containing protein 2; Probably plays a regulatory role in sperm development. |
| AL356273.5 | 4.86 | 0.00000072 | misc_RNA; unknown function. |
| AL513523.2 | 4.68 | 0.0000020 | misc_RNA; unknown function. |
| AC024575.1 | 4.58 | 0.00015 | misc_RNA; NAT to SWSAP1, unknown function. |
| AL513523.1 | 4.52 | 0.00000078 | misc_RNA; unknown function. |
| AC007242.1 | 4.42 | 0.00000050 | misc_RNA; unknown function. |
| AC113410.1 | 4.39 | 0.0000000097 | misc_RNA; unknown function. |
| AL138762.1 | 4.37 | 0.000010 | misc_RNA; unknown function. |
| AC017007.1 | 4.33 | 0.000103 | misc_RNA; unknown function. |
| AF093117.1 | 4.30 | 0.0000077 | misc_RNA; unknown function. |
| AL160313.1 | 4.20 | 0.00027 | misc_RNA; unknown function. |
| PTGS2 | 4.19 | 0.00016 | Prostaglandin G/H synthase 2; Converts arachidonate to prostaglandin H2 (PGH2), a committed step in prostanoid synthesis. Responsible for production of inflammatory prostaglandins. |
| SLC28A3 | -4.14 | 0.00057 | Solute carrier family 28 member 3; Involved in the homeostasis of endogenous nucleosides. |
| OASL | 3.98 | 0.0000032 | 2'-5'-oligoadenylate synthase-like protein; Does not have 2'-5'-OAS activity, but can bind double- stranded RNA. |

The STRING database was used to visualize the present interaction networks in coding DE RNAs (Figure 60). It is possible to see that the proteins encoded by the genes interact in one main network, comprising proteins of the immune system, and two smaller ones.

The genes expression and cellular localization were then investigated (Figure 61). Concerning tissue expression, genes pertaining to the switch from obesity to the diabetic comorbidity are ubiquitous (Figure 61a). The DE RNAs are also localized in the cytosol and nucleus, along with other organelles, and this kind of representation gives possible insights into where to functionally investigate the DE RNAs for further in vivo biological investigation (Figure 61b).

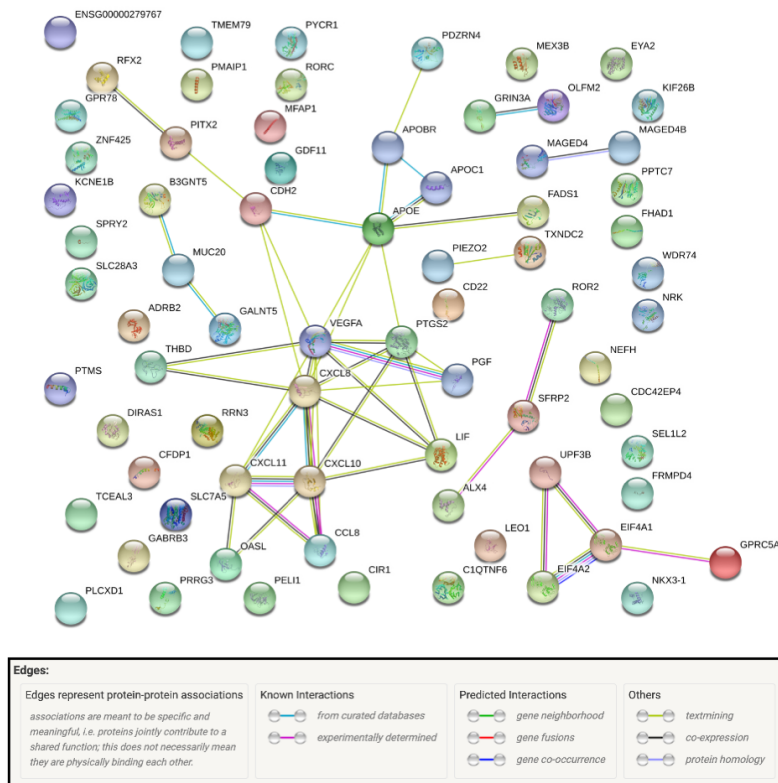


Figure 60: STRING Protein Network Interaction.

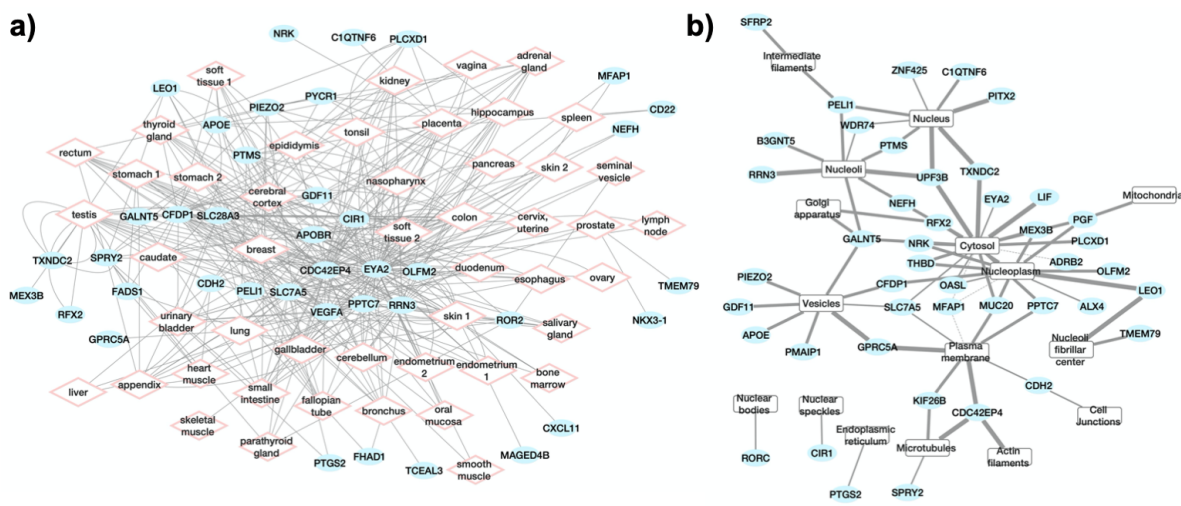


Figure 61: Tissue (a) and subcellular (b) localization of deregulated genes as obtained with the NDEx database.

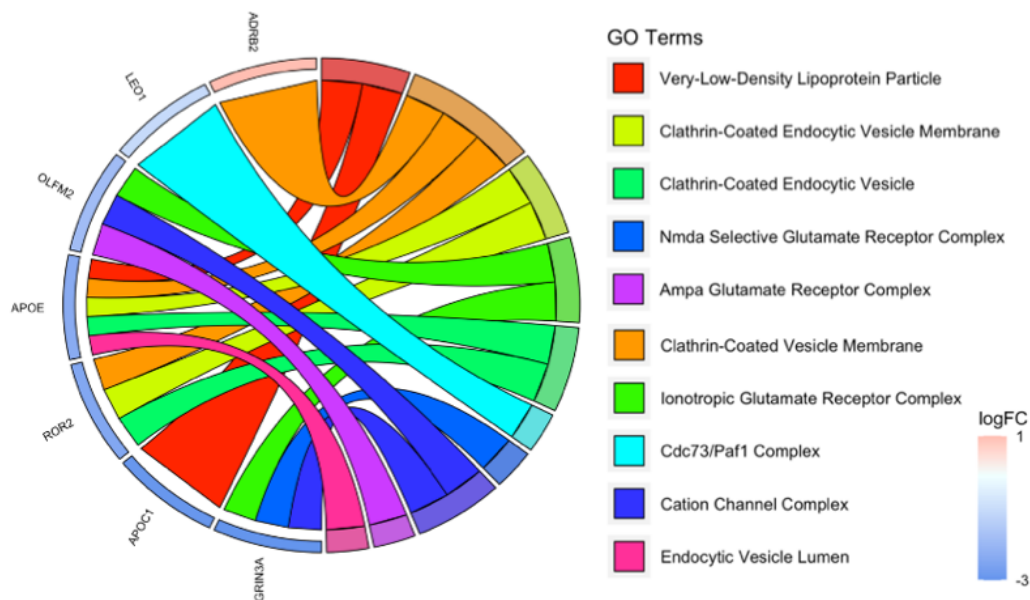


Figure 63: GO Chord Cellular Component analysis for DE genes in OBT2D vs. OBF. On the right the top 10 significant terms, whereas on the left the corresponding genes ordered according to log2FC.

The implication for chylomicron was supported by ClueGO analysis (Figure 64a) and by BiNGO analysis (Figure 64b).

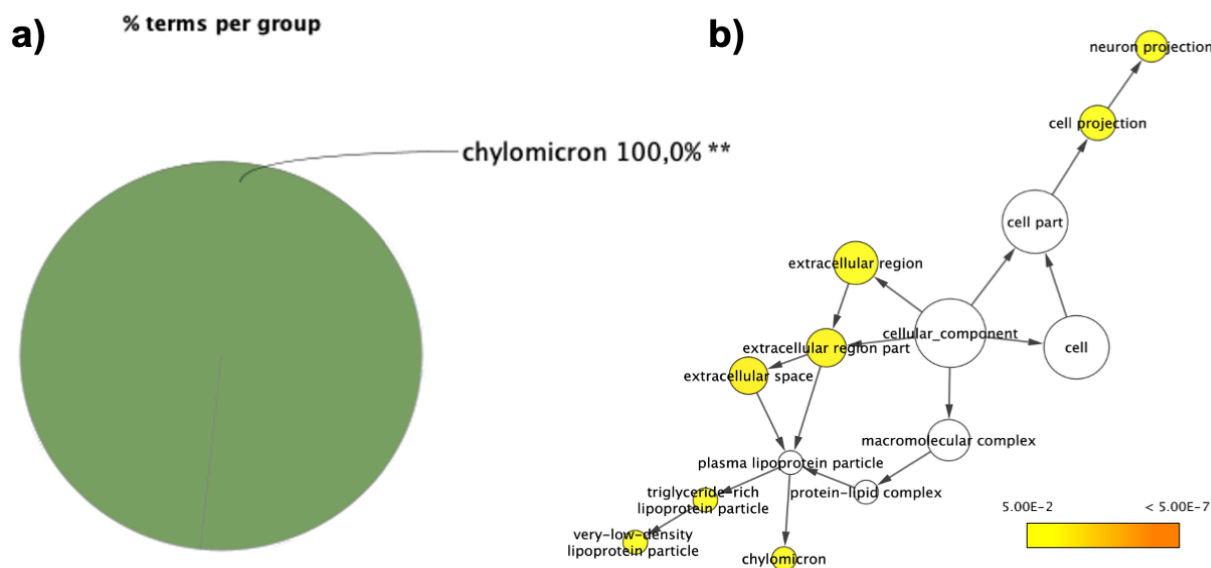


Figure 64: GO Cellular Component analysis. (a) ClueGO analysis for Cellular Component in OBT2D vs. OBF. Each pie segment refers to the % of terms present per group (** $p < 0.01$ vs Obese SAT) (b) BiNGO analysis for overrepresented Cellular Component terms in OBT2D vs. OBF. The hubs reported show the overrepresented terms.

The GO terms analysis in Molecular Function highlighted 179 pathways. The top 10 GO Molecular Functions highlighted again an implication for the immune system, with chemokine and cytokine activity (Figure 65). Moreover, the RNA polymerase I core binding activity is implicated, along with growth factor activity.

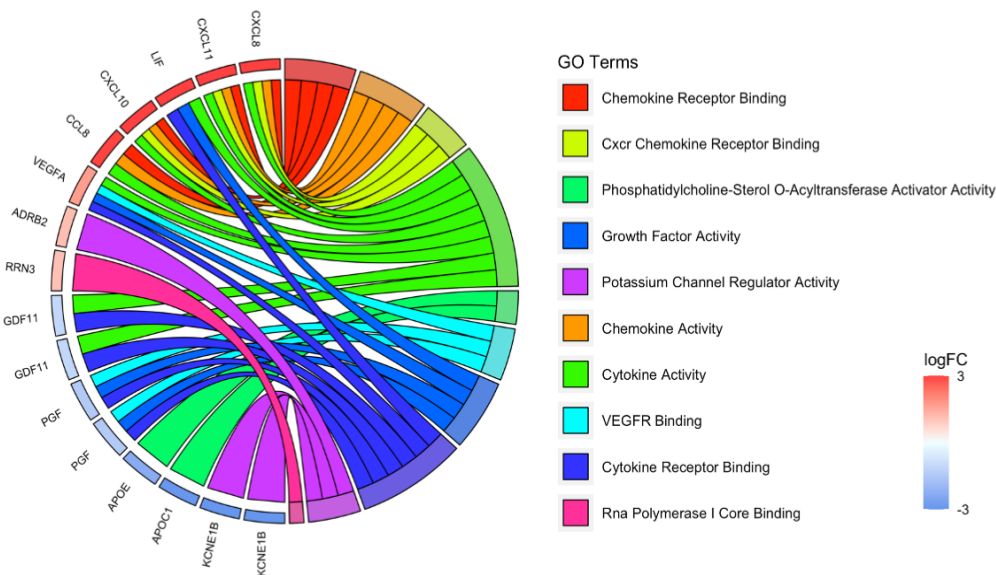


Figure 65: GO Chord Molecular Function analysis for DE genes in SAT from OBT2D vs. OBF. On the right the top 10 significant GO term, whereas on the left the corresponding genes ordered according to log2FC.

The ClueGO analysis implicated again chemokine and chemoattractant activity, (Figure 66a) and this is true also for the overrepresented terms in BiNGO analysis (Figure 66b).

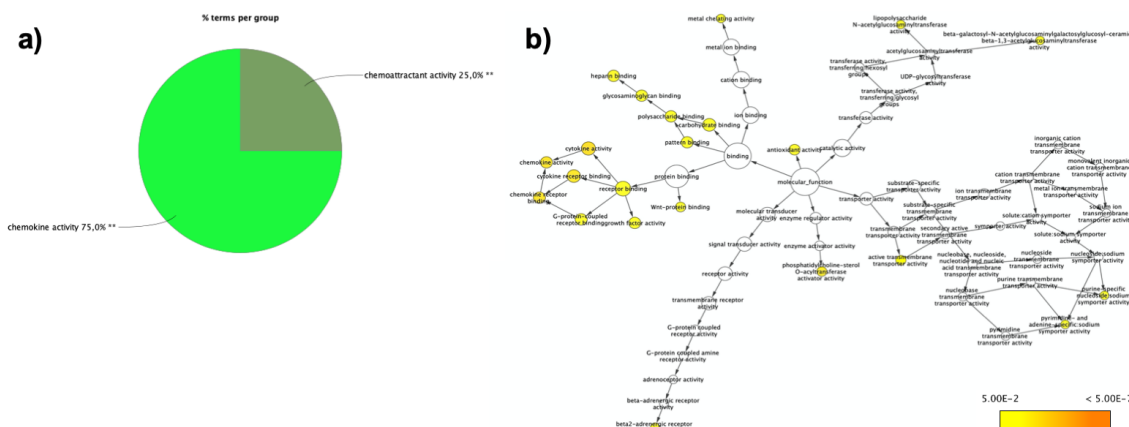


Figure 66: GO Molecular Function (a) ClueGO analysis in OBT2D vs. OBF. Each pie segment refers to the % of terms present per group (*p<0.05, **p<0.01 vs Control SAT) (b) BiNGO analysis in OBT2D vs. OBF. The hubs reported show the overrepresented terms.

The GO terms analysis for Biological Processes highlighted 934 deregulated pathways, and the GO Chord graph reports the top 10 deregulated processes according to their significance (Figure 67). Again, 7 out of 10 of these processes pertained immune-related functions, along with chylomicron clearance and cAMP signaling.

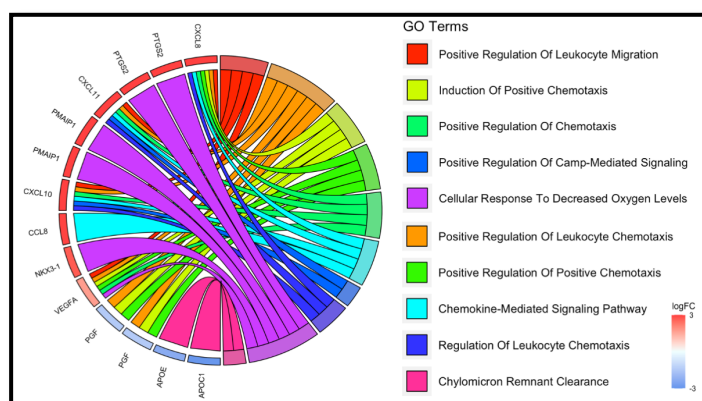


Figure 67: GO Biological Processes analysis for DE RNAs in SAT from OBT2D vs. OBF. On the right the top 10 significant GO terms, whereas on the left the corresponding genes ordered according to log2FC.

The ClueGO analysis shows a strong representation for induction of positive chemotaxis (Figure 68a), whilst the most over-represented term is the regulation of cell proliferation (Figure 68b).

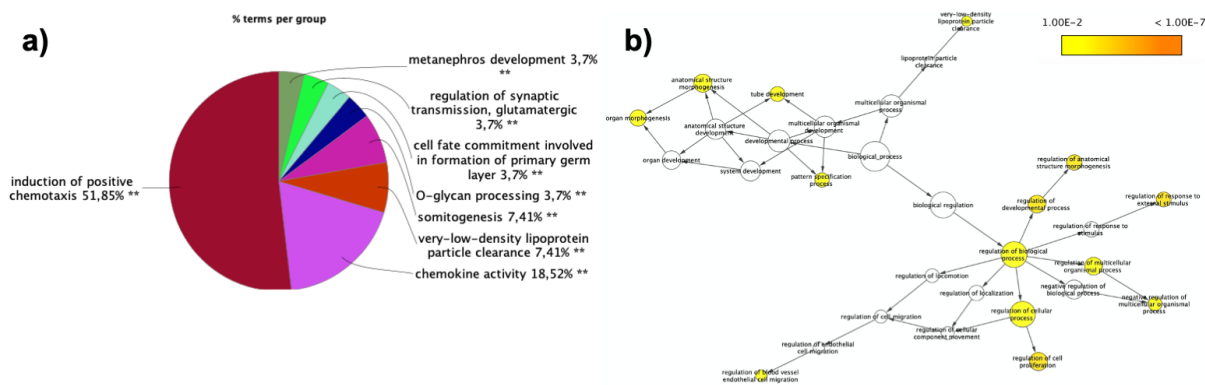


Figure 68: GO Biological Process. (a) ClueGO analysis in OBT2D vs. OBF. Each pie segment refers to the % of terms present per group (** $p < 0.01$ vs Control SAT) (b) BiNGO analysis in OBT2D vs. OBF. The hubs reported show the overrepresented terms.

4.2.3.6. Pathways characterization: top deregulated processes and implications for metabolic components

DE RNAs were then subjected to KEGG and WikiPathways and the outcomes were displayed through a dot plot graph. The top 20 deregulated pathways ranked for their significance were visualized for KEGG (Figure 69a) and WikiPathways (Figure 69b). Numerous pathways are implicated in the immunogenic response, along with pathways implicated in cancers and even the “AGE-RAGE signaling pathway in diabetic complications”.

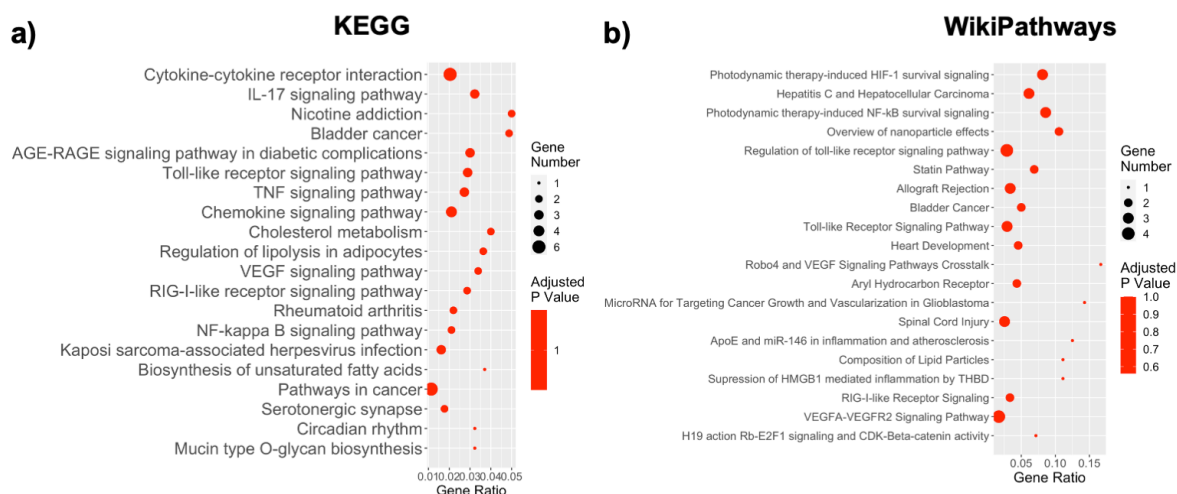


Figure 69: Dotplot of top 20 KEGG 2019 (a) and WikiPathways (b) analysis. The y-axis represents the name of the pathway, the x-axis represents the Rich factor, dot size represents the number of different genes and the color indicates the adjusted p value.

The ClueGO analysis for KEGG interestingly highlighted RNA transport as most significant deregulated component ($p < 0.01$), along with viral protein interaction with cytokine and cytokine receptor (Figure 70a), whilst WikiPathways implicated the hepatitis C and hepatocellular carcinoma, along with HIF-1 survival signaling (Figure 70b). The Reactome databases highlighted the IL-10 signaling, transcriptional regulation, glycosylation and plasma lipoprotein clearance (Figure 70c).

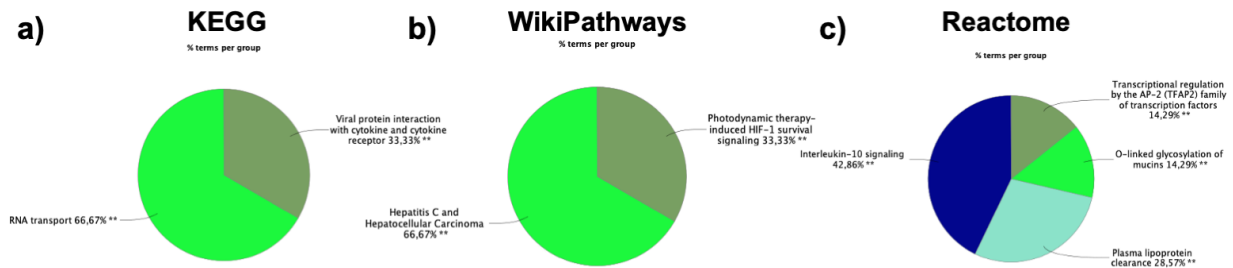


Figure 70: ClueGO analysis for KEGG (a), WikiPathways (b) and Reactome (c) in OBT2D vs. OBF. Each pie segment refers to the % of terms present per group (** $p < 0.01$ vs OBF).

The deregulated pathways related to these metabolisms are reported in Figure 71. Specifically, 1/101 KEGG and 5/120 terms for WikiPathways related to aa metabolism (Figure 71a), 6/101 for KEGG and 5/120 for WikiPathways related to lipids metabolism (Figure 71b) and 1/101 for KEGG and 1/120 for WikiPathways related to

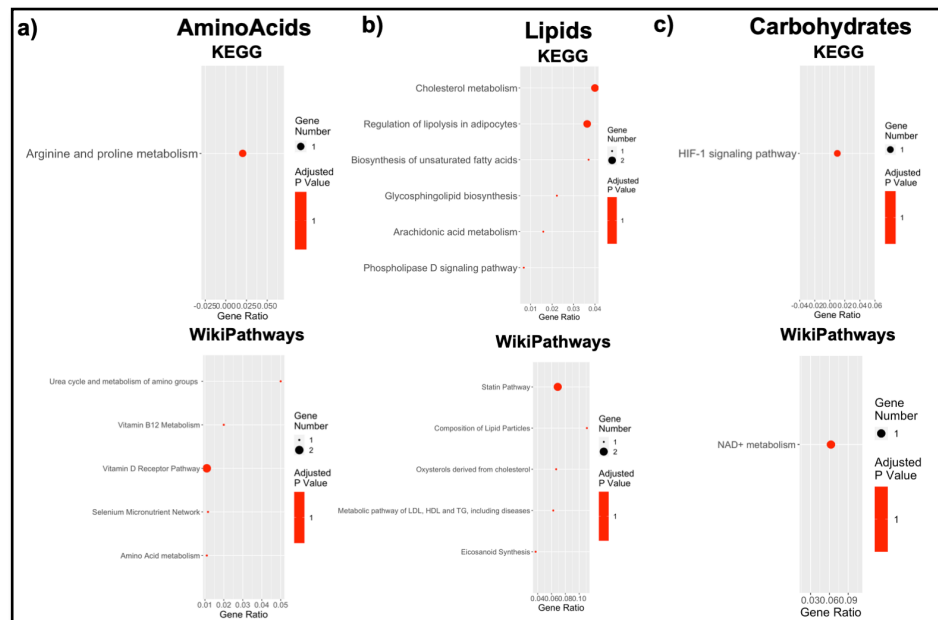


Figure 71: Dotplot of KEGG 2019 and WikiPathways analysis of pathways correlated with (a) aa, (b) lipids and (c) carbohydrates metabolism. The y-axis represents the name of the pathway, the x-axis represents the Rich factor, dot size represents the number of different genes and the color indicates the adjusted p-value.

Carbohydrates (Figure 71c). It is possible to observe how in this case, the metabolic component seems to be less implicated, suggesting that this could not be responsible for the differences in diabetic patients with respect to obese ones.

4.2.3.7. Role of the immunological component in SAT from OBT2D vs. OBF

An in-depth analysis was performed concerning immunological processes. 42 out of the 101 KEGG deregulated terms (41.6%) and 27 out of the 120 WikiPathways deregulated terms (22.5%) were correlated with the immunogenic phenomenon, suggesting that the increased immunogenic response may exacerbate the obesogenic phenotype, ultimately leading to diabetes insurgence (Figure 72).

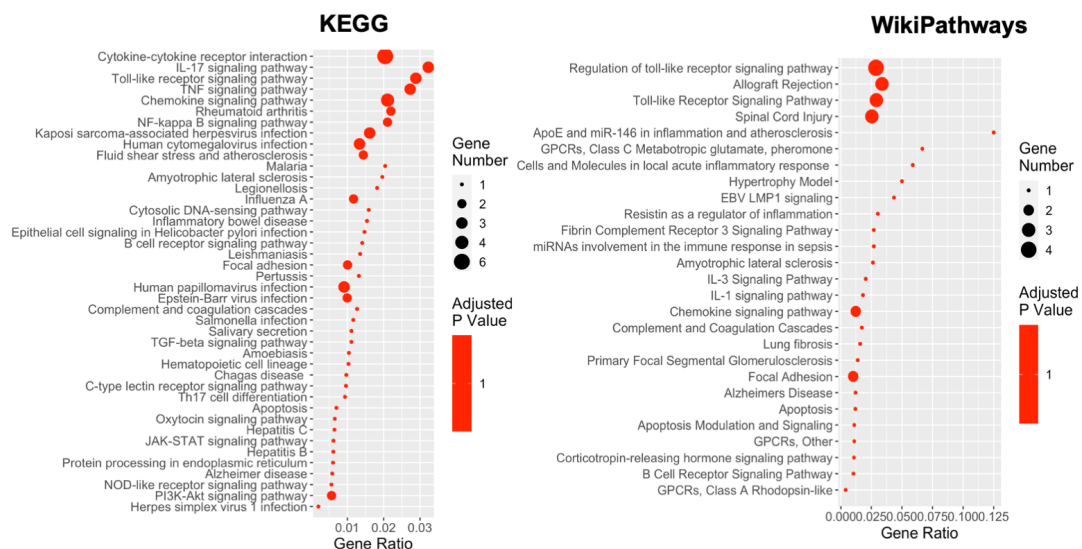


Figure 72: Dotplot of KEGG 2019 and WikiPathways analysis of immune system pathways. The y-axis represents the name of the pathway, the x-axis represents the Rich factor, dot size represents the number of genes and the color the adj p-value.

Moreover, via ClueGO GO Immune System Processes database, it was possible to see that the two most represented categories were lymphocyte chemotaxis and macrophage differentiation (Figure 73).

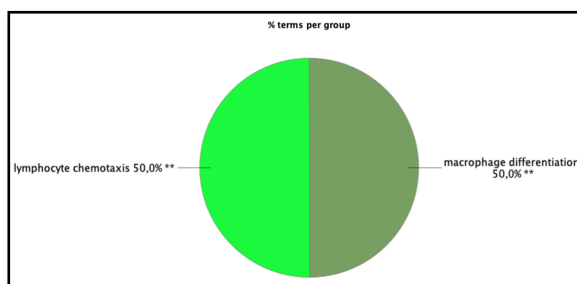


Figure 73: ClueGO analysis for GO Immune System Processes in OBT2D vs. OBF. (** $p < 0.01$ vs OBF)

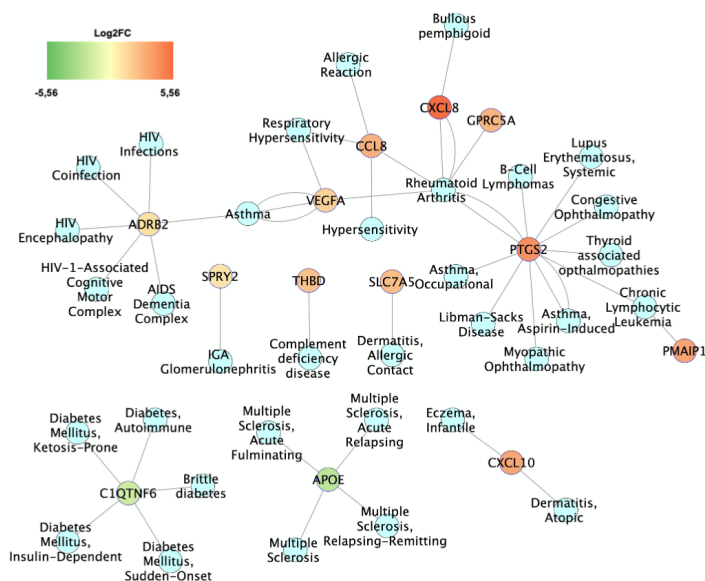


Figure 74: DisGeNET analysis shows the terms implicated in Immune Diseases in SAT from OBT2D vs. OBF. The lines connecting the genes to the disease term represent the literature evidence for the terms' implication in the disease. The color scale represents the genes FC.

The following step was to interrogate the DisGeNET curated database, finding a number of genes correlated with multiple immunological diseases (Figure 74). PTGS2 is the gene implicated in the highest number of disease conditions, whilst the CXCL8, is the most upregulated gene. This codes for the primary cytokine involved in the recruitment of neutrophils to the site of damage or infection.

4.2.3.8. Potential cancer implications: susceptibility in OBT2D vs. OBF

When comparing the DE RNAs in SAT from diabetic patients versus obese ones, we wished to see if there would be an even higher predisposition to the development of certain cancer types. Indeed, 22 out of the 101 KEGG deregulated terms (21.8%) and 31 out of the 120 WikiPathways deregulated terms (25.8%) were identified as correlated with oncogenesis (Figure 75).

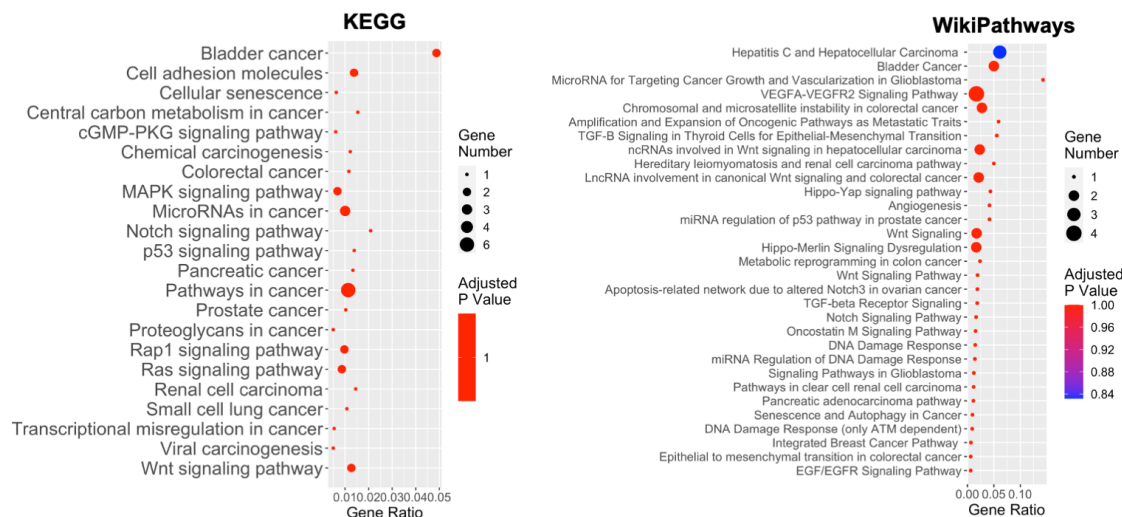


Figure 75: Dotplot of KEGG 2019 and WikiPathways analysis of oncogenesis-related pathways. The y-axis represents the name of the pathway, the x-axis represents the Rich factor, dot size represents the number of different genes and the color indicates the adjusted p-value.

The DisGeNET database was investigated highlighting a susceptibility network with CXCL8 as most upregulated gene and correlated with gastric cancer. PTGS2 was correlated with multiple conditions such as adrenal cancer, gastric cancer and a general precancerous condition (Figure 76). The investigation of the NDEx database allowed the identification of a higher number of implicated genes. Interestingly, as it was for diabetes versus control conditions, there seems to be an increased susceptibility for renal cancer when switching to a diabetic phenotype (Figure 76).

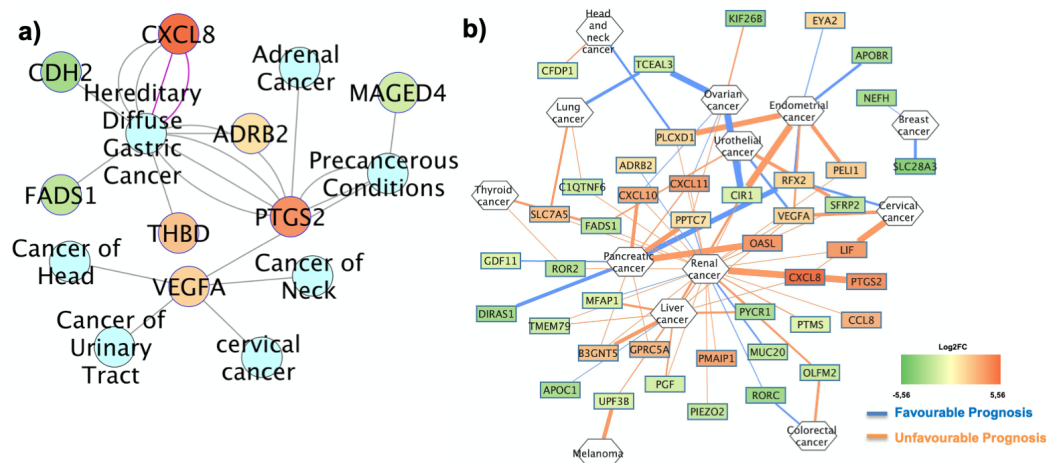


Figure 76: (a) DisGeNET analysis shows the terms implicated in cancer in SAT from OBT2D vs. OBF. The lines connecting the genes to the disease term represent the literature evidence for the terms' implication in the disease. The color scale for the genes represents the FC (b) Gene-Cancer correlation network as obtained with the NDEx database. The edges color indicates the prognosis (favorable in blue and unfavorable in orange) and the color scale for the genes represents the FC.

4.2.3.9. DE RNAs correlations with nutritional and metabolic diseases

The DisGeNET database was investigated in order to identify the interactions between DE RNAs and Nutritional and Metabolic Diseases, as obtained from curated databases (Figure 77a). It is possible to notice how these diseases include also central nervous system diseases with a metabolic component, along with other metabolic diseases such as hyperlipoproteinemia, highly linked with the APOE gene. When expanding the search to all known databases 24 genes were found to be associated with obesity (Figure 77b) and 18 with diabetes (Figure 77c). APOE and VEGFA seem to be the most annotated genes correlated with obesity and diabetes, with more than 10 evidence per gene (Figure 77b and Figure 77c respectively).

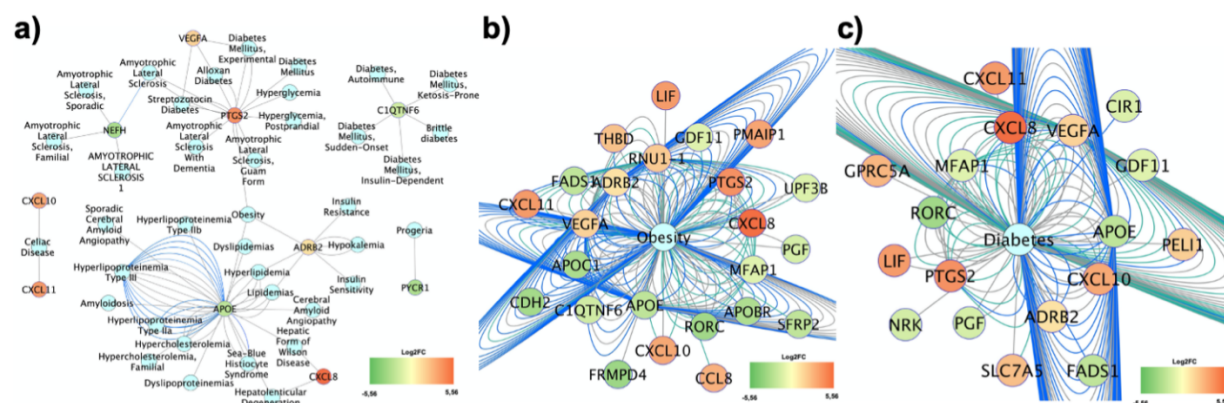


Figure 77: DisGeNET analysis shows the terms implicated in nutritional and metabolic diseases (a) obesity (b) and diabetes (c) in OBT2D vs. OBF.

4.2.3.10. Identification of DE RNAs associated diseases

The last analysis performed for this dataset consisted in investigating the ClinVar database. This highlights all diseases potentially associated with a list of DE RNAs (Figure 78).

Interestingly, numerous diseases emerge, and amongst the most represented are Familial type 3 hyperlipoproteinemia, Gordon's syndrome, anterior segment dysgenesis 4, atypical hemolytic-uremic syndrome and even epilepsy.

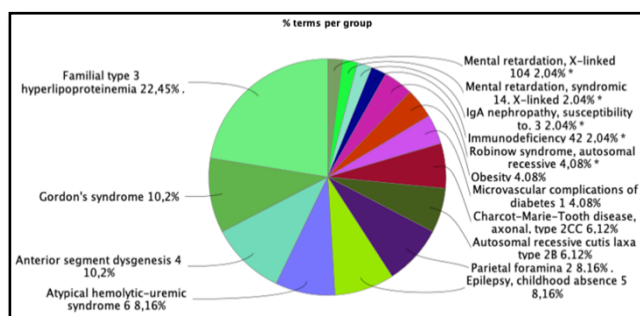


Figure 78: ClueGO analysis for ClinVar database. Each pie segment refers to the % of terms present per group (* $p < 0.05$ vs OBF)

4.3. Role of ncRNAs in disease pathogenesis: a focus on lncRNAs in obesity

The last part of this research work focused on the identification and characterization of the non-coding transcriptome in obesity and diabetes pathogenesis. Indeed, RNA-seq analyses in SAT obtained from 5 NW, 5 OBF, and 5 OBT2D highlighted a strong component of non-coding genes, and as this particular class of molecules are showing to have more and more of a relevant function in the pathogenesis of numerous diseases it is worth analyzing the role that these could play in obesity and diabetes.

4.3.1. Role of ncRNAs in obesity and diabetes

4.3.1.1. Increase of the non-coding biological component in the diabetic comorbidity

From the RNA-results, several coding and non-coding DE RNAs emerged as differentially expressed in each analyzed condition, and these are reported as a volcano plot graph highlighting only the non-coding component (Figure 79).

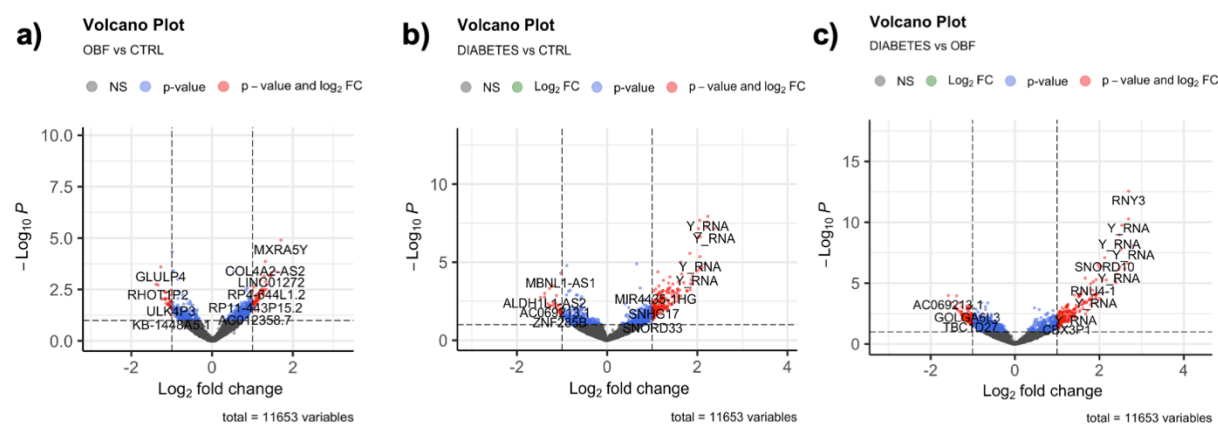


Figure 79: Transcriptomic profile reported as volcano plot for (a) SAT of OBF versus CTRL, (b) SAT of DIABETES versus control and (c) SAT of DIABETES versus OBF, where genes that respected the condition in terms of \log_2FC and FDR are reported in red, non-differentially expressed genes in grey, while genes that respected only one condition in blue.

When comparing the different biotypes, it was found that the ratio between the coding and non-coding compartment was different amongst the categories (Figure 80). It is remarkable to note how the number of non-coding DE RNAs increases when switching from an obesogenic condition to a diabetic one. Specifically, whilst non-coding DE RNAs are 6.43% of total DE RNAs in obese subjects, this percentage increases to up to 32.43% in diabetic subjects. Even more interesting is the fact that when considering the molecular underlining responsible for the additional diabetic phenotype (OBT2D vs. OBF), more than 50% of the DE RNAs are ncRNAs. This highlights how the non-coding epigenome could be of crucial relevance in the development of specific comorbidities, highlighting the possibility of new targets for future therapeutic intervention and prevention.

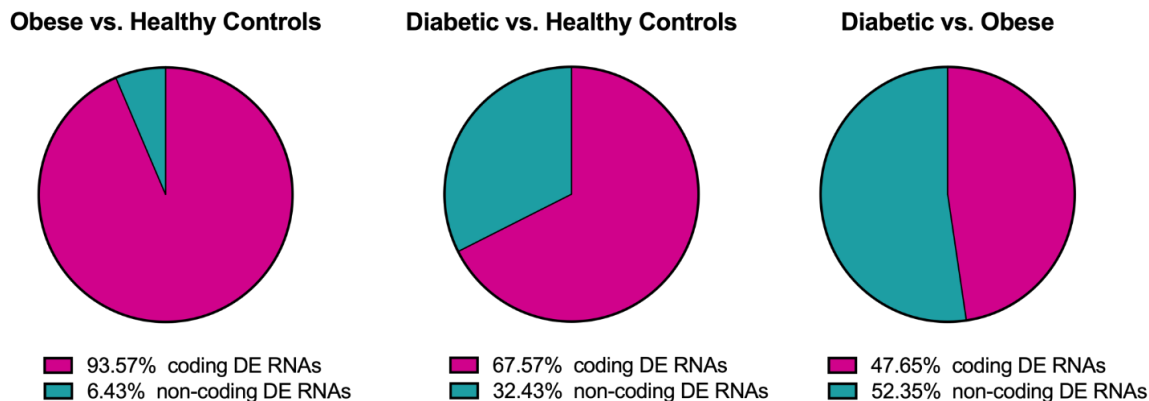


Figure 80: % of coding and non-coding DE RNAs in the three experimental conditions.

4.3.1.2. Network interaction of coding and non-coding DE RNAs in obesity and diabetes

As the non-coding component seems to be widely deregulated in SAT from obese and diabetic patients, the next step was to investigate whether the coding and non-coding component interact. This was done performing a WGCNA, which creates a correlation-network of the DE RNAs through the obtainment of an adjacency matrix which weights the possible interactions amongst genes. The obtained networks with a weighted correlation threshold of 0.1 are reported in Figure 81.

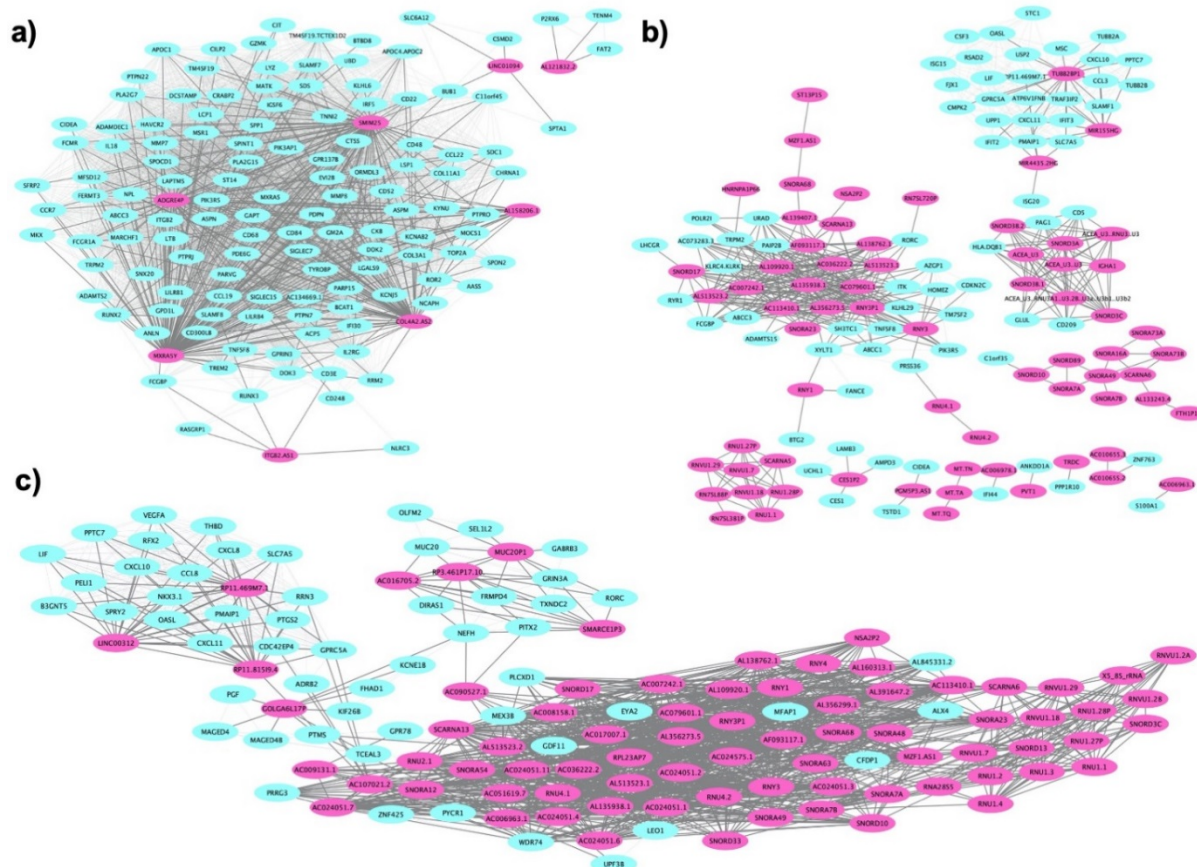


Figure 81: WGCNA of (a) OBF vs. NW (b) OBT2D vs. NW and (c) OBT2D vs. OBF. The correlation threshold was set to 0.1 and the ncRNAs are reported in pink. The thicker edges refer to the first degree interactions of non-coding DE RNAs.

Firstly, in obese versus healthy SAT, 8 ncRNAs, reported in pink, emerge as part of the interactome (Figure 81a). Specifically, all but AL121832.2 (NAT to RPS21) are found to be part of a main interaction network, although not directly with one-another. They could possibly influence numerous coding genes found altered via RNA-seq, thus suggesting that they also play a fundamental role in the altered signaling pathways present in obesity. In the OBT2D versus NW SAT, 62 ncRNAs present a correlation threshold higher than 0.1, and are thus displayed as interaction networks (Figure 81b). These ncRNAs interact in 13 separate networks. It is interesting to note the presence of one network composed solely of non-coding DE RNAs, one of solely mitochondrial non-coding DE RNAs and one of all ncRNAs but one. Indeed, in this case, the non-coding component seems to act not through an interaction with the coding genome, but rather as a separate interacting entity which could ultimately lead to phenotypic changes. Lastly, 67 ncRNAs participate in a correlation network in when considering the differential expression present in diabetic versus obese SAT (Figure 81c). These ncRNAs, the highest component found, interacts with the target coding DE RNAs in one single network, suggesting that they, together, influence the dynamics of diabetic tissues. Indeed, a center core is made up of ncRNAs interacting at multiple levels with one another, whilst two distinguished edges (still connected to the network) include a higher number of coding DE RNAs. Overall, these results indicate that the non-coding epigenome might play a significant role in the development of the diabetic comorbidity

4.3.2. Computational and functional analyses of lncRNAs in OBF

As lncRNAs are being more and more implicated in metabolic diseases, along with physiological function of the adipose tissue, the last aim of this work was the characterization of the deregulated lncRNAs which emerged through RNA-Seq in OBF.

4.3.2.1. Computational characterization of lncRNAs in OBF

Out of the 11 deregulated DE RNAs which emerge from transcriptional analysis of OBF vs. NW SAT, 6 belong to the lncRNAs category (Table 15). Most are uncharacterized genes, with no known function, and interestingly three of them are NATs to coding genes (COL4A2, ITGB2, and RPS21). The common aliases for each will be used for now on: SMIM25, COL4-AS2, CTEPHA1, RPS21-AS, ITGB2-AS1, ACER2-AS.

Table 15: List of lncRNAs DE in OBF vs NW SAT.

| Gene name | Log2FC | Aliases | Function |
|------------|--------|---------------------------|---|
| SMIM25 | 2.74 | GCRL1, LINC01272, PELATON | Nuclear expressed, monocyte- and macrophage-specific lncRNA, upregulated in unstable atherosclerotic plaque. |
| COL4A2-AS2 | 5.93 | | NAT to COL4A2, which plays a role in osteogenic differentiation and is differentially secreted in adipogenic differentiation. |
| LINC01094 | 1.74 | CTEPHA1 | Deregulated in post-menopausal osteoporosis, implicated in Chronic Thromboembolic Pulmonary Hypertension |
| AL121832.2 | 2.36 | RPS21-AS1 | NAT to RPS21, unknown function |
| ITGB2-AS1 | 2.23 | | NAT to ITGB2 and polymorphism in ITGB2 were associated with obesity. |
| AL158206.1 | -1.07 | ACER2-AS | NAT to ACER2, an alkaline ceramidase implicated in lipids metabolism. |

As insights into the genomic localization could provide useful information on neighboring genes and thus coordinated loci regulation, the chromosomal localization and neighboring genes were identified using the ensemble database and reported in Figure 82. The specific genes are highlighted in green. The most interesting observation can be made on SMIM25. Indeed, it is localized near the C/EBP β gene, activator of early adipogenesis.

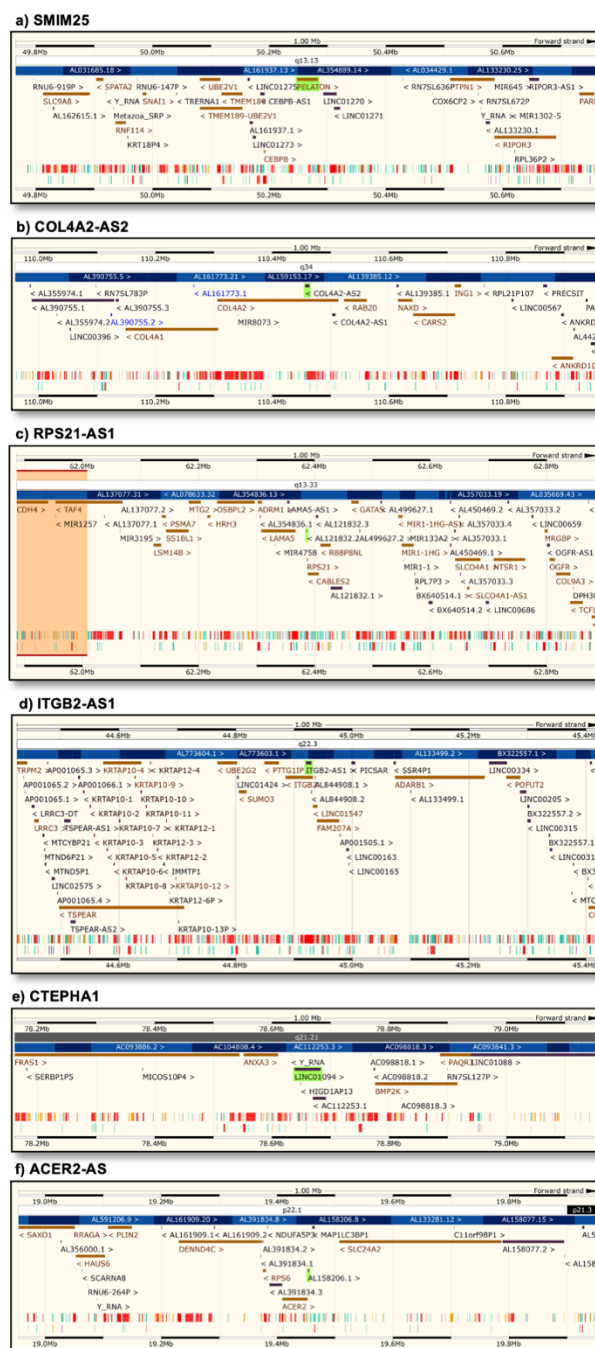


Figure 82: Genomic localization of (a) SMIM25, (b) COL4A2-AS2, (c) RPS21-AS1, (d) ITGB2-AS1, (e) CTEPHA1, (f), ACER2-AS as obtained from the ensemble database. Specific genes are highlighted in green.

A deeper analysis was performed looking at the specific gene structure, when present: this highlights the presence of exons and the genes localization with respect to overlapping genes (Figure 83). The sequence was obtained using *Geneious version 2020.2* created by Biomatters.

Specifically, the gene sequence is reported in green, whilst the ncRNA organization is reported in red. The thicker segments represent the exons whilst the interconnecting lines the introns.

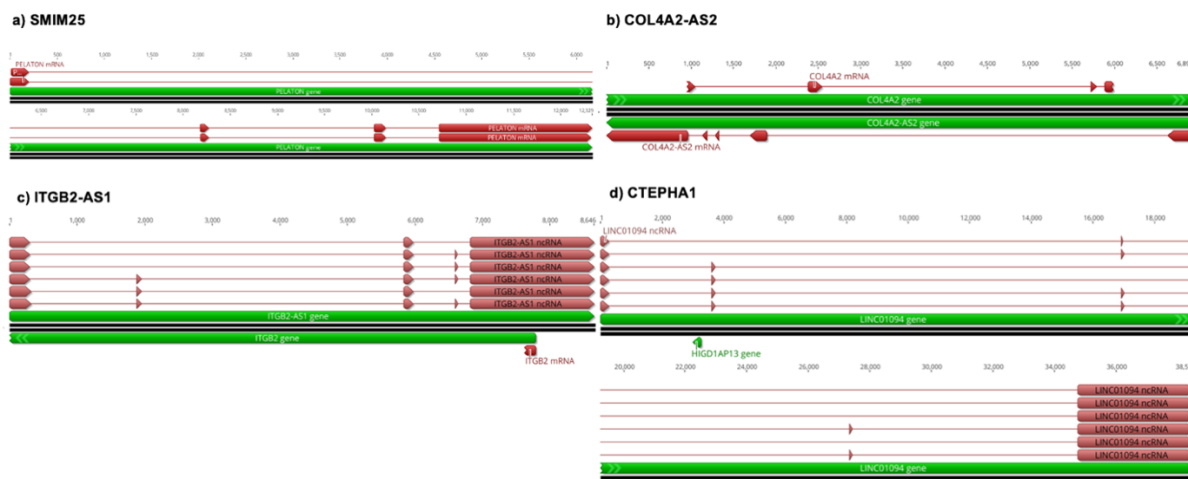


Figure 83: Genomic structure of (a) SMIM25, (b) COL4A2-AS2, (c) ITGB2-AS1, (d) CTEPHA1, as obtained with Geneious version 2020.2 created by Biomatters.

Evolutionarily, lncRNAs are present in all vertebrate species and their sequences cover the portion of the DNA previously termed as “junk DNA”, non-protein coding and thus previously thought of no value, although this view is now surpassed. Typically evolutionary conservation is based on sequence similarities between nucleotide or amino acid sequences (Diederichs 2014). LncRNAs sequences are overall less conserved than protein coding-genes, but more than introns or random intergenic regions. When looking for sequence similarity, it was found that only short sequence stretches are typically conserved, as lncRNAs evolve rapidly and often lack orthologs (Diederichs 2014). This is also the case for the lncRNAs analyzed in this work, as the phylogenetic trees reported in Figure 84 highlight. These were obtained blasting the ncRNAs for sequence similarity across species, and the predicted sequences were used to construct the trees. It is possible to observe how these lncRNAs sequences present the highest similarity in mammals, especially primates. For ACER2-AS, it was not possible to construct the tree as the only similarity was found in *Macaca Mulatta*. Even so, the gene presented homology with its sense gene ACER in other species.

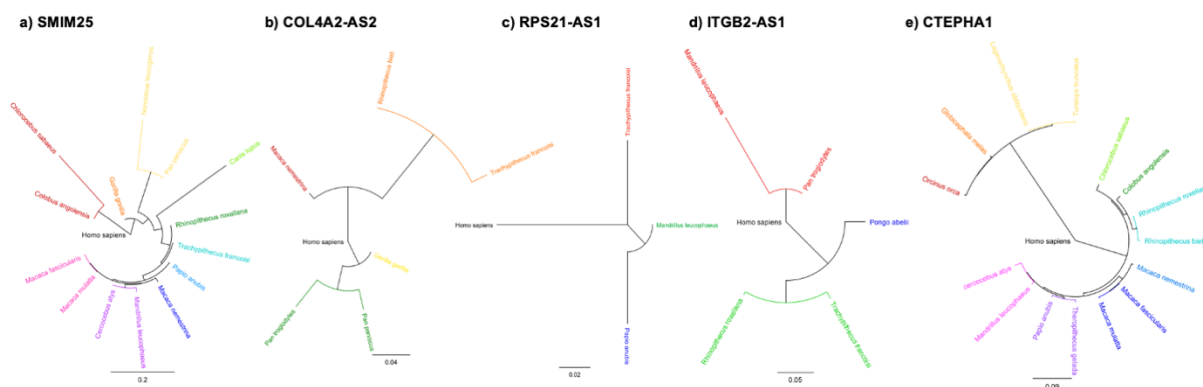


Figure 84: Phylogenetic tree of sequence similarity for (a) SMIM25, (b) COL4A2-AS2, (c) RPS21-AS1, (d) ITGB2-AS1, (e) CTEPHA1 as constructed with Geneious version 2020.2 created by Biomatters.

The specific sequence alignment is shown in Figure 85. It is possible to see that longer segments of the sequences are maintained when considering primates, whereas when considering other species (e.g. *Canis Lupus* for SMIM25) the similar sequence fragment is shorter.

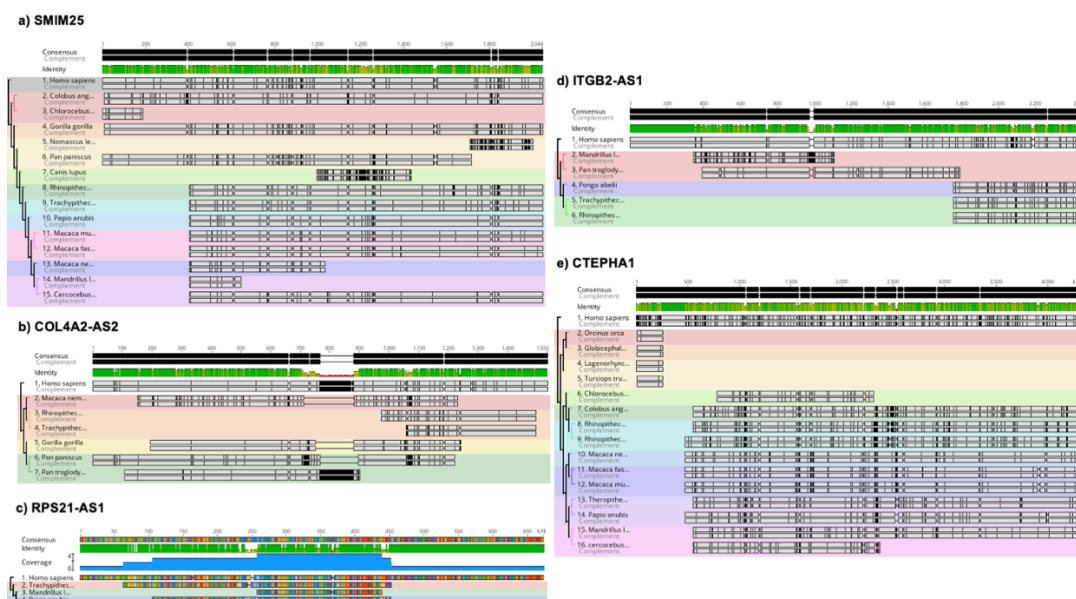


Figure 85: Alignment of (a) SMIM25, (b) COL4A2-AS2, (c) RPS21-AS1, (d) ITGB2-AS1, (e) CTEPHA1 across species as constructed with Geneious version 2020.2 created by Biomatters.

Interestingly, lncRNAs present higher structural conservation rather than nucleotide sequence conservation, as it is the structure which seems to be fundamental for their subsequent function (Zampetaki, Albrecht, and Steinhofel 2018). Insights into the secondary structure are useful for motives identification, which could determine the lncRNAs protein interactors and targets. Indeed, lncRNAs can fold into complex secondary structures and subsequently interact with proteins, DNA or other RNAs, modulating their function. The RNA secondary structure was predicted using the RNA fold web server for base pair probability (Figure 86).

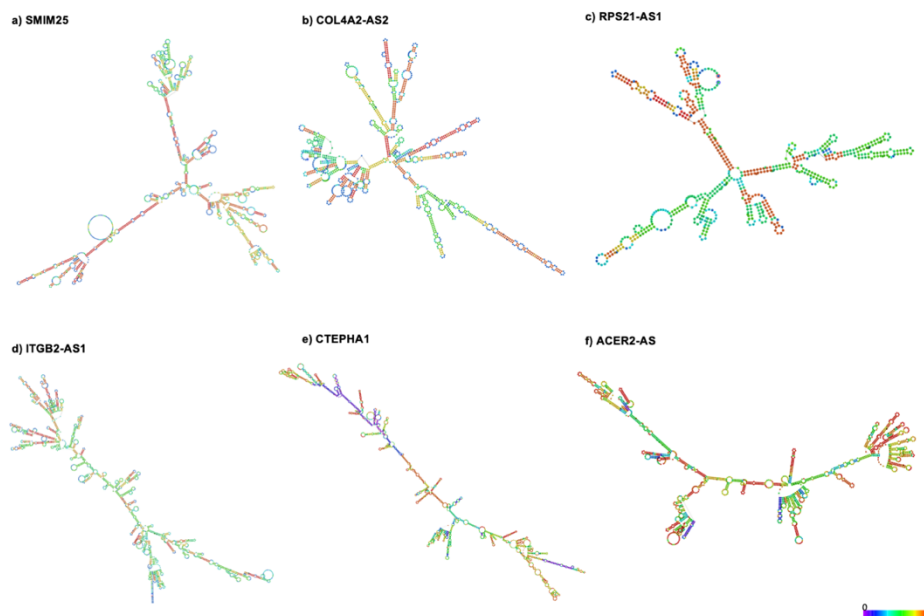


Figure 86: Secondary structure of (a) SMIM25, (b) COL4A2-AS2, (c) RPS21-AS1, (d) ITGB2-AS1, (e) CTEPHA1, (f) ACER2-AS as obtained RNA Fold Web Server. The color legend represents the base pair probability.

The last computational analysis performed involved the promoter of each specific lncRNA. Using the Ciiider software, it was possible to predict the presence of binding sites for PPAR γ , C/EBP α , C/EBP β and C/EBP δ (Figure 87). SMIM25 was the only one which did not present any binding site for these four TFs.

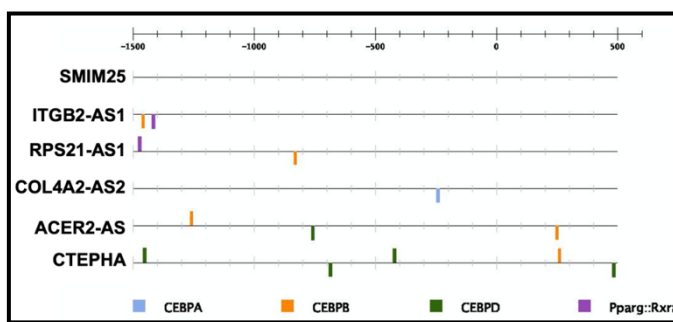


Figure 87: Analysis of binding sites for C/EBPs and PPAR in the promoter region of the different lncRNAs obtained using CiiDER.

4.3.2.2. In vitro characterization of lncRNAs regulation

As these lncRNAs have been found to be deregulated in SAT of obese patients, in vitro biological experiments were performed in order to investigate their role in adipogenesis, along with a study of their possible regulation. From here on, the lncRNAs SMIM25, COL4A2-AS2, RPS21-AS1, CTEPHA1 were considered for in vitro analysis. Furthermore, COL4A2 and RPS21, sense gene of respectively COL4A2-AS2 and RPS21-AS1, were also analyzed. The first step was to analyze the expression of these genes in SAT and VAT in adipogenesis, at different time points. SAT and VAT differentiated samples were obtained from 2 obese patients and subsequent gene expression was investigated via Real Time PCR. The results obtained are reported in Figure 88. All of the lncRNAs present changes in expression along different phases of differentiation. SMIM25 appears to be differentially expressed in VAT versus SAT tissue, and RPS21-AS1 appears to be the most upregulated during differentiation, with a peak at Day 6 of adipogenic induction and a subsequent decrease. RPS21 is also upregulated in VAT tissue, significantly at Day 4 and Day 8. Moreover, COL4A2 was significantly upregulated in VAT 8 days after differentiation.

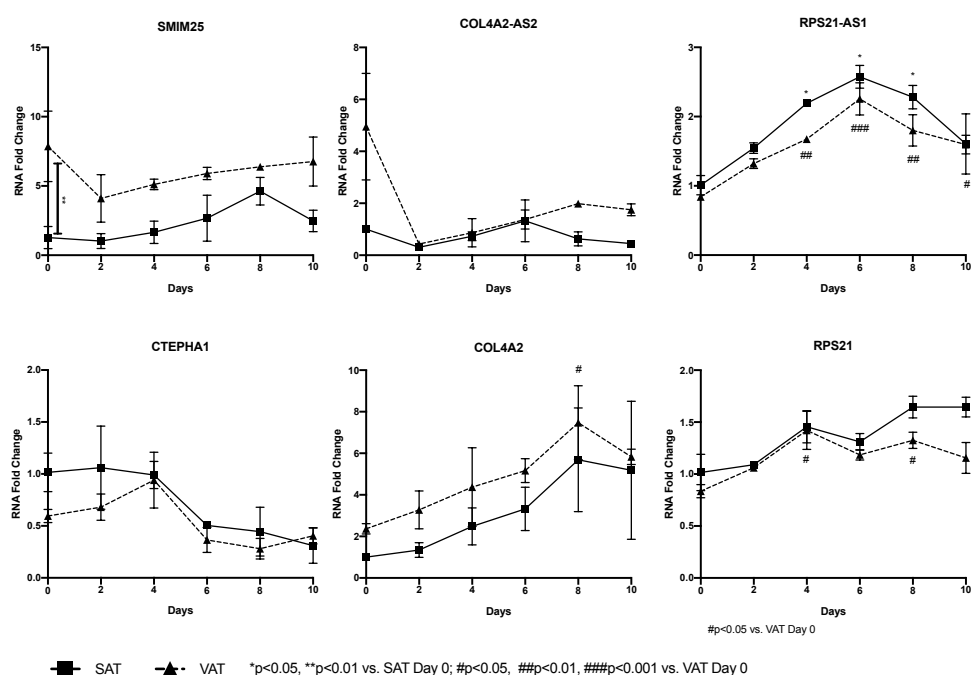


Figure 88: Differential expression of lncRNAs and sense genes in SAT and VAT tissue from obese patients was verified by Real Time PCR. 18S was used as housekeeping gene. Data are expressed as mean of 2 samples \pm SEM ($n = 2$), * $p < 0.05$, ** $p < 0.01$ vs. SAT Day 0, # $p < 0.05$, ## $p < 0.01$, ### $p < 0.001$ vs. VAT Day 0.

The genes expression was then analyzed during the differentiation in hADSCs obtained from the lipoaspirate of a NW subject. hADSCs were differentiated for 14 days, and samples collected at day 0, 2, 4, 7, 10 and 14. Also in this case the expression of the lncRNAs and sense genes changes at the different phasis of the adipogenesis process, and they all seem to present a peak at day 7 (Figure 89). This upregulation is extremely significant at day 7 for SMIM25, RPS21-AS1, CTEPHA1, COL4A2 and RPS21. Interestingly, in the case of CTEPHA1 e COL4A2, the expression seems to peak at day 7, with a subsequent decrease. On the contrary, for RPS21-AS1 and RPS21, the increase seems to be stable and maintained even after 14 days.

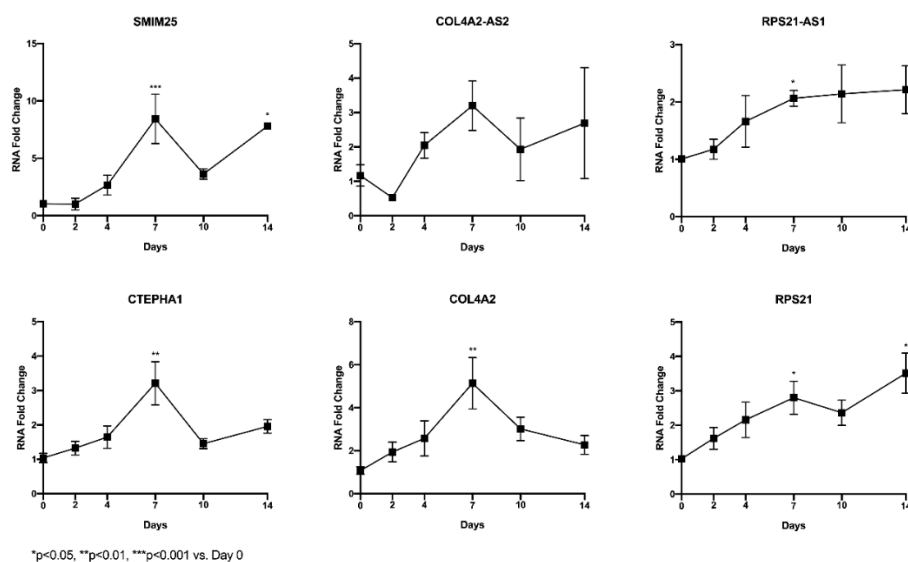


Figure 89: Differential expression of lncRNAs and sense genes in lipoaspirate of a NW subject was verified by Real Time PCR. GAPDH was used as housekeeping gene. Data are expressed as mean of 3 experiments each performed in duplicates \pm SEM ($n = 6$), * $p < 0.05$, ** $p < 0.01$, *** $p < 0.001$ vs. Day 0.

To ensure that efficient differentiation had taken place, the expression of C/EBP β , C/EBP δ , C/EBP α , PPAR γ and FABP4 was also assessed via Real Time PCR (Figure 90), and results demonstrate their specific increase.

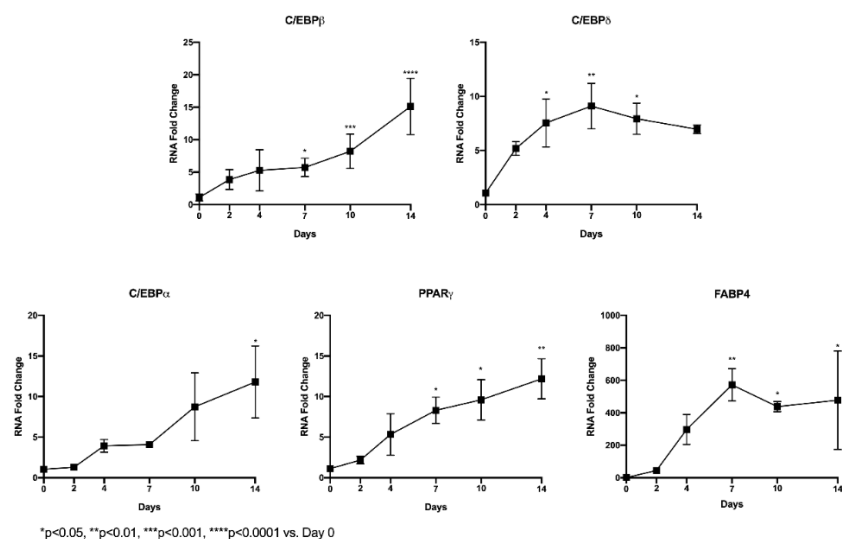


Figure 90: Differential expression of adipogenesis genes in hADSCs was verified by Real Time PCR. GAPDH was used as housekeeping gene. Data are expressed as mean of 3 experiments each performed in duplicates \pm SEM ($n = 6$), * $p < 0.05$, ** $p < 0.01$, *** $p < 0.001$, **** $p < 0.0001$ vs. Day 0.

The work then aimed to identify if adipogenesis-related TFs influenced the lncRNAs and relative sense genes expression in hADSCs. To do so, RNA interference was firstly used to inhibit the expression of C/EBP β , C/EBP δ 's and C/EBP α , regulators of adipogenesis. The efficiency of silencing was measured evaluating the respective expression of C/EBP β , C/EBP δ and C/EBP α , (Figure 91).

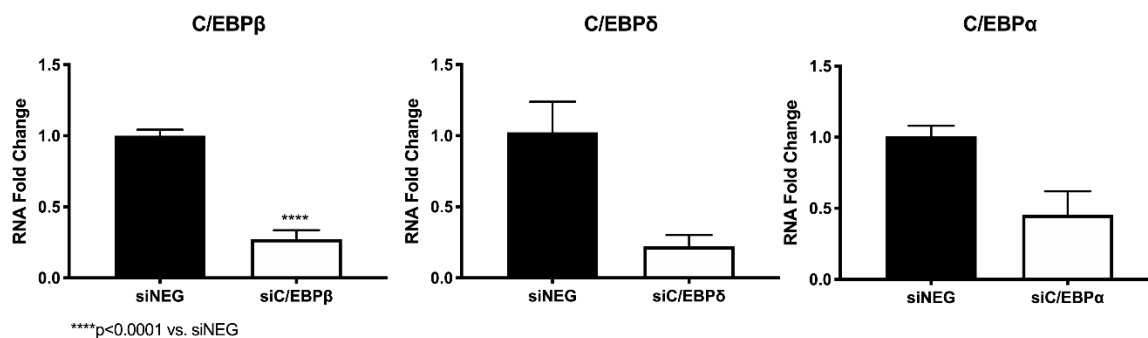


Figure 91: Efficiency of silencing was verified by Real Time PCR. GAPDH was used as housekeeping gene. Data are expressed as mean of 2 experiments each performed in duplicates \pm SEM ($n = 4$) for C/EBP β and as mean of 1 experiment performed in duplicate \pm SEM ($n = 2$) for C/EBP δ and C/EBP α . **** $p < 0.0001$ vs siNEG.

When C/EBP β 's expression was silenced, all but SMIM25 were found to be downregulated, suggesting that C/EBP β is necessary for their expression (Figure 92).

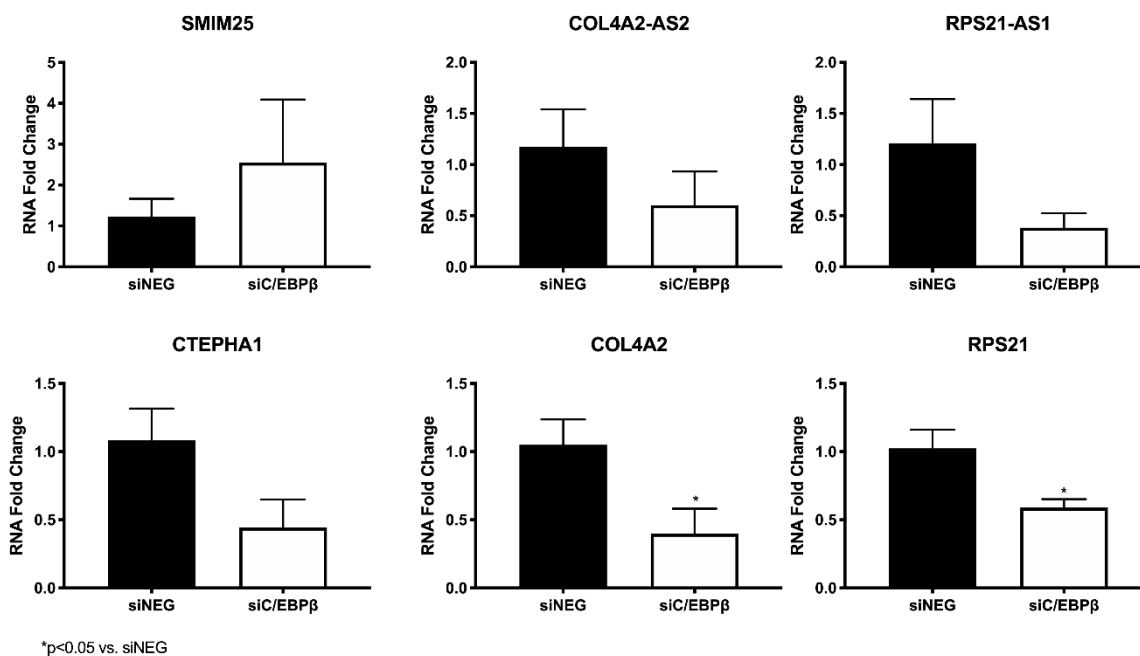


Figure 92: Differential expression of lncRNAs and sense genes in hADSCs silenced for C/EBP β versus control (siNEG) was verified by Real Time PCR. GAPDH was used as housekeeping gene. Data are expressed as mean of 2 experiments each performed in duplicates \pm SEM ($n = 4$), * $p < 0.05$ vs siNEG.

Similarly, when C/EBP δ 's expression was silenced, all the genes were found to be downregulated, except for COL4A2-AS2, suggesting that C/EBP δ is necessary for their expression (Figure 93).

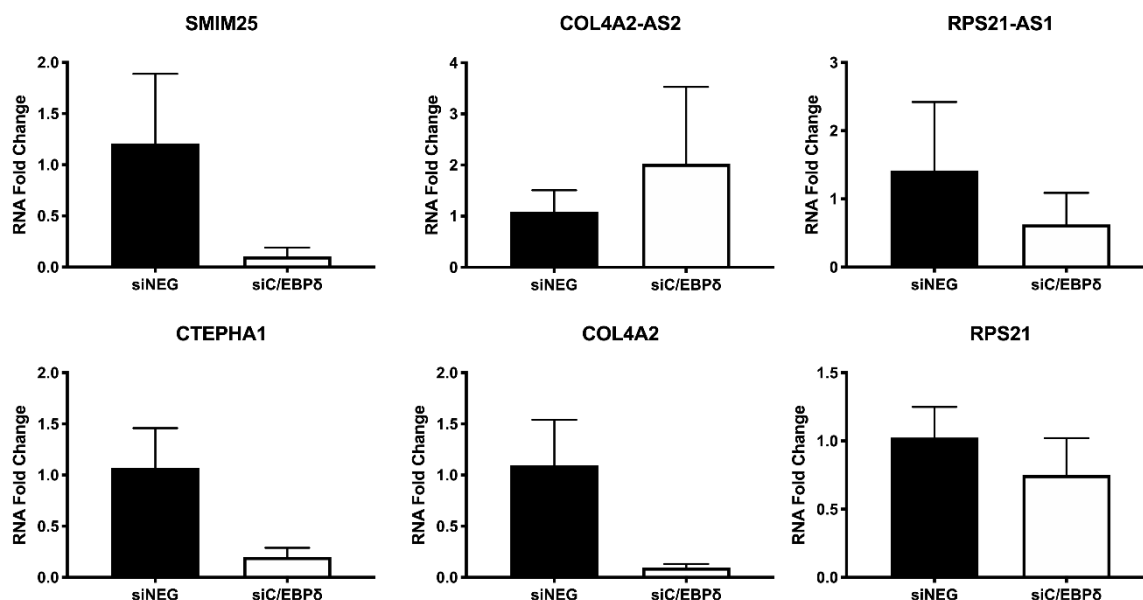


Figure 93: Expression of lncRNAs and sense genes in hADSCs silenced for C/EBP δ versus control (siNEG) was verified by Real Time PCR. GAPDH was used as housekeeping gene. Data are expressed as mean of 1 experiment in duplicate \pm SEM ($n = 2$).

When C/EBP α was silenced, all the genes were found to be downregulated, except for COL4A2-AS2, suggesting that C/EBP δ is necessary for their expression (Figure 94)

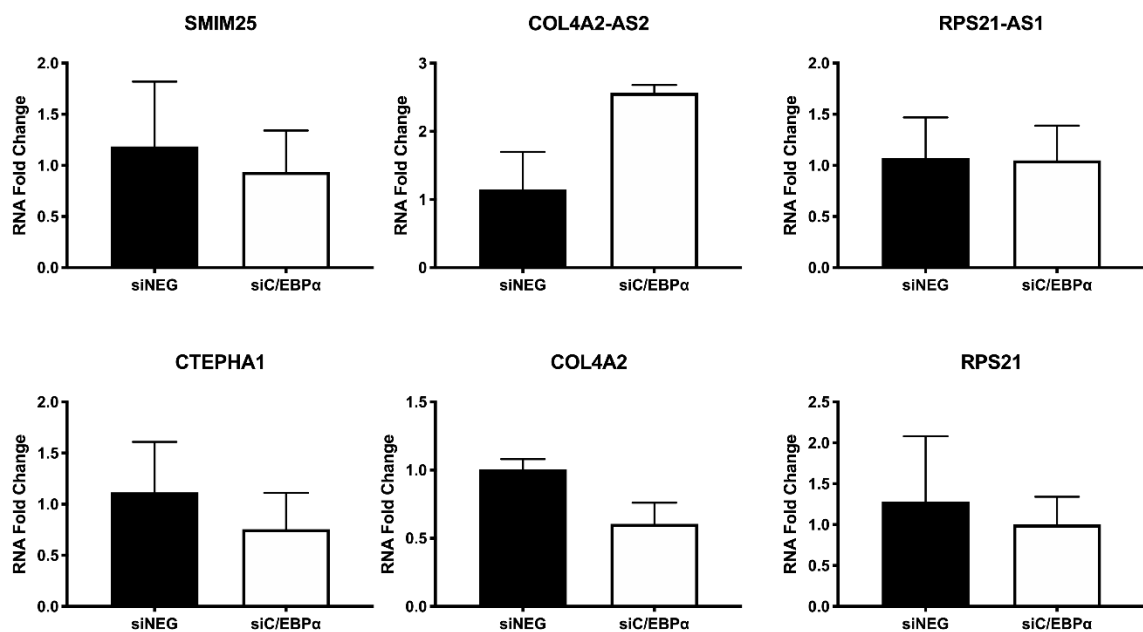


Figure 94: Expression of lncRNAs and sense genes in hADSCs silenced for C/EBP α versus control (siNEG) was verified by Real Time PCR. GAPDH was used as housekeeping gene. Data are expressed as mean of 1 experiments in duplicate \pm SEM ($n = 2$).

As PPAR γ is known to be adipogenesis' master regulator, its influence on the lncRNAs and respective sense genes was analyzed. To do so, its expression was firstly induced with its activator troglitazone (Figure 95). All the lncRNAs and respective sense genes were induced by PPAR γ 's activation, and this is significantly true for SMIM25, RPS21 and CTEPHA1.

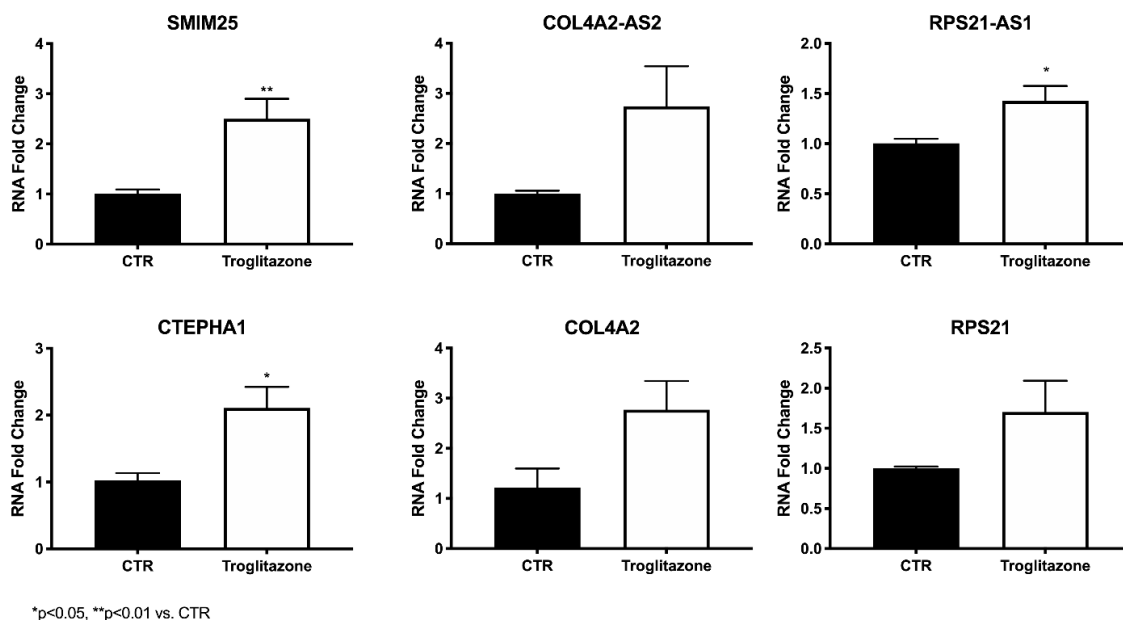


Figure 95: Expression of lncRNAs and sense genes in hADSCs treated with Troglitazone was verified by Real Time PCR. GAPDH was used as housekeeping gene. Data are expressed as mean of 3 experiments each performed in duplicates \pm SEM (n = 6), * p < 0.05, **p<0.01 vs CTR.

To verify that this induction was specific, hADSCs were differentiated in presence or absence of PPAR γ 's inhibitor T0070907 (Figure 96). When this was done, it was possible to notice that the SMIM25 and RPS21-AS1 specific induction after 7 days of differentiation was inverted with the PPAR γ 's inhibitor, suggesting that it is these two targets specifically which are modulated by it.

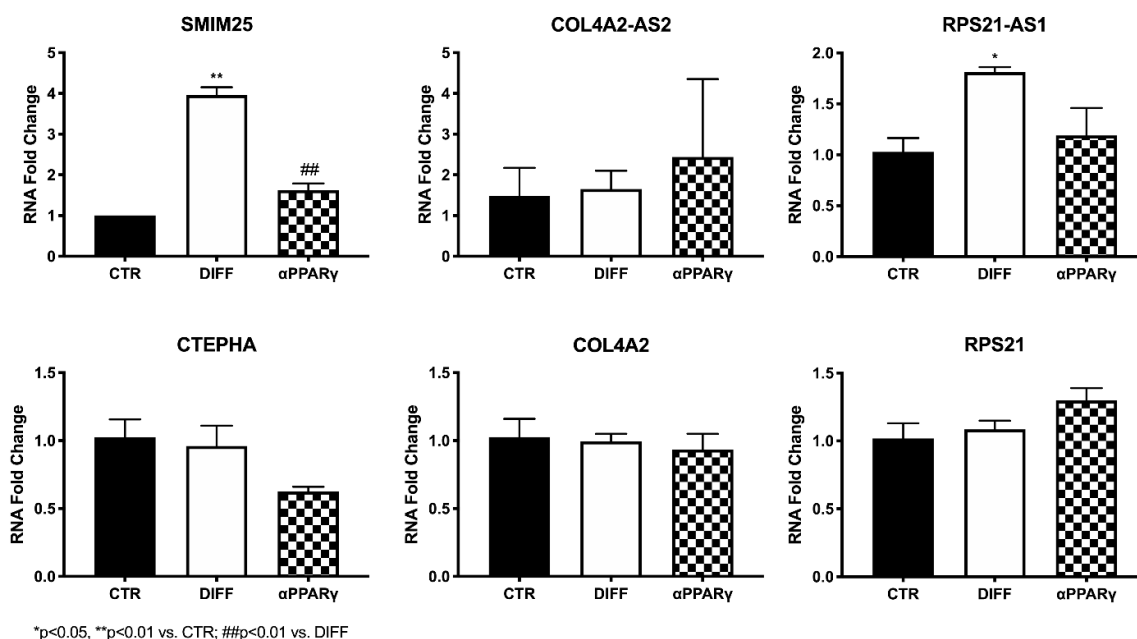
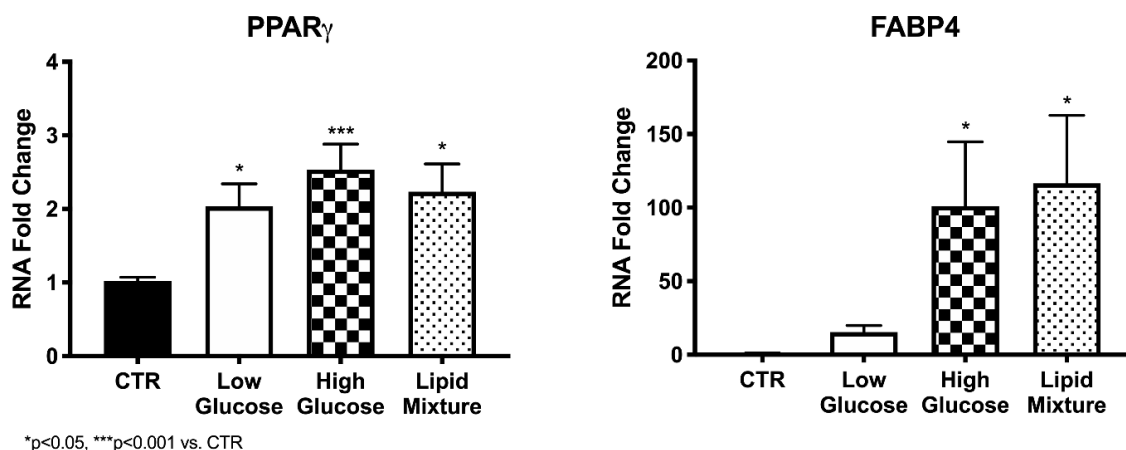


Figure 96: Expression of lncRNAs and sense genes in hADSCs differentiated in absence (DIFF) or presence of T0070907 (α PPAR γ) was verified by Real Time PCR. GAPDH was used as housekeeping gene. Data are expressed as mean of 2 experiments each performed in duplicates \pm SEM (n = 4), * p < 0.05, **p<0.01 vs CTR.

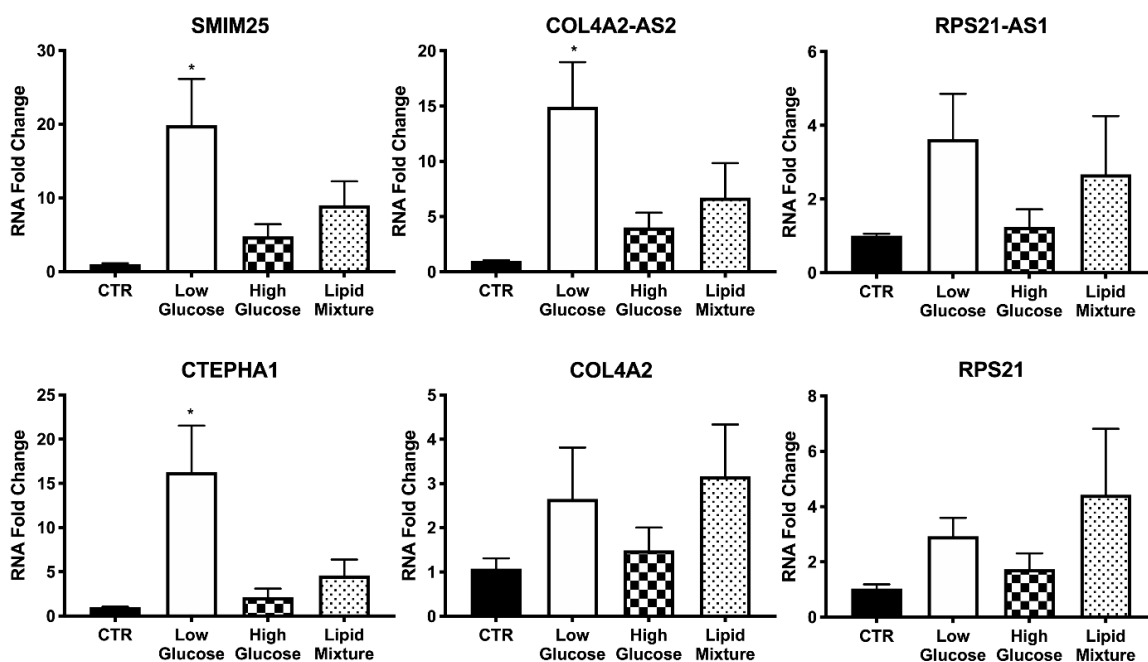
As obesity is strictly influenced by the nutritional component, the last experiment consisted in differentiation of hADSCs in three different medium: a standard one with high glucose, one with low glucose, and one supplemented with a lipid mixture of free fatty acids. The efficiency of the differentiation was firstly verified assessing the expression of PPAR γ and FABP4, as reported in Figure 97.



*p<0.05, ***p<0.001 vs. CTR

Figure 97: Expression of PPAR γ and FABP4 in hADSCs differentiated in a differentiation medium with low glucose, with high glucose, and with a lipid mixture was verified by Real Time PCR. GAPDH was used as housekeeping gene. Data are expressed as mean of 2 experiments each performed in duplicates \pm SEM (n = 4), * p < 0.05, ***p<0.001 vs CTR.

Interestingly, SMIM25, COL4A2-AS2 and CTEPHA1 seem to be significantly upregulated in the differentiation medium composed of low glucose, suggesting that this molecule could highly influence their expression (Figure 98).



*p<0.05 vs. CTR

Figure 98: Expression of PPAR γ and FABP4 in hADSCs differentiated in a differentiation medium with low glucose, with high glucose, and with a lipid mixture was verified by Real Time PCR. GAPDH was used as housekeeping gene. Data are expressed as mean of 2 experiments each performed in duplicates \pm SEM (n = 4), * p < 0.05, ***p<0.001 vs CTR.

5. Discussion

Obesity is defined by the WHO as a condition of abnormal or excessive accumulation of body fat that presents a risk to health. It can lead to an increase in associated morbidities for many chronic diseases such as T2D, hypertension, coronary artery disease, dyslipidemia, stroke, osteoarthritis, certain forms of cancer (Haslam, Sattar, and Lean 2006, Lawrence and Kopelman 2004, WHO 2020a), and even result in an increased mortality rate (WHO 2020a). To this day, it is not possible to conclude what is the relative contribution of either genetic or the environment in obesity onset. Indeed, behavior and genes are different levels of the same causal framework, and epigenetics through RNA biology might play a central role in elucidating new targetable pathways.

The aim of this research work was the investigation of the transcriptional differences present in obesity and T2D. Indeed, the identification of a subset of DE RNAs in obese and diabetic SAT allows the identification of new targetable disease pathways. Moreover, the study of the specific transcriptional differences between obese subjects who develop the diabetic comorbidity and those who do not could specifically highlight the DE RNAs responsible for the insurgence of this secondary disease. These targets could become useful for screening of patients at risk for comorbidities insurgence, and even allow the development of therapies based on precision medicine. Moreover, the work focused on the role of the non-coding part of the genome in diseases development, as the role of these molecules in physiological processes and diseases mechanisms is becoming more and more prominent. Specifically, RNA-seq was performed on the SAT obtained from 5 healthy NW females, 5 obese females, and 5 obese females with T2D. Three experimental conditions were subsequently analyzed: the differences occurring between obese and healthy subjects, the differences occurring between diabetic and healthy subjects, and moreover the differences occurring between diabetic and obese subjects. For each condition, a global bioinformatics characterization of the DE RNAs and the pathways in which they are involved was performed.

In SAT from obese versus healthy patients, 171 DE RNAs were identified, and of these 160 were coding genes whilst 11 were non-coding DE RNAs. Remarkably, 81 of these genes had never been correlated to obesity before and could thus be of great relevance for future characterization in the obesogenic context. Amongst the top deregulated genes, a significant implication was found for the immune system, to be expected as the SAT from obese patients presents a high degree of flogosis, along with tissue remodeling and, interestingly, the biology of the striatal muscle. Indeed, obesity can cause a decline in contractile function of skeletal muscle, thereby reducing mobility and leading to the development of even more obesity-associated health risks (Tallis, James, and Seebacher 2018). The proteins codified by the DE RNAs co-interact in two main networks, are expressed in multiple organs of the body and are localized in numerous different cellular organelles. Although this is quite a general characterization, the use of these databases allows for a comprehensive screening, and open the future works aimed at characterizing the role of one specific DE RNA could benefit from this preliminary information, knowing already which could be the DE RNA's co-interactors and localization. Moreover, the DE RNAs are governed by a highly complex network of 18 TFs, of

which the most implicated seems to be SPI1, involved in both the activation of gene expression during myeloid and B-lymphoid cell development and in adipogenesis (Dispirito et al. 2013, Lefterova et al. 2014). Indeed, when it is expressed in mature adipocytes, it leads to the increased expression of macrophage genes and a global repression of genes with nearby adipocyte-specific PPAR γ binding sites (Dispirito et al. 2013, Lefterova et al. 2014). Other TFs implicated in this network previously associated to adipogenesis are HSF1 (Ma et al. 2015), EP300 (Lee et al. 2019, Takahashi et al. 2002), EBF1 (Jimenez et al. 2007, Gao et al. 2014), NFkB1 (Berg et al. 2004), SRF (Rosenwald et al. 2017, Jones et al. 2020), CREB1 (Reusch, Colton, and Klemm 2000), TWIST2 (Lee et al. 2003, Franco et al. 2011), TP53 (Krstic et al. 2018, Huang et al. 2014), and, remarkably, C/EBP δ , key regulator of early adipogenesis (Hishida et al. 2009, Lee et al. 2019). Moreover, PTC1 knock out has been correlated with adult-onset obesity (Perks et al. 2017), whilst early over-nutrition leads to a decrease of PDX1 (Glavas et al. 2019). Members of the NFAT family have been implicated in adipogenesis and insulin resistance, but NFATc1 specifically was never reported to have a role in this process (Yang et al. 2006). The implicated EVX2, ZNF622, C9orf156, MTA3 and FLI1 have not been correlated with adipogenesis to date. This identification of new TFs could prove helpful in directing scientists towards their characterization in adipogenesis-related contexts.

The DE RNAs were analyzed for GO terms enrichment, in order to better understand the possible genes, cellular localization (Cellular Component), Molecular Functions and Biological Processes. DE RNAs in SAT from obese patients were strongly implicated in the vesicle formation component, granule formations, lytic vacuoles, lipoproteins, association with the immunological synapse, and even morphological changes in the plasma membrane. Indeed, the molecular functions mostly involved implicate morphological components such as actin and integrin binding, along with matrix remodeling with metalloproteinase activity, biochemical alterations such as carboxy-lyase and phosphoric ester hydrolase activity, lipid kinase activity, catalytic activities and signal transduction complexes such as the PI3K regulator subunit, phosphatase activity and protein tyrosine phosphatase activity. Lastly, the biological processes mainly involved pertained immune-related functions, with a specific role for tumor necrosis factor production. A subsequent analysis allowed the identification of the deregulated pathways through KEGG and WikiPathways enrichment. Specifically, the most significant pathways were implicated in immunological responses and specific metabolic pathways. This analysis approach highlights also a possible deregulation in the gene expression signature correlated with specific diseases, related with obesity, such as rheumatoid arthritis (Crowson et al. 2013, George and Baker 2016), inflammatory bowel disease (Bryant et al. 2018), gastric cancer (Yang et al. 2009) and others. Interestingly, these diseases had been previously related to obesity, and this pathway analysis highlight the possible specific molecular signature responsible for the disease insurgence. Moreover, amongst the deregulated pathways a number of them are correlated with pathogens infection (e.g. Human T-cell leukemia virus 1 infection, Malaria, Staphylococcus aureus infection, and Ebola virus), suggesting that this specific deregulated molecular signature could be implicated in the worse disease prognosis observed in obese patients (Falagas and Kompoti 2006, Hegde and Dhurandhar 2013). Indeed, individuals with obesity are also linked with large significant increases in morbidity and mortality from COVID-19 (Popkin et al. 2020, Wadman 2020).

As metabolic complications of obesity can lead to the development of metabolic diseases, a focus was given on those pathways identified as correlated with dysfunctions in specific metabolisms (Grundy et al. 2004). The most implicated component found were aminoacids (aa), previously studied in relation to obesity as these patients present with a reduction of branched chain aa catabolic enzyme activity, changes in methionine oxidation and cysteine/cystine generation, and tissue redox balance (NADH/NAD⁺) (Adams 2011). Even so, most studies focused on the peripheral or muscular deregulation in aa present in obese patients (Suzuki et al. 2019, Adams 2011, Takashina et al. 2016, Guillet et al. 2016) whilst this study highlights how this deregulation is also present in SAT. Lipids metabolism has also been found to be deregulated, and this is in agreement with studies showing that obesity is associated with increased basal lipolysis in adipose tissue, elevated circulating free fatty acids and increased tissue lipid accumulation in the liver, skeletal muscle, and heart (Singla, Bardoloi, and Parkash 2010, Shulman 2014, Galgani, Cortés, and Carrasco 2014). Lastly, the carbohydrates metabolism was found deregulated, and indeed more and more studies are identifying glucose uptake into fat as modulator of systemic glucose homeostasis (Singla, Bardoloi, and Parkash 2010).

An in-depth analysis was performed pertaining the immune system in SAT tissue from obese patients. Indeed, 67 out of the 171 KEGG deregulated terms (39%) and 44 out of the 158 WikiPathways deregulated terms (28%) were correlated with the immune system, suggesting that the DE RNAs deregulation reported profoundly impacts this system, with a higher susceptibility for subsequent co-morbidities insurgence. The GO Immune System Processes database implicated dendritic cells, antigen processing and presentation, and T cell activation whilst the DisGeNET database allowed the identification of specific genes leading to increased susceptibility for specific immune diseases, such as Lupus Erythematosus Systemic, Rheumatoid Arthritis, Immunologic Deficiency Syndromes, Multiple Sclerosis, defects in the leucocyte adhesion process, dermal diseases. Moreover, as the emerging link between obesity and multiple cancer types is gaining more and more relevance in recent years (Avgerinos et al. 2019, Kompella and Vasquez 2019, Ungefroren et al. 2015) the identification of the molecular signature occurring in obesity responsible for the insurgence of related carcinogenesis is of crucial importance. Indeed, 25 out of the 171 KEGG deregulated terms (15%) and 31 out of the 158 WikiPathways deregulated terms (20%) were correlated with the oncogenic phenomenon and diseases, whilst the specific gene association with each cancer was also displayed, with a focus on favorable and unfavorable prognosis, as studies are highlighting how obesity can be a predictor of better overall survival in metastatic patients (Tsang et al. 2016) and moreover, in lung cancer, renal cell carcinoma and melanoma, obesity was found to be protective in terms of outcome (Petrelli et al. 2020). These results highlight a more specific cancer-signature, and possibly allow for early intervention. Lastly, the genes were correlated with specific metabolic complications, including central nervous system inborn metabolic diseases, brain metabolic diseases, amyotrophic lateral sclerosis, semantic dementia, celiac disease, Tay-Sachs diseases and many more.

In SAT from diabetic versus healthy patients, 259 DE RNA was identified, and of these 175 were coding genes whilst 84 were non-coding DE RNAs. 164 of these genes had never been

correlated to diabetes before, and amongst the top 20 deregulated genes immune-related genes were identified, along with 3 ncRNAs. The coding DE RNAs co-interact in two main networks, are ubiquitarily expressed in multiple organs of our body and are localized in numerous different cellular organelles. Moreover, the DE RNAs are governed by 17 TFs, of which NFIC (Muhammad et al. 2017), MTA3 (He et al. 2016), STAT5 (Jackerott et al. 2006), NFE2 (Jin et al. 2020, Xiao et al. 2019), HSF1 (Chen, Ding, et al. 2017) have been previously correlated with T2D. Moreover, HSF1 inhibition has been correlated with glucolipotoxicity-induced beta cell apoptosis (Purwana et al. 2017), FOXM1 was found to be induced by obesity and stimulate β -cell proliferation, (Davis et al. 2010, Golson et al. 2015), SRY has been correlated with insulin resistance (Goldsworthy et al. 2008) whilst mice with the knock out in the TF PGR have improved glucose homeostasis (Picard et al. 2002). SMAD4 and SMAD1 impact autoimmune diabetes development (Kim, Lee, and Jun 2017, Seong, Manoharan, and Ha 2018, Kim et al. 2007) whilst LTF has also been found very recently to be differentially expressed in a Chinese cohort of type 1 diabetic patients (Yang et al. 2020). FLI1 and NFATc1 were identified to regulate the obesity DE RNAs network, but they were never previously correlated to either diabetes or obesity. POLR2A, T (TBXT), ELF1 and BCLAF1 have never been correlated with obesity nor diabetes.

All three terms in GO analysis revealed again a significant implication of the immune system (MHC complex), with the DE RNAs HLA-DQB2, HLA-DQB1 and HLA-DRA, along with specific chemokines and immune system regulators. Other components implicated are the sarcoplasm, the vesicular component and even nuclear TF complexes and the Golgi apparatus. In addition, RNA polymerase II TF activity is also impaired, suggesting profound transcriptional deregulation. Amongst the top deregulated pathways, a strong metabolic component is present, with nitrogen metabolism, glycolysis/gluconeogenesis, metabolism of xenobiotics, fatty acid omega oxidation, aa metabolism and indeed metabolic complications can often aggravate obesity and be highly dysfunctional in diabetic patients (Grundy et al. 2004, Goetzman et al. 2018). Several pathways also implicated in immunological responses and RNA transport is also implicated as one of the most significantly deregulated pathways. Interestingly, RNA-binding proteins (RBPs) were found dysregulated in diabetes and are being studied for the potential to design RNA-based therapeutic effects, but not much is known about the role of RNA metabolism in this disease (Nutter and Kuyumcu-Martinez 2018). 39% of the KEGG deregulated terms and 22% WikiPathways deregulated terms were correlated with the immunogenic phenomenon, suggesting that the DE RNAs deregulation reported profoundly impacts this system, with a focus on type I interferon signaling pathway and the positive regulation of antigen processing and presentation. Focusing of specific genes, the upregulated CSF2 and HLA-DQB1 appear to be implicated in the highest number of conditions, respectively mainly lymphoma and diabetes. There is also a known correlation between diabetes and cancer (Giovannucci et al. 2010) and indeed 15% KEGG deregulated terms and 23% WikiPathways deregulated terms (23%) were correlated with oncogenesis. BRCA2, known for its implications in breast cancer, is upregulated, and there is also a deregulation in many genes, such as MMP7 and SERPINE1 implicated in gastric cancer along with a high number of genes with unfavorable prognosis correlated with renal cancer. DE RNAs are also associated with numerous metabolic diseases.

The last transcriptional condition analyzed was that pertaining the SAT of diabetic subjects versus obese ones, where 149 DE RNAs were detected. 71 were coding genes whilst 78 were non-coding DE RNAs and 71.14% of the DE RNAs had never been correlated to diabetes before. It is extremely interesting to note that most of the top deregulated DE RNAs consists in ncRNAs, suggesting that this class is of significant relevance in the development of the diabetic co-morbidity. The proteins encoded by the genes interact in one main network, comprising proteins of the immune system, and two smaller ones, also in this case genes are ubiquitarily expressed in multiple organs of our body and are localized in numerous different cellular organelles. 18 TFs were identified to govern this network, such as RXRA which acts synergistically with PPAR receptors (Ravnskjaer et al. 2005), the master adipogenesis regulator C/EBP β (Guo, Li, and Tang 2015) and RARG, who modulates adipogenesis through the regulation of FRA1, PPARG2 and C/EBP α (Xie et al. 2020). Moreover, A polymorphism in the NR1H2 gene has been associated with T2D and obesity (Solaas et al. 2010), a variant in NR3C1 has been associated with obesity (Lin et al. 2003), FHL2 is involved in Wnt signaling in diabetic kidney disease (Li et al. 2015) and JAZF1 has been found to inhibit adipose tissue inflammation in diet-induced diabetic mice (Meng et al. 2018). E2F6, YEATS4, EXOSC3, GAR1, ZNF622, CHURC1-FNTB, POLR2A, RFX4, DLX1, HOXA10 and ZMAT4 have to this day never been correlated with obesity nor diabetes.

GO ontologies indicated a role for lipoproteins and vesicular compartments, transmembrane receptors, the immune system, RNA polymerase I core binding activity and even cellular proliferation. Amongst the top deregulated pathways numerous are associated with the immune system and cancers, and indeed 42 out of the 101 KEGG deregulated terms (41.6%) and 27 out of the 120 WikiPathways deregulated terms (22.5%) were correlated with the immunogenic phenomenon, whilst 22 out of the 101 KEGG deregulated terms (21.8%) and 31 out of the 120 WikiPathways deregulated terms (25.8%) were identified as correlated with oncogenesis. Interestingly, as it was for diabetes versus control conditions, there seems to be an increased susceptibility for renal cancer when switching to a diabetes. Metabolism-associated diseases include central nervous system diseases with a metabolic component, along with other metabolic diseases such as hyperlipoproteinemia, highly linked with the APOE gene.

The last part of this research work focused on the identification and characterization of the non-coding transcriptome in obesity and diabetes pathogenesis, as this class of molecules are showing to have more and more of a relevant function in the pathogenesis of numerous diseases. It is remarkable to note how the number of non-coding DE RNAs increases when switching from an obesogenic condition to a diabetic one. Specifically, whilst non-coding DE RNAs are 6.43% of total DE RNAs in obese subjects, this percentage increases to up to 32.43% in diabetic subjects. Even more interesting is the fact that when considering the molecular underlining responsible for the additional diabetic phenotype (diabetic vs. obese), more than 50% of the DE RNAs are ncRNAs. This highlights how the non-coding epigenome could be of crucial relevance in the development of specific comorbidities, highlighting the possibility of new targets for future therapeutic intervention and prevention. The identification of co-interaction networks allowed to identify numerous targets through which the ncRNAs might exert their functions, along with strong non-coding specific deregulated networks.

A focus was then given on the lncRNAs deregulated in obesity. 6 specific lncRNAs were identified, SMIM25, COL4A2-AS2, CTEPHA1, RPS21-AS1, ITGB2-AS1, ACER2-AS, and a comprehensive computational characterization was performed to identify their genomic localization, structure and phylogenetic conservation. Indeed, lncRNAs sequences are overall less conserved than protein coding-genes and when looking for sequence conservation, it was found that only short sequence stretches are typically conserved, as lncRNAs evolve rapidly and often lack orthologs (Diederichs 2014). Interestingly, lncRNAs present higher structural conservation rather than nucleotide sequence conservation, as it is the structure which seems to be fundamental for their subsequent function (Zampetaki, Albrecht, and Steinhofel 2018). Moreover, it was found that all but SMIM25 presented binding sites for PPAR γ , C/EBP α , C/EBP β and C/EBP δ at the promoter level, suggesting further biological validation would be of relevance.

LncRNAs SMIM25, COL4A2AS2, RPS21-AS1, CTEPHA1 and COL4A2 and RPS21, sense gene of respectively COL4A2AS2 and RPS21-AS1, were considered for in vitro analysis. When analyzing their deregulation in different adipogenesis phases, in obese subjects SMIM25 appears to be differentially expressed in VAT versus SAT tissue, whilst RPS21 appears to be the most upregulated during differentiation. In hADSCs of lean subjects differentiated for 14 days, all the considered lncRNAs and sense genes change at the different phasis of the adipogenesis process, presenting a peak at day 7. RNA interference studies were performed in order to assess whether a decrease for of C/EBP β and C/EBP δ could result in alteration of the lncRNAs. When C/EBP β 's expression was silenced, all but SMIM25 were found to be downregulated, suggesting that C/EBP β is necessary for their expression. Similarly, when C/EBP δ 's expression was silenced, all the genes were found to be downregulated. As PPAR γ is known to be adipogenesis' master regulator, its influence on the lncRNAs and respective sense genes was analyzed. To do so, its expression was firstly induced with its activator troglitazone and indeed all the lncRNAs and respective sense genes were induced by PPAR γ 's activation. To verify that this induction was specific, hADSCs were differentiated in presence or absence of the PPAR γ 's inhibitor T0070907. SMIM25 and RPS21-AS1 specific induction after 7 days of differentiation was inverted in presence of the PPAR γ inhibitor, suggesting that it is these two targets specifically which are modulated by it. Lastly, as obesity is strictly modulated by the nutritional component, hADSCs were differentiated in three different culture media: a standard one with high glucose, one with low glucose, and one supplemented with a lipid mixture of free fatty acids. Interestingly, SMIM25, COL4A2-AS2 and CTEPHA1 seem to be significantly upregulated in the differentiation medium composed of low glucose, suggesting that glucose levels and glucose metabolism could highly influence their expression.

Overall, the results presented in this work highlight the fundamental role that transcriptional deregulation could have in the development of obesity and subsequent diabetes co-morbidities. The work provides a comprehensive database of who these DE RNAs are, what function they exert, which pathways they influence and their potential disease implications. It will be of great relevance for future analysis seeking to identify new targets in obesity and diabetes pathogenesis, providing a crucial starting point for further omics analyses and specific functional evaluations. Indeed, further in-depth analysis of the transcriptional profiles of the

three categories could provide insights also into splicing or mutational events. Specifically, differential splicing is a post-transcriptional biological process which enables the production of multiple mRNAs from one gene. As this is an emerging approach, a number of computational approaches have been developed to identify and quantify differentially spliced genes from RNA-seq data, in order to obtain further insights into the analyzed conditions (Mehmood et al. 2019). Moreover, somatic mutations, typically detected through an analysis of the DNA sequence, can now be identified in RNAseq data, providing even more information for a certain disease condition (Sheng et al. 2016, Prodduturi et al. 2018). The results obtained here also clearly highlight the role of the non-coding component in the development of the diabetic co-morbidity, and functional investigation of this molecules could be of crucial relevance in understanding a new disease-mechanism never before analyzed, and even highlight why certain patients are at a higher risk for developing a specific co-morbidity, paving the way for early intervention and precision medicine strategies.

6. Acknowledgments

I would like to acknowledge and thank the Fondazione Fratelli Confalonieri for financial support during my PhD.

7. Bibliography

- Adams, S. H. 2011. "Emerging perspectives on essential amino acid metabolism in obesity and the insulin-resistant state." *Adv Nutr* 2 (6):445-56. doi: 10.3945/an.111.000737.
- Allum, Fiona, and Elin Grundberg. 2020. "Capturing functional epigenomes for insight into metabolic diseases." *Molecular Metabolism* 38:100936. doi: 10.1016/j.molmet.2019.12.016.
- Alvarez-Dominguez, J. R., Z. Bai, D. Xu, B. Yuan, K. A. Lo, M. J. Yoon, Y. C. Lim, M. Knoll, N. Slavov, S. Chen, C. Peng, H. F. Lodish, and L. Sun. 2015. "De Novo Reconstruction of Adipose Tissue Transcriptomes Reveals Long Non-coding RNA Regulators of Brown Adipocyte Development." *Cell Metab* 21 (5):764-776. doi: 10.1016/j.cmet.2015.04.003.
- Arcinas, Camille, Wilson Tan, Wenning Fang, Tresha P. Desai, Diana Chee Siang Teh, Ufuk Degirmenci, Dan Xu, Roger Foo, and Lei Sun. 2019. "Adipose circular RNAs exhibit dynamic regulation in obesity and functional role in adipogenesis." *Nature Metabolism* 1 (7):688-703. doi: 10.1038/s42255-019-0078-z.
- Arnes, L., I. Akerman, D. A. Balderes, J. Ferrer, and L. Sussel. 2016. "βlinc1 encodes a long noncoding RNA that regulates islet β-cell formation and function." *Genes Dev* 30 (5):502-7. doi: 10.1101/gad.273821.115.
- Avgerinos, K. I., N. Spyrou, C. S. Mantzoros, and M. Dalamaga. 2019. "Obesity and cancer risk: Emerging biological mechanisms and perspectives." *Metabolism* 92:121-135. doi: 10.1016/j.metabol.2018.11.001.
- Batista, P. J., and H. Y. Chang. 2013. "Long noncoding RNAs: cellular address codes in development and disease." *Cell* 152 (6):1298-307. doi: 10.1016/j.cell.2013.02.012.
- Beamish, A. J., S. E. Johansson, and T. Olbers. 2015. "Bariatric surgery in adolescents: what do we know so far?" *Scand J Surg* 104 (1):24-32. doi: 10.1177/1457496914553150.
- Beamish, A. J., and T. Reinehr. 2017. "Should bariatric surgery be performed in adolescents?" *Eur J Endocrinol* 176 (4):D1-D15. doi: 10.1530/EJE-16-0906.
- Berg, A. H., Y. Lin, M. P. Lisanti, and P. E. Scherer. 2004. "Adipocyte differentiation induces dynamic changes in NF-κB expression and activity." *Am J Physiol Endocrinol Metab* 287 (6):E1178-88. doi: 10.1152/ajpendo.00002.2004.
- Bessesen, D. H. 2011. "Regulation of body weight: what is the regulated parameter?" *Physiol Behav* 104 (4):599-607. doi: 10.1016/j.physbeh.2011.05.006.
- Bindea, G., B. Mlecnik, H. Hackl, P. Charoentong, M. Tosolini, A. Kirilovsky, W. H. Fridman, F. Pagès, Z. Trajanoski, and J. Galon. 2009. "ClueGO: a Cytoscape plug-in to decipher functionally grouped gene ontology and pathway annotation networks." *Bioinformatics* 25 (8):1091-3. doi: 10.1093/bioinformatics/btp101.
- Bleich, S. N., K. A. Vercammen, L. Y. Zatz, J. M. Frelief, C. B. Ebbeling, and A. Peeters. 2018. "Interventions to prevent global childhood overweight and obesity: a systematic review." *Lancet Diabetes Endocrinol* 6 (4):332-346. doi: 10.1016/S2213-8587(17)30358-3.
- Bost, F., M. Aouadi, L. Caron, and B. Binétry. 2005. "The role of MAPKs in adipocyte differentiation and obesity." *Biochimie* 87 (1):51-6. doi: 10.1016/j.biochi.2004.10.018.

- Bryant, R. V., C. G. Schultz, S. Ooi, C. Goess, S. P. Costello, A. D. Vincent, S. N. Schoeman, A. Lim, F. D. Bartholomeusz, S. P. L. Travis, and J. M. Andrews. 2018. "Obesity in Inflammatory Bowel Disease: Gains in Adiposity despite High Prevalence of Myopenia and Osteopenia." *Nutrients* 10 (9). doi: 10.3390/nu10091192.
- Cai, R., Y. Sun, N. Qimuge, G. Wang, Y. Wang, G. Chu, T. Yu, G. Yang, and W. Pang. 2018. "Adiponectin AS lncRNA inhibits adipogenesis by transferring from nucleus to cytoplasm and attenuating Adiponectin mRNA translation." *Biochim Biophys Acta Mol Cell Biol Lipids* 1863 (4):420-432. doi: 10.1016/j.bbaliip.2018.01.005.
- Cai, R., G. Tang, Q. Zhang, W. Yong, W. Zhang, J. Xiao, C. Wei, C. He, G. Yang, and W. Pang. 2019. "A Novel lnc-RNA, Named lnc-ORA, Is Identified by RNA-Seq Analysis, and Its Knockdown Inhibits Adipogenesis by Regulating the PI3K/AKT/mTOR Signaling Pathway." *Cells* 8 (5). doi: 10.3390/cells8050477.
- Carelli, S., F. Messaggio, A. Canazza, D. M. Hebda, F. Caremoli, E. Latorre, M. G. Grimoldi, M. Colli, G. Bulfamante, C. Tremolada, A. M. Di Giulio, and A. Gorio. 2015. "Characteristics and Properties of Mesenchymal Stem Cells Derived From Microfragmented Adipose Tissue." *Cell Transplant* 24 (7):1233-52. doi: 10.3727/096368914X681603.
- Carter, G., B. Miladinovic, A. A. Patel, L. Deland, S. Mastorides, and N. A. Patel. 2015. "Circulating long noncoding RNA GAS5 levels are correlated to prevalence of type 2 diabetes mellitus." *BBA Clin* 4:102-7. doi: 10.1016/j.bbacli.2015.09.001.
- Chen, J., X. Cui, C. Shi, L. Chen, L. Yang, L. Pang, J. Zhang, X. Guo, J. Wang, and C. Ji. 2015. "Differential lncRNA expression profiles in brown and white adipose tissues." *Mol Genet Genomics* 290 (2):699-707. doi: 10.1007/s00438-014-0954-x.
- Chen, J., Y. Liu, S. Lu, L. Yin, C. Zong, S. Cui, D. Qin, Y. Yang, Q. Guan, X. Li, and X. Wang. 2017. "The role and possible mechanism of lncRNA U90926 in modulating 3T3-L1 preadipocyte differentiation." *Int J Obes (Lond)* 41 (2):299-308. doi: 10.1038/ijo.2016.189.
- Chen, X., D. G. Robinson, and J. D. Storey. 2019. "The functional false discovery rate with applications to genomics." *Biostatistics*. doi: 10.1093/biostatistics/kxz010.
- Chen, Y., K. Li, X. Zhang, J. Chen, M. Li, and L. Liu. 2020. "The novel long noncoding RNA lncRNA-Adi regulates adipogenesis." *Stem Cells Transl Med*. doi: 10.1002/sctm.19-0438.
- Chen, Y., W. Ye, Y. Zhang, and Y. Xu. 2015. "High speed BLASTN: an accelerated MegaBLAST search tool." *Nucleic Acids Res* 43 (16):7762-8. doi: 10.1093/nar/gkv784.
- Chen, Z., L. Ding, W. Yang, J. Wang, L. Chen, Y. Chang, B. Geng, Q. Cui, Y. Guan, and J. Yang. 2017. "Hepatic Activation of the FAM3C-HSF1-CaM Pathway Attenuates Hyperglycemia of Obese Diabetic Mice." *Diabetes* 66 (5):1185-1197. doi: 10.2337/db16-0993.
- Childerhose, J. E., A. Alsamawi, T. Mehta, J. E. Smith, S. Woolford, and B. A. Tarini. 2017. "Adolescent bariatric surgery: a systematic review of recommendation documents." *Surg Obes Relat Dis* 13 (10):1768-1779. doi: 10.1016/j.soard.2017.08.008.
- Conesa, A., P. Madrigal, S. Tarazona, D. Gomez-Cabrero, A. Cervera, A. McPherson, M. W. Szcześniak, D. J. Gaffney, L. L. Elo, X. Zhang, and A. Mortazavi. 2016. "A survey of

- best practices for RNA-seq data analysis." *Genome Biol* 17:13. doi: 10.1186/s13059-016-0881-8.
- Consortium, ENCODE Project. 2012. "An integrated encyclopedia of DNA elements in the human genome." *Nature* 489 (7414):57-74. doi: 10.1038/nature11247.
- Cooper, D. R., G. Carter, P. Li, R. Patel, J. E. Watson, and N. A. Patel. 2014. "Long Non-Coding RNA NEAT1 Associates with SRp40 to Temporally Regulate PPAR γ 2 Splicing during Adipogenesis in 3T3-L1 Cells." *Genes (Basel)* 5 (4):1050-63. doi: 10.3390/genes5041050.
- Crowson, C. S., E. L. Matteson, J. M. Davis, and S. E. Gabriel. 2013. "Contribution of obesity to the rise in incidence of rheumatoid arthritis." *Arthritis Care Res (Hoboken)* 65 (1):71-7. doi: 10.1002/acr.21660.
- Dalton, B., I. C. Campbell, and U. Schmidt. 2017. "Neuromodulation and neurofeedback treatments in eating disorders and obesity." *Curr Opin Psychiatry* 30 (6):458-473. doi: 10.1097/YCO.0000000000000361.
- Davis, D. B., J. A. Lavine, J. I. Suhonen, K. A. Krautkramer, M. E. Rabaglia, J. M. Sperger, L. A. Fernandez, B. S. Yandell, M. P. Keller, I. M. Wang, E. E. Schadt, and A. D. Attie. 2010. "FoxM1 is up-regulated by obesity and stimulates beta-cell proliferation." *Mol Endocrinol* 24 (9):1822-34. doi: 10.1210/me.2010-0082.
- DeBerardinis, R. J., and C. B. Thompson. 2012. "Cellular metabolism and disease: what do metabolic outliers teach us?" *Cell* 148 (6):1132-44. doi: 10.1016/j.cell.2012.02.032.
- Diederichs, S. 2014. "The four dimensions of noncoding RNA conservation." *Trends Genet* 30 (4):121-3. doi: 10.1016/j.tig.2014.01.004.
- Dispirito, J. R., B. Fang, F. Wang, and M. A. Lazar. 2013. "Pruning of the adipocyte peroxisome proliferator-activated receptor γ cistrome by hematopoietic master regulator PU.1." *Mol Cell Biol* 33 (16):3354-64. doi: 10.1128/MCB.00599-13.
- Dobin, A., and T. R. Gingeras. 2016. Mapping RNA-seq Reads with STAR.
- Duren, D. L., R. J. Sherwood, S. A. Czerwinski, M. Lee, A. C. Choh, R. M. Siervogel, and W. Cameron Chumlea. 2008. "Body composition methods: comparisons and interpretation." *J Diabetes Sci Technol* 2 (6):1139-46. doi: 10.1177/193229680800200623.
- Durrer Schutz, D., L. Busetto, D. Dicker, N. Farpour-Lambert, R. Pryke, H. Toplak, D. Widmer, V. Yumuk, and Y. Schutz. 2019. "European Practical and Patient-Centred Guidelines for Adult Obesity Management in Primary Care." *Obes Facts* 12 (1):40-66. doi: 10.1159/000496183.
- Falagas, Matthew E., and Maria Kompoti. 2006. "Obesity and infection." *The Lancet Infectious Diseases* 6 (7):438-446. doi: 10.1016/S1473-3099(06)70523-0.
- Fan, L., H. Xu, D. Li, H. Li, and D. Lu. 2020. "A novel long noncoding RNA, AC092834.1, regulates the adipogenic differentiation of human adipose-derived mesenchymal stem cells via the DKK1/Wnt/ β -catenin signaling pathway." *Biochem Biophys Res Commun* 525 (3):747-754. doi: 10.1016/j.bbrc.2020.02.140.
- Farooqi, I. S., and S. O'Rahilly. 2004. "Monogenic human obesity syndromes." *Recent progress in hormone research* 59:409-424. doi: 10.1210/rp.59.1.409.
- Farooqi, I. Sadaf, and Stephen O'Rahilly. 2016. "Chapter 28 - Genetic Syndromes Associated with Obesity**Chapter titles shaded in green indicate chapters dedicated predominantly

- to pediatric endocrinology content." In *Endocrinology: Adult and Pediatric (Seventh Edition)*, edited by J. Larry Jameson, Leslie J. De Groot, David M. de Kretser, Linda C. Giudice, Ashley B. Grossman, Shlomo Melmed, John T. Potts and Gordon C. Weir, 491-497.e2. Philadelphia: W.B. Saunders.
- Fawzy, M. S., A. A. Abdelghany, E. A. Toraih, and A. M. Mohamed. 2020. "Circulating long noncoding RNAs H19 and GAS5 are associated with type 2 diabetes but not with diabetic retinopathy: A preliminary study." *Bosn J Basic Med Sci*. doi: 10.17305/bjbms.2019.4533.
- Franco, H. L., J. Casasnovas, J. R. Rodríguez-Medina, and C. L. Cadilla. 2011. "Redundant or separate entities?--roles of Twist1 and Twist2 as molecular switches during gene transcription." *Nucleic Acids Res* 39 (4):1177-86. doi: 10.1093/nar/gkq890.
- Galateanu, B., S. Dinescu, A. Cimpean, A. Dinischiotu, and M. Costache. 2012. "Modulation of adipogenic conditions for prospective use of hADSCs in adipose tissue engineering." *Int J Mol Sci* 13 (12):15881-900. doi: 10.3390/ijms131215881.
- Galgani, Jose E., Victor Cortés, and Fernando Carrasco. 2014. "Carbohydrate, Fat and Protein Metabolism in Obesity." In *Metabolic Syndrome: A Comprehensive Textbook*, edited by Rexford S. Ahima, 1-22. Cham: Springer International Publishing.
- Gao, H., A. Kerr, H. Jiao, C. C. Hon, M. Rydén, I. Dahlman, and P. Arner. 2018. "Long Non-Coding RNAs Associated with Metabolic Traits in Human White Adipose Tissue." *EBioMedicine* 30:248-260. doi: 10.1016/j.ebiom.2018.03.010.
- Gao, H., N. Mejhert, J. A. Fretz, E. Arner, S. Lorente-Cebrián, A. Ehrlund, K. Dahlman-Wright, X. Gong, S. Strömblad, I. Douagi, J. Laurencikiene, I. Dahlman, C. O. Daub, M. Rydén, M. C. Horowitz, and P. Arner. 2014. "Early B cell factor 1 regulates adipocyte morphology and lipolysis in white adipose tissue." *Cell Metab* 19 (6):981-92. doi: 10.1016/j.cmet.2014.03.032.
- Gearing, L. J., H. E. Cumming, R. Chapman, A. M. Finkel, I. B. Woodhouse, K. Luu, J. A. Gould, S. C. Forster, and P. J. Hertzog. 2019. "CiiiDER: A tool for predicting and analysing transcription factor binding sites." *PLoS One* 14 (9):e0215495. doi: 10.1371/journal.pone.0215495.
- George, M. D., and J. F. Baker. 2016. "The Obesity Epidemic and Consequences for Rheumatoid Arthritis Care." *Curr Rheumatol Rep* 18 (1):6. doi: 10.1007/s11926-015-0550-z.
- Ghaben, Alexandra L., and Philipp E. Scherer. 2019. "Adipogenesis and metabolic health." *Nature Reviews Molecular Cell Biology* 20 (4):242-258. doi: 10.1038/s41580-018-0093-z.
- Giovannucci, E., D. M. Harlan, M. C. Archer, R. M. Bergental, S. M. Gapstur, L. A. Habel, M. Pollak, J. G. Regensteiner, and D. Yee. 2010. "Diabetes and cancer: a consensus report." *Diabetes Care* 33 (7):1674-85. doi: 10.2337/dc10-0666.
- Glavas, M. M., Q. Hui, E. Tudurí, S. Erener, N. L. Kasteel, J. D. Johnson, and T. J. Kieffer. 2019. "Early overnutrition reduces Pdx1 expression and induces β cell failure in Swiss Webster mice." *Sci Rep* 9 (1):3619. doi: 10.1038/s41598-019-39177-3.
- Goetzman, E. S., Z. Gong, M. Schiff, Y. Wang, and R. H. Muzumdar. 2018. "Metabolic pathways at the crossroads of diabetes and inborn errors." *J Inherit Metab Dis* 41 (1):5-17. doi: 10.1007/s10545-017-0091-x.

- Goldsworthy, M., A. Hugill, H. Freeman, E. Horner, K. Shimomura, D. Bogani, G. Pieleas, V. Mijat, R. Arkell, S. Bhattacharya, F. M. Ashcroft, and R. D. Cox. 2008. "Role of the transcription factor sox4 in insulin secretion and impaired glucose tolerance." *Diabetes* 57 (8):2234-44. doi: 10.2337/db07-0337.
- Golson, M. L., J. C. Dunn, M. F. Maulis, P. K. Dadi, A. B. Osipovich, M. A. Magnuson, D. A. Jacobson, and M. Gannon. 2015. "Activation of FoxM1 Revitalizes the Replicative Potential of Aged β -Cells in Male Mice and Enhances Insulin Secretion." *Diabetes* 64 (11):3829-38. doi: 10.2337/db15-0465.
- Grundey, S. M., H. B. Brewer, J. I. Cleeman, S. C. Smith, C. Lenfant, L. ng National Heart, and Blood Institute, and American Heart Association. 2004. "Definition of metabolic syndrome: report of the National Heart, Lung, and Blood Institute/American Heart Association conference on scientific issues related to definition." *Arterioscler Thromb Vasc Biol* 24 (2):e13-8. doi: 10.1161/01.ATV.0000111245.75752.C6.
- Guillet, C., C. Domingues-Faria, S. Walrand, and Y. Boirie. 2016. "Chapter 8 - Specificity of Amino Acids and Protein Metabolism in Obesity." In *The Molecular Nutrition of Amino Acids and Proteins*, edited by Dominique Dardevet, 99-108. Boston: Academic Press.
- Guindon, S., J. F. Dufayard, V. Lefort, M. Anisimova, W. Hordijk, and O. Gascuel. 2010. "New algorithms and methods to estimate maximum-likelihood phylogenies: assessing the performance of PhyML 3.0." *Syst Biol* 59 (3):307-21. doi: 10.1093/sysbio/syq010.
- Guo, L., X. Li, and Q. Q. Tang. 2015. "Transcriptional regulation of adipocyte differentiation: a central role for CCAAT/enhancer-binding protein (C/EBP) β ." *J Biol Chem* 290 (2):755-61. doi: 10.1074/jbc.R114.619957.
- Haidar, Y. M., and B. C. Cosman. 2011. "Obesity epidemiology." *Clin Colon Rectal Surg* 24 (4):205-10. doi: 10.1055/s-0031-1295684.
- Hartford, C. C. R., and A. Lal. 2020. "When Long Noncoding Becomes Protein Coding." *Mol Cell Biol* 40 (6). doi: 10.1128/MCB.00528-19.
- Haslam, D., N. Sattar, and M. Lean. 2006. "ABC of obesity. Obesity--time to wake up." *BMJ* 333 (7569):640-2. doi: 10.1136/bmj.333.7569.640.
- Hausman, G. J., M. V. Dodson, K. Ajuwon, M. Azain, K. M. Barnes, L. L. Guan, Z. Jiang, S. P. Poulos, R. D. Sainz, S. Smith, M. Spurlock, J. Novakofski, M. E. Fernyhough, and W. G. Bergen. 2009. "Board-invited review: the biology and regulation of preadipocytes and adipocytes in meat animals." *J Anim Sci* 87 (4):1218-46. doi: 10.2527/jas.2008-1427.
- He, K., H. Qu, H. Wang, S. Zhang, X. H. Qian, and W. Li. 2016. "Regulated and Functional Expression of the Corepressor MTA3 in Rodent Testis." *Endocrinology* 157 (11):4400-4410. doi: 10.1210/en.2016-1213.
- Hegde, V., and N. V. Dhurandhar. 2013. "Microbes and obesity--interrelationship between infection, adipose tissue and the immune system." *Clin Microbiol Infect* 19 (4):314-20. doi: 10.1111/1469-0691.12157.
- Hishida, T., M. Nishizuka, S. Osada, and M. Imagawa. 2009. "The role of C/EBPdelta in the early stages of adipogenesis." *Biochimie* 91 (5):654-7. doi: 10.1016/j.biochi.2009.02.002.
- Hossain, P., B. Kavar, and M. El Nahas. 2007. "Obesity and diabetes in the developing world--a growing challenge." *N Engl J Med* 356 (3):213-5. doi: 10.1056/NEJMp068177.

- Huang, Q., M. Liu, X. Du, R. Zhang, Y. Xue, Y. Zhang, W. Zhu, D. Li, A. Zhao, and Y. Liu. 2014. "Role of p53 in preadipocyte differentiation." *Cell Biol Int* 38 (12):1384-93. doi: 10.1002/cbin.10334.
- Huang, X., C. Fu, W. Liu, Y. Liang, P. Li, Z. Liu, Q. Sheng, and P. Liu. 2019. "Chemerin-induced angiogenesis and adipogenesis in 3 T3-L1 preadipocytes is mediated by lncRNA Meg3 through regulating Dickkopf-3 by sponging miR-217." *Toxicol Appl Pharmacol* 385:114815. doi: 10.1016/j.taap.2019.114815.
- Huang, Y., C. Jin, Y. Zheng, X. Li, S. Zhang, Y. Zhang, L. Jia, and W. Li. 2017. "Knockdown of lncRNA MIR31HG inhibits adipocyte differentiation of human adipose-derived stem cells via histone modification of FABP4." *Sci Rep* 7 (1):8080. doi: 10.1038/s41598-017-08131-6.
- Huang, Y., Y. Zheng, C. Jin, X. Li, L. Jia, and W. Li. 2016. "Long Non-coding RNA H19 Inhibits Adipocyte Differentiation of Bone Marrow Mesenchymal Stem Cells through Epigenetic Modulation of Histone Deacetylases." *Sci Rep* 6:28897. doi: 10.1038/srep28897.
- Indrio, F., S. Martini, R. Francavilla, L. Corvaglia, F. Cristofori, S. A. Mastrolia, J. Neu, S. Rautava, G. Russo Spina, F. Raimondi, and G. Loverro. 2017. "Epigenetic Matters: The Link between Early Nutrition, Microbiome, and Long-term Health Development." *Front Pediatr* 5:178. doi: 10.3389/fped.2017.00178.
- Jackerott, M., A. Møldrup, P. Thams, E. D. Galsgaard, J. Knudsen, Y. C. Lee, and J. H. Nielsen. 2006. "STAT5 activity in pancreatic beta-cells influences the severity of diabetes in animal models of type 1 and 2 diabetes." *Diabetes* 55 (10):2705-12. doi: 10.2337/db06-0244.
- Jackson, V. M., D. M. Breen, J. P. Fortin, A. Liou, J. B. Kuzmiski, A. K. Loomis, M. L. Rives, B. Shah, and P. A. Carpino. 2015. "Latest approaches for the treatment of obesity." *Expert Opin Drug Discov* 10 (8):825-39. doi: 10.1517/17460441.2015.1044966.
- Janky, R., A. Verfaillie, H. Imrichová, B. Van de Sande, L. Standaert, V. Christiaens, G. Hulselmans, K. Hertel, M. Naval Sanchez, D. Potier, D. Svetlichnyy, Z. Kalender Atak, M. Fiers, J. C. Marine, and S. Aerts. 2014. "iRegulon: from a gene list to a gene regulatory network using large motif and track collections." *PLoS Comput Biol* 10 (7):e1003731. doi: 10.1371/journal.pcbi.1003731.
- Jimenez, M. A., P. Akerblad, M. Sigvardsson, and E. D. Rosen. 2007. "Critical role for Ebf1 and Ebf2 in the adipogenic transcriptional cascade." *Mol Cell Biol* 27 (2):743-57. doi: 10.1128/MCB.01557-06.
- Jin, S., J. Li, M. Barati, S. Rane, Q. Lin, Y. Tan, Z. Zheng, L. Cai, and M. J. Rane. 2020. "Loss of NF-E2 expression contributes to the induction of profibrotic signaling in diabetic kidneys." *Life Sci* 254:117783. doi: 10.1016/j.lfs.2020.117783.
- Jones, J. E. C., N. Rabhi, J. Orofino, R. Gamini, V. Perissi, C. Vernochet, and S. R. Farmer. 2020. "The Adipocyte Acquires a Fibroblast-Like Transcriptional Signature in Response to a High Fat Diet." *Sci Rep* 10 (1):2380. doi: 10.1038/s41598-020-59284-w.
- Jéquier, E. 2002. "Pathways to obesity." *Int J Obes Relat Metab Disord* 26 Suppl 2:S12-7. doi: 10.1038/sj.ijo.0802123.

- Kawaji, A., Y. Ohnaka, S. Osada, M. Nishizuka, and M. Imagawa. 2010. "Gelsolin, an actin regulatory protein, is required for differentiation of mouse 3T3-L1 cells into adipocytes." *Biol Pharm Bull* 33 (5):773-9.
- Kenney, E. L., and S. L. Gortmaker. 2017. "United States Adolescents' Television, Computer, Videogame, Smartphone, and Tablet Use: Associations with Sugary Drinks, Sleep, Physical Activity, and Obesity." *J Pediatr* 182:144-149. doi: 10.1016/j.jpeds.2016.11.015.
- Kim, D., S. M. Lee, and H. S. Jun. 2017. "Impact of T-cell-specific Smad4 deficiency on the development of autoimmune diabetes in NOD mice." *Immunol Cell Biol* 95 (3):287-296. doi: 10.1038/icb.2016.98.
- Kim, S., H. S. Kim, K. W. Chung, S. H. Oh, J. W. Yun, S. H. Im, M. K. Lee, K. W. Kim, and M. S. Lee. 2007. "Essential role for signal transducer and activator of transcription-1 in pancreatic beta-cell death and autoimmune type 1 diabetes of nonobese diabetic mice." *Diabetes* 56 (10):2561-8. doi: 10.2337/db06-1372.
- Kompella, P., and K. M. Vasquez. 2019. "Obesity and cancer: A mechanistic overview of metabolic changes in obesity that impact genetic instability." *Mol Carcinog* 58 (9):1531-1550. doi: 10.1002/mc.23048.
- Krstic, J., I. Reinisch, M. Schupp, T. J. Schulz, and A. Prokesch. 2018. "p53 Functions in Adipose Tissue Metabolism and Homeostasis." *Int J Mol Sci* 19 (9). doi: 10.3390/ijms19092622.
- Kumar, S., and A. S. Kelly. 2017. "Review of Childhood Obesity: From Epidemiology, Etiology, and Comorbidities to Clinical Assessment and Treatment." *Mayo Clin Proc* 92 (2):251-265. doi: 10.1016/j.mayocp.2016.09.017.
- Lackey, D. E., F. C. G. Reis, R. Isaac, R. C. Zapata, D. El Ouarrat, Y. S. Lee, G. Bandyopadhyay, J. M. Ofrecio, D. Y. Oh, and O. Osborn. 2019. "Adipocyte PU.1 knockout promotes insulin sensitivity in HFD-fed obese mice." *Sci Rep* 9 (1):14779. doi: 10.1038/s41598-019-51196-8.
- Landrier, J. F., A. Derghal, and L. Mounien. 2019. "MicroRNAs in Obesity and Related Metabolic Disorders." *Cells* 8 (8). doi: 10.3390/cells8080859.
- Lawrence, V. J., and P. G. Kopelman. 2004. "Medical consequences of obesity." *Clin Dermatol* 22 (4):296-302. doi: 10.1016/j.clindermatol.2004.01.012.
- Lee, G., F. Elwood, J. McNally, J. Weiszmann, M. Lindstrom, K. Amaral, M. Nakamura, S. Miao, P. Cao, R. M. Learned, J. L. Chen, and Y. Li. 2002. "T0070907, a selective ligand for peroxisome proliferator-activated receptor gamma, functions as an antagonist of biochemical and cellular activities." *J Biol Chem* 277 (22):19649-57. doi: 10.1074/jbc.M200743200.
- Lee, J. E., H. Schmidt, B. Lai, and K. Ge. 2019. "Transcriptional and Epigenomic Regulation of Adipogenesis." *Mol Cell Biol* 39 (11). doi: 10.1128/MCB.00601-18.
- Lee, Y. S., H. H. Lee, J. Park, E. J. Yoo, C. A. Glackin, Y. I. Choi, S. H. Jeon, R. H. Seong, S. D. Park, and J. B. Kim. 2003. "Twist2, a novel ADD1/SREBP1c interacting protein, represses the transcriptional activity of ADD1/SREBP1c." *Nucleic Acids Res* 31 (24):7165-74. doi: 10.1093/nar/gkg934.

- Lefterova, M. I., A. K. Haakonsson, M. A. Lazar, and S. Mandrup. 2014. "PPAR γ and the global map of adipogenesis and beyond." *Trends Endocrinol Metab* 25 (6):293-302. doi: 10.1016/j.tem.2014.04.001.
- Lekka, E., and J. Hall. 2018. "Noncoding RNAs in disease." *FEBS Lett* 592 (17):2884-2900. doi: 10.1002/1873-3468.13182.
- Li, Jianqiang, Doudou Zhou, Weiliang Qiu, Yuliang Shi, Ji-Jiang Yang, Shi Chen, Qing Wang, and Hui Pan. 2018. "Application of Weighted Gene Co-expression Network Analysis for Data from Paired Design." *Scientific Reports* 8 (1):622. doi: 10.1038/s41598-017-18705-z.
- Li, M., Q. Gao, Z. Tian, X. Lu, Y. Sun, Z. Chen, H. Zhang, Y. Mao, and Z. Yang. 2019. "MIR221HG Is a Novel Long Noncoding RNA that Inhibits Bovine Adipocyte Differentiation." *Genes (Basel)* 11 (1). doi: 10.3390/genes11010029.
- Li, M., X. Sun, H. Cai, Y. Sun, M. Plath, C. Li, X. Lan, C. Lei, F. Lin, Y. Bai, and H. Chen. 2016. "Long non-coding RNA ADNCR suppresses adipogenic differentiation by targeting miR-204." *Biochim Biophys Acta* 1859 (7):871-82. doi: 10.1016/j.bbagr.2016.05.003.
- Li, S. Y., P. H. Huang, D. C. Tarng, T. P. Lin, W. C. Yang, Y. H. Chang, A. H. Yang, C. C. Lin, M. H. Yang, J. W. Chen, G. W. Schmid-Schönbein, S. Chien, P. H. Chu, and S. J. Lin. 2015. "Four-and-a-Half LIM Domains Protein 2 Is a Coactivator of Wnt Signaling in Diabetic Kidney Disease." *J Am Soc Nephrol* 26 (12):3072-84. doi: 10.1681/ASN.2014100989.
- Li, Z., C. Jin, S. Chen, Y. Zheng, Y. Huang, L. Jia, W. Ge, and Y. Zhou. 2017. "Long non-coding RNA MEG3 inhibits adipogenesis and promotes osteogenesis of human adipose-derived mesenchymal stem cells via miR-140-5p." *Mol Cell Biochem* 433 (1-2):51-60. doi: 10.1007/s11010-017-3015-z.
- Lin, L., W. Pang, K. Chen, F. Wang, J. Gengler, Y. Sun, and Q. Tong. 2012. "Adipocyte expression of PU.1 transcription factor causes insulin resistance through upregulation of inflammatory cytokine gene expression and ROS production." *Am J Physiol Endocrinol Metab* 302 (12):E1550-9. doi: 10.1152/ajpendo.00462.2011.
- Lin, R. C., X. L. Wang, B. Dalziel, I. D. Caterson, and B. J. Morris. 2003. "Association of obesity, but not diabetes or hypertension, with glucocorticoid receptor N363S variant." *Obes Res* 11 (6):802-8. doi: 10.1038/oby.2003.111.
- Liu, S., L. Sheng, H. Miao, T. L. Saunders, O. A. MacDougald, R. J. Koenig, and B. Xu. 2014. "SRA gene knockout protects against diet-induced obesity and improves glucose tolerance." *J Biol Chem* 289 (19):13000-9. doi: 10.1074/jbc.M114.564658.
- Liu, S. X., F. Zheng, K. L. Xie, M. R. Xie, L. J. Jiang, and Y. Cai. 2019. "Exercise Reduces Insulin Resistance in Type 2 Diabetes Mellitus via Mediating the lncRNA MALAT1/MicroRNA-382-3p/Resistin Axis." *Mol Ther Nucleic Acids* 18:34-44. doi: 10.1016/j.omtn.2019.08.002.
- Liu, S., R. Xu, I. Gerin, W. P. Cawthorn, O. A. Macdougald, X. W. Chen, A. R. Saltiel, R. J. Koenig, and B. Xu. 2014. "SRA regulates adipogenesis by modulating p38/JNK phosphorylation and stimulating insulin receptor gene expression and downstream signaling." *PLoS One* 9 (4):e95416. doi: 10.1371/journal.pone.0095416.

- Liu, Y., Y. Ji, M. Li, M. Wang, X. Yi, C. Yin, S. Wang, M. Zhang, Z. Zhao, and Y. Xiao. 2018. "Integrated analysis of long noncoding RNA and mRNA expression profile in children with obesity by microarray analysis." *Sci Rep* 8 (1):8750. doi: 10.1038/s41598-018-27113-w.
- Liu, Y., Y. Wang, X. He, S. Zhang, K. Wang, H. Wu, and L. Chen. 2018. "LncRNA TINCR/miR-31-5p/C/EBP- α feedback loop modulates the adipogenic differentiation process in human adipose tissue-derived mesenchymal stem cells." *Stem Cell Res* 32:35-42. doi: 10.1016/j.scr.2018.08.016.
- Livak, K. J., and T. D. Schmittgen. 2001. "Analysis of relative gene expression data using real-time quantitative PCR and the 2(-Delta Delta C(T)) Method." *Methods* 25 (4):402-8. doi: 10.1006/meth.2001.1262.
- Lo, K. A., S. Huang, A. C. E. Walet, Z. C. Zhang, M. K. Leow, M. Liu, and L. Sun. 2018. "Adipocyte Long-Noncoding RNA Transcriptome Analysis of Obese Mice Identified." *Diabetes* 67 (6):1045-1056. doi: 10.2337/db17-0526.
- Loh, Marie, Li Zhou, Hong Kiat Ng, and John Campbell Chambers. 2019. "Epigenetic disturbances in obesity and diabetes: Epidemiological and functional insights." *Molecular Metabolism* 27:S33-S41. doi: <https://doi.org/10.1016/j.molmet.2019.06.011>.
- Lorenz, R., S. H. Bernhart, C. Höner Zu Siederdisen, H. Tafer, C. Flamm, P. F. Stadler, and I. L. Hofacker. 2011. "ViennaRNA Package 2.0." *Algorithms Mol Biol* 6:26. doi: 10.1186/1748-7188-6-26.
- Lu, X., D. Bai, X. Liu, C. Zhou, and G. Yang. 2017. "Sedentary lifestyle related exosomal release of Hotair from gluteal-femoral fat promotes intestinal cell proliferation." *Sci Rep* 7:45648. doi: 10.1038/srep45648.
- Ma, X., L. Xu, A. T. Alberobello, O. Gavrilova, A. Bagattin, M. Skarulis, J. Liu, T. Finkel, and E. Mueller. 2015. "Celastrol Protects against Obesity and Metabolic Dysfunction through Activation of a HSF1-PGC1 α Transcriptional Axis." *Cell Metab* 22 (4):695-708. doi: 10.1016/j.cmet.2015.08.005.
- Maass, P. G., F. C. Luft, and S. Bähring. 2014. "Long non-coding RNA in health and disease." *J Mol Med (Berl)* 92 (4):337-46. doi: 10.1007/s00109-014-1131-8.
- Maclaren, N. K., S. Gujral, S. Ten, and R. Motagheti. 2007. "Childhood obesity and insulin resistance." *Cell Biochem Biophys* 48 (2-3):73-8. doi: 10.1007/s12013-007-0017-6.
- Maere, S., K. Heymans, and M. Kuiper. 2005. "BiNGO: a Cytoscape plugin to assess overrepresentation of gene ontology categories in biological networks." *Bioinformatics* 21 (16):3448-9. doi: 10.1093/bioinformatics/bti551.
- Mameli, C., S. Mazzantini, and G. V. Zuccotti. 2016. "Nutrition in the First 1000 Days: The Origin of Childhood Obesity." *Int J Environ Res Public Health* 13 (9). doi: 10.3390/ijerph13090838.
- Mansoori, Z., H. Ghaedi, M. Sadatamini, R. Vahabpour, A. Rahimipour, M. Shanaki, L. Saeidi, and F. Kazerouni. 2018. "Downregulation of long non-coding RNAs LINC00523 and LINC00994 in type 2 diabetes in an Iranian cohort." *Mol Biol Rep* 45 (5):1227-1233. doi: 10.1007/s11033-018-4276-7.
- Mattick, J. S. 2009. "The genetic signatures of noncoding RNAs." *PLoS Genet* 5 (4):e1000459. doi: 10.1371/journal.pgen.1000459.

- Mehmood, A., A. Laiho, M. S. Venäläinen, A. J. McGlinchey, N. Wang, and L. L. Elo. 2019. "Systematic evaluation of differential splicing tools for RNA-seq studies." *Brief Bioinform.* doi: 10.1093/bib/bbz126.
- Meng, F., Y. Lin, M. Yang, M. Li, G. Yang, P. Hao, and L. Li. 2018. "JAZF1 Inhibits Adipose Tissue Macrophages and Adipose Tissue Inflammation in Diet-Induced Diabetic Mice." *Biomed Res Int* 2018:4507659. doi: 10.1155/2018/4507659.
- Mi, L., X. Y. Zhao, S. Li, G. Yang, and J. D. Lin. 2017. "Conserved function of the long noncoding RNA Blnc1 in brown adipocyte differentiation." *Mol Metab* 6 (1):101-110. doi: 10.1016/j.molmet.2016.10.010.
- Morán, I., I. Akerman, M. van de Bunt, R. Xie, M. Benazra, T. Nammo, L. Arnes, N. Nakić, J. García-Hurtado, S. Rodríguez-Seguí, L. Pasquali, C. Sauty-Colace, A. Beucher, R. Scharfmann, J. van Arensbergen, P. R. Johnson, A. Berry, C. Lee, T. Harkins, V. Gmyr, F. Pattou, J. Kerr-Conte, L. Piemonti, T. Berney, N. Hanley, A. L. Gloyn, L. Sussel, L. Langman, K. L. Brayman, M. Sander, M. I. McCarthy, P. Ravassard, and J. Ferrer. 2012. "Human β cell transcriptome analysis uncovers lncRNAs that are tissue-specific, dynamically regulated, and abnormally expressed in type 2 diabetes." *Cell Metab* 16 (4):435-48. doi: 10.1016/j.cmet.2012.08.010.
- Muhammad, S. A., W. Raza, T. Nguyen, B. Bai, X. Wu, and J. Chen. 2017. "Cellular Signaling Pathways in Insulin Resistance-Systems Biology Analyses of Microarray Dataset Reveals New Drug Target Gene Signatures of Type 2 Diabetes Mellitus." *Front Physiol* 8:13. doi: 10.3389/fphys.2017.00013.
- Nagano, T., and P. Fraser. 2011. "No-nonsense functions for long noncoding RNAs." *Cell* 145 (2):178-81. doi: 10.1016/j.cell.2011.03.014.
- Ng, M., T. Fleming, M. Robinson, B. Thomson, N. Graetz, C. Margono, E. C. Mullany, S. Biryukov, C. Abbafati, S. F. Abera, J. P. Abraham, N. M. Abu-Rmeileh, T. Achoki, F. S. AlBuhairan, Z. A. Alemu, R. Alfonso, M. K. Ali, R. Ali, N. A. Guzman, W. Ammar, P. Anwari, A. Banerjee, S. Barquera, S. Basu, D. A. Bennett, Z. Bhutta, J. Blore, N. Cabral, I. C. Nonato, J. C. Chang, R. Chowdhury, K. J. Courville, M. H. Criqui, D. K. Cundiff, K. C. Dabhadkar, L. Dandona, A. Davis, A. Dayama, S. D. Dharmaratne, E. L. Ding, A. M. Durrani, A. Esteghamati, F. Farzadfar, D. F. Fay, V. L. Feigin, A. Flaxman, M. H. Forouzanfar, A. Goto, M. A. Green, R. Gupta, N. Hafezi-Nejad, G. J. Hankey, H. C. Harewood, R. Havmoeller, S. Hay, L. Hernandez, A. Husseini, B. T. Idrisov, N. Ikeda, F. Islami, E. Jahangir, S. K. Jassal, S. H. Jee, M. Jeffreys, J. B. Jonas, E. K. Kabagambe, S. E. Khalifa, A. P. Kengne, Y. S. Khader, Y. H. Khang, D. Kim, R. W. Kimokoti, J. M. Kinge, Y. Kokubo, S. Kosen, G. Kwan, T. Lai, M. Leinsalu, Y. Li, X. Liang, S. Liu, G. Logroscino, P. A. Lotufo, Y. Lu, J. Ma, N. K. Mainoo, G. A. Mensah, T. R. Merriman, A. H. Mokdad, J. Moschandreas, M. Naghavi, A. Naheed, D. Nand, K. M. Narayan, E. L. Nelson, M. L. Neuhouser, M. I. Nisar, T. Ohkubo, S. O. Oti, A. Pedroza, D. Prabhakaran, N. Roy, U. Sampson, H. Seo, S. G. Sepanlou, K. Shibuya, R. Shiri, I. Shiue, G. M. Singh, J. A. Singh, V. Skirbekk, N. J. Stapelberg, L. Sturua, B. L. Sykes, M. Tobias, B. X. Tran, L. Trasande, H. Toyoshima, S. van de Vijver, T. J. Vasankari, J. L. Veerman, G. Velasquez-Melendez, V. V. Vlassov, S. E. Vollset, T. Vos, C. Wang, X. Wang, E. Weiderpass, A. Werdecker, J. L. Wright, Y. C. Yang, H. Yatsuya, J. Yoon, S. J. Yoon, Y. Zhao, M. Zhou, S. Zhu, A. D. Lopez, C. J.

- Murray, and E. Gakidou. 2014. "Global, regional, and national prevalence of overweight and obesity in children and adults during 1980-2013: a systematic analysis for the Global Burden of Disease Study 2013." *Lancet* 384 (9945):766-81. doi: 10.1016/S0140-6736(14)60460-8.
- Nuermairmaiti, N., J. Liu, X. Liang, Y. Jiao, D. Zhang, L. Liu, X. Meng, and Y. Guan. 2018. "Effect of lncRNA HOXA11-AS1 on adipocyte differentiation in human adipose-derived stem cells." *Biochem Biophys Res Commun* 495 (2):1878-1884. doi: 10.1016/j.bbrc.2017.12.006.
- Nutter, C. A., and M. N. Kuyumcu-Martinez. 2018. "Emerging roles of RNA-binding proteins in diabetes and their therapeutic potential in diabetic complications." *Wiley Interdiscip Rev RNA* 9 (2). doi: 10.1002/wrna.1459.
- Ogden, C. L., M. D. Carroll, L. R. Curtin, M. M. Lamb, and K. M. Flegal. 2010. "Prevalence of high body mass index in US children and adolescents, 2007-2008." *JAMA* 303 (3):242-9. doi: 10.1001/jama.2009.2012.
- Pang, W. J., L. G. Lin, Y. Xiong, N. Wei, Y. Wang, Q. W. Shen, and G. S. Yang. 2013. "Knockdown of PU.1 AS lncRNA inhibits adipogenesis through enhancing PU.1 mRNA translation." *J Cell Biochem* 114 (11):2500-12. doi: 10.1002/jcb.24595.
- Park, M. J., J. H. Song, M. S. Shon, H. O. Kim, O. J. Kwon, S. S. Roh, C. Y. Kim, and G. N. Kim. 2016. "Anti-Adipogenic Effects of Ethanol Extracts Prepared from Selected Medicinal Herbs in 3T3-L1 Cells." *Prev Nutr Food Sci* 21 (3):227-235. doi: 10.3746/pnf.2016.21.3.227.
- Perks, K. L., N. Ferreira, T. R. Richman, J. A. Ermer, I. Kuznetsova, A. J. Shearwood, R. G. Lee, H. M. Viola, V. P. A. Johnstone, V. Matthews, L. C. Hool, O. Rackham, and A. Filipovska. 2017. "Adult-onset obesity is triggered by impaired mitochondrial gene expression." *Sci Adv* 3 (8):e1700677. doi: 10.1126/sciadv.1700677.
- Petrelli, Fausto, Alessio Cortellini, Alice Indini, Gianluca Tomasello, Michele Ghidini, Olga Nigro, Massimiliano Salati, Lorenzo Dottorini, Alessandro Iaculli, Antonio Varricchio, Valentina Rampulla, Sandro Barni, Antonio Bossi, Antonio Ghidini, and Alberto Zaniboni. 2020. "Obesity paradox in patients with cancer: A systematic review and meta-analysis of 6,320,365 patients." *medRxiv:2020.04.28.20082800*. doi: 10.1101/2020.04.28.20082800.
- Picard, F., M. Wanatabe, K. Schoonjans, J. Lydon, B. W. O'Malley, and J. Auwerx. 2002. "Progesterone receptor knockout mice have an improved glucose homeostasis secondary to beta -cell proliferation." *Proc Natl Acad Sci U S A* 99 (24):15644-8. doi: 10.1073/pnas.202612199.
- Piñero, J., J. M. Ramírez-Anguita, J. Saüch-Pitarch, F. Ronzano, E. Centeno, F. Sanz, and L. I. Furlong. 2020. "The DisGeNET knowledge platform for disease genomics: 2019 update." *Nucleic Acids Res* 48 (D1):D845-D855. doi: 10.1093/nar/gkz1021.
- Ponting, C. P., P. L. Oliver, and W. Reik. 2009. "Evolution and functions of long noncoding RNAs." *Cell* 136 (4):629-41. doi: 10.1016/j.cell.2009.02.006.
- Popkin, B. M., S. Du, W. D. Green, M. A. Beck, T. Algaith, C. H. Herbst, R. F. Alsukait, M. Alluhidan, N. Alazemi, and M. Shekar. 2020. "Individuals with obesity and COVID-19: A global perspective on the epidemiology and biological relationships." *Obes Rev*. doi: 10.1111/obr.13128.

- Pratt, D., J. Chen, D. Welker, R. Rivas, R. Pillich, V. Rynkov, K. Ono, C. Miello, L. Hicks, S. Szalma, A. Stojmirovic, R. Dobrin, M. Braxenthaler, J. Kuentzer, B. Demchak, and T. Ideker. 2015. "NDEx, the Network Data Exchange." *Cell Syst* 1 (4):302-305. doi: 10.1016/j.cels.2015.10.001.
- Prodduturi, N., A. Bhagwate, J. A. Kocher, and Z. Sun. 2018. "Indel sensitive and comprehensive variant/mutation detection from RNA sequencing data for precision medicine." *BMC Med Genomics* 11 (Suppl 3):67. doi: 10.1186/s12920-018-0391-5.
- Pulgaron, Elizabeth R., and Alan M. Delamater. 2014. "Obesity and type 2 diabetes in children: epidemiology and treatment." *Current diabetes reports* 14 (8):508-508. doi: 10.1007/s11892-014-0508-y.
- Purwana, I., J. J. Liu, B. Portha, and J. Buteau. 2017. "HSF1 acetylation decreases its transcriptional activity and enhances glucolipotoxicity-induced apoptosis in rat and human beta cells." *Diabetologia* 60 (8):1432-1441. doi: 10.1007/s00125-017-4310-7.
- Raut, S. K., and M. Khullar. 2018. "The Big Entity of New RNA World: Long Non-Coding RNAs in Microvascular Complications of Diabetes." *Front Endocrinol (Lausanne)* 9:300. doi: 10.3389/fendo.2018.00300.
- Ravnskjaer, K., M. Boergesen, B. Rubi, J. K. Larsen, T. Nielsen, J. Fridriksson, P. Maechler, and S. Mandrup. 2005. "Peroxisome proliferator-activated receptor alpha (PPARalpha) potentiates, whereas PPARgamma attenuates, glucose-stimulated insulin secretion in pancreatic beta-cells." *Endocrinology* 146 (8):3266-76. doi: 10.1210/en.2004-1430.
- Reddy, M. A., Z. Chen, J. T. Park, M. Wang, L. Lanting, Q. Zhang, K. Bhatt, A. Leung, X. Wu, S. Putta, P. Sætrom, S. Devaraj, and R. Natarajan. 2014. "Regulation of inflammatory phenotype in macrophages by a diabetes-induced long noncoding RNA." *Diabetes* 63 (12):4249-61. doi: 10.2337/db14-0298.
- Reusch, J. E., L. A. Colton, and D. J. Klemm. 2000. "CREB activation induces adipogenesis in 3T3-L1 cells." *Mol Cell Biol* 20 (3):1008-20. doi: 10.1128/mcb.20.3.1008-1020.2000.
- Rey, F., E. Lesma, D. Massihnia, E. Ciusani, S. Nava, C. Vasco, G. Al Haj, G. Ghilardi, E. Opocher, A. Gorio, S. Carelli, and A. M. Di Giulio. 2019. "Adipose-Derived Stem Cells from Fat Tissue of Breast Cancer Microenvironment Present Altered Adipogenic Differentiation Capabilities." *Stem Cells Int* 2019:1480314. doi: 10.1155/2019/1480314.
- Rosen, E. D., and O. A. MacDougald. 2006. "Adipocyte differentiation from the inside out." *Nat Rev Mol Cell Biol* 7 (12):885-96. doi: 10.1038/nrm2066.
- Rosen, E., J. Eguchi, and Z. Xu. 2009. "Transcriptional targets in adipocyte biology." *Expert Opin Ther Targets* 13 (8):975-86. doi: 10.1517/14728220903039706.
- Rosenwald, M., V. Efthymiou, L. Opitz, and C. Wolfrum. 2017. "SRF and MKL1 Independently Inhibit Brown Adipogenesis." *PLoS One* 12 (1):e0170643. doi: 10.1371/journal.pone.0170643.
- Ruan, Y., N. Lin, Q. Ma, R. Chen, Z. Zhang, W. Wen, H. Chen, and J. Sun. 2018. "Circulating LncRNAs Analysis in Patients with Type 2 Diabetes Reveals Novel Genes Influencing Glucose Metabolism and Islet β -Cell Function." *Cell Physiol Biochem* 46 (1):335-350. doi: 10.1159/000488434.
- Ryan, D. H., and S. Kahan. 2018. "Guideline Recommendations for Obesity Management." *Med Clin North Am* 102 (1):49-63. doi: 10.1016/j.mcna.2017.08.006.

- Saeidi, L., H. Ghaedi, M. Sadatamini, R. Vahabpour, A. Rahimipour, M. Shanaki, Z. Mansoori, and F. Kazerouni. 2018. "Long non-coding RNA LY86-AS1 and HCG27_201 expression in type 2 diabetes mellitus." *Mol Biol Rep* 45 (6):2601-2608. doi: 10.1007/s11033-018-4429-8.
- Salem, E. S. B., A. D. Vonberg, V. J. Borra, R. K. Gill, and T. Nakamura. 2019. "RNAs and RNA-Binding Proteins in Immuno-Metabolic Homeostasis and Diseases." *Front Cardiovasc Med* 6:106. doi: 10.3389/fcvm.2019.00106.
- Sathishkumar, C., P. Prabu, V. Mohan, and M. Balasubramanyam. 2018. "Linking a role of lncRNAs (long non-coding RNAs) with insulin resistance, accelerated senescence, and inflammation in patients with type 2 diabetes." *Hum Genomics* 12 (1):41. doi: 10.1186/s40246-018-0173-3.
- Saunders, K. H., D. Umashanker, L. I. Igel, R. B. Kumar, and L. J. Aronne. 2018. "Obesity Pharmacotherapy." *Med Clin North Am* 102 (1):135-148. doi: 10.1016/j.mcna.2017.08.010.
- Seidell, J. C., and J. Halberstadt. 2015. "The Global Burden of Obesity and the Challenges of Prevention." *Annals of Nutrition and Metabolism* 66(suppl 2) (Suppl. 2):7-12. doi: 10.1159/000375143.
- Seong, H. A., R. Manoharan, and H. Ha. 2018. "Smad proteins differentially regulate obesity-induced glucose and lipid abnormalities and inflammation via class-specific control of AMPK-related kinase MPK38/MELK activity." *Cell Death Dis* 9 (5):471. doi: 10.1038/s41419-018-0489-x.
- Shannon, P., A. Markiel, O. Ozier, N. S. Baliga, J. T. Wang, D. Ramage, N. Amin, B. Schwikowski, and T. Ideker. 2003. "Cytoscape: a software environment for integrated models of biomolecular interaction networks." *Genome Res* 13 (11):2498-504. doi: 10.1101/gr.1239303.
- Sheng, L., L. Ye, D. Zhang, W. P. Cawthorn, and B. Xu. 2018. "New Insights Into the Long Non-coding RNA SRA: Physiological Functions and Mechanisms of Action." *Front Med (Lausanne)* 5:244. doi: 10.3389/fmed.2018.00244.
- Sheng, Q., S. Zhao, C. I. Li, Y. Shyr, and Y. Guo. 2016. "Practicability of detecting somatic point mutation from RNA high throughput sequencing data." *Genomics* 107 (5):163-9. doi: 10.1016/j.ygeno.2016.03.006.
- Shepherd, P. R., L. Gnudi, E. Tozzo, H. Yang, F. Leach, and B. B. Kahn. 1993. "Adipose cell hyperplasia and enhanced glucose disposal in transgenic mice overexpressing GLUT4 selectively in adipose tissue." *J Biol Chem* 268 (30):22243-6.
- Shi, X., D. Ma, M. Li, L. Zeng, J. Chen, and Y. Yang. 2019. "Nuclear receptor TLX regulates islet beta cell proliferation via E2F6." *Biochem Biophys Res Commun* 513 (3):560-566. doi: 10.1016/j.bbrc.2019.04.033.
- Shulman, G. I. 2014. "Ectopic fat in insulin resistance, dyslipidemia, and cardiometabolic disease." *N Engl J Med* 371 (23):2237-8. doi: 10.1056/NEJMc1412427.
- Sievers, F., and D. G. Higgins. 2014. "Clustal Omega, accurate alignment of very large numbers of sequences." *Methods Mol Biol* 1079:105-16. doi: 10.1007/978-1-62703-646-7_6.
- Singh, R. K., P. Kumar, and K. Mahalingam. 2017. "Molecular genetics of human obesity: A comprehensive review." *C R Biol* 340 (2):87-108. doi: 10.1016/j.crv.2016.11.007.

- Singla, P., A. Bardoloi, and A. A. Parkash. 2010. "Metabolic effects of obesity: A review." *World J Diabetes* 1 (3):76-88. doi: 10.4239/wjd.v1.i3.76.
- Solaas, K., V. Legry, K. Retterstol, P. R. Berg, K. B. Holven, J. Ferrières, P. Amouyel, S. Lien, J. Romeo, J. Valtueña, K. Widhalm, J. R. Ruiz, J. Dallongeville, S. Tonstad, H. Rootwelt, B. Halvorsen, M. S. Nenseter, K. I. Birkeland, P. M. Thorsby, A. Meirhaeghe, and H. I. Nebb. 2010. "Suggestive evidence of associations between liver X receptor β polymorphisms with type 2 diabetes mellitus and obesity in three cohort studies: HUNT2 (Norway), MONICA (France) and HELENA (Europe)." *BMC Med Genet* 11:144. doi: 10.1186/1471-2350-11-144.
- St Laurent, G., C. Wahlestedt, and P. Kapranov. 2015. "The Landscape of long noncoding RNA classification." *Trends Genet* 31 (5):239-51. doi: 10.1016/j.tig.2015.03.007.
- Stanhope, K. L., J. M. Schwarz, N. L. Keim, S. C. Griffen, A. A. Bremer, J. L. Graham, B. Hatcher, C. L. Cox, A. Dyachenko, W. Zhang, J. P. McGahan, A. Seibert, R. M. Krauss, S. Chiu, E. J. Schaefer, M. Ai, S. Otokoza, K. Nakajima, T. Nakano, C. Beysen, M. K. Hellerstein, L. Berglund, and P. J. Havel. 2009. "Consuming fructose-sweetened, not glucose-sweetened, beverages increases visceral adiposity and lipids and decreases insulin sensitivity in overweight/obese humans." *J Clin Invest* 119 (5):1322-34. doi: 10.1172/JCI37385.
- Stavropoulos-Kalinoglou, A., G. S. Metsios, Y. Koutedakis, and G. D. Kitas. 2011. "Obesity in rheumatoid arthritis." *Rheumatology (Oxford)* 50 (3):450-62. doi: 10.1093/rheumatology/keq266.
- Stefater, Margaret A., Hilary E. Wilson-Pérez, Adam P. Chambers, Darleen A. Sandoval, and Randy J. Seeley. 2012. "All Bariatric Surgeries Are Not Created Equal: Insights from Mechanistic Comparisons." *Endocrine Reviews* 33 (4):595-622. doi: 10.1210/er.2011-1044.
- Stöger, R. 2008. "Epigenetics and obesity." *Pharmacogenomics* 9 (12):1851-60. doi: 10.2217/14622416.9.12.1851.
- Sun, L., L. A. Goff, C. Trapnell, R. Alexander, K. A. Lo, E. Hacısuleyman, M. Sauvageau, B. Tazon-Vega, D. R. Kelley, D. G. Hendrickson, B. Yuan, M. Kellis, H. F. Lodish, and J. L. Rinn. 2013. "Long noncoding RNAs regulate adipogenesis." *Proc Natl Acad Sci U S A* 110 (9):3387-92. doi: 10.1073/pnas.1222643110.
- Suzuki, Y., J. Kido, S. Matsumoto, K. Shimizu, and K. Nakamura. 2019. "Associations among amino acid, lipid, and glucose metabolic profiles in childhood obesity." *BMC Pediatr* 19 (1):273. doi: 10.1186/s12887-019-1647-8.
- Szklarczyk, D., A. L. Gable, D. Lyon, A. Junge, S. Wyder, J. Huerta-Cepas, M. Simonovic, N. T. Doncheva, J. H. Morris, P. Bork, L. J. Jensen, and C. V. Mering. 2019. "STRING v11: protein-protein association networks with increased coverage, supporting functional discovery in genome-wide experimental datasets." *Nucleic Acids Res* 47 (D1):D607-D613. doi: 10.1093/nar/gky1131.
- Takahashi, N., T. Kawada, T. Yamamoto, T. Goto, A. Taimatsu, N. Aoki, H. Kawasaki, K. Taira, K. K. Yokoyama, Y. Kamei, and T. Fushiki. 2002. "Overexpression and ribozyme-mediated targeting of transcriptional coactivators CREB-binding protein and p300 revealed their indispensable roles in adipocyte differentiation through the

- regulation of peroxisome proliferator-activated receptor gamma." *J Biol Chem* 277 (19):16906-12. doi: 10.1074/jbc.M200585200.
- Takashina, C., I. Tsujino, T. Watanabe, S. Sakaue, D. Ikeda, A. Yamada, T. Sato, H. Ohira, Y. Otsuka, N. Oyama-Manabe, Y. M. Ito, and M. Nishimura. 2016. "Associations among the plasma amino acid profile, obesity, and glucose metabolism in Japanese adults with normal glucose tolerance." *Nutr Metab (Lond)* 13:5. doi: 10.1186/s12986-015-0059-5.
- Tallis, J., R. S. James, and F. Seebacher. 2018. "The effects of obesity on skeletal muscle contractile function." *J Exp Biol* 221 (Pt 13). doi: 10.1242/jeb.163840.
- Tang, Q. Q., T. C. Otto, and M. D. Lane. 2003. "Mitotic clonal expansion: a synchronous process required for adipogenesis." *Proc Natl Acad Sci U S A* 100 (1):44-9. doi: 10.1073/pnas.0137044100.
- Thenappan, A., and E. Nadler. 2019. "Bariatric Surgery in Children: Indications, Types, and Outcomes." *Curr Gastroenterol Rep* 21 (6):24. doi: 10.1007/s11894-019-0691-8.
- Tronieri, J. S., T. A. Wadden, A. M. Chao, and A. G. Tsai. 2019. "Primary Care Interventions for Obesity: Review of the Evidence." *Curr Obes Rep*. doi: 10.1007/s13679-019-00341-5.
- Tsai, A. G., and D. H. Bessesen. 2019. "Obesity." *Ann Intern Med* 170 (5):ITC33-ITC48. doi: 10.7326/AITC201903050.
- Tsang, N. M., P. C. Pai, C. C. Chuang, W. C. Chuang, C. K. Tseng, K. P. Chang, T. C. Yen, J. D. Lin, and J. T. Chang. 2016. "Overweight and obesity predict better overall survival rates in cancer patients with distant metastases." *Cancer Med* 5 (4):665-75. doi: 10.1002/cam4.634.
- Tseng, Y. H., A. M. Cypess, and C. R. Kahn. 2010. "Cellular bioenergetics as a target for obesity therapy." *Nat Rev Drug Discov* 9 (6):465-82. doi: 10.1038/nrd3138.
- Ungefroren, H., F. Gieseler, S. Fliedner, and H. Lehnert. 2015. "Obesity and cancer." *Horm Mol Biol Clin Investig* 21 (1):5-15. doi: 10.1515/hmbci-2014-0046.
- van der Klaauw, A. A., and I. S. Farooqi. 2015. "The hunger genes: pathways to obesity." *Cell* 161 (1):119-132. doi: 10.1016/j.cell.2015.03.008.
- Vance, Keith W., and Chris P. Ponting. 2014. "Transcriptional regulatory functions of nuclear long noncoding RNAs." *Trends in Genetics* 30 (8):348-355. doi: 10.1016/j.tig.2014.06.001.
- Wadman, Meredith. 2020. "Why obesity worsens COVID-19." *Science* 369 (6509):1280. doi: 10.1126/science.369.6509.1280.
- Wang, D., Y. Zhou, W. Lei, K. Zhang, J. Shi, Y. Hu, G. Shu, and J. Song. 2009. "Signal transducer and activator of transcription 3 (STAT3) regulates adipocyte differentiation via peroxisome-proliferator-activated receptor gamma (PPARgamma)." *Biol Cell* 102 (1):1-12. doi: 10.1042/BC20090070.
- Wang, J., D. Xiang, S. Mei, Y. Jin, D. Sun, C. Chen, D. Hu, S. Li, H. Li, Y. Wang, D. W. Wang, and H. Ding. 2020. "The novel long noncoding RNA Lnc19959.2 modulates triglyceride metabolism-associated genes through the interaction with Purb and hnRNPA2B1." *Mol Metab* 37:100996. doi: 10.1016/j.molmet.2020.100996.
- Wang, K. C., and H. Y. Chang. 2011. "Molecular mechanisms of long noncoding RNAs." *Mol Cell* 43 (6):904-14. doi: 10.1016/j.molcel.2011.08.018.

- Wei, N., Y. Wang, R. X. Xu, G. Q. Wang, Y. Xiong, T. Y. Yu, G. S. Yang, and W. J. Pang. 2015. "PU.1 antisense lncRNA against its mRNA translation promotes adipogenesis in porcine preadipocytes." *Anim Genet* 46 (2):133-40. doi: 10.1111/age.12275.
- Wei, S., M. Du, Z. Jiang, G. J. Hausman, L. Zhang, and M. V. Dodson. 2016. "Long noncoding RNAs in regulating adipogenesis: new RNAs shed lights on obesity." *Cell Mol Life Sci* 73 (10):2079-87. doi: 10.1007/s00018-016-2169-2.
- WHO. 2020a. "Obesity and Overweight." <https://www.who.int/news-room/factsheets/detail/obesity-and-overweight>.
- WHO. 2020b. "The WHO Child Growth Standards." <https://www.who.int/childgrowth/en/>.
- Wright, S. M., and L. J. Aronne. 2012. "Causes of obesity." *Abdom Imaging* 37 (5):730-2. doi: 10.1007/s00261-012-9862-x.
- Wu, P., X. Zuo, H. Deng, X. Liu, L. Liu, and A. Ji. 2013. "Roles of long noncoding RNAs in brain development, functional diversification and neurodegenerative diseases." *Brain Res Bull* 97:69-80. doi: 10.1016/j.brainresbull.2013.06.001.
- Wyatt, H. R. 2013. "Update on treatment strategies for obesity." *J Clin Endocrinol Metab* 98 (4):1299-306. doi: 10.1210/jc.2012-3115.
- Xiao, Q., Y. Zhao, J. Xu, W. J. Li, Y. Chen, and H. J. Sun. 2019. "NFE2/miR-423-5p/TFF1 axis regulates high glucose-induced apoptosis in retinal pigment epithelial cells." *BMC Mol Cell Biol* 20 (1):39. doi: 10.1186/s12860-019-0223-2.
- Xiao, T., L. Liu, H. Li, Y. Sun, H. Luo, T. Li, S. Wang, S. Dalton, R. C. Zhao, and R. Chen. 2015. "Long Noncoding RNA ADINR Regulates Adipogenesis by Transcriptionally Activating C/EBP α ." *Stem Cell Reports* 5 (5):856-865. doi: 10.1016/j.stemcr.2015.09.007.
- Xie, L., L. Zou, J. Chen, and Y. Liu. 2020. "All-Trans Retinoic Acid Inhibits Bone Marrow Mesenchymal Stem Cell Commitment to Adipocytes via Upregulating FRA1 Signaling." *Int J Endocrinol* 2020:6525787. doi: 10.1155/2020/6525787.
- Xiong, Y., F. Yue, Z. Jia, Y. Gao, W. Jin, K. Hu, Y. Zhang, D. Zhu, G. Yang, and S. Kuang. 2018. "A novel brown adipocyte-enriched long non-coding RNA that is required for brown adipocyte differentiation and sufficient to drive thermogenic gene program in white adipocytes." *Biochim Biophys Acta Mol Cell Biol Lipids* 1863 (4):409-419. doi: 10.1016/j.bbalip.2018.01.008.
- Xu, B., I. Gerin, H. Miao, D. Vu-Phan, C. N. Johnson, R. Xu, X. W. Chen, W. P. Cawthorn, O. A. MacDougald, and R. J. Koenig. 2010. "Multiple roles for the non-coding RNA SRA in regulation of adipogenesis and insulin sensitivity." *PLoS One* 5 (12):e14199. doi: 10.1371/journal.pone.0014199.
- Yang, P., Y. Zhou, B. Chen, H. W. Wan, G. Q. Jia, H. L. Bai, and X. T. Wu. 2009. "Overweight, obesity and gastric cancer risk: results from a meta-analysis of cohort studies." *Eur J Cancer* 45 (16):2867-73. doi: 10.1016/j.ejca.2009.04.019.
- Yang, S., C. Cao, Z. Xie, and Z. Zhou. 2020. "Analysis of potential hub genes involved in the pathogenesis of Chinese type 1 diabetic patients." *Ann Transl Med* 8 (6):295. doi: 10.21037/atm.2020.02.171.
- Yang, T. T., H. Y. Suk, X. Yang, O. Olabisi, R. Y. Yu, J. Durand, L. A. Jelicks, J. Y. Kim, P. E. Scherer, Y. Wang, Y. Feng, L. Rossetti, I. A. Graef, G. R. Crabtree, and C. W. Chow.

2006. "Role of transcription factor NFAT in glucose and insulin homeostasis." *Mol Cell Biol* 26 (20):7372-87. doi: 10.1128/MCB.00580-06.
- Yao, R. W., Y. Wang, and L. L. Chen. 2019. "Cellular functions of long noncoding RNAs." *Nat Cell Biol* 21 (5):542-551. doi: 10.1038/s41556-019-0311-8.
- Yi, F., P. Zhang, Y. Wang, Y. Xu, Z. Zhang, W. Ma, B. Xu, Q. Xia, and Q. Du. 2019. "Long non-coding RNA slincRAD functions in methylation regulation during the early stage of mouse adipogenesis." *RNA Biol* 16 (10):1401-1413. doi: 10.1080/15476286.2019.1631643.
- You, L. H., L. J. Zhu, L. Yang, C. M. Shi, L. X. Pang, J. Zhang, X. W. Cui, C. B. Ji, and X. R. Guo. 2015. "Transcriptome analysis reveals the potential contribution of long noncoding RNAs to brown adipocyte differentiation." *Mol Genet Genomics* 290 (5):1659-71. doi: 10.1007/s00438-015-1026-6.
- Yu, W., G. Q. Zhao, R. J. Cao, Z. H. Zhu, and K. Li. 2017. "LncRNA NONRATT021972 Was Associated with Neuropathic Pain Scoring in Patients with Type 2 Diabetes." *Behav Neurol* 2017:2941297. doi: 10.1155/2017/2941297.
- Zampetaki, A., A. Albrecht, and K. Steinhofel. 2018. "Long Non-coding RNA Structure and Function: Is There a Link?" *Front Physiol* 9:1201. doi: 10.3389/fphys.2018.01201.
- Zhang, L., and Y. M. Wang. 2019. "Expression and function of lncRNA ANRIL in a mouse model of acute myocardial infarction combined with type 2 diabetes mellitus." *J Chin Med Assoc* 82 (9):685-692. doi: 10.1097/JCMA.000000000000182.
- Zhang, L., D. Zhang, Z. Y. Qin, J. Li, and Z. Y. Shen. 2020. "The role and possible mechanism of long noncoding RNA PVT1 in modulating 3T3-L1 preadipocyte proliferation and differentiation." *IUBMB Life*. doi: 10.1002/iub.2269.
- Zhang, M., F. Li, J. W. Sun, D. H. Li, W. T. Li, R. R. Jiang, Z. J. Li, X. J. Liu, R. L. Han, G. X. Li, Y. B. Wang, Y. D. Tian, X. T. Kang, and G. R. Sun. 2019. "LncRNA IMFNCR Promotes Intramuscular Adipocyte Differentiation by Sponging miR-128-3p and miR-27b-3p." *Front Genet* 10:42. doi: 10.3389/fgene.2019.00042.
- Zhang, X., W. Wang, W. Zhu, J. Dong, Y. Cheng, Z. Yin, and F. Shen. 2019. "Mechanisms and Functions of Long Non-Coding RNAs at Multiple Regulatory Levels." *Int J Mol Sci* 20 (22). doi: 10.3390/ijms20225573.
- Zhang, X., C. Xue, J. Lin, J. F. Ferguson, A. Weiner, W. Liu, Y. Han, C. Hinkle, W. Li, H. Jiang, S. Gosai, M. Hachet, B. A. Garcia, B. D. Gregory, R. E. Soccio, J. B. Hogenesch, P. Seale, M. Li, and M. P. Reilly. 2018. "Interrogation of nonconserved human adipose lincRNAs identifies a regulatory role of." *Sci Transl Med* 10 (446). doi: 10.1126/scitranslmed.aar5987.
- Zhu, E., J. Zhang, Y. Li, H. Yuan, J. Zhou, and B. Wang. 2019. "Long noncoding RNA Plnc1 controls adipocyte differentiation by regulating peroxisome proliferator-activated receptor γ ." *FASEB J* 33 (2):2396-2408. doi: 10.1096/fj.201800739RRR.

8. Annex A - Publications

1. “Dissecting the Effect of a 3D Microscaffold on the Transcriptome of Neural Stem Cells with Computational Approaches: A Focus on Mechanotransduction” **Rey F***, Pandini C*, Barzaghini B* et al, *IJMS*, September 2020; 10.3390/ijms21186775
2. “Neural precursors cells expanded in a 3D micro-engineered niche present enhanced therapeutic efficacy in vivo” Carelli S, Giallongo T, **Rey F** et al, *Nanotheranostics*, September 2020; 10.7150/ntno.50633
3. “Advances in Tissue Engineering and Innovative Fabrication Techniques for 3-D-Structures: Translational Applications in Neurodegenerative Diseases” **Rey F** et al, *Cells*, July 2020; 10.3390/cells9071636
4. “A New Selective PPAR γ Modulator Inhibits Triglycerides Accumulation during Murine Adipocytes’ and Human Adipose-Derived Mesenchymal Stem Cells Differentiation” Al Haj G*, **Rey F*** et al, *IJMS*, June 2020; 10.3390/ijms21124415
5. “Biomaterials in Neurodegenerative Disorders: A Promising Therapeutic Approach” Bordoni M*, Scarian E*, **Rey F** et al, *IJMS*, May 2020; 10.3390/ijms21093243
6. “Erythropoietin as a neuroprotective molecule: an overview of its therapeutic potential in neurodegenerative diseases” **Rey F** et al., *ASN Neuro*, July 2019; 10.1177/1759091419871420
7. “Adipose Derived Stem Cells from Fat Tissue of Breast Cancer microenvironment present altered adipogenic differentiation capabilities” **Rey F***, Lesma E* et al., *Stem Cells International*, July 2019; 10.1155/2019/1480314
8. “HuR interacts with lincBRN1a and lincBRN1b during neuronal stem cells differentiation” Carelli S*, Giallongo T*, **Rey F*** et al., *RNA Biology*, July 2019; 10.1080/15476286.2019.1637698
9. “Neuroprotection, Recovery of Function and Endogenous Neurogenesis in Traumatic Spinal Cord Injury Following Transplantation of Activated Adipose Tissue” Carelli S*, Giallongo T*, **Rey F** et al., *Cells*, April 2019; 10.3390/cells8040329
10. “From Neuronal Differentiation of iPSCs to 3D Neuro-Organoids: Modelling and Therapy of Neurodegenerative Diseases” Bordoni M*, **Rey F***, Fantini V* et al., *IJMS*, Dec 2018; 10.3390/ijms19123972
11. “Counteracting neuroinflammation in experimental Parkinson's disease favors recovery of function: Effects of Er-NPCs administration” Carelli S, Giallongo T, Gombalova Z, **Rey F** et al., *J Neuroinflammation*, Nov 2018; 10.1186/s12974-018-1375-2

*These authors contributed equally to this work

9. Annex B – Abstracts

1. “Application of the nichoid culture substrate to enhance multipotency of neural precursors.” Giallongo T*, Barzaghini B*, **Rey F** et al., DISS Congress 9 November 2019
2. “Role of the oncogenic lncRNA ZEB1-AS1 in sporadic ALS: at a cross-road between neurodegeneration and cancer.” **Rey F** et al., DISS Congress 9 November 2019
3. “Global deregulation of lncRNAs involved in neuronal development could play a role in ALS.” **Rey F** et al., DISS Congress 9 November 2019
4. “Neuroprotective role for Erythropoietin in Parkinson’s Disease: evidence from in vitro and in vivo models of the disease.” **Rey F** et al., DISS Congress 9 November 2019
5. “HuR’s interaction with lincBRN1a and lincBRN1b is implicated in neuronal stem cells differentiation” Giallongo T, **Rey F** et al., 2nd BraYn, Milan, November 14-16th 2019
6. “Neural Stem Cells transplantation in pre-clinical experimental model of Parkinson’s: counteraction of neuroinflammation and promotion of functional recovery” Giallongo T, **Rey F** et al., 2nd BraYn, Milan, November 14-16th 2019
7. “Therapeutic effect of neural progenitor cells expanded in the 3D nano-engineered Nichoid substrate in a Parkinson’s disease preclinical model” Barzaghini B, Giallongo T, **Rey F** et al., 2nd BraYn, Milan, November 14-16th 2019
8. “Study of the oncogenic lncRNA ZEB1-AS1 in sporadic ALS: identification of a new deregulated pathway” **Rey F** et al., 2nd BraYn, Milan, November 14-16th 2019
9. “Implication of the oncogenic lncRNA ZEB1-AS1 mediated pathway in sporadic ALS pathogenesis” **Rey F** et al., XVIII SINS, Perugia, September 26-29 2019
10. “LncRNAs involved in neuronal development seem to play a role in ALS pathology” **Rey F** et al., XVIII SINS, Perugia, September 26-29 2019
11. “Therapeutic effect of neural progenitor cells expanded in the 3D nano-engineered Nichoid substrate in a Parkinson’s disease preclinical model” Barzaghini B, Giallongo T, **Rey F** et al., XVIII SINS, Perugia, September 26-29 2019
12. “Neural Stem Cells transplantation in pre-clinical experimental model of Parkinson’s: counteraction of neuroinflammation and promotion of functional recovery” Giallongo T, **Rey F** et al., XVIII SINS, Perugia, September 26-29 2019
13. “HuR’s interaction with lincBRN1a and lincBRN1b is implicated in neuronal stem cells differentiation” Carelli S, Giallongo T, **Rey F** et al XVIII SINS, Perugia, September 26-29 2019
14. “Therapeutic Effect of Neural Progenitor cells in the Nichoid substrate in a Parkinson’s Disease preclinical model” Carelli S, Giallongo T, **Rey F** et al, ESB-ITA Meeting 2019, 30 September – 1 October 2019, Bologna, Italy
15. “Expansion and characterization of human adipose derived stem cells in the 3D nano-engineered Nichoid substrate” Barzaghini B, Giallongo T, **Rey F** et al, ESB-ITA Meeting 2019, 30 September – 1 October 2019, Bologna, Italy
16. “Therapeutic Effect of Neural Progenitor cells expanded in the 3D nano-engineered Nichoid substrate in a Parkinson’s disease preclinical model” Carelli S, Giallongo T, **Rey F** et al., TERMIS EU 2019, 27-31 May 2019, Rhodes, Greece
17. “LncRNAs involved in neuronal development seem to play a role in ALS pathology” **Rey F** et al., National Meeting of PhD Students in Neuroscience 01 March 2019

18. "AU-rich elements associated with HuR are essential for lncRNAs turnover in murine neural stem cells differentiation" Giallongo T, Carelli S, **Rey F** et al, DISS Congress 9 November 2018
19. "Counteracting neuroinflammation in experimental Parkinson's disease favors recovery of function. Effects of Er-NPCs administration" Carelli S, Giallongo T, Gombalova Z, **Rey F** et al, DISS Congress 9 November 2018
20. "LncRNAs involved in neuronal development seem to play a role in ALS pathology" **Rey F** et al, Focus on ALS 2018, 27-29 September, 2018
21. "Oncogenes and transcription factors long non-coding RNA: new actors in ALS pathogenesis" Gagliardi S, Zucca S, Pandini C, Sproviero D, Palmieri I, Pansarasa O, Garofalo M, **Rey F**, et al, Focus on ALS 2018, 27-29 September, 2018
22. "AU-rich elements associated with HuR are essential for lncRNAs turnover in murine neuronal stem cells differentiation" **Rey F** et al, FENS 2018, Berlin, 7-11 July, 2018
23. "Anti-inflammatory action of erythropoietin releasing neural precursors transplanted in a murine model of Parkinson's Disease" Giallongo T, Carelli S, Gombalova Z, **Rey F**, et al, FENS 2018, Berlin, 7-11 July, 2018
24. "Genetic testing of sporadic ALS patients reveals pathogenetic mutations in non-ALS genes" Valente M, Zucca S, Palmieri I, Garau J, **Rey F** et al, The 28th International Symposium on ALS/MND, Boston, USA, 8-10 December 2017.
25. "Mutational analysis of the GBA gene in an Italian population affected by Parkinson's disease" Palmieri I, Valente M, **Rey F** et al, XX SIGU, 15-18 Novembre 2017, Napoli
26. "The differential view of genotype phenotype relationships in neurodegenerative diseases" Cereda C, Valente M, Palmieri I, **Rey F** et al, XLVIII Congresso Società Italiana di Neurologia, Napoli, 14-17 Ottobre 2017.
27. "Natural Antisense Transcripts and Long Non-Coding RNA in Amyotrophic Lateral Sclerosis" Gagliardi S, Zucca S, Arigoni M, Pandini C, **Rey F** et al, XVII SINS, Ischia, 1-4 Ottobre 2017

Ringraziamenti

Ho la fortuna di avere tantissime persone che mi sono state accanto e indispensabili nello svolgimento di questo percorso, e servirebbe un'altra tesi intera per rendergli giustizia.

Vorrei innanzitutto ringraziare le Prof. Di Giulio e Prof. Barassi, per avermi fatto da tutor, permettendomi di continuare a lavorare in un campo che tanto mi appassiona. A Stephana devo dire un grazie infinito per avermi supportata in questo percorso, per avermi insegnato a guardare la ricerca con nuovi occhi, per avermi incoraggiata e per avermi dato fiducia, aiutandomi a ottenere i risultati che speravo e anche tanto di più. Grazie inoltre per essere stato un capo con cui è possibile confrontarsi, imparando tanto. Un grandissimo grazie va ai miei colleghi, che mi hanno accompagnata e sostenuta insegnandomi moltissimo in questi anni. A Tonia, che mi è stata vicina dal primo giorno, guidandomi in un ambiente del tutto nuovo, che ha da subito avuto a cuore il mio bene, aiutandomi in tutti i modi, consigliandomi e tutelandomi sempre, e che continua ancora oggi a supportarmi, con una gentilezza incredibile. A Ghina, che ha affrontato con me questo percorso, districandosi con me in tutto quello che questo dottorato ha richiesto. Grazie anche ai colleghi e amici di Pavia, che dopo tre anni di distanza ancora mi supportano e sono sempre disponibili e pronti a rispondere a tutti i miei dubbi.

Vorrei inoltre ringraziare tutti i miei "studentini", che dal primo all'ultimo mi hanno aiutata tantissimo insegnandomi spesso più di quanto io ho insegnato loro e diventando, oltre che colleghi, amici preziosi. Ad Andrea e Riccardo, i primi ingegneri, per essere stati da subito una presenza rassicurante, e per avermi ricordato di sorridere facendo diventare questo percorso più di un semplice lavoro. Ad Alice, che mi è stata vicina per più di un anno e mezzo, per avermi aiutata a superare le numerose difficoltà che questo lavoro sicuramente crea, per essere stata presente anche nei momenti di gioia e di grande soddisfazioni e per aver posto con me delle basi solide per quelli che sono i lavori che più mi appassiano. A Francesca, che è riuscita ad affrontare un percorso difficile senza mai perdersi d'animo e con una forza incredibile, per avermi insegnato a cercare sempre nuove soluzioni, facendo dei problemi un punto di partenza. Ad Alessandra, così determinata che sono sicura andrà molto lontano, per aver sempre dimostrato un interesse sincero, per la tanta voglia di imparare, e per avermi sempre aiutata con entusiasmo. A Valentina, per aver condiviso con me la forte passione per la ricerca. A Erika e Rossella, per avermi aiutata in queste battute finali, sempre con un sorriso e un'attitudine positiva nonostante le circostanze tutt'altro che facili.

Da questo elenco rimangono fuori due persone, che hanno deciso di continuare a condividere con me questa avventura anche dopo la laurea, e alle quali sarò eternamente grata. A Letizia, per la quale non esiste niente che non si possa imparare, che ha sempre accettato tutte le sfide, spesso impossibili, che le ho posto davanti riuscendo ad ottenere risultati incredibili, un grazie infinito per non esserti arresa e avermi aiutata in maniera fondamentale a creare un lavoro del quale essere orgogliosa. A Bianca, una delle rare persone sinceramente buone e umili, va un ringraziamento speciale per tutto il sostegno di questi anni. Grazie per essermi sempre stata d'incoraggiamento, credendo in me quando neanche io lo facevo, per avermi aiutata a superare paure e difficoltà, condividendo con me le sfide più difficili; superarle insieme è stata una bellissima soddisfazione. Grazie perché mi sei rimasta sempre accanto, sia dentro che fuori dal laboratorio, diventando un'amica così importante così in fretta. Grazie, perché so di potermi sempre fidare di te.

Il grazie che mi viene più difficile mettere per iscritto, per tutto quello che vorrei poter esprimere loro, va a mio padre, mia madre e Guido. A mio papà, che è così simile a me, ma che ha una forza così grande che posso solo sperare un giorno di avere. Vorrei riuscire ad avere la tua capacità di guardare qualsiasi problema come se fosse solo un piccolissimo incidente di percorso, mi hai insegnato ad apprezzare le cose belle della vita, a trovare sempre il lato positivo e ad affrontare ogni ostacolo con grinta e determinazione. Grazie per aver lottato con le unghie e con i denti, rimanendoci sempre vicino, sostenendoci, guidandoci e amandoci, e grazie, perché hai sempre fatto di tutto affinché potessi essere tutto quello che volevo e anche qualcosa in più. A mia mamma, il mio angolo di pace quando il mondo sembra crollarmi addosso. Sai sempre di cosa ho bisogno, quando devo essere incoraggiata e quando semplicemente consolata, mi basta parlarti per ritrovare di nuovo me stessa. Vorresti proteggerci da tutte le cose brutte di questo mondo e anche se questo è impossibile, sapere di averti al mio fianco ha sempre reso, e rende ancora, tutto molto meno spaventoso. Grazie, perché mi fai venire voglia di essere la versione migliore di me stessa, e grazie, perché mi basta guardarti negli occhi per veder riflesso tutto l'amore che provi per noi. A Guido, che riassume in un'unica persona i lati migliori dei miei genitori, mettendoci anche qualcosa di incredibile di suo. Sei una roccia, la persona che più ammiro, e ogni volta rimango stupita dalla tua capacità di sorridere, sorridere sempre. Quando penso che tu ormai non possa sorprendermi più, mostri un nuovo lato del tuo carattere, e improvvisamente mi accorgo che, ancora una volta, sei cresciuto senza che neanche me ne accorgessi. Grazie, perché senza di te sarei persa, e grazie, perché ti prendi cura di me.

Ho una bella, grande famiglia, che ringrazio di cuore, ma un ringraziamento speciale va alle mie nonne, per avermi sempre amata incondizionatamente e per aver gioito con me di ogni mio successo. A mia Nonna Betty, che condivide con me l'amore per quello che faccio e che mi supporta con entusiasmo in ogni mia decisione, capendomi sempre. A mia Nonna Pia, che mi ha sempre fatta sentire speciale e che avrebbe smosso le montagne per noi. Mi manchi tanto.

A Elena e Valentina va un ringraziamento speciale per essere sempre la mia prima cosa bella, il mio raggio di sole e le persone sulle quali so di poter sempre sempre sempre contare. Non so nemmeno chi sarei senza di voi. Ad Anna, un grande grazie per aver sempre guardato oltre, trovando il buono dove pochi riuscivano e rimanendomi accanto nonostante tutto. Vorrei inoltre ringraziare quegli amici che da cinque anni ormai hanno deciso di starmi accanto e sostenermi. Non sono incline alle manifestazioni d'affetto, e raramente riesco a dirvi quanto siete importanti per me, ma mi avete trovata in un momento in cui ero completamente persa, e, senza nemmeno saperlo, mi avete salvata. Grazie, perché avete frantumato tutte i miei muri più spessi e perché è solo grazie a voi se ho imparato a fidarmi di nuovo. Siete il mio jolly più fortunato.

E alla fine non potevi esserci che tu, Ceci, che sei un po' lavoro, un po' famiglia, e sicuramente tanto amica. Non so cosa ci abbia portato dall'essere "colleghe" alla definizione impossibile di oggi, so soltanto che non riesco a prescindere il mio percorso degli ultimi anni, e la mia vita ora, da te. Mi hai aiutata ad andare avanti in momenti in cui credevo di non riuscire, hai trovato soluzioni per problemi impossibili, e mi sei rimasta vicina in momenti in cui nemmeno io sopportavo me stessa. Sei rimasta con me anche nei momenti belli, quelli in cui tutto sembra facile ma che dimostrano quanto io abbia bisogno di condividere proprio tutto con te. Vorrei potessi vederti come ti vedo io, speciale e indispensabile, e vorrei che ti ricordassi sempre che non c'è assolutamente niente che tu non possa fare, e nessuno che tu non possa essere, perché hai la forza per ottenere tutto. Ti voglio bene.